Evidence-Based Complementary and Alternative Medicine

Medicinal Plant Extracts and Bioactive Compounds Targeting Inflammation in Skeletal Muscle Disease

Lead Guest Editor: Atul Kabra
Guest Editors: Rohit Sharma and Jelena Zivkovic

Medicinal Plant Extracts and Bioactive Compounds Targeting Inflammation in Skeletal Muscle Disease

Evidence-Based Complementary and Alternative Medicine

Medicinal Plant Extracts and Bioactive Compounds Targeting Inflammation in Skeletal Muscle Disease

Lead Guest Editor: Atul Kabra
Guest Editors: Rohit Sharma and Jelena Zivkovic

Contents

Herbal Formula Modified Bu-Shen-Huo-Xue Decoction Attenuates Intervertebral Disc Degeneration via Regulating Inflammation and Oxidative Stress
Jialiang Lin, Jionghui Gu, Dongwei Fan, and Weishi Li
Research Article (12 pages), Article ID 4284893, Volume 2022 (2022)

Wu-Teng-Gao External Treatment Improves Th17/Treg Balance in Rheumatoid Arthritis
Xueming Yao, Qiuyi Wang, Changming Chen, Ping Zeng, Lei Hou, Jing Zhou, Ying Huang, and Wukai Ma
Research Article (12 pages), Article ID 5105545, Volume 2022 (2022)

Jin-Wu-Jian-Gu Formulation Attenuates Rheumatoid Arthritis by Inhibiting the IL33-ST2 Signaling Pathway
Daomin Lu, Ying Huang, Wukai Ma, Changming Chen, and Lei Hou
Research Article (9 pages), Article ID 6821388, Volume 2022 (2022)

Hindawi
Evidence-Based Complementary and Alternative Medicine
Volume 2022, Article ID 8027987, 15 pages
https://doi.org/10.1155/2022/8027987

Research Article

Identification of Potential Therapeutic Target Genes in Osteoarthritis

Yang Hu,[1] Yinteng Wu,[1] Fu Gan,[2] Mingyang Jiang,[1] Dongxu Chen,[3] Mingjing Xie,[1] Yiji Jike,[1] and Zhandong Bo[1]

[1]*Department of Orthopedics, The First Affiliated Hospital of Guangxi Medical University, Nanning 530021, China*
[2]*Department of Urology Surgery, The Affiliated Hospital of Youjiang Medical University for Nationalities, Baise 533000, China*
[3]*Department of Joint Surgery and Sports Medicine, Nanxishan Hospital of Guangxi Zhuang Autonomous Region, Guilin 541002, China*

Correspondence should be addressed to Zhandong Bo; drrbozhandong@126.com

Received 10 March 2022; Revised 20 May 2022; Accepted 13 July 2022; Published 13 August 2022

Academic Editor: Atul Kabra

Objective. Osteoarthritis (OA), also known as joint failure, is characterized by joint pain and, in severe cases, can lead to loss of joint function in patients. Immune-related genes and immune cell infiltration play a crucial role in OA development. We used bioinformatics approaches to detect potential diagnostic markers and available drugs for OA while initially exploring the immune mechanisms of OA. *Methods*. The training set GSE55235 and validation set GSE51588 and GSE55457 were obtained from the Gene Expression Omnibus (GEO) database and differentially expressed genes (DEGs) were identified by the limma package. Gene set enrichment analysis (GSEA) was performed on the GSE55235 dataset using the cluster profiler package. At the same time, DEGs were analyzed by gene ontology (GO) and the Kyoto Encyclopedia of Genes and Genomes (KEGG). In addition, protein-protein interaction (PPI) analysis was performed on the common DEGs of the three datasets using the STRING database. Proteins with direct linkage were identified as hub genes, and the relation of hub genes was subsequently analyzed using the GOSemSim package. Hub genes' expression profiles and diagnostic capabilities (ROC curves) were analyzed and validated using three datasets. In addition, we performed RT-qPCR to validate the levels of hub genes. The immune microenvironment was analyzed using the CIBERSORT package, and the relationship between hub genes and immune cells was evaluated. In addition, we used a linkage map (CMAP) database to identify available drug candidates. Finally, the GSEA of hub genes was used to decipher the potential pathways corresponding to hub genes. *Results*. Three hub genes (*CX3CR1*, *MYC*, and *TLR7*) were identified. *CX3CR1* and *TLR7* were highly expressed in patients with OA, whereas the expression of *MYC* was low. The results of RT-qPCR validation were consistent with those obtained using datasets. Among these genes, *CX3CR1* and *TLR7* can be used as diagnostic markers. It was found that CX3CR1, MYC, and TLR7 affect the immune microenvironment of OA via different immune cells. In addition, we identified a potential drug for the treatment of OA. Altogether, CX3CR1, MYC, and TLR7 affect the immune response of OA through multiple pathways. *Conclusion*. CX3CR1, MYC, and TLR7 are associated with various immune cells and are the potential diagnostic markers and therapeutic targets for OA.

1. Background

Osteoarthritis (OA) refers to a common arthritic disease worldwide, featured by several changes such as synovial inflammation, cartilage degeneration, and subchondral bone sclerosis [1]. It affected more than 500 million people worldwide (~7% of the global population), with exceptionally high prevalence in those of advanced age (>65 years of age) [2]. Factors contributing to OA include joint trauma, age, obesity, joint shape, and alignment [3]. However, recently, more and more research has demonstrated the crucial function of immune molecules in the pathogenesis of OA, such that OA is gradually recognized as a chronic inflammatory response [4]. At present, OA is routinely diagnosed according to clinical presentations and a combination of imaging technologies [5]. Unfortunately, an

early, accurate OA diagnosis remains impossible, and there exists no effective drug for its treatment. Therefore, it is highly crucial to explore early diagnostic biomarkers that can also serve as drug targets to enhance the prognosis and treatment of patients undergoing OA.

Due to the development of bioinformatics technology, high-throughput platform-based gene chips have emerged as an effective tool to study gene expression profiles and explore molecular mechanisms underlying several diseases [6]. This approach is considered an efficient method for identifying diagnostic markers and therapeutic targets. CIBERSORT, an algorithm used to depict the immune cell constitution within complicated tissues using the corresponding gene expression patterns, is extensively adopted for assessing the relative abundances of 22 immune cells in multiple diseases [7]. Thus, it can be applied for analyzing infiltration degrees of immune cells within OA, which can thus facilitate to development of novel diagnostic biomarkers and immunotherapeutic targets.

We first downloaded three OA microarray datasets in Gene Expression Omnibus (GEO) database, and differentially expressed genes (DEGs) were analyzed. Afterward, the common DEGs in the two datasets were used for protein-protein interaction (PPI) studies for selecting and determining diagnostic markers for OA. In addition, this study identified drugs that acted on the product of these genes. We used CIBERSORT to explore the differences in immune infiltration degrees within OA compared with healthy tissue samples of 22 immune cell types. Apart from that, this work also investigated the association of diagnostic markers with infiltration degrees of immune cells. Finally, a single-gene Gene Set Enrichment Analysis (GSEA) was conducted to identify immune pathways related to diagnostic markers to better understand molecular immune mechanisms related to OA occurrence and progression.

2. Methods

2.1. Data Collection. To identify genome-wide gene expression datasets comparing gene expression in OA tissues and normal tissues, we searched and selected the GSE55235, GSE51588, and GSE55457 datasets for subsequent analysis using the Gene Expression Overview (GEO) database. We used GSE55235 as the training set, whereas GSE51588 and GSE55457 as validation sets.

2.2. Screening of Differentially Expressed Genes. Using the information obtained from the GPL96 platform, the probe identification number was first converted to a traditional gene symbol, and the maximum value was assigned to multiple probes of the same gene as the gene expression. Datasets were normalized and differentially expressed using the limma software package. The criteria for screening DEGs were adjusted $P < 0.05$ after correction; $|\log FC| > 1.5$, FC refers to the fold of difference.

2.3. Gene Set Enrichment Analysis. GSEA detects changes in expression in the sets of genes rather than individual genes. Therefore, subtle changes in the expression can be found, and better results can be obtained. To identify the biological processes and GO terms, together with KEGG pathways associated with OA, we performed GSEA on the GSE51588 dataset with cluster profiler *R* package, with $P < 0.05$ indicating statistical significance.

2.4. Functional Annotation of DEGs. Gene Ontology (GO) is classified into three types, namely, biological process (BP), cellular component (CC), and molecular function (MF). It is a broad and highly efficient method to interpret gene products and their functional characteristics. The KEGG analysis provides a data resource about known metabolic pathways to understand higher-level functions of genes and biological systems. As a package for annotation, visualization, and integrated discovery, a cluster profiler can be adopted for extracting meaningful biological information about genes. DEGs from the training set were examined with a cluster profiler software package, and a $P < 0.05$ threshold was considered significant.

2.5. Protein-Protein Interaction Network (PPI and Hub Gene Selection). We extracted DEGs from the GSE55235 dataset and intersected them with those from GSE51588 and GSE55457 datasets, respectively, to obtain the common DEGs between the two datasets. The online tool VennDetail was used to construct the common DEGs between two datasets, respectively. STRING database (https://string-db.org) was adopted to retrieve interacting genes/proteins, including approximately 24.6 million proteins and over 3.1 billion interactions in 5.09 K organisms. In the STRING database, we selected "multiple proteins," entered co-up-and down-regulated differential genes, selected "*Homo sapiens*" as the organism, and set the significant threshold to the lowest interaction score >0.4 (low confidence). Subsequently, the Cytoscape software the PPI network was constructed using. We analyzed the key genes using the GOSemSim package to analyze their functional similarity. This analysis was based on the assumption that if two gene products are functionally similar, they tend to be located together in the GOtree.

2.6. Expression-Level Validation of Hub Genes. The genes in the GSE55235 dataset were extracted, and their expression was analyzed and verified using the GSE51588 and GSE55457 datasets.

2.7. Experimental Validation of Hub Gene Expression. We obtained rat articular chondrocytes from Wuhan Procell Life Science and Technology Co., Ltd. Cells were cultured using DMEM/F12 medium containing 10% fetal bovine serum. The inflammation model group was stimulated with a medium containing IL-1β at a concentration of 10 ng/ml for 24 h. Total RNA was extracted with RNAeasy™ Animal RNA Extraction Kit (Beyotime Biotechnology, China), and quality control was conducted by NanoDrop one spectrophotometer. Then, reverse transcription was performed to produce

cDNA. The extracted RNA was reverse transcribed to cDNA using PrimeScript™ RT Master Mix (TAKARA, Japan). cDNA was extracted using PowerUp™ SYBR® Green Master Mix (Applied Biosystems, USA) and ABI 7500Real-TimePCR System. RT-qPCR was performed to detect the expression of differential genes. GAPDH was used as an internal reference. The relative mRNA expression level was calculated with the $2^{-\Delta\Delta Ct}$ method, and $P < 0.05$ indicated a significant difference. The primer sequences are shown in Table 1.

Table 1: | Primer sequences.

Gene		Primer (5′-3′)
GAPDH	Forward	GACATGCCGCCTGGAGAAAC
GAPDH	Reverse	AGCCCAGGATGCCCTTTAGT
CX3CR1	Forward	CACCAAAGCCAGCACATAGGAGAG
CX3CR1	Reverse	GTCTGCGGATCTTGGACAAACAAATG
MYC	Forward	AGCAGCGACTCTGAAGAAGAACAAG
MYC	Reverse	GGATGACCCTGACTCGGACCTC
TLR7	Forward	GTATGCCACCGAATCTAACGACTCTC
TLR7	Reverse	GCCAATCTCGCAGGGACAGTTG

2.8. ROC-Level Validation of Hub Genes. In the GSE55235 database, the total RNA was extracted from patients undergoing OA and healthy controls. The ROC curves were drawn. At the same time, the area under the curve (AUC) was computed using "proc" software to evaluate the ability of the selected genes, aiming to discriminate between patients with OA and controls. Both GSE51588 and GSE55457 datasets were used to validate their ROC levels.

2.9. Correlation Analysis of Hub Gene with Immune Cells. This work employed *R* package CiberSort to process the GSE55235 gene expression matrix data. Besides, samples satisfying $P < 0.05$ were chosen for obtaining the infiltration matrix of OA immune cells. For visualizing the proportions of 22 immune cell infiltrations within patients with OA, the cumulative histogram was plotted using the "ggplot2" software package. Correlations between 22 immune cells were analyzed and visualized using the "corrplot" software package. This study drew violin plots with "ggplot2" package for visualizing different infiltration degrees of immune cells in OA compared with normal groups.

2.10. Correlation Analysis of Hub Gene with Infiltration Degrees of Immune Cells. This work conducted Spearman's correlation on immune cells and hub genes, and immune cells satisfying $P < 0.05$ were chosen. The ggplot2 software package was used to visualize the results.

2.11. Small Molecule Drug Analysis. As an experimentally validated drug database, the CMAP database can be used to predict the potential molecular compounds acting on OA. CX3CR1, MYC, and TLR7 were submitted to the CMAP website to identify small-molecule drugs against OA. The correlation between the drug and the target is represented by a score of −1 to 1, with negative scores indicating that the drug has the potential to inhibit OA. Therefore, enrichment <0 and $P < 0.001$ were used for screening.

2.12. GSEA of Hub Genes. To further explore the potential functions of CX3CR1, MYC, and TLR7 in OA, GSEA was performed on CX3CR1, MYC, and TLR7. In the GSE51588 dataset, according to the expression of CX3CR1, MYC, and TLR7, Spearman's analysis was used to calculate their correlation coefficients with other genes. They were treated as an ordered gene list. The R package "cluster profile" was used to select hall.v7.4.sytmbols.gmt from the Molecular Signature Database (MSigDB) as the reference genome for GSEA, and a *P* -adjustment value < 0.05 was used as the screening criterion.

3. Results

3.1. Screening Results of DEGs. The limma software package analysis revealed 343 standard-compliant DEGs from the GSE55235 dataset, among which 167 showed up-regulation while 176 showed down-regulation (Figure 1(a)). In the GSE51588 dataset, 272 standard DEGs were discovered, including 108 with up-regulation, replaced by 164 with down-regulation (Figure 1(b)). In addition, we discovered 109 qualified DEGs from the GSE55457 dataset, including 26 with up-regulation and 83 with down-regulation (Figure 1(c)). The respective top 15 up-regulated and down-regulated genes in the GSE55235, GSE51588, and GSE55457 datasets are shown in the heatmap (Figures 1(d) and 1(f)).

3.2. GSEA. Gene set enrichment analysis revealed that compared with controls, the gastrointestinal system's smooth muscle contraction, glycosphingolipid catabolic process, response to UV-A, and glycolipid catabolic processes were enriched in BP (Figure 2(a)). The major histocompatibility complex (MHC) class II protein complex, immunoglobulin complex, banded collagen fibrils, and fibrillar collagen trimer were enriched in CC (Figure 2(b)). In MF, platelet-derived growth factor binding, immunoglobulin receptor binding, peptidoglycan binding, and immunoglobulin binding were mainly enriched (Figure 2(c)). The KEGG analysis revealed enrichment in asthma, autoimmune thyroid disease, N primary immunodeficiency as well as intestinal immune network for IgA production (Figure 2(d)).

3.3. DEGs Functional Enrichment Analysis Results. GO as well as KEGG enrichment analysis was conducted with the cluster profiler package in R for exploring DEGs' biological functions. In the BP group, we enriched DEGs in neutrophil degranulation, neutrophil activation, as well as neutrophil activation involved in immune response (Figure 3(a)). In the CC group, DEGs were majorly concentrated in secretory granule lumen, vesicle lumen, and cytoplasmic vesicle lumen (Figure 3(b)). In the MF group, DEGs were associated with glycosaminoglycan binding, extracellular matrix structural constituents, and heparin-binding (Figure 3(c)). In KEGG,

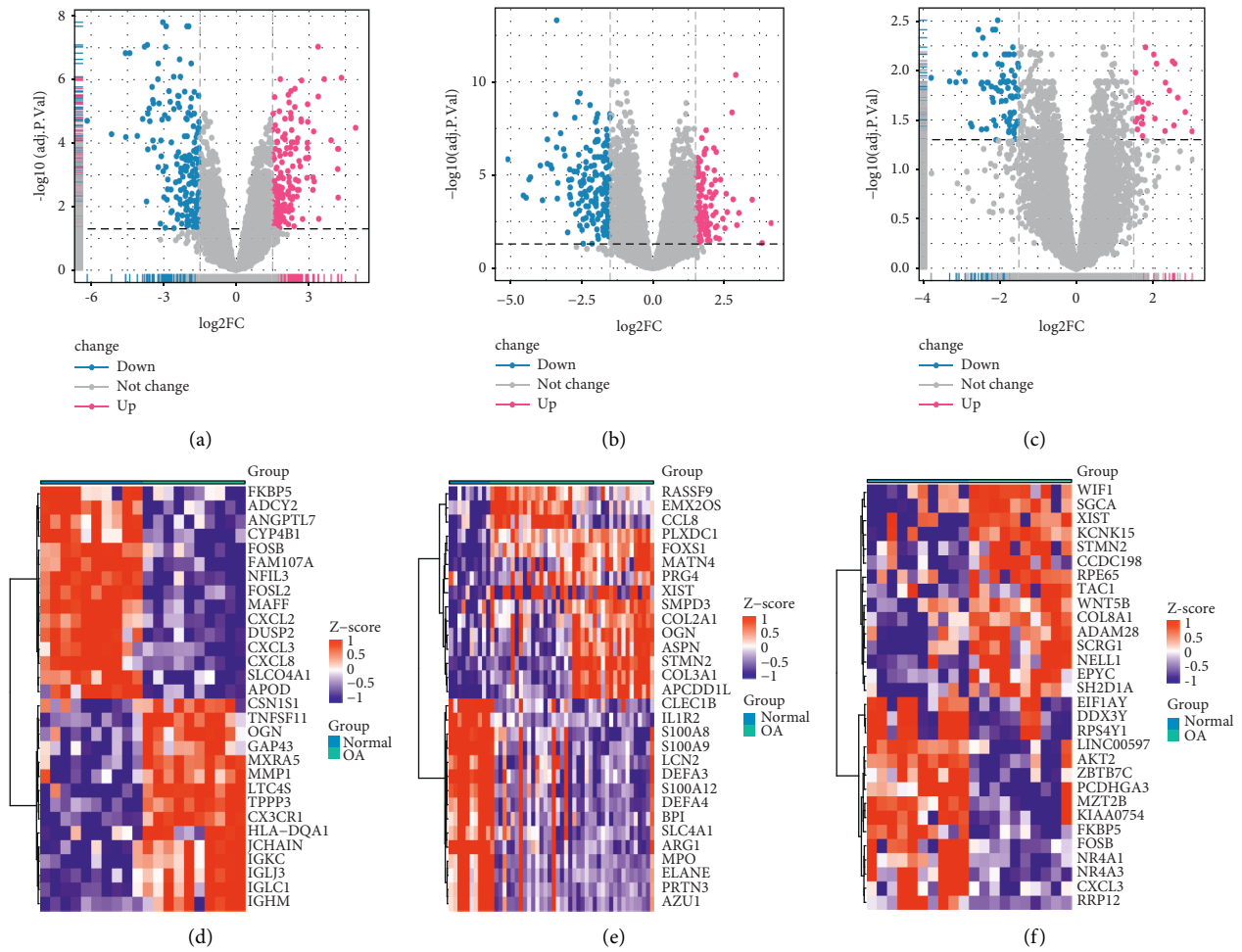

Figure 1: Analysis of EDGs (a): Volcano Plot of GSE55235 dataset:(b): Volcano Plot of GSE51588 dataset; (c): Volcano Plot of GSE55457 dataset; Up-regulated differentially expressed genes are indicated by red dots; down-regulated differentially expressed genes are indicated by blue dots; nonsignificant genes are indicated by gray dots. (d): Heat map of GSE55235 dataset; (e): Heat map of GSE51588 dataset (f): Heat map of GSE55457 dataset. Differential epigones that are highly expressed in the samples are marked in red, and differentially expressed genes that are low in the samples are indicated in blue.

DEGs were enriched in neutrophil extracellular trap formation, viral protein interaction with cytokines or their receptors, and *Staphylococcus aureus* infection (Figure 3(d)).

3.4. PPI Network Construction and Key Gene Screening. Two up-regulated DEGs (*CX3CR1* and *TLR7*) and two down-regulated DEGs (*MYC* and *NFIL3*) were shared across the three datasets (Figure 4(a)). The PPI results indicated a direct link between *CX3CR1*, *MYC*, and *TLR7* (Figure 4(b)). The functional similarity results showed a functional connection between *CX3CR1*, *MYC*, and *TLR7*, with *TLR7* occupying the most important position, followed by *CX3CR1* and *MYC* (Figure 4(c)).

3.5. Hub Gene Verification and Efficacy Evaluation. In the GSE55235 dataset, *CX3CR1* and *TLR7* levels increased, whereas *MYC* levels notably decreased, with a P-value <0.05 (Figures 5(a)–5(c)). In the validation datasets GSE51588 (Figures 5(d)–5(f)) and GSE55457 (Figures 5(g)–5(i)), the expression of the three genes was the same as that in the GSE51588 dataset, all of which were significant.

3.6. RT-qPCR Validation. The experimental results showed significantly increased expression of *CX3CR1* and *TLR7* in the OA group (Figures 6(a), 6(b)) and significantly decreased expression of *MYC* in the OA group (Figure 6(c)). The experimental results were in line with those obtained from the analysis of the three microarray datasets, demonstrating the reliability of our bioinformatics analysis results.

3.7. ROC Level Validation of Hub Genes. In the GSE55235 dataset, the true AUCs of CX3CR1 and TLR7 were greater than 0.9, and the true AUC of MYC was lesser than 0 (Figure 7(a)). In the validation datasets GSE51588 (Figure 7(b)) and GSE55457 (Figure 7(c)), the true AUCs of CX3CR1 and TLR7 were also greater than 0.9, and the true AUC of MYC was less than 0. CX3CR1 and TLR7 exhibited a strong ability to distinguish patients with OA from those without OA.

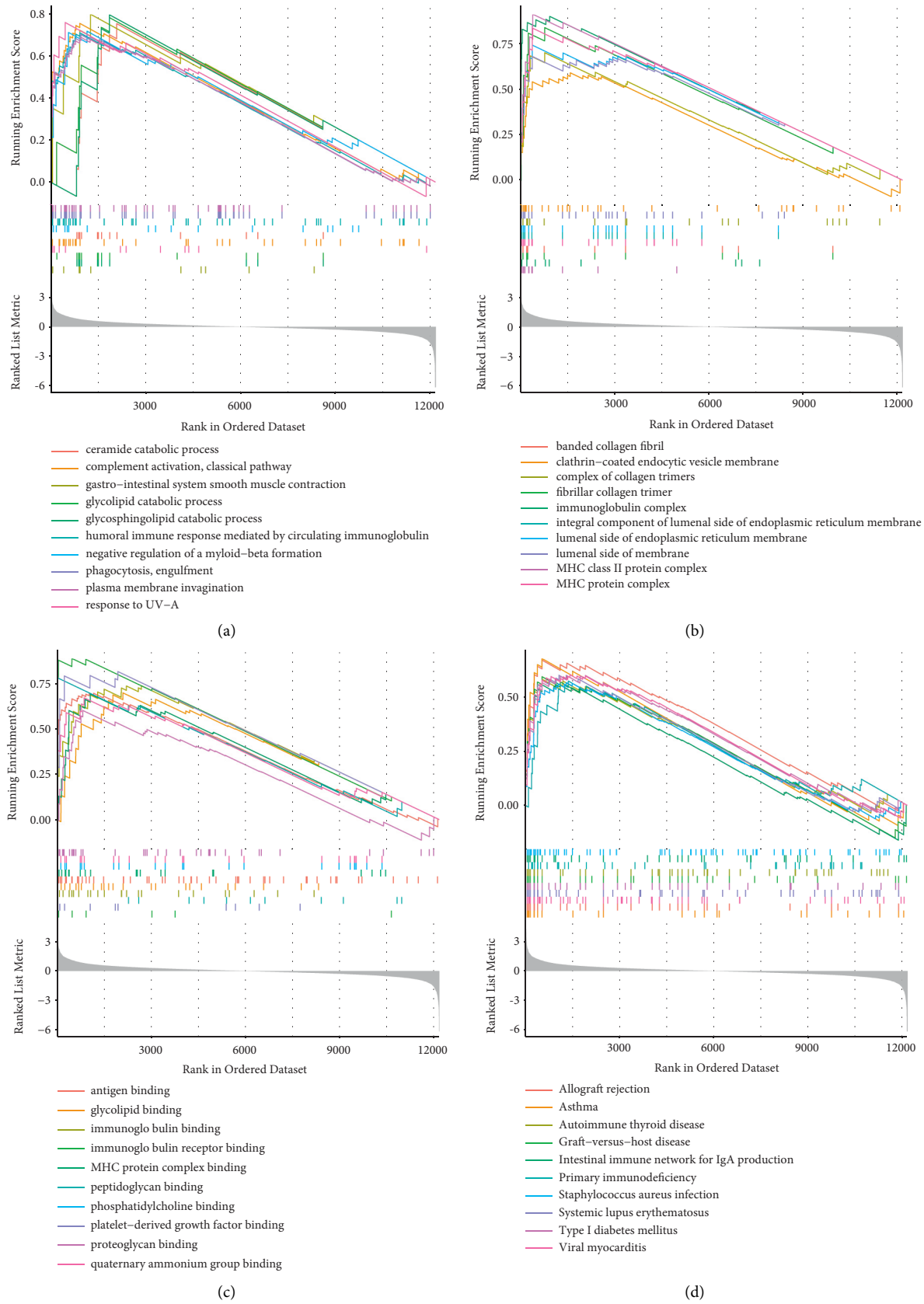

Figure 2: Gsea (a): BP; (b): CC; (c): Mf; (d): Kegg.

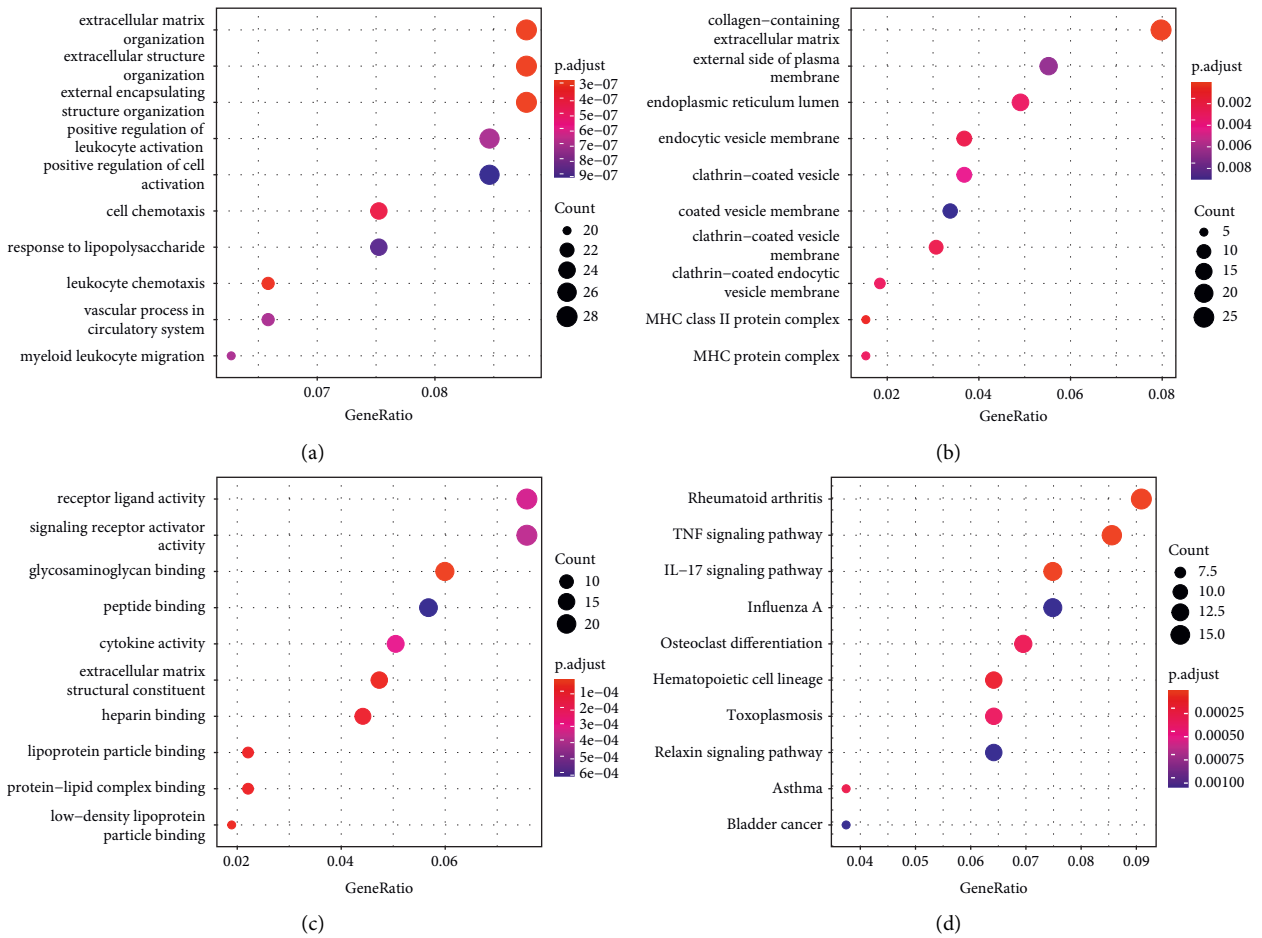

FIGURE 3: GO Enrichment Analysis (a): BP; (b): CC; (c): MF; (d): KEGG. The size of the circle represents the number of genes; darker red means a smaller corrected P -value, and darker blue means a larger corrected P -value.

3.8. Immune Cell Infiltration. To deeply study the differential expression of immune components in OA and normal groups, the CIBERSORT algorithm was adopted for evaluating the relationship of OA phenotype with immune cell infiltration. The relative proportions of immune cell subtypes are shown in cumulative histograms (Figure 8(a)). The results showed that activated mast cells, CD4 naïve T cells, resting NK cells, and neutrophils accounted for a major proportion. The correlation heat map for 22 immune cell types (Figure 8(b)) showed a significant positive correlation between monocytes and eosinophils, a positive correlation between neutrophils and monocytes, and a negative association between resting and activated NK cells, and between eosinophils and resting dendritic cells. Besides, the violin plot regarding the difference in immune cell infiltration (Figure 8(c)) presented significantly more naive CD4 T cells, resting dendritic cells as well as activated NK cells compared to the normal control group.

3.9. Correlation Analysis of Hub Genes with Infiltration Degrees of Immune Cells. According to correlation analysis, *CX3CR1* exhibited a positive correlation with activated mast cells, NK cells, gamma delta T cells, and M1 macrophages. It was adversely related to resting CD4 memory T cells, activated CD4 memory T cells, neutrophils, and activated dendritic cells (Figure 9(a)). *TLR7* was in positive correlation with M2 macrophages, activated NK cells, M1 macrophages, gamma delta T cells, and resting dendritic cells. It was negatively related to activated dendritic cells and resting NK cells (Figure 9(b)). *MYC* was positively associated with resting CD4 memory T cells, eosinophils, neutrophils, activated dendritic cells, monocytes, and activated mast cells. It showed a negative correlation between activated mast cells and CD4 naive T cells (Figure 9(c)).

3.10. Drug Analysis Results. We used three mRNAs (CX3CR1, MYC, and TLR7) in the connectivity map (CMAP) database to predict potential drugs against OA. We found a variety of drugs for the treatment of OA, including Thapsigargin, Meteneprost, Naftifine, Trimethobenzamide, and Fludrocortisone (Table 2).

3.11. GSEA of Hub Gene. The GSEA was used to identify a complete list of gene sets enriched in *CX3CR1* (Figure 10(a)), *TLR7* (Figure 10(b)), and *MYC* (Figure 10(c)). Next, we selected immune-related gene sets from the complete list for

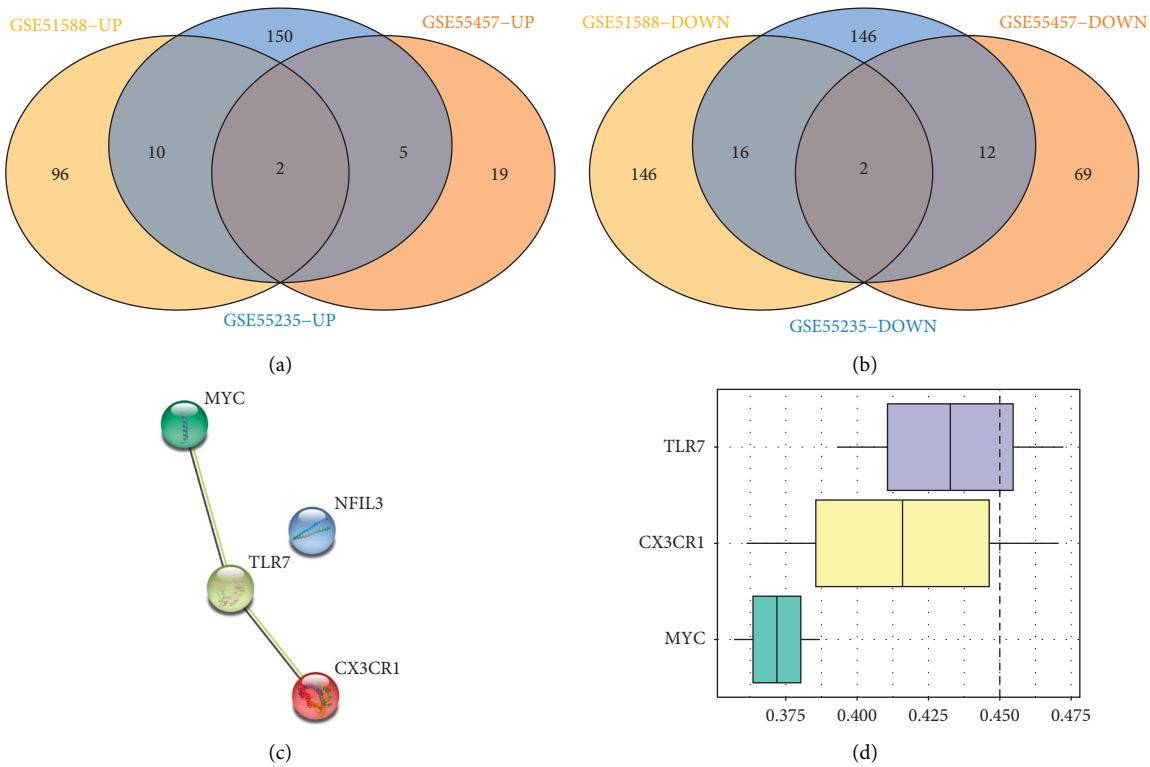

Figure 4: PPI network and Hub gene screening results. (a): Common up-regulated DGs of the three datasets; (b): Common down-regulated DGs of the three datasets; (c): PPI network of common DGs; (d): Function similarity analysis.

further analysis. Six groups of genes were enriched in samples for CX3CR1, including "interferon-alpha response," "allograft rejection," "PI3K-AKT-MTOR signaling," "inflammatory response," "IL2-STAT5 signaling," and "TNFA signaling via NF-KB" (Figure 11(a)). Similarly, "interferon-alpha response," "allograft rejection," "IL2-STAT5 signaling," and "TNFA signaling via NF-KB" were enriched in TLR7-related samples (Figure 11(b)). Furthermore, the genomes of "interferon-alpha response," "allograft rejection," "inflammatory response," "IL2-STAT5 signaling," as well as "TNFA signaling via NF-KB" were enriched in MYC-related samples (Figure 11(c)).

4. Discussion

OA is the most common disease among the elderly and causes irreversible bone erosion and cartilage destruction [8]. Due to the lack of timely and efficient treatment, OA is bound to greatly influence the functions of a patient's joints. Although multiple diagnostic methods are available for OA, clinical outcomes have remained unsatisfactory. Furthermore, no drug therapy with convincing disease-modifying effects has been approved by regulatory agencies [9,10].

We used three datasets and found three biomarkers (CX3CR1, MYC, and TLR7), of which the AUC values of CX3CL1 and TLR7 were greater than 0.9 in all three datasets with good discrimination of OA capacity between patients of OA and healthy individuals. CX3CL1 is the only member of the CX3C chemokine class that has chemoattractant and adhesion molecule properties. CX3CL1 activates c-RAF, MEK, ERK, and NFκB through the MMP-3 promoter of CX3CR1, thereby promoting the destruction of cartilage during OA [11]. CX3CR1 regulates the Wnt/β-catenin signaling, which consequently regulates the proliferation of chondrocytes and apoptosis in osteoarthropathy [12]. Toll-like receptor 7 (TLR7) is a single-stranded RNA pattern recognition receptor, and extracellular miR-21 released from synovial tissue mediates knee OA pain by activating the activation of TLR7 in surgical OA rat models [13]. TLR7 recognizes the microbes and endogenous RNAs, and nucleosides. Moreover, its aberrant activation has been implicated in numerous autoimmune diseases, including systemic lupus erythema (SLE) [14]. TLR7 detects viral RNA and can also be inappropriately activated by self-RNA, generating autoimmunity [15]. The *MYC* gene consists of three sub-branches, namely, *C-MYC*, *N-MYC*, and *L-MYC*, and is one of the most common runaway driver genes in human cancers [16]. The proto-oncogene *MYC* regulates several cellular processes, containing proliferation and metabolism. Keeping the homeostatic levels of *MYC* is vital for normal cell function; its overexpression is associated with several cancers. MYC stability can be regulated by phosphorylation, and phosphorylation signals at Thr58 degrade it, whereas Ser62 phosphorylation generates its stabilization and functional activation [17]. In addition, we used the CMAP database to identify multiple therapeutics targeting CX3CR1, MYC, and TLR7. However, their specific functions in OA and consequent side effects require further clinical

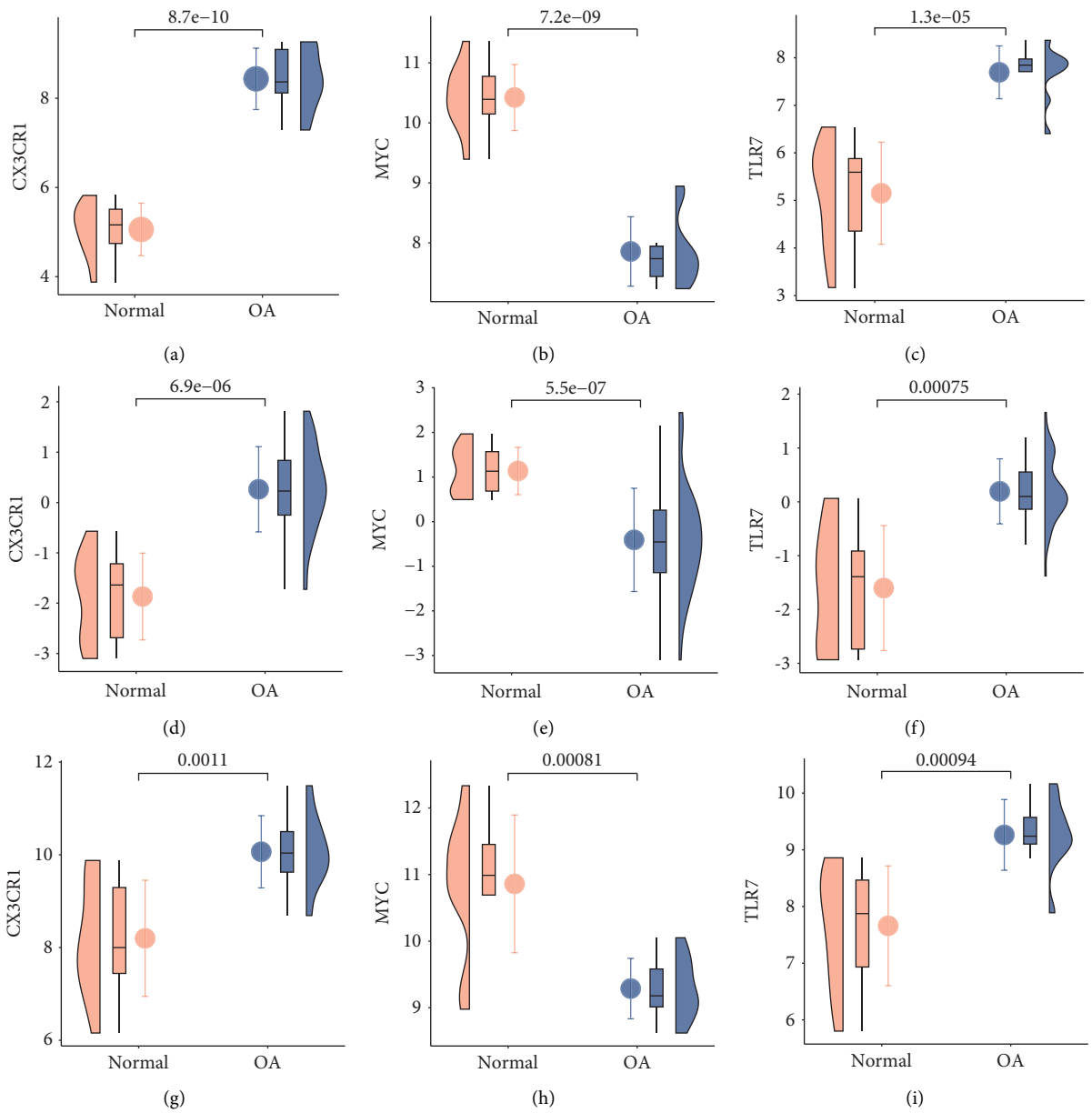

Figure 5: Expression levels of Hub genes (a): CX3CR1 expression levels in GSE55235 dataset; (b): MYC expression levels in GSE55235 dataset; (c): TLR7 expression levels in GSE55235 dataset; (d): CX3CR1 expression levels in GSE51588 dataset; (e): MYC expression levels in GSE51588 dataset; (f): TLR7 expression levels in GSE51588 dataset; (g): CX3CR1 expression levels in GSE55457 dataset; (h): MYC expression levels in GSE55457 dataset; (i): TLR7 expression levels in GSE55457 dataset.

studies. In the dataset GSE55235, the expression of CX3CR1 and TLR7 was significantly increased, and the expression of *MYC* was significantly reduced in patients with OA. The expression of the above three HUB genes was validated in the other two datasets. We found that the results of RT-qPCR validation for CX3CR1, MYC, and TLR7 were consistent with all three datasets, demonstrating the reliability of our results. Although the three studies used different gene expression analysis platforms and were conducted in highly distinct populations, the three gene levels remained unaffected. Furthermore, the above three genes were commonly expressed in different individuals. More investigations are needed to explore their levels and associated activities.

To further analyze the infiltration degree of immune cells within OA, a comprehensive evaluation of OA immune infiltration was performed using CIBERSORT. This study observed higher regulatory T cell and mast cell infiltration degrees, whereas reduced eosinophil, activated NK cell, and resting $CD4^+$ T cell infiltration degrees, were associated with OA occurrence. A prior study reported relatively high mast cell infiltration in synovial tissues from OA cases and was associated with structural damage [18]. M2 cells are closely related to inflammation, such as having anti-inflammatory activity, and being regulated by squid type II collagen, thereby promoting cartilage repair under inflammatory conditions [19, 20]. Cartilage proteoglycans located in the

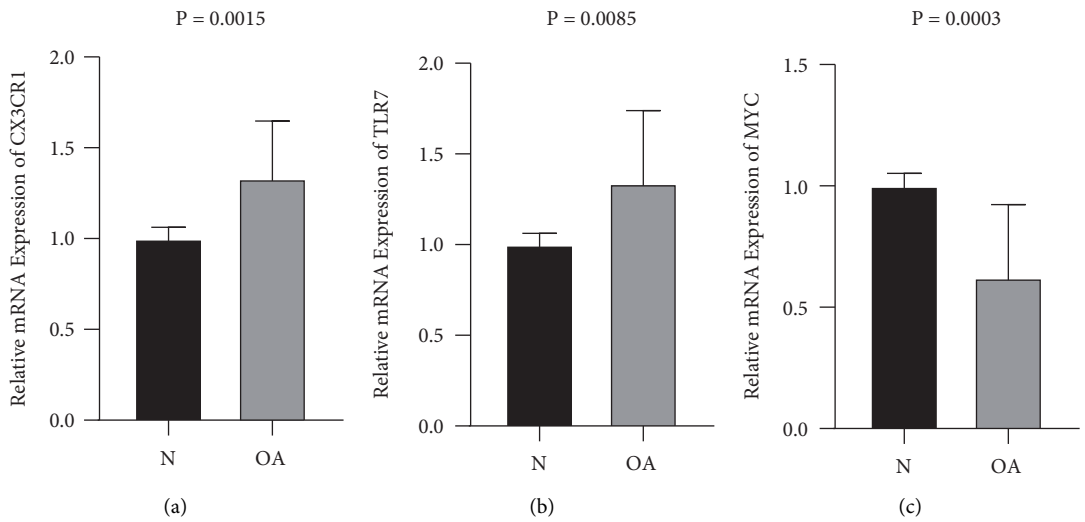

Figure 6: Relative mRNA expression of EDGs (a): Relative mRNA expression of CX3CR1; (b): Relative mRNA expression of TLR7; (c): Relative mRNA expression of Myc.

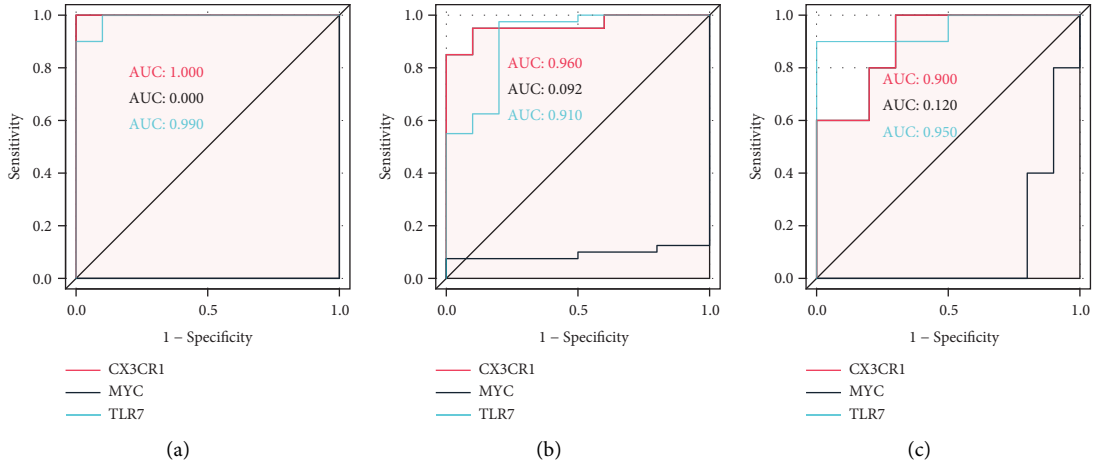

Figure 7: ROC(Receiver Operating Characteristic) curves of Hub gene. (a): ROC curves of Hub gene in GSE55235; (b): ROC curves of Hub gene in GSE51588; (c): ROC curves of Hub gene in GSE55457; A larger ROC value represents a greater ability of the key gene to distinguish between OA and normal individuals.

G1 region can induce T cell responses and promote the degradation of cartilage in patients undergoing OA [21]. Apart from that, researchers have pointed out the abundance of regulatory T cells within OA, with their levels being related to the levels of inflammatory molecules [22]. As reported by Ezawa and colleagues, memory $CD4^+$ T cells are universally accumulated in the case of local inflammatory response in joints, which are engaged in forming chronic OA [20]. Using *in vivo* experiments confirmed the important functions of neutrophils and NK cells in OA, and the interaction between them is stimulated via CXCL10/CXCR3 axis [23]. Based on this background and our findings, regulatory T cells, resting mast cells, activated NK cells, and resting $CD4^+$ memory T cells exert a vital effect on OA pathogenesis, which will become a future research focus. Nevertheless, no research currently exists regarding eosinophils' effect on OA, requiring deep experimental analysis. Furthermore, our results revealed the infiltration degrees of 22 immune cell types within OA. Regulatory T cell and activated mast cell infiltration degrees were intricately associated with activated NK cell and resting $CD4^+$ memory T cell infiltration. The infiltration degree of activated dendritic cells was in close correlation with eosinophilic infiltration. Again, specific mechanisms of the above-mentioned associations need the evidence of further experimental evidence.

An analysis of the association of CX3CR1, MYC, and TLR7 with immune cells revealed that CX3CR1 showed obvious positive relation to activated M1 macrophages, NK cells, gamma delta T cells, and activated mast cells, whereas activated $CD4^+$ memory T cells, neutrophils, resting $CD4^+$ memory T cell, and activated DCs were negatively correlated. TLR7 was significantly positively correlated with M1 macrophages, M2 macrophages, activated NK cells, resting

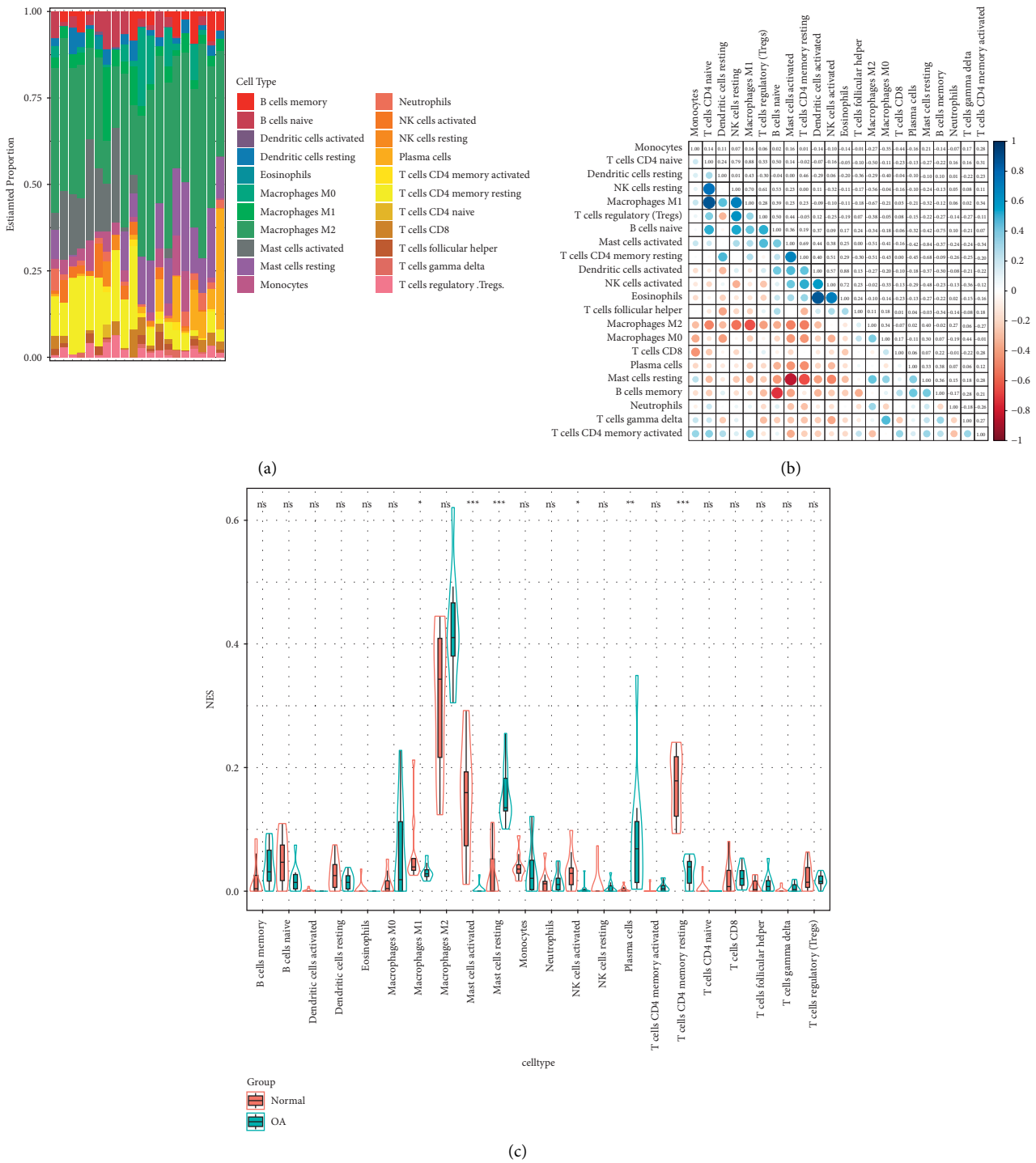

Figure 8: Immune cell infiltration analysis (a): Immune cell percentage chart; (b): Correlation diagram between immune cells; (c): Expression of immune cells in OA group and Control group.

dendritic cells, and gamma delta T cells, whereas notably adversely related to DCs and activated resting NK cells. MYC showed a significant positive relation with resting $CD4^+$ memory T cells, eosinophils, neutrophils, activated DCs, monocytes, as well as activated mast cells, whereas it was markedly adversely linked with activated mast cells and $CD4^+$ naive T cells. CX3CR1, MYC, and TLR7 are involved in immune processes. For instance, CX3CR1 is essential in airway inflammation and promotes the survival and maintenance of *T* helper cells in the inflamed lungs [24]. In addition, CX3CR1 modulates bacterial translocation, intestinal macrophage homeostasis, as well as colitis Th17 responses in mice [25]. CX3CR1 mediates the access of dendritic cells to the intestinal lumen and bacterial clearance. TLR7 induces anergic human $CD4^+$ T cells [26]. Plasmacytoid dendritic cells (pDCs) sense the viral RNA

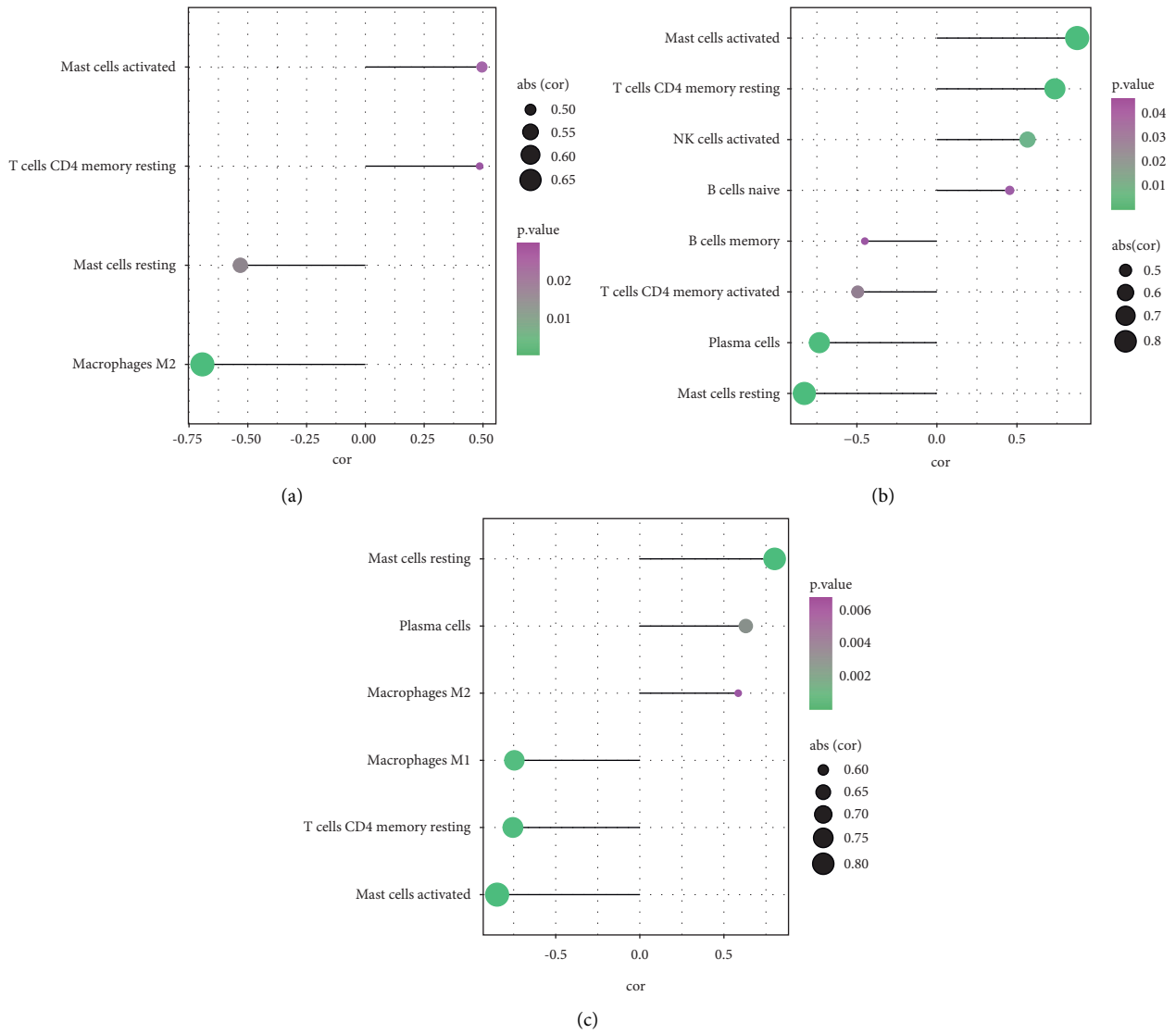

Figure 9: Correlation analysis of Hub genes and immune cells (a): Correlation analysis of CX3CR1 and immune cells; (b): Correlation analysis of MYC and immune cells; A Correlation analysis of TLR7 and immune cells; The magnitude of the absolute value of the correlation coefficient is indicated by the size of the circle. Larger P -values are indicated in dark purple, and smaller P -values are indicated in dark green.

Table 2: mRNA was used to predict potential drugs for the treatment of OA.

Cmap name	Mean	N	Enrichment	P	Specificity	Non-null percent
Thapsigargin	−0.828	3	−0.977	0.00004	0.0129	100
Meteneprost	−0.781	4	−0.853	0.00088	0	100
Naftifine	−0.78	4	−0.884	0.0004	0	100
Trimethobenzamide	−0.702	5	−0.779	0.00096	0.0067	100
Fludrocortisone	−0.371	8	−0.648	0.00092	0.0493	50

through toll-like receptor 7 (TLR7), leading to the formation of self-adhesive pDC–pDC clusters and yield type I interferons. Besides, such cell adhesion can enhance the production of type I interferons [27]. Autophagy exerts a vital function in TLR7-mediated activation of B cells to induce SLE by delivering RNA ligands to endosomes, where innate immune receptors are located [28]. The MYC pathway not only determines cancer cell pathophysiology but also suppresses host immune responses [29]. MYC is known to regulate antitumor immune responses through CD47 and PD-L1. In addition, c-Myc is required for maintaining homeostasis and transient activation of regulatory T cells [16]. Studies have reported significant functions of NK cells and mast cells in OA. Because the polarization of M1

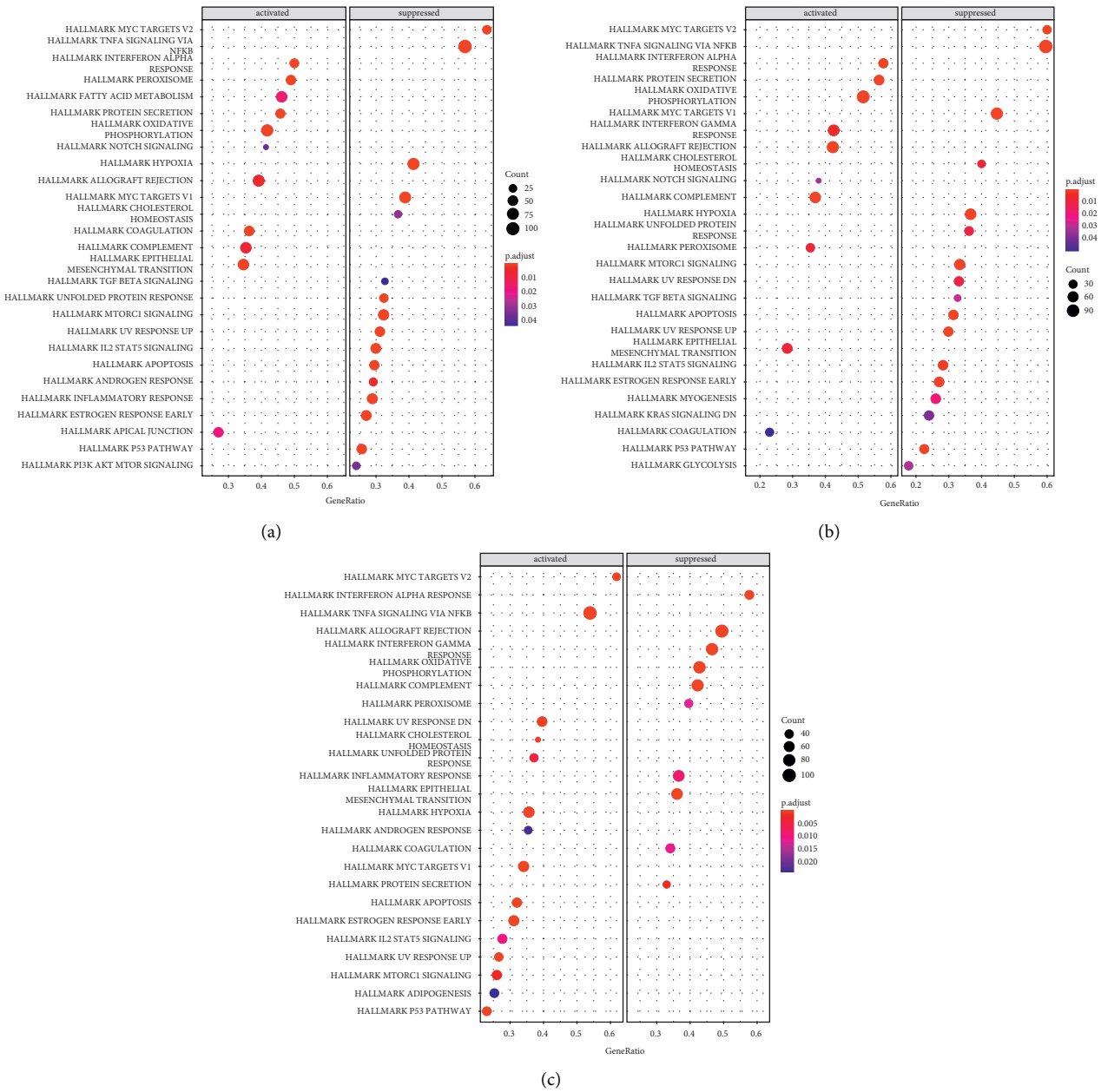

Figure 10: GSEA analysis of HUB genes (a): Complete GSEA results for CX3CR1; (b): Complete GSEA results for MYC; (c): Complete GSEA results for TLR7; The number of genes is indicated by the size of the circle; smaller corrected *P*-values are indicated in dark red, and larger corrected *P*-values are indicated in dark blue.

macrophages within synovium deteriorates OA [30], It can be speculated that CX3CR1 elevated the number of NK cells and naive $CD4^+$ T cells or decreased the number of M1 macrophages, whereas MYC and TLR7 decreased the number of mast cells related to OA occurrence. These hypotheses need future studies to elucidate the complicated gene-immune cell interactions.

Furthermore, single-gene GSEA analysis revealed that "interferon-alpha response," "allograft rejection," "PI3K-AKT-MTOR signaling," "inflammatory response," "IL2-STAT5 signaling." and "TNFA signaling via NFK-B" were involved in the OA immune process. Interferons can induce or exacerbate autoimmune diseases due to their immunomodulatory properties. For example, alpha-interferon can induce severe immune thrombocytopenia in those suffering from chronic hepatitis C. Moreover, probiotics that modulate the mTOR/PI3K/Akt signaling pathway can activate immune responses. PI3K and mTOR positively regulate the activation of immune cells of neutrophils and mast cells. In addition, T-cell receptors regulate the expression of Foxp3 through the PI3K/Akt/mTOR signaling network, thereby participating in immune processes. Dying neutrophils are known to produce anti-inflammatory effects by modulating surrounding cellular responses, especially macrophages that release inflammatory cytokines. Several cellular components of both adaptive and innate immune

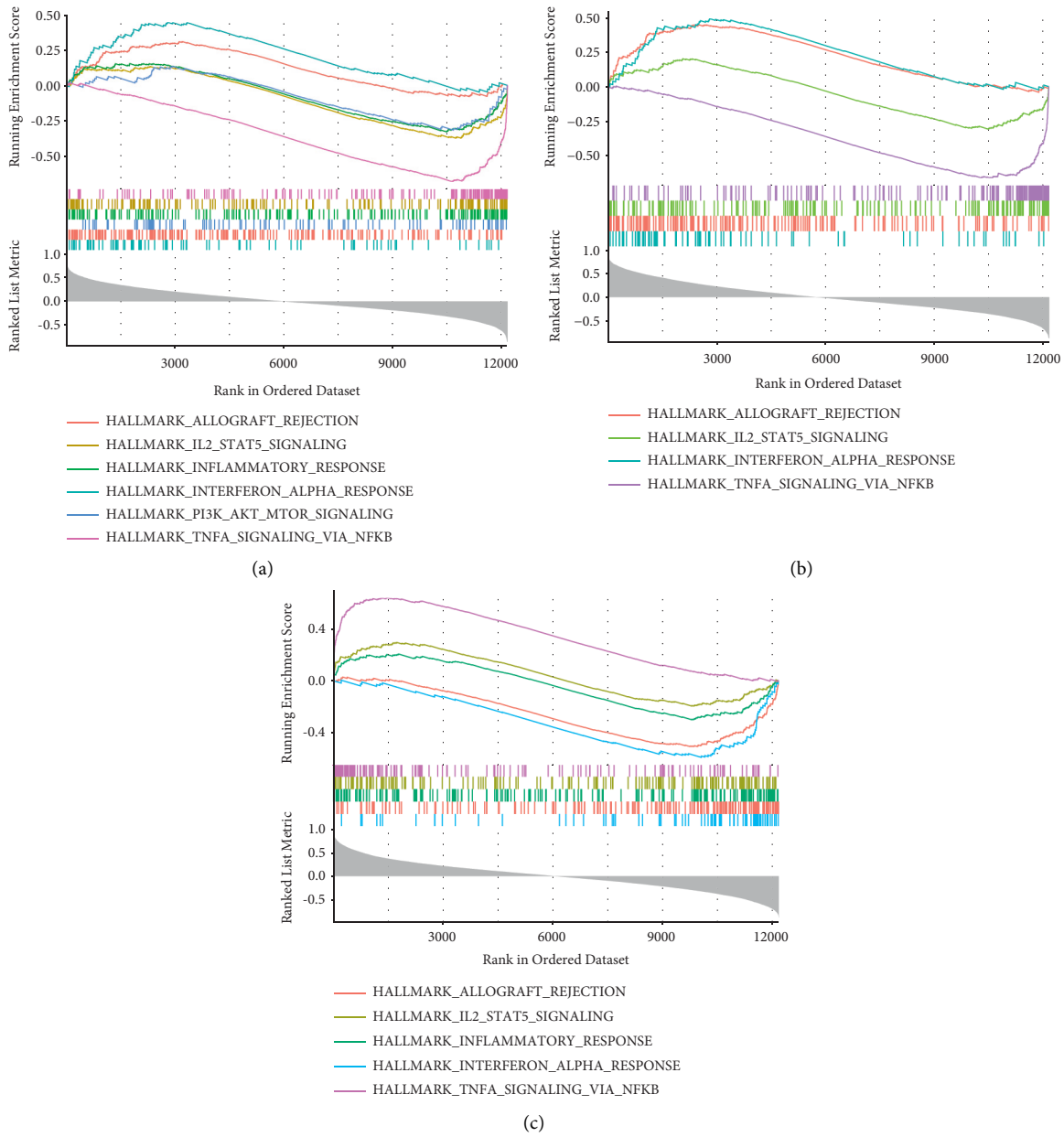

Figure 11: Immune-related pathways of Hub genes (a): Immune-related GSEA results of CX3CR1 (b): Immune-related GSEA results of MYC (c): Immune-effective GSEA results of TLR7.

responses are present at the sites of tissue inflammation. Targeted delivery of IL2 to the tumor stroma can enhance the effects of immune checkpoint inhibitors by preferentially activating NK and $CD8^+$ T cells. Furthermore, the tetramerization of STAT5 is important for cytokine responses and normal immune function, establishing its vital function *in vivo*. TTP53 GOF mutants up-regulate the expression of CC motif chemokine ligand 2 (CCL2) and TNFA via the NFκB signaling pathway, thereby increasing microglia-and monocyte-derived immunity cell infiltration. The complex functions of CX3CR1, MYC, and TLR7 and these pathways in OA require elucidation.

Our study had certain limitations. First, the data used in the current work were acquired from public databases, with no way to validate the reliability of the data. Second, this study explored the association of OA markers with immune cells. Meanwhile, the reliability of this result in OA needs to be experimentally verified. Third, we did not deeply experimentally investigate the exact mechanism of the hub gene identified in OA.

5. Conclusion

Our study identified three hub genes, their relationship with the immune microenvironment, and certain functional biological pathways associated with immune response, inflammatory response, and cytokines related to O pathogenic mechanism. In addition, potential drugs for the treatment of

OA were discovered. Although the obtained results offer new insights into OA genesis and progression, the exact molecular mechanism and functional pathway of HUB genes in OA still require to be deeply investigated.

Data Availability

The data used to support this manuscript are included within this manuscript.

Additional Points

1. In this study, we discovered that CX3CR1, MYC, and TLR7 could be used as a new diagnostic marker by bioinformatics methods and RT-qPCR, which provides a new direction for studying the pathogenesis of OA. 2. Using drug information from the CMAP database, we have identified multiple drugs that have effects on CX3CR1, MYC, and TLR7, providing potential therapeutic options for the treatment of OA. 3. Using GSEA, we have discovered multiple pathways involved in CX3CR1, MYC, and TLR7 in OA, further enriching our study of them.

Ethical Approval

These authors are responsible for all aspects of the work and for ensuring that issues related to the accuracy or completeness of any part of the work are properly investigated and resolved.

Conflicts of Interest

All authors have no conflicts of interest to declare.

Authors' Contributions

Yang Hu, Yinteng Wu, and Fu Gan contributed equally to this work.

Acknowledgments

Thanks are due to the experimental equipment support from the First Affiliated Hospital of Guangxi Medical University. This experiment was supported by the Guangxi Natural Science Foundation (2017JJA10088).

References

[1] W. Liao, Z. Li, H. Zhang, J. Li, K. Wang, and Y. Yang, "Proteomic analysis of synovial fluid as an analytical tool to detect candidate biomarkers for knee osteoarthritis," *International Journal of Clinical and Experimental Pathology*, vol. 8, no. 9, pp. 9975–9989, 2015.

[2] E. Sanchez-Lopez, R. Coras, A. Torres, N. E. Lane, and M. Guma, "Synovial inflammation in osteoarthritis progression," *Nature Reviews Rheumatology*, vol. 18, no. 5, pp. 258–275, 2022.

[3] S. Shen, Y. Wu, J. Chen et al., "CircSERPINE2 protects against osteoarthritis by targeting miR-1271 and ETS-related gene," *Annals of the Rheumatic Diseases*, vol. 78, no. 6, pp. 826–836, 2019.

[4] Z. Chen, Y. Ma, X. Li, Z. Deng, M. Zheng, and Q. Zheng, "The immune cell landscape in different anatomical structures of knee in osteoarthritis: a gene Expression-Based study," *BioMed Research International*, vol. 2020, Article ID 964707, 21 pages, 2020.

[5] B. E. M. Elsadek, A. A. Abdelghany, M. A. Abd El-Aziz et al., "Validation of the diagnostic and prognostic values of ADAMTS5 and FSTL1 in osteoarthritis rat model," *Cartilage*, vol. 13, pp. 1263S–1273S, 2021.

[6] G. R. Oliver, S. N. Hart, and E. W. Klee, "Bioinformatics for clinical next generation sequencing," *Clinical Chemistry*, vol. 61, no. 1, pp. 124–135, 2015.

[7] A. M. Newman, C. L. Liu, M. R. Green et al., "Robust enumeration of cell subsets from tissue expression profiles," *Nature Methods*, vol. 12, no. 5, pp. 453–457, 2015.

[8] A. Bhatia, P. Peng, and S. P. Cohen, "Radiofrequency procedures to relieve chronic knee pain: an Evidence-Based narrative review," *Regional Anesthesia and Pain Medicine*, vol. 41, no. 4, pp. 501–510, 2016.

[9] V. Gkretsi, T. Simopoulou, and A. Tsezou, "Lipid metabolism and osteoarthritis: lessons from atherosclerosis," *Progress in Lipid Research*, vol. 50, no. 2, pp. 133–140, 2011.

[10] F. C. Grandi and N. Bhutani, "Epigenetic therapies for osteoarthritis," *Trends in Pharmacological Sciences*, vol. 41, no. 8, pp. 557–569, 2020.

[11] S. M. Hou, C. H. Hou, and J. F. Liu, "CX3CL1 promotes MMP-3 production via the CX3CR1, c-Raf, MEK, ERK, and NF-κB signaling pathway in osteoarthritis synovial fibroblasts," *Arthritis Research and Therapy*, vol. 19, no. 1, 2017.

[12] Y. Sun, F. Wang, X. Sun, X. Wang, L. Zhang, and Y. Li, "CX3CR1 regulates osteoarthrosis chondrocyte proliferation and apoptosis via Wnt/β-catenin signaling," *Biomedicine & Pharmacotherapy*, vol. 96, pp. 1317–1323, 2017.

[13] N. Hoshikawa, A. Sakai, S. Takai, and H. Suzuki, "Targeting extracellular miR-21-TLR7 signaling provides Long-Lasting analgesia in osteoarthritis," *Molecular Therapy—Nucleic Acids*, vol. 19, pp. 199–207, 2020.

[14] S. Tojo, Z. Zhang, H. Matsui et al., "Structural analysis reveals TLR7 dynamics underlying antagonism," *Nature Communications*, vol. 11, no. 1, 2020.

[15] S. I. Saitoh, F. Abe, A. Kanno et al., "TLR7 mediated viral recognition results in focal type I interferon secretion by dendritic cells," *Nature Communications*, vol. 8, no. 1, 2017.

[16] M. J. Duffy, S. O'Grady, M. Tang, and J. Crown, "MYC as a target for cancer treatment," *Cancer Treatment Reviews*, vol. 94, Article ID 102154, 2021.

[17] B. N. Devaiah, J. Mu, B. Akman et al., "MYC protein stability is negatively regulated by BRD4," *Proceedings of the National Academy of Sciences*, vol. 117, no. 24, pp. 13457–13467, 2020.

[18] B. J. E. de Lange-Brokaar, M. Kloppenburg, S. N. Andersen et al., "Characterization of synovial mast cells in knee osteoarthritis: association with clinical parameters," *Osteoarthritis and Cartilage*, vol. 24, no. 4, pp. 664–671, 2016.

[19] M. Dai, B. Sui, Y. Xue, X. Liu, and J. Sun, "Cartilage repair in degenerative osteoarthritis mediated by squid type II collagen via immunomodulating activation of M2 macrophages, inhibiting apoptosis and hypertrophy of chondrocytes," *Biomaterials*, vol. 180, pp. 91–103, 2018.

[20] H. Zhang, C. Lin, C. Zeng et al., "Synovial macrophage M1 polarisation exacerbates experimental osteoarthritis partially through R-spondin-2," *Annals of the Rheumatic Diseases*, vol. 77, no. 10, pp. 1524–1534, 2018.

[21] H. de Jong, S. E. Berlo, P. Hombrink et al., "Cartilage proteoglycan aggrecan epitopes induce proinflammatory autoreactive T-cell responses in rheumatoid arthritis and osteoarthritis," *Annals of the Rheumatic Diseases*, vol. 69, pp. 255–262, 2009.

[22] J. Xia, Z. Ni, J. Wang, S. Zhu, and H. Ye, "Overexpression of lymphocyte activation gene-3 inhibits regulatory t cell responses in osteoarthritis," *DNA and Cell Biology*, vol. 36, no. 10, pp. 862–869, 2017.

[23] G. Benigni, P. Dimitrova, F. Antonangeli et al., "CXCR3/CXCL10 axis regulates neutrophil-NK cell Cross-Talk determining the severity of experimental osteoarthritis," *The Journal of Immunology*, vol. 198, no. 5, pp. 2115–2124, 2017.

[24] C. Mionnet, V. Buatois, A. Kanda et al., "CX3CR1 is required for airway inflammation by promoting T helper cell survival and maintenance in inflamed lung," *Nature Medicine*, vol. 16, no. 11, pp. 1305–1312, 2010.

[25] J. H. Niess, S. Brand, X. Gu et al., "CX3 CR1-Mediated dendritic cell access to the intestinal lumen and bacterial clearance," *Science*, vol. 307, no. 5707, pp. 254–258, 2005.

[26] M. Dominguez-Villar, A. S. Gautron, M. de Marcken, M. J. Keller, and D. A. Hafler, "TLR7 induces anergy in human $CD4^+$ T cells," *Nature Immunology*, vol. 16, no. 1, pp. 118–128, 2015.

[27] A. M. Krieg, "The toll of too much TLR7," *Immunity*, vol. 27, no. 5, pp. 695–697, 2007.

[28] C. G. Weindel, L. J. Richey, S. Bolland, A. J. Mehta, J. F. Kearney, and B. T. Huber, "B cell autophagy mediates TLR7-dependent autoimmunity and inflammation," *Autophagy*, vol. 11, no. 7, pp. 1010–1024, 2015.

[29] S. C. Casey, L. Tong, Y. Li et al., "MYC regulates the antitumor immune response through CD47 and PD-L1," *Science*, vol. 352, no. 6282, pp. 227–231, 2016.

[30] Y. J. Deng, E. H. Ren, W. H. Yuan, G. Z. Zhang, Z. L. Wu, and Q. Q. Xie, "GRB10 and E2F3 as diagnostic markers of osteoarthritis and their correlation with immune infiltration," *Diagnostics*, vol. 10, no. 3, 2020.

Hindawi
Evidence-Based Complementary and Alternative Medicine
Volume 2022, Article ID 4295802, 18 pages
https://doi.org/10.1155/2022/4295802

Review Article

Plant Bioactives in the Treatment of Inflammation of Skeletal Muscles: A Molecular Perspective

Dipanjan Karati,[1] **Ryan Varghese**,[1] **K. R. Mahadik**,[1] **Rohit Sharma**,[2] **and Dileep Kumar**[1]

[1]*Poona College of Pharmacy, Bharati Vidyapeeth (Deemed to be) University, Pune, Maharashtra 411038, India*
[2]*Department of Rasa Shastra and Bhaishajya Kalpana, Faculty of Ayurveda, Institute of Medical Sciences, Banaras Hindu University, Varanasi 221005, Uttar Pradesh, India*

Correspondence should be addressed to Rohit Sharma; rohitsharma@bhu.ac.in and Dileep Kumar; dileep.0@gmail.com

Received 17 December 2021; Revised 28 April 2022; Accepted 24 June 2022; Published 20 July 2022

Academic Editor: Smail Aazza

Skeletal muscle mass responds rapidly to growth stimuli, precipitating hypertrophies (increased protein synthesis) and hyperplasia (activation of the myogenic program). For ages, muscle degeneration has been attributed to changes in the intracellular myofiber pathways. These pathways are tightly regulated by hormones and lymphokines that ultimately pave the way to decreased anabolism and accelerated protein breakdown. Despite the lacunae in our understanding of specific pathways, growing bodies of evidence suggest that the changes in the myogenic/regenerative program are the major contributing factor in the development and progression of muscle wasting. In addition, inflammation plays a key role in the pathophysiology of diseases linked to the failure of skeletal muscles. Chronic inflammation with elevated levels of inflammatory mediators has been observed in a spectrum of diseases, such as inflammatory myopathies and chronic obstructive pulmonary disease (COPD). Although the pathophysiology of these diseases varies greatly, they all demonstrate sarcopenia and dysregulated skeletal muscle physiology as common symptoms. Medicinal plants harbor potential novel chemical moieties for a plenitude of illnesses, and inflammation is no exception. However, despite the vast number of potential antiinflammatory compounds found in plant extracts and isolated components, the research on medicinal plants is highly daunting. This review aims to explore the various phytoconstituents employed in the treatment of inflammatory responses in skeletal muscles, while providing an in-depth molecular insight into the latter.

1. Introduction

Skeletal muscles account for about 40% of the body's mass and are essential for performing normal physiological activities. This necessitates the need for maintaining skeletal muscle growth, metabolism, and contractile performance throughout life for total body health. However, the decline in muscle performance is frequently associated with increasing age and other morbid conditions [1].

In both developed and emerging countries, noncommunicable diseases are on the rise, and musculoskeletal disorders (MSDs) are no exception [2]. The global burden of MSDs is approximately 1.7 billion individuals, which precedes both disability and even death [3].

In response to the rapid muscular damage and acute exercise stimulation, the skeletal muscle tends to change its size, shape, and/or function, thereby demonstrating remarkable flexibility. Since time immemorial, exercise has been reported to demonstrate a substantial increase in muscle mass and function (reviewed in [4–6]). However, the elderly and patients with muscle morbidities are restrained due to their ailments and physical limitations. This has further facilitated the development of nonexercise and pharmacotherapeutic interventions as a hotspot for research on MSDs.

In morbid conditions such as Type-2 Diabetes Mellitus and obesity, insulin resistance in the skeletal muscles is a major contributor to impaired whole-body glucose clearance. Since antiquity, plants have been a rich source of pharmacologically active phytochemicals that have been employed in a spectrum of ailments. For example, the ethanolic extract of Russian tarragon (*Artemisia dracunculus*

L.) has been studied to be a potent blood sugar reducing agent, which concurrently improves insulin sensitivity in congenital as well as synthetically persuaded diabetic murine models [7, 8]. In addition, the tannase-converted green tea extract could potentially be utilized in the treatment regimen of sarcopenia, among other MSDs [9]. Despite the fact that western medicine (allopathy) and surgical interventions have gained acceptance in recent years, the masses still resort to plant-based medicine as it is highly efficacious, considered safe, and devoid of harmful side effects [10]. Researchers and physicians across the globe have developed an armamentarium of medicinal herbs that could potentially alleviate the symptoms associated with MSD-related disorders.

While several articles emphasise on the role of phytochemicals and plant extracts in the alleviation of symptoms associated with MSDs, the prime focus of this article is to summarize and critically evaluate recent studies, findings, and conclusions.

2. Insights into Musculoskeletal Disorders

Skeletal muscles make up about 40% of a person's total weight and are essential for good health. Skeletal muscles are in charge of keeping your posture and allowing you to perform your regular tasks. They help with important biological functions, including nutrition sensing, energy metabolism, core temperature regulation, and organ and bone protection. Muscle function deteriorates with age, resulting in decreased mobility. Fall-related injuries, impairment, loss of independence and a considerable increase in mortality in the elderly can all result. Sarcopenia is a term used to describe the progressive loss of muscle mass and function in the elderly and chronically ill due to muscular fiber atrophy and loss. It plays a significant role in the loss of independence, disability, the need for long-term care, and overall mortality. Sarcopenia is a complicated disease with little knowledge of its etiology. MSDs are a group of diseases that primarily affect the bones, joints, muscles, and connective tissues. These ailments are often reported to cause pain and loss of function and are among the most expensive and disabling conditions in the United States [11]. These MSDs could be a product of either genetic predisposition, congenital illness, or an acquired pathological process. Growing bodies of evidence have also associated their pathophysiology with infection, inflammation, degeneration, trauma, impaired development, neoplasia, as well as vascular and/or toxic/metabolic derangements [12]. With over 1.7 billion individuals being affected by MSDs globally, their disability and mortality rates pose a great health concern [2, 3]. The World Health Organization (WHO) ranks MSDs, such as arthritis, osteoarthritis, bone fractures, and back and neck discomfort, as the second most common cause of debility across the globe [13]. Other major MSDs include chronic lower back pain, osteoarthritis of the hip, knee, wrist, and hand, inflammatory arthropathies such as rheumatoid arthritis and psoriatic arthritis, and arthropathies of other joints [12].

Rheumatoid arthritis is a chronic autoimmune disorder characterized by polyarthralgia and joint inflammation. Antibodies that target self-neoepitopes are triggered by inflammatory cascade mechanisms. These mechanisms are allied by chronic arthritic assaults, which further result in the targeting of self-neoepitopes. The arsenal of macrophages, defense immunocytes, and biomarkers elicited in response to the self-epitopes have paved the way for the development of innovative theranostic modalities. These curative methods serve as effective suppressors of these cells and trigger antibodies, thereby curbing the disease progression as well as providing a deeper understanding of the disease etiopathophysiology [14].

Psoriatic arthritis is a chronic inflammatory condition primarily affecting the entheses, joints, and the spine [12]. The inflammatory effect is also profound in other tissues such as nail involvement and dactylitis, where it occurs in concurrence with psoriatic scaly patches (reviewed in [15]). In most cases, skin indications often precede the onset of arthritis; however, in some people, their symptoms appear at the same time. In about 10–15% of the cases, arthritis precedes the onset of these inflammatory patches [16, 17].

Another major social debility is muscular atrophy, which is a decrease in muscle mass and power, as well as the ability to regenerate. This condition could be precipitated by a plenitude of conditions, including blast distress, cachexia, chronic kidney disease (CKD), diabetes, high-speed accidents, immobility, obesity, preexisting orthopedic conditions, malnutrition, metabolic acidosis, and sepsis, to name a few [18]. However, despite an exhaustive list of potential causes, muscular atrophy is often attributed to an imbalance between the catabolic and anabolic signaling pathways [19]. Thus, with metabolic problems, changing lifestyles, and ageing, muscular atrophy poses a bigger health concern than ever before [20].

Conditions like sarcopenia that forms the quintessence of most MSDs is characterized by a reduction of muscle mass protein, which eventually culminates into a loss of muscle function [21]. It is often marked by a steady and extensive diminution of skeletal muscle potency, which often climaxes with physical impairment and muscle immobility [22]. It is often conspicuous in the elderly cohorts, as it is strongly corroborated by frailty development [21].

The current understanding of muscle damage and pain couples muscle damage and associated pain with the generation of reactive oxygen species (ROS), oxidative stress, and inflammation [23]. Mounting bodies of evidence have substantiated the utility of several plants, plant extracts, and phytochemicals as pharmacotherapeutic interventions to scavenge ROS and ameliorate inflammation, thereby intercepting the pathogenesis of these MSDs.

3. Signalling Pathways and Skeletal Muscle Homeostasis

In response to various environmental stresses, the skeletal muscles trigger a spectrum of signaling pathways that facilitate the latter to remodel and maintain muscular action. One of the quintessential pathways that are necessary for self-renewal and differentiation of adult muscle cells is the Wnt scheme. Recent studies have also elucidated its

importance not only in the proliferation of adult stem cells but also in the improvement of embryonic muscle cells [24]. Wnt signaling is an enduring and evolutionarily conserved system proven to be essential for adipose tissue formation. This path exerts its influence on a variety of biological processes, including muscle tissue development and the creation of the motor neuron-muscle synapse. Wnt signaling influences myogenesis by stimulating differentiation at early developmental stages. However, interception of this signaling would result in poor and deformed skeletal muscle formation. Wnt signaling also regulates the location of several proteins vital for synapse formation as well as precise muscle contraction throughout the maturation of the neuromuscular junction (NMJ). This signaling also plays a profound role in muscle fibrosis because it interacts with other profibrotic molecules such as connective tissue growth factor (CTGF) and transformative growth factor-β (TGF-β) [25].

Another key signaling effector involved in skeletal muscle development is the fibroblast growth factor (FGF) and the ubiquitin-proteasome pathway. The loss of FGFR1 signaling results in decreased skeletal mass, thereby disrupting the myofiber structure [26]. While some interventions have a favorable impact on the development of skeletal muscles, others may have an antagonistic effect. The induction of muscular atrophy is an interplay of various transcriptional mechanisms, which catalyze the degradation as well as the production of new proteins from the old ones [27, 28]. In addition, the expression of MurF1 and MAFbx/Atrogin-1 is considerably enhanced in the atrophies of skeletal muscles [29–32]. The FoxO transcription factor family, which is phosphorylated by Akt, is involved in the suppression of MuRF1 and MAFbx/Atrogin-1 [32, 33]. FoxO transcription factors, such as FoxO1 and FoxO3, translocate to the nucleus after being dephosphorylated and upregulating MurF1 and MAFbx/Atrogin-1 [32, 33].

In addition, Insulin-like Growth factor (IGF-1) has a profound effect on myoblast differentiation and proliferation of skeletal muscles. IGF-1 also stimulates the phosphatidylinositol-3 kinase (PI3K)/Akt and other downstream targets like mTOR, that facilitate the upregulation of protein synthesis, further resulting in the hypertrophy of skeletal muscle cells [34, 35].

Another signaling pathway involved in atrophy of the skeletal muscles is nuclear factor-kappa B (NF-κB). In the cultured C2C12 myoblasts without NF-κB, the addition of TNF-α mediated the suppression of muscle development [36]. Similarly, through the regulation of MuRF1, the overexpression of NF-κB endorsed an acute atrophy of the skeletal muscles. Upon injury, the adult skeletal muscle triggers a variety of important inflammatory mediators, which aid in controlling the healing environment to promote faster healing. However, some of the inflammatory cytokines have been attributed to both physiological as well as pathological activities [37–39]. These cytokines have been enlisted in Figure 1.

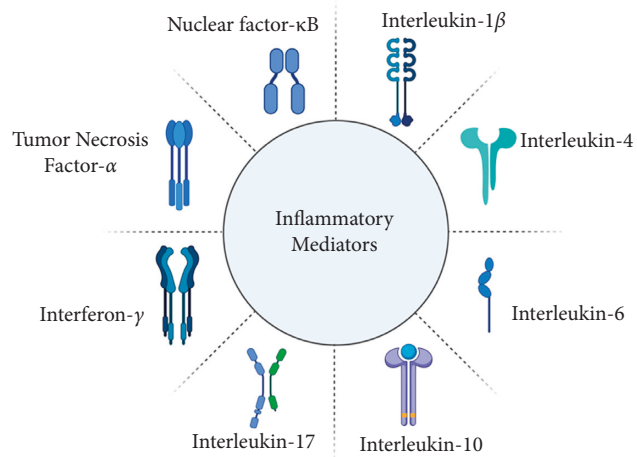

Figure 1: Inflammatory mediators involved in the pathophysiology of musculoskeletal diseases.

4. Phytomedicine in the Treatment of MSDs

Since antiquity, plants have been a rich source of pharmacologically active phytochemicals and therapeutic moieties. They have been used as a safe and efficient supplementary therapy for a plethora of disease processes [40–42]. These herbs not only increase the blood circulation but also repair the damaged skeletal tissue, thereby alleviating skeletal muscle inflammation and MSDs [7]. Over the years, several botanicals and medicinal herbs have been found to positively affect the treatment of skeletal muscle problems, including muscle thinning and muscle atrophy, thereby improving the treatment outcome [43]. The production of ROS, followed by inflammatory cascade and oxidative stress, often precedes the impairment of the muscle tissue and causes muscle ache [12]. The rationale behind the administration of herbal drugs as a curative for skeletal muscle inflammation among most MSDs is elucidated in Figure 2.

5. Role of Phytotherapy in the Management of Skeletal Inflammation in MSDs

With a paradigm shift in the dietary preferences, nature of work, and lifestyles of individuals, the prevalence of skeletal muscle inflammation and MSDs is on the rise. With this increment in MSDs, there is a pressing need for dietary management to alleviate the symptoms associated with the former. Nonetheless, the prevention strategy and medication regimen would largely be specific to the MSD, taking into account the rate of progression, comorbidities, and characteristics of the individual. However, the consumption of medicinal plants could potentially prevent muscle wasting and supplement the muscles with essential nutrients, while various bioactives could intercept the signaling pathways that progress the disease. Some of the prominent medicinal herbs employed for the treatment of the latter have been elucidated below.

5.1. Coffea arabica. The *Coffea arabica,* or coffee plant, is a subset of the family *Rubiaceae* and genus *Coffea*. It is generally a woody perennial tree that thrives at higher altitudes. Although caffeine is the major component of

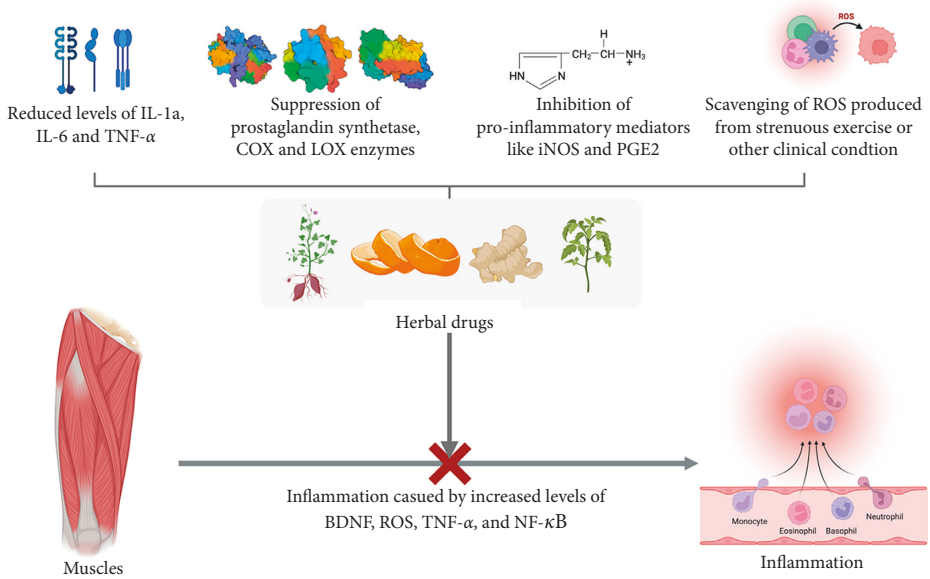

Figure 2: Mechanism of medicinal herbs and phytochemicals in the inhibition of skeletal muscle inflammation. (BDNF = brain-derived neurotropic factor; COX = cyclooxygenase; IL = interleukin; iNOS = inducible nitric oxide synthase; LOX = lipoxygenase; NF-κB = nuclear factor-κB; PGE2 = prostaglandin E2; ROS = reactive oxygen species; TNF-α = tumor necrosis factor-α).

C. arabica, it also contains dimethylxanthines, paraxanthine, theobromine, and theophylline, which are metabolized in the liver by CYP1A2 enzymes [44]. These phytochemicals demonstrate a spectrum of activities, ranging from boosting sensations to enhancing focus [45]. Other trace compounds present in coffee include polyphenols such as hydroxyhydroquinone (HHQ) and chlorogenic acids, among others [44].

The administration of *C. arabica* extract has been associated with a plummeting in levels of interleukins IL-1a, IL-6, and TNF-α, which have been attributed to grip strength and muscle mass. The results from an *in-vitro* murine model demonstrated an increment in the count of proliferating tissues and enhanced nucleic acid synthesis via the Akt signaling pathway, after administration of *C. arabica* extract. The latter also increased the activation of satellite cells while concurrently lowering inflammatory cytokines, thereby validating its antiinflammatory properties. These immunomodulatory properties and antioxidant potential are attributed to compounds like kahweol [46].

5.2. Zingiber officinale. Ginger (*Zingiber officinale*) is a subset of the *Zingiberaceae* family and is predominantly found in traditional medicine systems. It is generally cultivated in southeast Asia and then exported globally, to be employed both as a spice and a condiment [47]. The utility of ginger both as a dietary supplement and an herbal medicine is attributed to its rich phytochemistry (reviewed in [48]). Owing to its potential antioxidative and antiinflammatory properties, it finds its utility in antiageing and degenerative disorders such as arthritis and rheumatism. Additionally, its antimicrobial effect also helps in the treatment of sepsis-induced MSDs [48–52]. A recent study reported a moderate reduction in muscular discomfort progression for one to two days, when they consumed ginger 24 hours after their exercise session. However, the consumption of heat-triggered ginger did not potentiate this activity [53]. The gingerol, shogaol, and other chemical moieties present in ginger have been studied to inhibit prostaglandin and leukotriene biosynthesis via suppression of the prostaglandin synthetase and 5-lipoxygenase enzymes (reviewed in [52]). In addition, they also inhibit the synthesis of other pro-inflammatory cytokines, including IL-1, IL-8, and TNF-α [54, 55]. A study conducted by Pan et al. concluded that shogaol suppresses the expression of iNOS and COX-2 genes in macrophages [56]. In addition, Jung et al. demonstrated the inhibition of excessive NO, PGE (2), TNF-α, and IL-1β by the rhizome hexane fraction of ginger [57]. A study by Habib et al. showed that the extract of *Z. officinale* normalised the expression of TNF-α and NF-κB in liver cancer-induced murine models [58]. However, the study by Lantz et al. exhibited the inhibitory effect of LPS-induced COX-2 expression while shogaol-containing extracts had no effect on COX-2 expression [59]. These studies substantiate the utility of ginger extracts as a potential antiinflammatory and antioxidant [52]. However, the studies that evaluated the efficacy of ginger in osteoarthritis (OA) patients showed conflicting results. While one study proved its effectiveness to be statistically significant in alleviating the symptoms associated with knee OA [60], the other opined its utility to be confined only to the first half of the treatment regimen [61]. However, recent evidence validates the efficacy of [6] shogaol in gouty arthritis, owing to its potential antioxidant and antiinflammatory activity [62]. These effects render ginger and its extract as a potential treatment modality in alleviating the inflammation associated with MSDs.

5.3. Curcuma longa. Turmeric is a spice that has garnered attention from both the medical as well as the culinary communities [63–65]. Turmeric (*Curcuma longa*) is a

rhizomatous herbaceous perennial plant and a subset of the *Zingiberaceae* family [66]. Despite the knowledge of its therapeutic benefits for ages, its exact mechanism of action has only been elucidated in the recent years [67]. The chemical compound predominantly found in *C. longa* is curcumin (4) or diferuloylmethane, which is attributed to its antioxidant, antibacterial, antimicrobial, antimutagenic, antiinflammatory, and anticancer properties [67–73]. Its utility has been demonstrated in the alleviation of pain [74], metabolic syndrome [75], inflammatory and degenerative conditions [67, 76, 77]. Recent studies have underscored the positive effect of curcumin on muscles by reducing the activation of the NF-κB signaling pathway. This is imperative for the alleviation of the delayed onset muscle syndrome (DOMS), as the NF-κB pathway is involved in the control of proteolysis and muscle inflammation, thereby exerting a muscle-protective effect. The administration of curcumin has not only been attributed to the reduction of muscle loss following sepsis and endotoxemia but also to inducing the regeneration of the wasted muscle after the traumatic injury. Curcumin exerts its antiinflammatory and antioxidant properties via the inhibition of NF-κB signaling, induction of heat shock response, abrogating the p38 kinase activity, inhibition of oxygen free radical formation, and prevention of the biosynthesis and release of pro-inflammatory cytokines (reviewed in [78]). Furthermore, curcumin reduces the inflammation associated with exertive exercise-induced muscle damage. This is achieved by the neutralization of pro-inflammatory cytokines and muscle injury markers such as creatine kinase (Ck) [79]. It also increases the expression of glucose-regulated protein 94 kDa (Grp94) in myogenic cells, which often plummets in unloaded muscles but is essential in the prevention of myofiber atrophy [80, 81].

5.4. Aloe barbadensis. *Aloe vera*, or *Aloe barbadensis*, is a tropical, drought-resistant succulent plant, belonging to the family *Liliaceae*. It is native to the Mediterranean region, India, China, and eastern Africa (reviewed in [82]). Aloes contain a copious amount of bioactive compounds, such as anthraquinones (7), fatty acids, flavonoids, lectins, terpenoids, monosaccharides, and polysaccharides (glucomannan, hemicelluloses, and pectins), tannins, sterols (campesterol and β-sitosterol), enzymes, salicylic acid, minerals (Fe, Cr, Cu, Ca, Mg, Na, K, P, Zn, and Mn), and vitamins (including Vit-A, Vit-C, Vit-E, β-carotene, Vit-B1, Vit-B2, Vit-B3, Vit-B6, choline, Vit-B12, and folic acid) (reviewed in [83–88]). The abundance of these compounds in *A. barbadensis* accounts for its potent antiinflammatory and antiarthritic effects (reviewed in [89]). Despite its utility in a spectrum of fields, *A. barbadensis* is very effective in the treatment of allergic reactions, arthritis, and rheumatoid fever. Growing bodies of evidence attribute this antiinflammatory property to the bioactive compound aloe-emodin, an anthraquinone alkaloid that exerts its effect by inhibiting prostaglandin-E2 and inducible nitric oxide [90, 91]. These properties could be extrapolated for the treatment of inflammation associated with MSDs.

5.5. Citrus limon. *Citrus limon,* or lemon, is a subset of the family *Rutaceae*. It is a tree with evergreen leaves and yellow edible fruits, which upon processing yields the juice and essential oil (reviewed in [92, 93]). The pharmacologically active phytoconstituents of *C. limon* juice extract and essential oils include flavones (apigenin (9), diosmin, orientin, and vitexin); flavanones (eriodyctiol, hesperidin (1), hesperitin, naringin, and neohesperidin); flavanols (quercetin (8), limocitrin, and spinacetin) and their derivatives. Other trace quantities in *C. limon* include eriocitrin, limonin, and nomilin (reviewed in [94]). The *C. limon* leaf extract is also known to scavenge the free radical levels and inhibit the redox reaction of xanthine, thereby proving as a potent antioxidant [95]. Concurrently, there is also a decrease in the levels of pro-inflammatory molecules such as ROS and prostaglandin scaffolds. Thus, owing to its potential antiinflammatory actions, several preparations of this plant can alleviate joint inflammation and arthritis [96].

5.6. Glycyrrhiza glabra. Liquorice (*Glycyrrhiza glabra*) is a plant belonging to the *Leguminosae* family. It is grown in China, India, Italy, Iran, Russia, and Spain [97]. A spectrum of components has been isolated from the roots of *G. glabra*, which was made up of simple sugars, triterpenes, saponins, flavonoids, polysaccharides, pectins, amino acids, mineral salts, asparagines, bitters, essential oil, fat, estrogen, gums, mucilage (rhizome), proteins, resins, starches, sterols, volatile oils, tannins, glycosides, among other substances [98–100]. The flavonoid component of *G. glabra* contains liquiritin, isoliquiritin (a chalcone), and other chemicals that give its characteristic yellow hue [101]. In addition, isoflavones like glabridin and hispaglabridins A and B have substantial antioxidant action [102], while both glabridin and glabrene exhibit estrogen-like activity [103]. Estradiol has been proven to exert a beneficial effect on skeletal muscles by stimulating the proliferation of satellite cells. Owing to the presence of estradiol-specific receptors on muscle fibers, skeletal muscles tend to respond to differences in estrogenic hormones. Furthermore, estradiol potentially limits and mitigates the stress damage imparted on the skeletal muscle [104]. Recent studies have attributed the antiinflammatory properties of liquorice to its inhibitory effect on the production of IL-6, NO, PGE2, and TNF-α [105]. Furthermore, the hydromethanolic liquorice root extract demonstrated potent antioxidant activity in an *in-vitro* system [106]. Additionally, licochalcones B and D have the ability to substantially reduce microsomal lipid peroxidation [97]. Moreover, retrochalcones show mitochondrial lipid peroxidation and inhibit oxidative hemolysis in red blood corpuscles (RBCs). Additionally, compounds like glabridin, hispaglabridin A, 3′hydroxy-4-O-methylglabridin, and dehydrostilbene derivatives such as dihydro-3,5,4-trihydroxy-4,5-diiodopentenylstilbene have also been reported for their potential antioxidant capacities [97, 107–109]. Growing bodies of evidence have validated the antiinflammatory effect of glycyrrhizin to be comparable to that of hydrocortisone and other corticosteroid hormones upon being broken down in the gut [97].

5.7. Citrus aurantium. The *Citrus aurantium*, popularly known as bitter orange is a subset of the family *Rutaceae* [110, 111]. It is mainly employed as a flavoring and acidifying agent in the food industry [112, 113]. The plant is rich in essential oils, vitamins, minerals, phenolic compounds, terpenoids, and flavonoid-type compounds that demonstrate a spectrum of biological effects, ranging from anxiety and obesity to lung and prostate cancers [110, 112, 114–119]. Among the diverse phytoconstituents present in *C. aurantium*, the pharmacological activity is attributed to the flavonoids present in them [110, 120–122]. The flavonoids (such as hesperidin, nobiletin (2), and naringin (3)) in *C. aurantium* prevent the inflammatory sensation in L6 skeletal muscle cells that is propagated by the lipopolysaccharides (LPS). Furthermore, the flavonoids isolated from Korean *C. aurantium* potentially inhibit the inducible nitric oxide synthase (iNOS), cyclooxygenase-2 (COX-2), IL-6, and TNF-α by intercepting the mitogen-activated protein kinases (MAPKs) and NF-κB signaling pathways. Moreover, these flavonoids demonstrated antiinflammatory properties by modulating the proteins involved in the immunological response. Furthermore, pretreatment with the flavonoids substantially reduced the quantity of cleaved caspase-3, a protein generated during muscle inflammation and highlighted in muscle proteolysis and atrophy [123]. These studies validate its utility in reducing the inflammation associated with MSDs.

5.8. Alstonia scholaris. Saptaparni or *Alstonia scholaris*, belonging to the family *Apocynaceae*, has been an integral part of the ethnopharmacological armamentarium, especially in the "dai" ethnopharmacy in the treatment of respiratory ailments [124]. This utility has reinforced its potential in other inflammatory ailments. The comprehensive investigation of various plant parts of *A. scholaris* reported a spectrum of indole alkaloids, iridoids, monoterpenoids, and terpenoids [124–133]. It is also rich in alkaloids (like echitamine, tubotaiwine, akuammicine, echitamidine, picrinine, and strictamine) and terpenes, which are used as antiinflammatory agents [134, 135]. The ethanolic extract of *A. scholaris* leaves in a dose of 100–200 mg/kg demonstrated a significant reduction in the total leukocyte migration, while concurrently reducing the levels of pro-inflammatory mediators like COX, LOX, PGE2, and NO in animal models [136]. The plant has also afforded protection in various pain and inflammation models, including the formalin test, acetic acid-induced writhing, and the air pouch model in rodents [124]. A study by Subraya and Gupta concluded the significant antiinflammatory effect of the methanolic extract of *A. scholaris* stem bark compared to indomethacin against carrageenan-induced acute pedal edema, cotton pellet-induced, and dextran-induced edema [137–139]. The dextran-mediated inflammation was thought to be alleviated by the antihistaminic property of the extract. However, the antiinflammatory effect of the cotton pellet granuloma test reflected its efficacy in inhibiting the proliferation of fibroblasts and synthesis of collagen and mucopolysaccharide during the formation of granuloma tissues [137, 138]. Despite the various studies underscoring its utility as an antiinflammatory agent, substantial bodies of evidence are required to substantiate its efficacy in the treatment of MSDs.

5.9. Eysenhardtia polystachya. E. polystachya is a subset of the family *Fabaceae* and is predominantly found throughout Mexico and in the southeastern United States [140, 141]. The various parts of the tree is copious in a variety of secondary metabolites, including chalcones, coumarins, dihydrochalcones, fatty acids, flavonoids, flavones, flavanones, isoflavonoids, phenols, pterocarpan, and sugars to name a few [141]. These active congeners have antiinflammatory properties and have been used in the treatment of arthritis [142–144]. A recent study explored the antiinflammatory potential of *E. polystachya* bark in its hexane, chloroform, and methanolic extracts on Wistar rat models. These studies were also supplemented with the carrageenan and croton oil-induced edema tests, following which the PGE2, IL-1β, TNF-α, and leukotriene B4 (LTB4) levels were quantified. Furthermore, the methanolic extract of *E. polystachya* bark showed antiinflammatory activity in the different models by inhibiting the expression of cytokines like PGE2, IL-1β, TNF-α, LTB4, and the enzymes lipoxygenase and xanthine-oxidase linked to the inflammatory problems [141, 145]. In addition, the researchers elucidated the effects of an ethanolic extract from the bark of E. polystachya on Complete Freund's Adjuvant (CFA)-induced rheumatoid arthritis. The secondary metabolites of *E. polystachya*, mainly flavonoids, inhibited the secondary inflammation in arthritic rats, promoting the histopathological alterations while concurrently lowering the levels of circulating pro-inflammatory cytokines [143]. Moreover, the study on the antiinflammatory effect of the leaves and branches of *E. polystachya* used *in-vitro* tests that stimulated the macrophages using LPS. These results validated a reduction in H_2O_2 (IC50 = 43.9 ± 3.8 μg/mL) and IL-6 (73.3 ± 6.9 μg/mL) [142]. These studies corroborate the utility of this plant in treating inflammation and could be extrapolated for alleviating the inflammation associated with MSDs.

5.10. Ipomoea batatas. The sweet potato, or *I. batatas,* is a plant often associated with being a major crop food worldwide. It is widely produced and consumed in East Asia, Oceania, and sub-Saharan Africa, with China being the highest producer, with 76.07% of the world's production [146–148]. The leaves of *I. batatas* are widely regarded as a functional food that poses a variety of health-promoting benefits [146, 149]. *I. batatas* is a subset of the *Convolvulaceae* family and is a rich source of antiinflammatory phytonutrients such as rutin, gallic acid, quercetin, and kaempferol (5). The flowers of the latter show their antiinflammatory effect by modulating the levels of IL-1b, IL-6, and NO [150]. The latter is rich in Vit B1, Vit B5, Vit B6, niacin, riboflavin, polyphenols (anthocyanin), phenolic compounds (including caffeic, monocaffeoylquinic, dicaffeoylquinic, and tricaffeoylquinic acids), triterpenes (such as β-carotene and boehmeryl acetate), trace elements (calcium,

iron, and zinc), and other proteins [151–155]. The leaves and areal parts of *I. batatas* contain more polyphenols than most vegetables, with atleast 15 anthocyanins and 6 polyphenolic compounds [151]. The dry powder of *I. batatas* tuber and roots were extracted using ethyl acetate and methanol. Various tests, including carrageenan-induced paw edema test, croton oil-induced ear, and anal edema inhibition, and CFA-induced antiarthritic experiments, were performed on Sprague-Dawley rats at a dose of 300 mg/kg body weight. Their antiinflammatory potential was attributed to the suppression of pro-inflammatory cytokines (such as PGE2, IL-1β, and TNF-α), with a concurrent reduction in NO levels, in the ethyl acetate root extract and methanolic tuber extract, respectively [150]. These studies validate their efficacy in ameliorating inflammation in most tissues.

5.11. Swertia chirayita. *S. chirayita* is a popular herbal plant that has been used for ages [156, 157]. The plant mainly matures at tall altitudes of 1200–1500 metres in sub-temperature regions, specifically on the slopes of the Himalayas, ranging from Bhutan to Kashmir [158] (reviewed in [159]). The medicinal plant has been employed for a multitude of clinical applications, including vomiting, hepatitis, constipation, inflammation, weak stomach, and indigestion [157, 160, 161]. Growing bodies of evidence have analyzed the hepatoprotective activity of this plant extract to be associated with its antioxidant property [157]. An oral dose (200 mg/kg) of *S. chirayita* ethanolic leave extract decreases pro-inflammatory cytokines such as TNF-α and IL-1α, as well as paw edema in arthritic rats [162]. Chen et al. used many common *in-vitro* methods to investigate the antioxidant potential of *S. chirayita* plant extract against CCl4-induced toxicity in murine models. The characteristics of malondialdehyde (MDA) and antioxidant enzymes such as glutathione (GSH), superoxide dismutase (SOD), and catalase (CAT) have also been elucidated using standard investigation techniques. Furthermore, the powder obtained by evaporating and lyophilizing an ethanolic extract of *S. chirayita* was found to have strong antioxidant properties [161]. A study by Das and Barman explored the analgesic and antiinflammatory properties of the ethanolic plant root extract in the carrageenan-induced rat paw edema model. In order to determine the analgesic property of the extract, a writhing test based on acetic acid induction and radiant heat tail-flick methods were used. At a 400 mg/kg dose, the extract was efficient in reducing the development of edema, resulting in a 57.81% reduction in edema volume, 3 hours after administration. This study substantiates its utility in having analgesic and antiinflammatory activities [163]. Banerjee et al. tested a xanthone derivative for inflammation from *S. chirayita* in acute, sub-acute, and chronic male rats. Their research concluded its antiinflammatory activity to be comparable to that of diclofenac [164]. Therefore, these studies underscore its utility in inflammation and could be a potential treatment modality in inflammation in MSDs.

5.12. Strychnos nux-vomica. The strychnine tree, or *Strychnos nux-vomica,* belongs to the *Loganiaceae* family and has demonstrated remarkable treatment potential for several disorders. They have been employed for a variety of therapeutic outcomes, including analgesic, antipyretic, cytotoxic, and antiinflammatory activities. These phytotherapeutic effects have been attributed to the compounds present in them, like 7-hydroxy coumarin, Kaempferol-3-rutinoside, Kaempferol-7-glucoside, Quercetin-3-rhamnoside, and rutin. A study by Eldahshan and Daim validated the antiinflammatory, antipyretic, and antinociceptive effects of *S. nux-vomica* leaf extract in animal models. These activities were attributed to the inhibitory effect of the extract and its phytoconstituents on inflammatory mediators such as PGE2 and TNF-α [165]. In addition, the *S. nux-vomica* extract demonstrated a reduction in PGE2, with a concurrent decrease in vascular permeability, thereby demonstrating potent antiarthritic and antiinflammatory activities, which are profound in the case of joint inflammation [166–168]. However, for preclinical applications, the effects and potential toxicities must be elucidated through further tests.

5.13. Rosemarinus officinalis. Rosemary, or *Rosmarinus officinalis,* is a medicinal plant, based out of the Mediterranean region, but eventually cultivated across the globe. Besides its potential therapeutic utility, it is commonly employed as a condiment and a food preservative. By virtue of its phytoconstituents, the plant demonstrates potential pharmacological activities, including antioxidant, antiinflammatory, antimicrobial, antitumour, antiproliferative, protective, inhibitory, and attenuating effects [169–173]. The phytoconstituents present in *R. officinalis* mainly include α-pinene, caffeic acid (10), camphor, carnosic acid, carnosol, chlorogenic acid, eucalyptol, monomeric acid, oleanolic acid, rosmarinic acid, rosmadial, rosmanol, rosmaquinones A and B, secohinokio, ursolic acid, and the derivatives of eugenol (6), and luteolin [173–178]. The effects of *R. officinalis* were evaluated in patients with osteoarthritis, rheumatoid arthritis, and fibromyalgia for four weeks in an open-label trial; the hs-CRP levels that mark the presence of inflammation had also reduced substantially in patients who had demonstrated the augmentation in this index. Though the reduction in inflammation was related to the pain score, no remission was observed in fibromyalgia scores [179]. Recent shreds of evidence corroborate the antiinflammatory effect of *R. officinalis*. This effect is attributed to the disruptive effect of rosmarinic acid on the activation of the complement system by reducing the C3b attachment, while the dose required for the latter is relatively low (34 μM) [180]. This plant has also been demonstrated to have topical antiinflammatory effects in murine models [181]. These effects validate its efficacy as a potential antioxidant and antiinflammatory agent.

5.14. Borago officinalis. The borage, or *Borago officinalis,* is a member of the *Boraginaceae* family and is native to the European area as well as the north of Africa [182]. Since antiquity, borage and its derivatives have formed a part of the traditional medicine armamentarium, especially in the

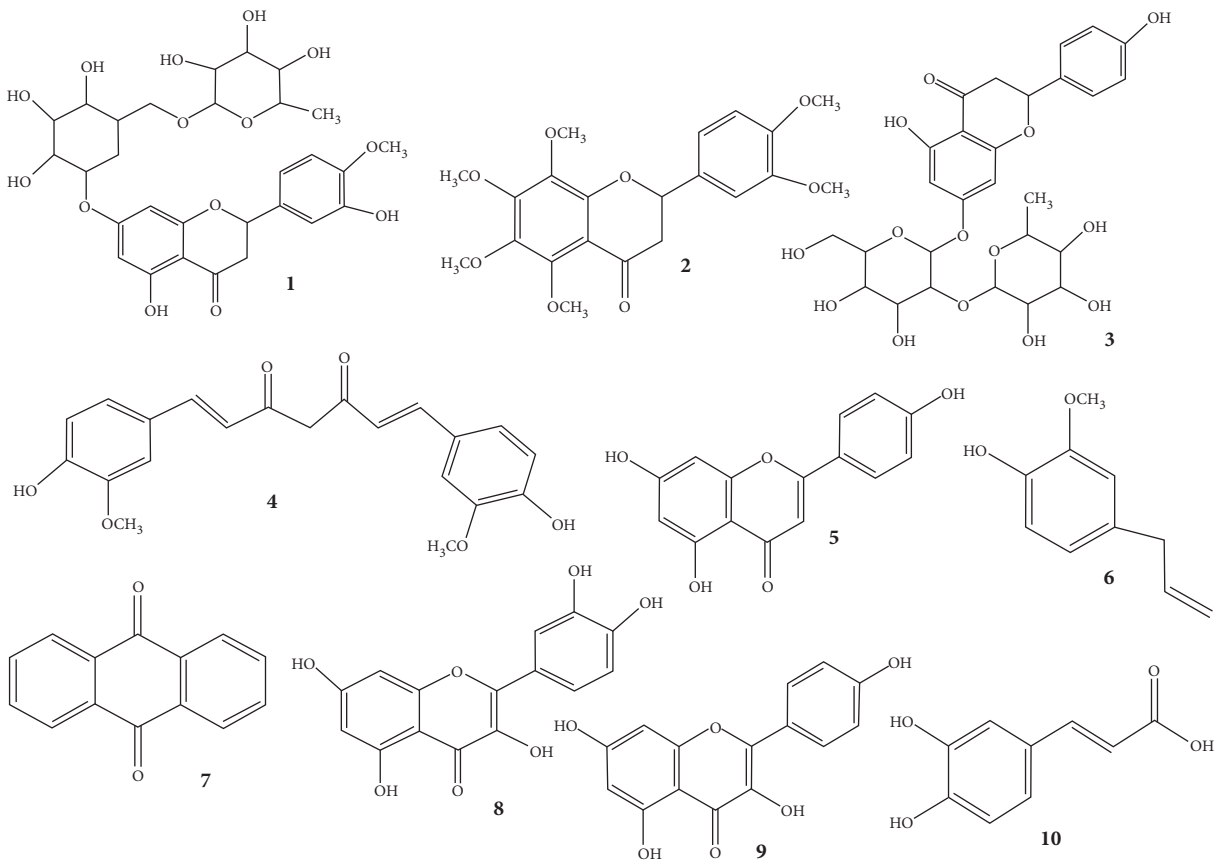

Figure 3: Various phytochemicals that exert their effects on inflammation in musculoskeletal disorders.

treatment of allergic disorders, owing to their immunomodulatory properties [183]. The plant is a rich source of gamma linoleic acid (GLA), containing about 25% of GLA. The GLA augments the cyclic adenosine monophosphate (cAMP) by elevating the prostaglandin-E (PGE) levels, as well as being a strong suppressor of TNF-α [184]. Its activity is associated with its ability to suppress the TNF-α, while delivering gamma-linolenic acid [183]. This mechanism explains its antiinflammatory effect in the alleviation of symptoms associated with rheumatoid arthritis. However, this treatment modality has been contraindicated as an intervention in pregnant women, as it is associated with an increased risk of miscarriage [184]. The antirheumatoid arthritis potential of borage seed oil of 1.4 gm/day when compared to the placebo group exhibited 36.8% amelioration post 6 months of therapy. Additionally, a 2.8 gm/day administration of borage seed oil in the treatment of rheumatoid arthritis demonstrated a 64% amelioration in the treatment group compared to the 21% in the control group post 6 months of therapy (reviewed in [185, 186]). These clinical studies underscore their utility as a potential antirheumatoid arthritis and antiinflammatory medication.

5.15. Harpagophytum procumbens. The Devil's claw, or *Harpagophytum procumbens,* is a member of the *Pedaliaceae* family [187]. The pharmacological activity of its extract is mainly associated with its copiousness of an

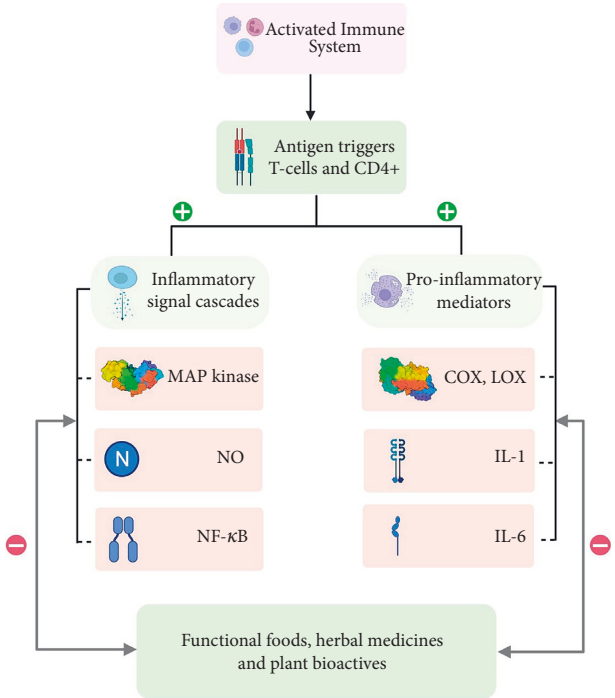

Figure 4: General protective actions mediated by functional food, herbal medicines, and their derived phytoconstituents.

Table 1: Plant bioactives in the management of musculoskeletal disorders.

Dietary food or medicinal herb	Family	Phytochemical molecule	Research summary	References
Coffea arabica	*Rubiaceae*	Caffeine dimethylxanthines, paraxanthine, theobromine, theophylline	↓ in IL-1a, IL-6, and TNF-α ↑ proliferation of the tissues ↑ in the nucleic acid synthesis via the Akt signaling pathway ↓ in the levels of circulating inflammatory cytokines ↑ activatin of satellite cells	[46]
Zingiber officinale	*Zingiberaceae*	Gingerol, shogaol	↓ in the production of prostaglandins and leukotrienes, via the suppression of the prostaglandin synthetase 5-lipoxygenase enzymes ↓ the IL-1, IL-8, and TNF-α synthesis ↓ the expression of iNOS and COX-2 genes Hexane fraction of ginger extract ↓the excessive NO, PGE2, TNF-α, and IL-1β	[51, 52, 54–57]
Curcuma longa	*Zingiberaceae*	Curcumin or diferuloylmethane	↓ the activation of the NF-κB signaling pathway ↑ expression of glucose-regulated protein 94 kDa (Grp94) in myogenic cells	[78, 80, 81]
Aloe vera or *Aloe barbadensis*	*Liliaceae*	Campesterol, β-sitosterol	↑ the inhibition and ↓ the expression of PGE2 and inducible nitric oxide.	[90, 91]
Citrus limon	*Rutaceae*	Quercetin, limocitrin, and spinacetin	↓ the pro-inflammatory molecules such as ROS, PG scaffolds, and precursors ↓ free radical levels, by means of scavenging, in its leaf extract Inhibition of xanthine redox reaction	[95, 96]
Glycyrrhiza glabra	*Leguminosae*	Hispaglabridins A and B	↓ the synthesis of IL-6, NO, PGE2, and TNF-α ↓ in the microsomal lipid peroxidation Potent antioxidant effect in its hydromethanolic extract	[97, 106–109]
Citrus aurantium	*Rutaceae*	Essential oils, vitamins, minerals, phenolic compounds, terpenoids	Inhibition of iNOS, COX-2, IL-6, and TNF-α, by inhibiting the MAPKs and NF-κB signaling pathways	[123]
Alstonia scholaris	Apocynaceae	Echitamine, tubotaiwine, akuammicine, echitamidine, picrinine and strictamine	↓in total leukocyte migration ↓ in the biosynthesis of pro-inflammatory mediators such as COX, LOX, PGE2, and NO, upon validation of its ethanolic extract	[136]
Eysenhardtia polystachya	*Fabaceae*	Coumarins, dihydrochalcones, fatty Acids, flavonoids	↓ in the expression of PGE2, IL-1β, TNF-α, LTB4, in a methanolic extract ↓ in the expression of enzymes LOX and xanthine-oxidase when a methanolic extract was used	[140, 141]
Ipomoea batatas	*Convolvulaceae*	Vit B1, vit B5, vit B6, niacin, riboflavin, polyphenols	Modulation of IL-1β, IL-6, and NO ↓ in the activity of PGE2, IL-1β, and TNF-α, upon methanolic tuber extraction ↓ in NO levels, upon administration of ethyl acetate root extract	[150]
Swertia chirayita	*Gentianaceae*	Chiratin, xanthone derivative	Ethanolic leaves extract ↓ the activity of TNF-α and IL-1α	[162]
Strychnos nux-vomica	*Loganiaceae*	Quercetin-3-rhamnoside, and rutin	Leaves extract ↓ the effect exerted by PGE2 and TNF-α Antiarthritic and antiinflammatory effect attributed to the ↓ of PGE2 levels	[165–168]
Rosemarinus officinalis	*Lamiaceae*	Rosmarinic acid, rosmadial, rosmanol, rosmaquinones	Rosmarinic acid disrupts the activation of complement system ↓ in the C3b attachment at low doses	[180]

Table 1: Continued.

Dietary food or medicinal herb	Family	Phytochemical molecule	Research summary	References
Borago officinalis	*Boraginaceae*	Gamma-linolenic acid (GLA),	↓ in the expression and activity of TNF-α	[183, 184]
Harpagophytum procumbens	*Pedaliaceae*	Harpagoside	↓ in the total levels of NO, PGE2, IL-6, IL-1β, and TNF-α Intercepts the metabolism of arachidonic acid and the synthesis of eicosanoids, thereby inhibiting COX-2 enzyme	[189–191]

↓ represents a decreasing trend and ↑ represents an increasing trend.

Table 2: Clinical trials testing the efficacy of the medicinal herbs and plant bioactives in the treatment of musculoskeletal inflammation.

Sr. no.	Title	Status	Conditions	Interventions	Characteristics	NCT number
1.	Aloe vera ointment application and skeletal muscle recovery	Completed	(i) Skeletal muscle damage (ii) Exercise-induced aseptic inflammation (iii) Performance	(i) Biological: placebo (ii) Biological: natural aloe vera (iii) Biological: aloe vera soup	Study type: interventional Phase: not applicable Study design: (i) Allocation: randomized (ii) Intervention model: crossover assignment (iii) Masking: double (participant, investigator) (iv) Primary purpose: treatment Outcome measures: (v) Change in creatine kinase activity in plasma (vi) Change in performance of knee extensor muscles (vii) Change in delayed onset of muscle soreness	NCT03934762
2.	Describing Chinese herbal medicine telehealth care for symptoms related to infectious diseases such as COVID-19	Recruiting	(i) Coronavirus infection	(i) Dietary supplement: Chinese herbal medicine	Study type: observational Phase: study design: (i) Observational model: ecologic or community (ii) Time perspective: prospective Outcome measures: (iii) Patient reported main complaint (iv) Conduct qualitative analyses of data	NCT04380870

Table 2: Continued.

Sr. no.	Title	Status	Conditions	Interventions	Characteristics	NCT number
3.	PB125, osteoarthritis, pain, mobility, and energetics	Recruiting	(i) Osteoarthritis, knee (ii) Muscle weakness (iii) Pain, joint	(i) Dietary supplement: PB125 (ii) Dietary supplement: placebo	Study type: interventional Phase: not applicable Study design: (i) Allocation: nonrandomized (ii) Intervention model: single group assignment (iii) Masking: double (participant, outcomes assessor) (iv) Primary purpose: treatment Outcome measures: (v) Mobility-6 min self-paced walk (vi) Mobility-sit to stand (vii) Mobility-static balance (viii) Mobility-6 min fast-paced walk (ix) Intermittent and constant knee pain (x) Energetics-submaximal oxygen consumption (xi) Energetics-maximal oxygen consumption (xii) Energetics-hydrogen peroxide emission (xiii) Bone mineral density (xiv) Knee range of motion (xv) Leg extensor strength	NCT04638387

antiinflammatory compound, Harpagoside [188]. The Devil's claw root extract has been claimed to inhibit NO levels and other pro-inflammatory cytokines (including PGE2, IL-6, IL-1β, and TNF-α). It also prevents the metabolism of arachidonic acid and the biosynthesis of eicosanoids, which further inhibits the COX-2 enzyme, thereby reducing inflammation [189–191]. A pilot study has been carried out on patients suffering from rheumatoid arthritis and psoriatic arthritis. The patients were administered 410 mg of the devil's claw liquid extract TDS. However, the patients did not show any remission or subjective and objective improvement in their clinical condition [192]. Additionally, another preclinical study involving devil's claw showed no efficacy in improvement in the carrageenan-induced edema in the hind foot of the rat [193]. These studies have described the potential of devil's claw extract in inflammatory MSDs including rheumatoid arthritis and psoriatic arthritis. However, further studies need to be carried out to substantiate their utility and toxicity profiles.

Various phytochemicals effective in inflammatory pathophysiology involved in musculoskeletal disorders have been elucidated in Figure 3, while their protective actions have been demonstrated in Figure 4. Further investigations are warranted to understand the clinical efficacy of these bioactive phytomedicines along with the exploration of new potential botanicals. Safety studies play a crucial role in the drug development process [194, 195], therefore they should also be carried out. The research summary has been concisely presented in Table 1. Additionally, the recent clinical advances have been curated and tabulated in Table 2.

6. Conclusion and Outlook

Although the utility of various medicinal plants and their derived phytochemicals has been established in the treatment of various musculoskeletal disorders, especially rheumatoid and psoriatic arthritis, however, their ethnopharmacological studies and evidences presented are not convincing, and thorough evidence needs to be provided to substantiate their utility, toxicity profiles, dosing, and formulation in the mitigation and management of inflammation in the MSDs. Additionally, it aims to review the various plants that have been long lost as a potential modality in alleviating the inflammation and pain associated with various MSDs and their role as a part of the diet or as a medicinal treatment intervention. The current literature available is limited and more detailed *in vitro* and *in vivo* studies are required to provide a better view of the current treatment landscape of inflammation and related diseases of the musculoskeletal system. However, the authors also opine on the need for further preclinical and clinical studies to corroborate the effects in humans. In addition, these phytochemicals could be extracted to potentially fabricate them into a viable formulation, for clinical administration. Moreover, more cogent and exhaustive data is required for understanding the molecular and signaling mechanisms and the way in which these crude drugs and/or phytoconstituents must be administered and their potential adverse effects and toxicity must be catered after consumption.

Data Availability

The data used to support the findings of this study are available from the corresponding author upon request.

Conflicts of Interest

The authors declare that they have no conflicts of interest.

Authors' Contributions

Dipanjan Karati conceptualized the study, provided resources, curated the data, wrote the original draft, reviewed and edited the manuscript, visualized the study, and did project administration. Ryan Varghese conceptualized the study, provided resources, curated the data, wrote the original draft, writing-reviewed and edited the manuscript, visualized the study, and did project administration. K. R. Mahadik supervised the study, reviewed and edited the manuscript, and did project administration. Rohit Sharma supervised the study, reviewed and edited the manuscript, and did project administration. Dileep Kumar provided resources, supervised the study, and did project administration.

Acknowledgments

The images have been created with the aid of https://BioRender.com.

References

[1] S. D. Anker, A. J. S. Coats, J. E. Morley et al., "Muscle wasting disease: a proposal for a new disease classification," *Journal of Cachexia Sarcopenia and Muscle*, vol. 5, no. 1, pp. 1–3, 2014.

[2] R. Puntumetakul, W. Siritaratiwat, Y. Boonprakob, W. Eungpinichpong, and M. Puntumetakul, "Prevalence of musculoskeletal disorders in farmers: case study in Sila, Muang Khon Kaen, Khon Kaen province," *Journal of Medical Technology Physical Therapy*, vol. 23, no. 3, pp. 297–303, 2011.

[3] S. Hignett and M. Fray, "Manual handling in healthcare," in *Proceedings of the 1st Conference of the Federation of the European Ergonomics Societies [FEES]*, pp. 10–12, Institute of Ergonomics and Human Factors, Bruges, Belgium, 2010.

[4] B. Egan and J. R. Zierath, "Exercise metabolism and the molecular regulation of skeletal muscle adaptation," *Cell Metabolism*, vol. 17, no. 2, pp. 162–184, 2013.

[5] D. W. Gould, I. Lahart, A. R. Carmichael, Y. Koutedakis, and G. S. Metsios, "Cancer cachexia prevention via physical exercise: molecular mechanisms," *Journal of Cachexia Sarcopenia and Muscle*, vol. 4, no. 2, pp. 111–124, 2013.

[6] A. J. Cruz-Jentoft, F. Landi, S. M. Schneider et al., "Prevalence of and interventions for sarcopenia in ageing adults: a systematic review. Report of the international sarcopenia initiative (EWGSOP and IWGS)," *Age and Ageing*, vol. 43, no. 6, pp. 748–759, 2014.

[7] D. N. Obanda, A. Hernandez, D. Ribnicky et al., "Bioactives of *Artemisia dracunculus* L. mitigate the role of ceramides in attenuating insulin signaling in rat skeletal muscle cells," *Diabetes*, vol. 61, no. 3, pp. 597–605, 2012.

[8] Z. Q. Wang, D. Ribnicky, X. H. Zhang et al., "An extract of *Artemisia dracunculus* L. enhances insulin receptor signaling and modulates gene expression in skeletal muscle in KK-Ay mice," *The Journal of Nutritional Biochemistry*, vol. 22, no. 1, pp. 71–78, 2011.

[9] K.-B. Hong, H.-S. Lee, J. S. Hong, D. H. Kim, J. M. Moon, and Y. Park, "Effects of tannase-converted green tea extract on skeletal muscle development," *BMC Complement Medical Therapy*, vol. 20, no. 1, p. 47, 2020.

[10] S. Nimesh, V. D. Ashwlayan, R. Rani, and O. Prakash, "Advantages of herbal over allopathic medicine in the management of kidney and urinary stones disease," *Borneo Jornal of Pharmacy*, vol. 3, no. 3, pp. 179–189, 2020.

[11] A. J. Benham and K. A. Geier, "How well are nurse practitioners prepared to treat common musculoskeletal conditions?" *Orthopaedic Nursing*, vol. 35, no. 5, pp. 325–329, 2016.

[12] National Academies of Sciences and Medicine, Health and Medicine Division, Board on Health Care Services, and Committee on Identifying Disabling Medical Conditions Likely to Improve with Treatment, *Selected Health Conditions and Likelihood of Improvement with Treatment*, National Academies Press, Washington, DC, USA, 2020.

[13] World Health Organization, *Musculoskeletal Conditions*, World Health Organization, Geneva, Switzerland, 2021.

[14] S. Singh, T. G. Singh, K. Mahajan, and S. Dhiman, "Medicinal plants used against various inflammatory biomarkers for the management of rheumatoid arthritis," *Journal of Pharmacy and Pharmacology*, vol. 72, no. 10, pp. 1306–1327, 2020.

[15] L. C. Coates and P. S. Helliwell, "Psoriatic arthritis: state of the art review," *Clinical Medicine*, vol. 17, no. 1, pp. 65–70, 2017.

[16] J. M. H. Moll and V. Wright, "Psoriatic arthritis," *Seminars in Arthritis and Rheumatism*, vol. 3, pp. 55–78, 1973.

[17] A. Ogdie and P. Weiss, "The epidemiology of psoriatic arthritis," *Rheumatic Disease Clinics of North America*, vol. 41, no. 4, pp. 545–568, 2015.

[18] Y. Huang, K. Chen, Q. Ren et al., "Dihydromyricetin attenuates dexamethasone-induced muscle atrophy by improving mitochondrial function via the PGC-1α pathway," *Cellular Physiology and Biochemistry*, vol. 49, no. 2, pp. 758–779, 2018.

[19] V. Guasconi and P. L. Puri, "Epigenetic drugs in the treatment of skeletal muscle atrophy," *Current Opinion in Clinical Nutrition and Metabolic Care*, vol. 11, no. 3, pp. 233–241, 2008.

[20] D. J. Glass, "Signalling pathways that mediate skeletal muscle hypertrophy and atrophy," *Nature Cell Biology*, vol. 5, no. 2, pp. 87–90, 2003.

[21] Y. Rolland, S. Czerwinski, G. A. Van Kan et al., "Sarcopenia: its assessment, etiology, pathogenesis, consequences and future perspectives," *The Journal of Nutrition, Health & Aging*, vol. 12, no. 7, pp. 433–450, 2008.

[22] A. J. Cruz-Jentoft, J. P. Baeyens, J. M. Bauer et al., "Sarcopenia: European consensus on definition and diagnosis: report of the European working group on sarcopenia in older people," *Age and Ageing*, vol. 39, no. 4, pp. 412–423, 2010.

[23] J. Díaz-Castro, R. Guisado, N. Kajarabille et al., "*Phlebodium decumanum* is a natural supplement that ameliorates the oxidative stress and inflammatory signalling induced by strenuous exercise in adult humans," *European Journal of Applied Physiology*, vol. 112, no. 8, pp. 3119–3128, 2012.

[24] J. von Maltzahn, N. C. Chang, C. F. Bentzinger, and M. A. Rudnicki, "Wnt signaling in myogenesis," *Trends in Cell Biology*, vol. 22, no. 11, pp. 602–609, 2012.

[25] P. Cisternas, J. P. Henriquez, E. Brandan, and N. C. Inestrosa, "Wnt signaling in skeletal muscle dynamics: myogenesis, neuromuscular synapse and fibrosis," *Molecular Neurobiology*, vol. 49, no. 1, pp. 574–589, 2014.

[26] H. Flanagan-Steet, K. Hannon, M. J. McAvoy, R. Hullinger, and B. B. Olwin, "Loss of FGF receptor 1 signaling reduces skeletal muscle mass and disrupts myofiber organization in the developing limb," *Developmental Biology*, vol. 218, no. 1, pp. 21–37, 2000.

[27] F. Haddad, R. R. Roy, H. Zhong, V. R. Edgerton, and K. M. Baldwin, "Atrophy responses to muscle inactivity II. Molecular markers of protein deficits," *Journal of Applied Physiology*, vol. 95, no. 2, pp. 791–802, 2003.

[28] S. H. Lecker, R. T. Jagoe, A. Gilbert et al., "Multiple types of skeletal muscle atrophy involve a common program of changes in gene expression," *The FASEB Journal*, vol. 18, no. 1, pp. 39–51, 2004.

[29] S. C. Bodine, E. Latres, S. Baumhueter et al., "Identification of ubiquitin ligases required for skeletal muscle atrophy," *Science*, vol. 294, no. 5547, pp. 1704–1708, 2001.

[30] M. J. M. Dehoux, R. P. van Beneden, L. F. Celemín, P. L. Lause, and J.-P. M. Thissen, "Induction of MafBx and Murf ubiquitin ligase mRNAs in rat skeletal muscle after LPS injection," *FEBS Letters*, vol. 544, no. 1-3, pp. 214–217, 2003.

[31] M. D. Gomes, S. H. Lecker, R. T. Jagoe, A. Navon, and A. L. Goldberg, "Atrogin-1, a muscle-specific F-box protein highly expressed during muscle atrophy," *Proceedings of the National Academy of Sciences*, vol. 98, no. 25, Article ID 14445, 2001.

[32] H.-H. Li, V. Kedar, C. Zhang et al., "Atrogin-1/muscle atrophy F-box inhibits calcineurin-dependent cardiac hypertrophy by participating in an SCF ubiquitin ligase complex," *Journal of Clinical Investigation*, vol. 114, no. 8, pp. 1058–1071, 2004.

[33] M. Sandri, C. Sandri, A. Gilbert et al., "Foxo transcription factors induce the atrophy-related ubiquitin ligase atrogin-1 and cause skeletal muscle atrophy," *Cell*, vol. 117, no. 3, pp. 399–412, 2004.

[34] S. C. Bodine, T. N. Stitt, M. Gonzalez et al., "Akt/mTOR pathway is a crucial regulator of skeletal muscle hypertrophy and can prevent muscle atrophy *in vivo*," *Nature Cell Biology*, vol. 3, no. 11, pp. 1014–1019, 2001.

[35] C. Rommel, S. C. Bodine, B. A. Clarke et al., "Mediation of IGF-1-induced skeletal myotube hypertrophy by PI(3)K/Akt/mTOR and PI(3)K/Akt/GSK3 pathways," *Nature Cell Biology*, vol. 3, no. 11, pp. 1009–1013, 2001.

[36] D. C. Guttridge, M. W. Mayo, L. V. Madrid, C.-Y. Wang, and A. S. Baldwin Jr, "NF-κB-induced loss of MyoD messenger RNA: possible role in muscle decay and cachexia," *Science*, vol. 289, no. 5488, pp. 2363–2366, 2000.

[37] P. Londhe and D. C. Guttridge, "Inflammation induced loss of skeletal muscle," *Bone*, vol. 80, pp. 131–142, 2015.

[38] E. A. Bach, M. Aguet, and R. D. Schreiber, "The IFNγ receptor: a paradigm for cytokine receptor signaling," *Annual Review of Immunology*, vol. 15, no. 1, pp. 563–591, 1997.

[39] H. A. Young, "Regulation of interferon-γ gene expression," *Journal of Interferon and Cytokine Research*, vol. 16, no. 8, pp. 563–568, 1996.

[40] R. Sharma, N. Martins, K. Kuca et al., "Chyawanprash: a traditional Indian bioactive health supplement," *Biomolecules*, vol. 9, no. 5, p. 161, 2019.

[41] A. Nagral, K. Adhyaru, O. S. Rudra, A. Gharat, and S. Bhandare, "Herbal immune booster-induced liver injury in the COVID-19 pandemic-a case series," *Journal of Clinical and Experimental Hepatology*, vol. 11, no. 6, pp. 732–738, 2021.

[42] R. Sharma, K. Kuca, E. Nepovimova, A. Kabra, M. M. Rao, and P. K. Prajapati, "Traditional ayurvedic and herbal remedies for alzheimer's disease: from bench to bedside," *Expert Review of Neurotherapeutics*, vol. 19, no. 5, pp. 359–374, 2019.

[43] Y.-H. Lee, D.-H. Kim, Y. S. Kim, and T.-J. Kim, "Prevention of oxidative stress-induced apoptosis of C2C12 myoblasts by a *Cichorium intybus* root extract," *Bioscience, Biotechnology, and Biochemistry*, vol. 77, no. 2, pp. 375–377, 2013.

[44] M. S. Butt and M. T. Sultan, "Coffee and its consumption: benefits and risks," *Critical Reviews in Food Science and Nutrition*, vol. 51, no. 4, pp. 363–373, 2011.

[45] R. Pardo Lozano, Y. alvarez García, D. Barral Tafalla, and M. Farré Albaladejo, "Cafeína: un nutriente, un fármaco, o una droga de abuso," *Adicciones*, vol. 19, no. 3, p. 225, 2007.

[46] N. P. Evans, J. A. Call, J. Bassaganya-Riera, J. L. Robertson, and R. W. Grange, "Green tea extract decreases muscle pathology and NF-κB immunostaining in regenerating muscle fibers of mdx mice," *Clinical Nutrition*, vol. 29, no. 3, pp. 391–398, 2010.

[47] E. J. Park and J. M. Pezzuto, "Botanicals in cancer chemoprevention," *Cancer and Metastasis Reviews*, vol. 21, no. 3-4, pp. 231–255, 2002.

[48] Y. Shukla and M. Singh, "Cancer preventive properties of ginger: a brief review," *Food and Chemical Toxicology*, vol. 45, no. 5, pp. 683–690, 2007.

[49] B. H. Ali, G. Blunden, M. O. Tanira, and A. Nemmar, "Some phytochemical, pharmacological and toxicological properties of ginger (*Zingiber officinale* Roscoe): a review of recent

research," *Food and Chemical Toxicology*, vol. 46, no. 2, pp. 409–420, 2008.

[50] M. Thomson, K. K. Al-Qattan, S. M. Al-Sawan, M. A. Alnaqeeb, I. Khan, and M. Ali, "The use of ginger (*Zingiber officinale* Rosc.) as a potential anti-inflammatory and antithrombotic agent," *Prostaglandins, Leukotrienes and Essential Fatty Acids*, vol. 67, no. 6, pp. 475–478, 2002.

[51] R. Nicoll and M. Y. Henein, "Ginger (*Zingiber officinale* Roscoe): a hot remedy for cardiovascular disease?" *International Journal of Cardiology*, vol. 131, no. 3, pp. 408-409, 2009.

[52] N. S. Mashhadi, R. Ghiasvand, G. Askari, M. Hariri, L. Darvishi, and M. R. Mofid, "Anti-oxidative and anti-inflammatory effects of ginger in health and physical activity: review of current evidence," *International Journal of Preventive Medicine*, vol. 4, no. 1, pp. S36–S42, 2013.

[53] C. D. Black, M. P. Herring, D. J. Hurley, and P. J. O'Connor, "Ginger (*Zingiber officinale*) reduces muscle pain caused by eccentric exercise," *The Journal of Pain*, vol. 11, no. 9, pp. 894–903, 2010.

[54] E. Tjendraputra, V. H. Tran, D. Liu-Brennan, B. D. Roufogalis, and C. C. Duke, "Effect of ginger constituents and synthetic analogues on cyclooxygenase-2 enzyme in intact cells," *Bioorganic Chemistry*, vol. 29, no. 3, pp. 156–163, 2001.

[55] S. K. Verma, M. Singh, P. Jain, and A. Bordia, "Protective effect of ginger, *Zingiber officinale* Rosc on experimental atherosclerosis in rabbits," *Indian Journal of Experimental Biology*, vol. 24, no. 7, 2004.

[56] M. H. Pan, M. C. Hsieh, P. C. Hsu et al., "6-shogaol suppressed lipopolysaccharide-induced up-expression of iNOS and COX-2 in murine macrophages," *Molecular Nutrition and Food Research*, vol. 52, no. 12, pp. 1467–1477, 2008.

[57] H. W. Jung, C.-H. Yoon, K. M. Park, H. S. Han, and Y.-K. Park, "Hexane fraction of *Zingiberis* Rhizoma Crudus extract inhibits the production of nitric oxide and proinflammatory cytokines in LPS-stimulated BV2 microglial cells via the NF-kappaB pathway," *Food and Chemical Toxicology*, vol. 47, no. 6, pp. 1190–1197, 2009.

[58] S. H. M. Habib, S. Makpol, N. A. A. Hamid, S. Das, W. Z. W. Ngah, and Y. A. M. Yusof, "Ginger extract (*Zingiber officinale*) has anti-cancer and anti-inflammatory effects on ethionine-induced hepatoma rats," *Clinics*, vol. 63, no. 6, pp. 807–813, 2008.

[59] R. C. Lantz, G. J. Chen, M. Sarihan, A. M. Solyom, S. D. Jolad, and B. N. Timmermann, "The effect of extracts from ginger rhizome on inflammatory mediator production," *Phytomedicine*, vol. 14, no. 2-3, pp. 123–128, 2007.

[60] R. D. Altman and K. C. Marcussen, "Effects of a ginger extract on knee pain in patients with osteoarthritis," *Arthritis & Rheumatism*, vol. 44, no. 11, pp. 2531–2538, 2001.

[61] H. Bliddal, A. Rosetzsky, P. Schlichting et al., "A randomized, placebo-controlled, cross-over study of ginger extracts and ibuprofen in osteoarthritis," *Osteoarthritis and Cartilage*, vol. 8, no. 1, pp. 9–12, 2000.

[62] R. Grzanna, L. Lindmark, and C. G. Frondoza, "Ginger—an herbal medicinal product with broad anti-inflammatory actions," *Journal of Medicinal Food*, vol. 8, no. 2, pp. 125–132, 2005.

[63] D. Shah, M. Gandhi, A. Kumar, N. Cruz-Martins, R. Sharma, and S. Nair, "Current insights into epigenetics, noncoding RNA interactome and clinical pharmacokinetics of dietary polyphenols in cancer chemoprevention," *Critical Reviews in Food Science and Nutrition*, pp. 1–37, 2021.

[64] R. Sharma, A. Kabra, M. M. Rao, and P. K. Prajapati, "Herbal and holistic solutions for neurodegenerative and depressive disorders: leads from ayurveda," *Current Pharmaceutical Design*, vol. 24, no. 22, pp. 2597–2608, 2018.

[65] S. J. Hewlings and D. S. Kalman, "Curcumin: a review of its effects on human health," *Foods*, vol. 6, no. 10, p. 92, 2017.

[66] K. I. Priyadarsini, "The chemistry of curcumin: from extraction to therapeutic agent," *Molecules*, vol. 19, no. 12, pp. 20091–20112, 2014.

[67] S. C. Gupta, S. Patchva, and B. B. Aggarwal, "Therapeutic roles of curcumin: lessons learned from clinical trials," *The AAPS Journal*, vol. 15, no. 1, pp. 195–218, 2013.

[68] B. B. Aggarwal and K. B. Harikumar, "Potential therapeutic effects of curcumin, the anti-inflammatory agent, against neurodegenerative, cardiovascular, pulmonary, metabolic, autoimmune and neoplastic diseases," *The International Journal of Biochemistry & Cell Biology*, vol. 41, no. 1, pp. 40–59, 2009.

[69] M. L. A. D. Lestari and G. Indrayanto, "Curcumin," *Profiles of Drug Substances, Excipients and Related Methodology*, vol. 39, pp. 113–204, 2014.

[70] G. B. Mahady, S. L. Pendland, G. Yun, and Z. Z. Lu, "Turmeric (*Curcuma longa*) and curcumin inhibit the growth of *Helicobacter pylori*, a group 1 carcinogen," *Anticancer Research*, vol. 22, no. 6C, pp. 4179–4181, 2002.

[71] R. C. Reddy, P. G. Vatsala, V. G. Keshamouni, G. Padmanaban, and P. N. Rangarajan, "Curcumin for malaria therapy," *Biochemical and Biophysical Research Communications*, vol. 326, no. 2, pp. 472–474, 2005.

[72] L. Vera-Ramirez, P. Pérez-Lopez, A. Varela-Lopez, M. C. Ramirez-Tortosa, M. Battino, and J. L. Quiles, "Curcumin and liver disease," *BioFactors*, vol. 39, no. 1, pp. 88–100, 2013.

[73] L. Wright, J. Frye, B. Gorti, B. Timmermann, and J. Funk, "Bioactivity of turmeric-derived curcuminoids and related metabolites in breast cancer," *Current Pharmaceutical Design*, vol. 19, no. 34, pp. 6218–6225, 2013.

[74] V. Kuptniratsaikul, P. Dajpratham, W. Taechaarpornkul et al., "Efficacy and safety of *Curcuma domestica* extracts compared with ibuprofen in patients with knee osteoarthritis: a multicenter study," *Clinical Interventions in Aging*, vol. 9, pp. 451–458, 2014.

[75] Y. Panahi, M. S. Hosseini, N. Khalili et al., "Effects of curcumin on serum cytokine concentrations in subjects with metabolic syndrome: a post-hoc analysis of a randomized controlled trial," *Biomedicine & Pharmacotherapy*, vol. 82, pp. 578–582, 2016.

[76] F. Mazzolani and S. Togni, "Oral administration of a curcumin-phospholipid delivery system for the treatment of central serous chorioretinopathy: a 12-month follow-up study," *Clinical Ophthalmology*, vol. 7, pp. 939–945, 2013.

[77] P. Allegri, A. Mastromarino, and P. Neri, "Management of chronic anterior uveitis relapses: efficacy of oral phospholipidic curcumin treatment. Long-term follow-up," *Clinical Ophthalmology*, vol. 4, pp. 1201–1206, 2010.

[78] N. Alamdari, P. O'Neal, and P.-O. Hasselgren, "Curcumin and muscle wasting—a new role for an old drug?" *Nutrition*, vol. 25, no. 2, pp. 125–129, 2009.

[79] A. Shehzad and Y. S. Lee, "Molecular mechanisms of curcumin action: signal transduction," *BioFactors*, vol. 39, no. 1, pp. 27–36, 2013.

[80] M. Vitadello, E. Germinario, B. Ravara, L. D. Libera, D. Danieli-Betto, and L. Gorza, "Curcumin counteracts loss of force and atrophy of hindlimb unloaded rat soleus by

hampering neuronal nitric oxide synthase untethering from sarcolemma," *Journal of Physiology*, vol. 592, no. 12, pp. 2637–2652, 2014.

[81] G. Gutierrez-Salmean, T. P. Ciaraldi, L. Nogueira et al., "Effects of (−)-epicatechin on molecular modulators of skeletal muscle growth and differentiation," *The Journal of Nutritional Biochemistry*, vol. 25, no. 1, pp. 91–94, 2014.

[82] M. H. Radha and N. P. Laxmipriya, "Evaluation of biological properties and clinical effectiveness of *Aloe vera*: a systematic review," *Journal of Traditional and Complementary Medicine*, vol. 5, no. 1, pp. 21–26, 2015.

[83] A. Gupta and S. Rawat, "Clinical importance of *Aloe vera*: review," *Research Journal of Topical and Cosmetic Sciences*, vol. 8, no. 1, p. 30, 2017.

[84] M. Hęś, K. Dziedzic, D. Górecka, A. Jędrusek-Golińska, and E. Gujska, "*Aloe vera* (L.) Webb.: natural sources of antioxidants–a review," *Plant Foods for Human Nutrition*, vol. 74, no. 3, pp. 255–265, 2019.

[85] L. L. O. Rodrigues, A. C. L. de Oliveira, S. Tabrez et al., "Mutagenic, antioxidant and wound healing properties of Aloe vera," *Journal of Ethnopharmacology*, vol. 227, pp. 191–197, 2018.

[86] P. K. Sahu, D. D. Giri, R. Singh et al., "Therapeutic and medicinal uses of *Aloe vera*: a review," *Pharmacology &Pharmacy*, vol. 4, no. 8, pp. 599–610, 2013.

[87] A. Surjushe, R. Vasani, and D. G. Saple, "*Aloe vera*: a short review," *Indian Journal of Dermatology*, vol. 53, no. 4, p. 163, 2008.

[88] M. D. Boudreau and F. A. Beland, "An evaluation of the biological and toxicological properties of *Aloe barbadensis* (Miller), *Aloe vera*," *Journal of Environmental Science and Health, Part C*, vol. 24, no. 1, pp. 103–154, 2006.

[89] P. Sharma, A. C. Kharkwal, H. Kharkwal, M. Z. Abdin, and A. Varma, "A review on pharmacological properties of *Aloe vera*," *International Journal of Pharmaceutical Sciences Review and Research*, vol. 29, no. 2, pp. 31–37, 2014.

[90] M. M. Budai, A. Varga, S. Milesz, J. Tőzsér, and S. Benkő, "Aloe vera downregulates LPS-induced inflammatory cytokine production and expression of NLRP3 inflammasome in human macrophages," *Molecular Immunology*, vol. 56, no. 4, pp. 471–479, 2013.

[91] A. D. Kshirsagar, P. V. Panchal, U. N. Harle, R. K. Nanda, and H. M. Shaikh, "Anti-inflammatory and antiarthritic activity of anthraquinone derivatives in rodents," *International Journal of Inflammation*, vol. 2014, Article ID 690596, 12 pages, 2014.

[92] M. Klimek-Szczykutowicz, A. Szopa, and H. Ekiert, "*Citrus limon* (Lemon) phenomenon—a review of the chemistry, pharmacological properties, applications in the modern pharmaceutical, food, and cosmetics industries, and biotechnological studies," *Plants*, vol. 9, no. 1, p. 119, 2020.

[93] P. Goetz, "*Citrus limon* (L) Burm. f. (Rutacées) citronnier," *Phytothérapie*, vol. 12, no. 2, pp. 116–121, 2014.

[94] K. Robards and M. Antolovich, "Analytical chemistry of fruit bioflavonoids a review," *The Analyst*, vol. 122, no. 2, pp. 11R–34R, 1997.

[95] G.-S. Zou, S.-J. Li, S. L. Zheng, X. Pan, and Z. P Huang, "Lemon-peel extract ameliorates rheumatoid arthritis by reducing xanthine oxidase and inflammatory cytokine levels," *Journal of the Taiwan Institute of Chemical Engineers*, vol. 93, pp. 54–62, 2018.

[96] B. H. Kim, J. H. Yoon, J. I. Yang et al., "Guggulsterone attenuates activation and survival of hepatic stellate cell by inhibiting nuclear factor kappa B activation and inducing apoptosis," *Journal of Gastroenterology and Hepatology*, vol. 28, no. 12, pp. 1859–1868, 2013.

[97] V. Sharma, A. Katiyar, and R. C. Agrawal, "*Glycyrrhiza glabra*: chemistry and pharmacological activity," *Sweeteners. Published online*, p. 87, 2018.

[98] P. Bradley, *British herbal compendium a Handbook of Scientific Information of Widely Used Plant Drugs*, British Herbal Medicine Association, Exeter, UK, 2006.

[99] D. Hoffmann, *Medical Herbalism: The Science and Practice of Herbal Medicine*, Simon and Schuster, New York, NY, USA, 2003.

[100] R. Sharma and N. Martins, "Telomeres, DNA damage and ageing: potential leads from ayurvedic rasayana (anti-ageing) drugs," *Journal of Clinical Medicine*, vol. 9, no. 8, p. 2544, 2020.

[101] Y. Yamamura, J. Kawakami, T. Santa et al., "Pharmacokinetic profile of glycyrrhizin in healthy volunteers by a new high-performance liquid chromatographic method," *Journal of Pharmaceutical Sciences*, vol. 81, no. 10, pp. 1042–1046, 1992.

[102] J. Vaya, P. A. Belinky, and M. Aviram, "Antioxidant constituents from licorice roots: isolation, structure elucidation and antioxidative capacity toward LDL oxidation," *Free Radical Biology and Medicine*, vol. 23, no. 2, pp. 302–313, 1997.

[103] S. Tamir, M. Eizenberg, D. Somjen, S. Izrael, and J. Vaya, "Estrogen-like activity of glabrene and other constituents isolated from *licorice* root," *The Journal of Steroid Biochemistry and Molecular Biology*, vol. 78, no. 3, pp. 291–298, 2001.

[104] A. Geraci, R. Calvani, E. Ferri, E. Marzetti, B. Arosio, and M. Cesari, "Sarcopenia and menopause: the role of estradiol," *Frontiers in Endocrinology*, vol. 12, Article ID 682012, 2021.

[105] S. K. Maurya, K. Raj, and A. K. Srivastava, "Anti-dyslipidaemic activity of *Glycyrrhiza glabra* in high fructose diet induced dsyslipidaemic Syrian golden hamsters," *Indian Journal of Clinical Biochemistry*, vol. 24, no. 4, pp. 404–409, 2009.

[106] S. Varsha, R. C. Agrawal, and P. Sonam, "Phytochemical screening and determination of anti-bacterial and anti-oxidant potential of *Glycyrrhiza glabra* root extracts," *Journal of Environmental Research And Development*, vol. 7, no. 4A, p. 1552, 2013.

[107] D. M. Biondi, C. Rocco, and G. Ruberto, "New dihydrostilbene derivatives from the leaves of *Glycyrrhiza glabra* and evaluation of their antioxidant activity," *Journal of Natural Products*, vol. 66, no. 4, pp. 477–480, 2003.

[108] M. Malek Jafarian and K. Ghazvini, "*In vitro* susceptibility of *Helicobacter pylori* to licorice extract," *Iranian Journal of Pharmaceutical Research*, vol. 1, pp. 69–72, 2010.

[109] A. M. Aly, L. Al-Alousi, and H. A. Salem, "Licorice: a possible anti-inflammatory and anti-ulcer drug," *AAPS PharmSciTech*, vol. 6, no. 1, pp. E74–E82, 2005.

[110] I. Suntar, H. Khan, S. Patel, R. Celano, and L. Rastrelli, "An overview on *Citrus aurantium* L.: its functions as food ingredient and therapeutic agent," *Oxidative Medicine and Cellular Longevity*, vol. 2018, Article ID 7864269, 1-12 pages, 2018.

[111] Ş Karabıyıklı, H. Değirmenci, and M. Karapınar, "Inhibitory effect of sour orange (*Citrus aurantium*) juice on *Salmonella* typhimurium and *Listeria monocytogenes*," *LWT—Food Science and Technology*, vol. 55, no. 2, pp. 421–425, 2014.

[112] T. M. Moraes, H. Kushima, F. C. Moleiro et al., "Effects of limonene and essential oil from *Citrus aurantium* on gastric

mucosa: role of prostaglandins and gastric mucus secretion," *Chemico-Biological Interactions*, vol. 180, no. 3, pp. 499–505, 2009.

[113] I. Süntar, H. Haroon, S. Patel, R. Celano, and L. Rastrelli, "An overview on Citrus aurantium L.: its functions as food ingredient and therapeutic agent," *Oxidative Medicine and Cellular Longevity*, vol. 2018, Article ID 7864269, pp. 1–12, 2018.

[114] D. Hamdan, M. L. Ashour, S. Mulyaningsih, A. El-Shazly, and M. Wink, "Chemical composition of the essential oils of variegated pink-fleshed lemon (*Citrusx limon* L. Burm. f.) and their anti-inflammatory and antimicrobial activities," *Zeitschrift für Naturforschung C*, vol. 68, no. 7-8, p. 275, 2013.

[115] S. R. Kang, K. I. L. Park, H. S. Park et al., "Anti-inflammatory effect of flavonoids isolated from Korea *Citrus aurantium* L. on lipopolysaccharide-induced mouse macrophage RAW 264.7 cells by blocking of nuclear factor-kappa B (NF-κB) and mitogen-activated protein kinase (MAPK) signalling pathways," *Food Chemistry*, vol. 129, no. 4, pp. 1721–1728, 2011.

[116] L. Liu, S. Shan, K. Zhang, Z. Q. Ning, X. P. Lu, and Y. Y. Cheng, "Naringenin and hesperetin, two flavonoids derived from *Citrus aurantium* up-regulate transcription of adiponectin," *Phytotherapy Research*, vol. 22, no. 10, pp. 1400–1403, 2008.

[117] A. de Moraes Pultrini, L. Almeida Galindo, and M. Costa, "Effects of the essential oil from *Citrus aurantium* L. in experimental anxiety models in mice," *Life Sciences*, vol. 78, no. 15, pp. 1720–1725, 2006.

[118] K.-I. Park, H.-S. Park, M.-K. Kim et al., "Flavonoids identified from Korean *Citrus aurantium* L. inhibit non-small cell lung cancer growth *in vivo* and *in vitro*," *Journal of Functional Foods*, vol. 7, pp. 287–297, 2014.

[119] A. Fugh-Berman and A. Myers, "*Citrus aurantium*, an ingredient of dietary supplements marketed for weight loss: current status of clinical and basic research," *Experimental Biology and Medicine*, vol. 229, no. 8, pp. 698–704, 2004.

[120] H. Khan, S. M. Nabavi, A. Sureda et al., "Therapeutic potential of songorine, a diterpenoid alkaloid of the genus *Aconitum*," *European Journal of Medicinal Chemistry*, vol. 153, pp. 29–33, 2018.

[121] S. F. Nabavi, H. Khan, G. D'onofrio et al., "Apigenin as neuroprotective agent: of mice and men," *Pharmacological Research*, vol. 128, pp. 359–365, 2018.

[122] H. Khan, H. Khan, S. M. Nabavi, and S. Habtemariam, "Antidiabetic potential of peptides: future prospects as therapeutic agents," *Life Sciences*, vol. 193, pp. 153–158, 2018.

[123] J. A. Kim, H. S. Park, S. R. Kang et al., "Suppressive effect of flavonoids from Korean *Citrus aurantium* L. on the expression of inflammatory mediators in L6 skeletal muscle cells," *Phytotherapy Research*, vol. 26, no. 12, pp. 1904–1912, 2012.

[124] J.-H. Shang, X.-H. Cai, T. Feng et al., "Pharmacological evaluation of *Alstonia scholaris*: anti-inflammatory and analgesic effects," *Journal of Ethnopharmacology*, vol. 129, no. 2, pp. 174–181, 2010.

[125] Y. Xu, T. Feng, X. H. Cai, and X. D. Luo, "A new C13-norisoprenoid from leaves of *Alstonia scholaris*," *Chinese Journal of Natural Medicines*, vol. 7, no. 1, pp. 21–23, 2009.

[126] T. Feng, X. H. Cai, Z. Z. Du, and X. D. Luo, "Iridoids from the bark of *Alstonia scholaris*," *Helvetica Chimica Acta*, vol. 91, no. 12, pp. 2247–2251, 2008.

[127] T. Feng, X.-H. Cai, P.-J. Zhao, Z.-Z. Du, W.-Q. Li, and X.-D. Luo, "Monoterpenoid indole alkaloids from the bark of *Alstonia scholaris*," *Planta Medica*, vol. 75, no. 14, pp. 1537–1541, 2009.

[128] D. U. Guo-Shun, S. Jian-Hua, C. A. I. Xiang-Hai, and L. U. O. Xiao-Dong, "Antitussive constituents from roots of *Alstonia scholaris* (Apocynaceae)," *Plant Divers*, vol. 29, no. 03, p. 366, 2007.

[129] G. S. Du, X. H. Cai, J. H. Shang, and X. D. Luo, "Non-alkaline constituents from the leaf of *Alstonia scholaris*," *Chinese Journal of Natural Medicines*, vol. 5, pp. 259–262, 2007.

[130] X.-H. Cai, Z.-Z. Du, and X.-D. Luo, "Unique monoterpenoid indole alkaloids from *Alstonia scholaris*," *Organic Letters*, vol. 9, no. 9, pp. 1817–1820, 2007.

[131] X.-H. Cai, Y.-P. Liu, T. Feng, and X.-D. Luo, "Picrinine-type alkaloids from the leaves of *Alstonia scholaris*," *Chinese Journal of Natural Medicines*, vol. 6, no. 1, pp. 20–22, 2008.

[132] X.-H. Cai, Q.-G. Tan, Y.-P. Liu et al., "A cage-monoterpene indole alkaloid from *Alstonia scholaris*," *Organic Letters*, vol. 10, no. 4, pp. 577–580, 2008.

[133] Y.-L. Zhao, Z.-F. Yang, J.-H. Shang et al., "Effects of indole alkaloids from leaf of *Alstonia scholaris* on post-infectious cough in mice," *Journal of Ethnopharmacology*, vol. 218, pp. 69–75, 2018.

[134] A. Yagi and B. Pal Yu, "Prophylactic aloe components on autoimmune diseases: barbaloin, aloe-emodin, emodin, and fermented butyrate," *Journal of Gastroenterology and Hepatology Research*, vol. 7, no. 2, pp. 2535–2541, 2018.

[135] M. S. Khyade, N. P. Vaikos, and N. P. Vaikos, "Phytochemical and antibacterial properties of leaves of *Alstonia scholaris* R. Br," *African Journal of Biotechnology*, vol. 8, no. 22, pp. 6434–6436, 2009.

[136] O. P. Tiwari and M. Sharma, "Anti-arthritic evaluation of some traditionally used medicinal plants in FCA induced arthritis in rats," *Journal of Drug Delivery and Therapeutics*, vol. 7, no. 5, pp. 74–79, 2017.

[137] C. K. Subraya and D. Gupta, "Antioxidant anti-inflammatory activity of *Alstonia scholaris* R," *Br. Stem Bark Extract. Free Radicals Antioxidants*, vol. 2, no. 2, pp. 55–57, 2012.

[138] M. N. Ghosh, R. M. Banerjie, and S. K. Mukherji, "Capillary permeability-i creasing property of hyaluronidase in rat," *Indian Journal of Physiology Pharmacology*, vol. 7, pp. 17–21, 1963.

[139] J. A. Castro, H. A. Sasame, H. Sussman, and J. R. Gillette, "Diverse effects of SKF 525-A and antioxidants on carbon tetrachloride-induced changes in liver microsomal P-450 content and ethylmorphine metabolism," *Life Sciences*, vol. 7, no. 3, pp. 129–136, 1968.

[140] L. Gutierrez, H. Sumano, F. Rivero, and Y. Alcala-Canto, "Ixodicide activity of eysenhardtia polystachya against *Rhipicephalus* (boophilus) microplus1," *Journal of Animal Science*, vol. 93, no. 4, pp. 1980–1986, 2015.

[141] A. Garcia-Campoy, E. Garcia, and A. Muñiz-Ramirez, "Phytochemical and pharmacological study of the *Eysenhardtia* genus," *Plants*, vol. 9, no. 9, p. 1124, 2020.

[142] A. J. Alonso-Castro, J. R. Zapata-Morales, V. Arana-Argáez et al., "Pharmacological and toxicological study of a chemical-standardized ethanol extract of the branches and leaves from *Eysenhardtia polystachya* (Ortega) Sarg. (Fabaceae)," *Journal of Ethnopharmacology*, vol. 224, pp. 314–322, 2018.

[143] S. S. Pablo-Pérez, B. Parada-Cruz, O. C. Barbier, and M. E. Meléndez-Camargo, "The ethanolic extract of *Eysenhardtia polystachya* (Ort.) Sarg. bark and its fractions delay the progression of rheumatoid arthritis and show antinociceptive activity in murine models," *Iranian Journal of*

Pharmaceutical Research: Iranian Journal of Pharmaceutical Research, vol. 17, no. 1, pp. 236–248, 2018.

[144] F. Pan, L. Chen, Y. Jiang et al., "Bio-based UV protective films prepared with polylactic acid (PLA) and *Phoebe zhennan* extractives," *International Journal of Biological Macromolecules*, vol. 119, pp. 582–587, 2018.

[145] M. P. G. Rosa, "Evaluation of anti-inflammatory activity of the bark of *Eysenhardtia polystachya* in experimental animal models," *African Journal of Pharmacy and Pharmacology*, vol. 9, no. 8, pp. 230–236, 2015.

[146] H. C. Nguyen, C.-C. Chen, K.-H. Lin, P.-Y. Chao, H.-H. Lin, and M.-Y. Huang, "Bioactive compounds, antioxidants, and health benefits of sweet potato leaves," *Molecules*, vol. 26, no. 7, p. 1820, 2021.

[147] H. H. Ishida, N. S. Suzuno, S. Innami, T. Todokoro, and A. Mackawa, "Nutritive evaluation on chemical components of leaves, stalks and stems of sweet potatoes (*Ipomoea batatas* poir)," *Food Chemistry*, vol. 68, no. 3, pp. 359–367, 2000.

[148] S. Shekhar, D. Mishra, A. K. Buragohain, S. Chakraborty, and N. Chakraborty, "Comparative analysis of phytochemicals and nutrient availability in two contrasting cultivars of sweet potato (*Ipomoea batatas* L.)," *Food Chemistry*, vol. 173, pp. 957–965, 2015.

[149] S. Nakachi, A. Tokeshi, R. Takamatsu et al., "The modifying effects of the extract from Okinawan sweet potato leaves in mouse colon carcinogenesis," *Cancer Research*, vol. 76840 pages, 2016.

[150] M. Majid, B. Nasir, S. S. Zahra, M. R. Khan, B. Mirza, and I. U Haq, "*Ipomoea batatas* L. Lam. ameliorates acute and chronic inflammations by suppressing inflammatory mediators, a comprehensive exploration using *in vitro* and *in vivo* models," *BMC Complementary and Alternative Medicine*, vol. 18, no. 1, p. 216, 2018.

[151] S. Islam, *Nutritional and Medicinal Qualities of Sweet Potato Tops and Leaves*, Cooperative Extension Service, University of Arkansas, Fayetteville, AR, USA, 2014.

[152] K. Ishiguro, J. Toyama, M. D. S. Islam et al., "Suioh, a new sweetpotato cultivar for utilization in vegetable greens," *Acta Hortic*, vol. 637, pp. 339–346, 2004.

[153] M. S. Islam, M. Yoshimoto, S. Yahara, S. Okuno, K. Ishiguro, and O. Yamakawa, "Identification and characterization of foliar polyphenolic composition in sweetpotato (*Ipomoea batatas* L.) genotypes," *Journal of Agricultural and Food Chemistry*, vol. 50, no. 13, pp. 3718–3722, 2002.

[154] M. S. Islam, M. Yoshimoto, and O. Yamakawa, "Distribution and physiological functions of caffeoylquinic acid derivatives in leaves of sweetpotato genotypes," *Journal of Food Science*, vol. 68, no. 1, pp. 111–116, 2003.

[155] J. H. Choi, Y. P. Hwang, C. Y. Choi, Y. C. Chung, and H. G. Jeong, "Anti-fibrotic effects of the anthocyanins isolated from the purple-fleshed sweet potato on hepatic fibrosis induced by dimethylnitrosamine administration in rats," *Food and Chemical Toxicology*, vol. 48, no. 11, pp. 3137–3143, 2010.

[156] S. Tabassum, S. Mahmood, J. Hanif, M. Hina, and B. Uzair, "An overview of medicinal importance of *Swertia chirayita*," *International Journal of Applied Research*, vol. 2, no. 1, 2012.

[157] P. Dey, J. Singh, J. K. Suluvoy, K. J. Dilip, and J. Nayak, "Utilization of *Swertia chirayita* plant extracts for management of diabetes and associated disorders: present status, future prospects and limitations," *Nature Products Bioprospect*, vol. 10, pp. 1–13, 2020.

[158] R. D. Gaur, *Flora of the District Garhwal, North West Himalaya*, Transmedia, Srinagar, India, 1999.

[159] V. Kumar and J. Van Staden, "A review of *Swertia chirayita* (Gentianaceae) as a traditional medicinal plant," *Frontiers in Pharmacology*, vol. 6, p. 308, 2015.

[160] S. K. Bhattacharya, "Chemical constituents of gentianaceae XI: antipsychotic activity of gentianine," *Journal of Pharmaceutical Sciences*, vol. 63, no. 8, pp. 1314–1320, 1974.

[161] Y. Chen, B. Huang, J. He, L. Han, Y. Zhan, and Y. Wang, "*In vitro* and *in vivo* antioxidant effects of the ethanolic extract of *Swertia chirayita*," *Journal of Ethnopharmacology*, vol. 136, no. 2, pp. 309–315, 2011.

[162] "*Terminalia chebula* Retz. fruit extracts inhibit bacterial triggers of some autoimmune diseases and potentiate the activity of tetracycline," *Indian Journal of Microbiology*, vol. 58, no. 4, pp. 496–506, 2018.

[163] S. Das and S. Barman, "Antidiabetic and antihyperlipidemic effects of ethanolic extract of leaves of *Punica granatum* in alloxan-induced non-insulin-dependent diabetes mellitus albino rats," *Indian Journal of Pharmacology*, vol. 44, no. 2, p. 219, 2012.

[164] S. Banerjee, T. K. Sur, S. Mandal, P. C. Das, and S. Sikdar, "Assessment of the anti-inflammatory effects of *Swertia chirata* in acute and chronic experimental models in male albino rats," *Indian Journal of Pharmacology*, vol. 32, no. 1, pp. 21–24, 2000.

[165] O. A. Eldahshan and M. M. A. Daim, "Phytochemical study, cytotoxic, analgesic, antipyretic and anti-inflammatory activities of *Strychnos nux-vomica*," *Cytotechnology*, vol. 67, no. 5, pp. 831–844, 2015.

[166] S. Chaurasia, "Anti-inflammatory and antioxidant activity of *Strychnos nux vomica* Linn," *American-Eurasian Journal of Sustainable Agriculture*, vol. 3, no. 2, pp. 244–252, 2009.

[167] S. Ekambaram, S. S. Perumal, and V. Subramanian, "Evaluation of antiarthritic activity of *Strychnos potatorum* Linn seeds in freund's adjuvant induced arthritic rat model," *BMC Complementary and Alternative Medicine*, vol. 10, no. 1, p. 56, 2010.

[168] H. Lad and D. Bhatnagar, "Amelioration of oxidative and inflammatory changes by *Swertia chirayita* leaves in experimental arthritis," *Inflammopharmacology*, vol. 24, no. 6, pp. 363–375, 2016.

[169] M. E. González-Trujano, E. I. Peña, A. L. Martínez et al., "Evaluation of the antinociceptive effect of *Rosmarinus officinalis* L. using three different experimental models in rodents," *Journal of Ethnopharmacology*, vol. 111, no. 3, pp. 476–482, 2007.

[170] L. Perez-Fons, M. T. Garzon, and V. Micol, "Relationship between the antioxidant capacity and effect of rosemary (*Rosmarinus officinalis* L.) polyphenols on membrane phospholipid order," *Journal of Agricultural and Food Chemistry*, vol. 58, no. 1, pp. 161–171, 2010.

[171] M. S. Brewer, "Natural antioxidants: sources, compounds, mechanisms of action, and potential applications," *Comprehensive Reviews in Food Science and Food Safety*, vol. 10, no. 4, pp. 221–247, 2011.

[172] A. Rašković, I. Milanović, N. Pavlović, T. Ćebović, S. Vukmirović, and M. Mikov, "Antioxidant activity of rosemary (*Rosmarinus officinalis* L.) essential oil and its hepatoprotective potential," *BMC Complementary and Alternative Medicine*, vol. 14, no. 1, p. 225, 2014.

[173] J. R. De Oliveira, S. E. A. Camargo, and L. D. De Oliveira, "*Rosmarinus officinalis* L. (rosemary) as therapeutic and prophylactic agent," *Journal of Biomedical Science*, vol. 26, no. 1, p. 5, 2019.

[174] R. S. Borges, B. L. S. Ortiz, A. C. M. Pereira, H. Keita, and J. C. T. Carvalho, "*Rosmarinus officinalis* essential oil: a review of its phytochemistry, anti-inflammatory activity, and mechanisms of action involved," *Journal of Ethnopharmacology*, vol. 229, pp. 29–45, 2019.

[175] L. S. Einbond, H. A. Wu, R. Kashiwazaki et al., "Carnosic acid inhibits the growth of ER-negative human breast cancer cells and synergizes with curcumin," *Fitoterapia*, vol. 83, no. 7, pp. 1160–1168, 2012.

[176] G. A. Gonçalves, R. C. G. Corrêa, L. Barros et al., "Effects of *in vitro* gastrointestinal digestion and colonic fermentation on a rosemary (*Rosmarinus officinalis* L) extract rich in rosmarinic acid," *Food Chemistry*, vol. 271, pp. 393–400, 2019.

[177] M. A. Medina, B. Martínez-Poveda, M. I. Amores-Sánchez, and A. R. Quesada, "Hyperforin: more than an antidepressant bioactive compound?" *Life Sciences*, vol. 79, no. 2, pp. 105–111, 2006.

[178] A. L. Martínez, M. E. González-Trujano, F. Pellicer, F. J. López-Muñoz, and A. Navarrete, "Antinociceptive effect and GC/MS analysis of *Rosmarinus officinalis* L. essential oil from its aerial parts," *Planta Medica*, vol. 75, no. 05, pp. 508–511, 2009.

[179] D. Lukaczer, G. Darland, M. Tripp et al., "A Pilot trial evaluating meta050, a proprietary combination of reduced iso-alpha acids, rosemary extract and oleanolic acid in patients with arthritis and fibromyalgia," *Phytotherapy Research*, vol. 19, no. 10, pp. 864–869, 2005.

[180] A. Sahu, N. Rawal, and M. K. Pangburn, "Inhibition of complement by covalent attachment of rosmarinic acid to activated C3b," *Biochemical Pharmacology*, vol. 57, no. 12, pp. 1439–1446, 1999.

[181] M. A. Abu-Al-Basal, "Healing potential of *Rosmarinus officinalis* L. on full-thickness excision cutaneous wounds in alloxan-induced-diabetic BALB/c mice," *Journal of Ethnopharmacology*, vol. 131, no. 2, pp. 443–450, 2010.

[182] A. Miceli, A. Aleo, O. Corona, M. T. Sardina, C. Mammina, and L. Settanni, "Antibacterial activity of *Borago officinalis* and *Brassica juncea* aqueous extracts evaluated *in vitro* and in situ using different food model systems," *Food Control*, vol. 40, pp. 157–164, 2014.

[183] M. Mirsadraee, S. Khashkhashi Moghaddam, P. Saeedi, and S. Ghaffari, "Effect of *Borago officinalis* extract on moderate persistent asthma: a phase two randomized, double blind, placebo-controlled clinical trial," *Tanaffos*, vol. 15, no. 3, pp. 168–174, 2016.

[184] R. E. Kast, "Borage oil reduction of rheumatoid arthritis activity may be mediated by increased cAMP that suppresses tumor necrosis factor-alpha," *International Immunopharmacology*, vol. 1, no. 12, pp. 2197–2199, 2001.

[185] K. L. Soeken, S. A. Miller, and E. Ernst, "Herbal medicines for the treatment of rheumatoid arthritis: a systematic review," *Rheumatology*, vol. 42, no. 5, pp. 652–659, 2003.

[186] M. Ghasemian, S. Owlia, and M. B. Owlia, "Review of anti-inflammatory herbal medicines," *Advances in Pharmacological Sciences*, vol. 2016, Article ID 9130979, 11 pages, 2016.

[187] A. R. Setty and L. H. Sigal, "Herbal medications commonly used in the practice of rheumatology: mechanisms of action, efficacy, and side effects," *Seminars in Arthritis and Rheumatism*, vol. 34, pp. 773–784, 2005.

[188] T. H.-W. Huang, V. H. Tran, R. K. Duke et al., "Harpagoside suppresses lipopolysaccharide-induced iNOS and COX-2 expression through inhibition of NF-κB activation," *Journal of Ethnopharmacology*, vol. 104, no. 1-2, pp. 149–155, 2006.

[189] V. Gyurkovska, K. Alipieva, A. Maciuk et al., "Anti-inflammatory activity of Devil's claw *in vitro* systems and their active constituents," *Food Chemistry*, vol. 125, no. 1, pp. 171–178, 2011.

[190] B. L. Fiebich, B. Fiebich, M. Heinrich, K. Hiller, and N. Kammerer, "Inhibition of TNF-α synthesis in LPS-stimulated primary human monocytes by *Harpagophytum* extract SteiHap 69," *Phytomedicine*, vol. 8, no. 1, pp. 28–30, 2001.

[191] D. Loew, J. Möllerfeld, A. Schrödter, S. Puttkammer, and M. Kaszkin, "Investigations on the pharmacokinetic properties of *Harpagophytum* extracts and their effects on eicosanoid biosynthesis *in vitro* and *ex vivo*," *Clinical Pharmacology and Therapeutics (St. Louis)*, vol. 69, no. 5, pp. 356–364, 2001.

[192] R. Grahame and B. V. Robinson, "Devils's claw (*Harpagophytum procumbens*): pharmacological and clinical studies," *Annals of the Rheumatic Diseases*, vol. 40, no. 6, p. 632, 1981.

[193] L. W. Whitehouse, M. Znamirowska, and C. J. Paul, "Devil's claw (*Harpagophytum procumbens*): no evidence for anti-inflammatory activity in the treatment of arthritic disease," *Canadian Medical Association Journal*, vol. 129, no. 3, pp. 249–251, 1983.

[194] R. Sharma, J. Hazra, and P. K. Prajapati, "Knowledge and awareness of pharmacovigilance among ayurveda physicians in Himachal Pradesh," *Ancient Science of Life*, vol. 36, no. 4, p. 234, 2017.

[195] R. Sharma, R. Galib, and P. K. Prajapati, "Good pharmacovigilance practice: accountability of ayurvedic pharmaceutical companies," *Ancient Science of Life*, vol. 36, no. 3, p. 167, 2017.

Hindawi
Evidence-Based Complementary and Alternative Medicine
Volume 2022, Article ID 1488905, 19 pages
https://doi.org/10.1155/2022/1488905

Research Article

CUL3 and COPS5 Related to the Ubiquitin-Proteasome Pathway Are Potential Genes for Muscle Atrophy in Mice

Qun Xu, Jinyou Li, Ji Yang, and Zherong Xu

Department of Geriatrics, The First Affiliated Hospital, Zhejiang University, School of Medicine, No. 79, Qingchun Road, Hangzhou, Zhejiang, China

Correspondence should be addressed to Zherong Xu; zherongxu0809@outlook.com

Received 17 February 2022; Revised 29 April 2022; Accepted 3 May 2022; Published 30 June 2022

Academic Editor: Atul Kabra

Sarcopenia is a condition that reduces muscle mass and exercise capacity. Muscle atrophy is a common manifestation of sarcopenia and can increase morbidity and mortality in specific patient populations. The aim of this study was to identify novel prognostic biomarkers for muscle atrophy and associated pathway analysis using bioinformatics methods. The samples were first divided into different age groups and different muscle type groups, respectively, and each of these samples was analyzed for differences to obtain two groups of differentially expressed genes (DEGs). The two groups of DEGs were intersected using Venn diagrams to obtain 1,630 overlapping genes, and enrichment analysis was performed to observe the Gene Ontology (GO) functional terms of overlapping genes and the enrichment of the Kyoto Encyclopedia of Genes and Genomes (KEGG) pathway. Subsequently, WGCNA (weighted gene coexpression network analysis) was used to find gene modules associated with both the age and muscle type to obtain the lightgreen module. The genes in the key modules were analyzed using PPI, and the top five genes were obtained using the MCC (maximum correntropy criterion) algorithm. Finally, CUL3 and COPS5 were obtained by comparing gene expression levels and analyzing the respective KEGG pathways using gene set enrichment analysis (GSEA). In conclusion, we identified that CUL3 and COPS5 may be novel prognostic biomarkers in muscle atrophy based on bioinformatics analysis. CUL3 and COPS5 are associated with the ubiquitin-proteasome pathway.

1. Introduction

The skeletal muscle consists of muscle fibers and bundles that play an important role in regulating the metabolic aspects of the body. Universally, increased exercise leads to increased muscle mass, while decreased or restricted rates of exercise can lead to muscle atrophy [1]. Muscle atrophy is a response that can weaken patients with hunger and some systemic diseases, often leading to muscle mass loss [2], and this phenomenon is also defined as sarcopenia in a broad sense. Muscular dystrophy is usually manifested as generalized muscular atrophy and fat infiltration, which is associated with the incidence rate and mortality in the context of aging and cancer [3]. For muscle atrophy, when muscles are inactive for a long period of time, muscle contractile function and muscle fiber size decrease as a result of increased degradation and decreased synthesis of muscle proteins [4]. Muscle atrophy can occur in a variety of individuals who are suffering from diseases, such as diabetes, cancer, muscle genetic disorders, and neurodegenerative diseases, or under mechanical unloading conditions, such as prolonged bed rest and reduced step count [5]. Muscle atrophy can lead to a poorer functional status, reducing the quality of life of patients and increasing morbidity and mortality in specific patient groups [6].

Muscle atrophy is the direct manifestation of sarcopenia, and its main cause is excessive protein degradation. The Forkhead box O (FOXO) family of transcription factors and the progrowth IGF-AKT pathway are key mediators of muscle atrophy and are important for the protein degradation pathway in muscle atrophy [7]. Also, mitochondrial dysfunction is associated with disuse muscle atrophy [8]. Mitochondrial oxidative stress (OS) can stimulate muscle proteolysis by increasing the involvement in protein degradation pathways and protein expression [9], and excessive

oxidative stress can lead to muscle damage and, consequently, muscle atrophy [10]. The occurrence of muscle atrophy is both "active" and "passive"; therefore, its study is of high clinical necessity. "Active" muscle atrophy is often caused by denervation. Nutritional factors that maintain skeletal muscle function require the innervation of motor neurons, and when muscle innervation deteriorates, it can lead to inadequate nerve input, resulting in muscle weakness or even atrophy [11]. This loss of muscle mass and function caused by peripheral nervous system injury or motor neuron disease is called neurogenic muscle atrophy and, in some cases, can reduce survival rates [12], which is also considered to be the main cause of the progression of sarcopenia. "Passive" muscle atrophy, on the other hand, is usually the result of other conditions that require reduced or limited activity. It is called disuse muscle atrophy and promotes skeletal muscle atrophy by stimulating protein decomposition [13]. Generally speaking, with the progress of aging, reactive oxygen species produced by muscle mitochondria will increase [14], which is another reason to promote the occurrence of sarcopenia. In contrast, muscle atrophy associated with wasting after a musculoskeletal injury is often difficult to overcome and can persist despite efforts at rehabilitation [15].

Several studies have shown that the development of muscle atrophy is associated with the regulation of proteins or RNAs. Li et al. [6] showed that miR-29b causes several types of muscle atrophy, while Li et al. demonstrated that lncIRS1 indirectly controls the production of muscle atrophy [16]. In this study, we will use bioinformatics approaches to find potential genes associated with muscle atrophy by grouping mice and obtaining sequencing information.

2. Materials and Methods

2.1. Establishment of the Animal Model. In this study, a total of 30 6-week-old male mice were selected from Institute of Cancer Research (ICR) (Cavens Lab, China) and divided into different age groups and muscle types groups. Firstly, 30 mice were reared at 25°C in light/dark cycle environment for 12 h each, without restriction of movement and feeding. At 2 months, 15 mice were sacrificed by neck removal, extensor digitorum longus atrophy(EDLA) tissues were obtained from 7 mice, and soleus longus atrophy (SOLA) tissues were obtained from 8 mice, the remaining 15 mice were sacrificed by neck removal at 29 months, and EDLA tissues were obtained from 7 mice. SOLA tissues were obtained from 8 mice. Finally, 30 muscle atrophy samples were obtained, including 7 2-month-old EDLA muscle atrophy samples, 8 2-month-old SOLA muscle atrophy samples, 8 29-month-old EDLA muscle atrophy samples, and 7 29-month-old SOLA muscle atrophy samples. The samples were sent for sequencing to obtain the muscle atrophy-related gene expression profile. Animal experiments were carried out in the First Affiliated Hospital of Zhejiang University, and the experimental program was carried out in an accredited animal facility (no. 2017-038).

2.2. Differential Expression Analysis. Samples were grouped according to the monthly age or muscle type, and two groups of differentially expressed genes (DEGs) were obtained using the R package and the limma package for differential analysis of two-month-old and 29-month-old mice or EDLA and SOLA muscle atrophy mice, respectively. Genes with differential expression in the two groups were selected using $|\log2FC| > 1$, $P < 0.05$, as a screening condition. The overlapping genes were obtained by taking the intersection of the two groups of DEGs using a Venn diagram.

2.3. Weighted Gene Coexpression Network Analysis (WGCNA). WGCNA was conducted using the R package to analyze the co-expression of DEGs associated with muscle atrophy in mice. A soft threshold β was calculated using the scale-free topology criterion to generate a weighted adjacency matrix. Subsequently, gene modules were cut using the dynamic tree-cutting method. Additionally, the correlation between each gene module and sample phenotype was analyzed by the WGCNA package, and the module that correlated the most with both the monthly age and muscle type was selected as the target gene module.

2.4. Protein-Protein Interaction (PPI) Network. The Search Tool for the Retrieval of Interacting Genes/Proteins (STRING) database was used to explore the known and predicted interactions between proteins, including direct and indirect relationships, construct protein expression networks in key gene modules from the STRING database, and link disease-causing gene-to-gene features via Cytoscape. The top five extracted genes were processed using the maximum correntropy criterion (MCC) algorithm in the cytoHubba plugin and used as pivotal genes.

2.5. Gene Expression Validation. To understand the differences in the expression of each pivotal gene between different phenotypes in mice, the expression level distribution was achieved using the R package ggplot2. The samples were grouped according to monthly age and muscle type, and *t*-tests were used to analyze the significance of differences in pivotal gene expression. $P < 0.05$ was considered statistically significant.

2.6. Enrichment Analysis. To better understand the pathogenic role of mRNA, overlapping genes were analyzed for Gene Ontology (GO) function and Kyoto Encyclopedia of Genes (KEGG) pathways using the R package ClusterProfiler. GO is used to annotate genes with function, and it contains a molecular function (MF), biological process (BP), and cellular component (CC). In contrast, KEGG can be used to analyze the gene functions and functional information of the related genomes and to explore the functional pathways of pathogenic genes. In the enrichment results, $P < 0.05$ or $\mathrm{FDR} < 0.05$ was considered significant for the enriched pathway. Gene set enrichment analysis (GSEA) was used to analyze the association of hub genes with the mouse muscle atrophy pathway. KEGG pathways in the top three of

significance were selected for analysis using the screening conditions of |NES| >1, NOM p val <0.05, and FDR q val <0.25.

3. Analysis of Results

3.1. Differential Expression Analysis. The mice were divided into two groups according to their age and the type of muscle atrophy, and each group was analyzed for differences. A total of 2,721 genes were downregulated, and 1,298 genes were upregulated in the two-month-old and 29-month-old groups of muscle atrophy mice (Figures 1(a) and 1(b)). In the EDLA muscle atrophy group and the SOLA muscle atrophy group, a total of 2,651 genes were downregulated and 1,148 genes were upregulated (Figures 1(c) and 1(d)). For the potential causative genes of muscle atrophy in mice, this study used Venn diagrams to take the intersection of the months and muscle groups, and obtained 1,630 overlapping genes associated with both the monthly age and muscle type (Figure 1(e)).

3.2. GO Function and the KEGG Pathway. To understand the function of overlapping genes in muscle atrophy in mice, we used enrichment analysis to observe the main functions and pathways of these genes. The top 20 KEGG pathways and GO function terms were enriched and presented using bubble plots. The results showed that the target genes were associated with KEGG processes, such as Parkinson's disease, Alzheimer's disease, and oxidative phosphorylation (Figure 2(a)). For GO functional terms, the target genes were significantly enriched for energy metabolic processes, such as purine nucleotide metabolic processes; energy production from oxidation of organic compounds; ribonucleoside monophosphate metabolic processes (Figure 2(b)); cellular components, such as organelle inner membrane; mitochondrial inner membrane; mitochondrial protein complexes (Figure 2(c)); and molecular functions, such as cell adhesion molecule binding, electron transfer activity, and NADH dehydrogenase activity (Figure 2(d)).

3.3. WGCNA Selection of Key Gene Modules. In WGCNA, when the correlation coefficient is greater than 0.85, the optimal soft threshold value $\beta = 24$ (Figures 3(a) and 3(b)). At this time, the genes can be clustered using the average chain hierarchy clustering method, and five color modules can be obtained (Figure 3(c)). The lightgreen, cyan, blue, grey, and magenta modules contain 224, 1074, 175, 93, and 64 genes, respectively (Figure 3(d)). Among them, the lightgreen module was significantly and positively correlated with both mouse month age (cor = 0.59, P = 0.0003) and muscle type (cor = 0.6, P = 0.0003).

3.4. Protein Interaction Network to Find Pivotal Genes. To further identify pivotal genes affecting the progression of muscle atrophy in mice, we used the STRING database to identify the interactions between proteins in the lightgreen module and obtained a total of 223 nodes and 196 edges (Figure 4(a)). The top five genes in terms of correlation ranking such as ubiquitin-specific peptidase 7(USP7), ubiquitin-protein ligase E3A (UBE3A), Cullin 3 (CUL3), ubiquitin-specific peptidase 9, X-linked (USP9X), and COP9 constitutive photomorphogenic homolog subunit 5 (COPS5) were then derived using the MCC algorithm and used as pivotal genes for subsequent analysis (Figure 4(b)).

3.5. CUL3 and COPS5 as Pivotal Genes. Correlation analysis of pivotal genes revealed high correlation coefficients among all five genes and significant results (Figure 5(a)). The expression levels of the five genes were then analyzed, and the mouse samples were divided into 29-month-old and two-month-old to observe the difference in the expression of pivotal genes in the EDLA muscle and the SOLA muscle, respectively. The results showed that only the expression levels of CUL3 and COPS5 were significant at the same time (Figures 5(b)–5(f)), which indicated that CUL3 and COPS5 were correlated with both months of age and muscle type during the development of muscle atrophy in mice.

3.6. GSEA Analysis of the KEGG Pathway of Key Genes. To further understand the functional pathways involved in the key genes in mouse muscle atrophy, this study focused on the KEGG pathway using GSEA. Analysis showed that CUL3 was associated with signaling pathways, such as Parkinson's disease, ECM-receptor interaction, and oxidative phosphorylation (Figures 6(a)–6(c)), while COPS5 was associated with signaling pathways, such as the proteasome, protein export, and ubiquitin-mediated protein hydrolysis (Figures 6(d)–6(f)).

4. Discussion

Muscle reduction is the main cause of muscle strength and muscle mass loss in the elderly. It is also an important complication of chronic kidney disease [17], cardiac cachexia [18], diabetes mellitus [19], and cancer [20]. Factors associated with sarcopenia include neurological factors, oxidative stress, mitochondrial dysfunction, fat accumulation, mild inflammation, nutritional deficiency, hormone changes, reduction of the number of microcells, and regenerative capacity. Some studies have shown that moderate exercise enhances mitochondrial adaptation and function, which facilitates skeletal muscle recovery and myocyte regeneration [21]. In addition, many types of drugs have the potential to treat muscle atrophy, including anabolic drugs, enzyme inhibitors, and anti-inflammatory drugs [22]. But so far, no drugs have been approved for the treatment of sarcopenia, which makes the search for appropriate intervention targets become the focus of clinical research. Advances in transcriptome technology and high-throughput analysis allow the detection of a variety of cytokines, such as growth factors, transcription factors, cell signal pathway activators, and noncoding RNA, which are involved in the regulation of gene expression during skeletal muscle aging changes and adaptation [23]. In this study, an expression matrix containing 18234 genes was obtained by sequencing

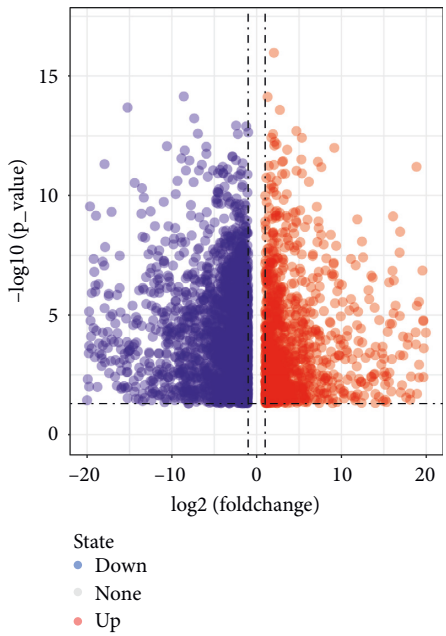

(a)

Figure 1: Continued.

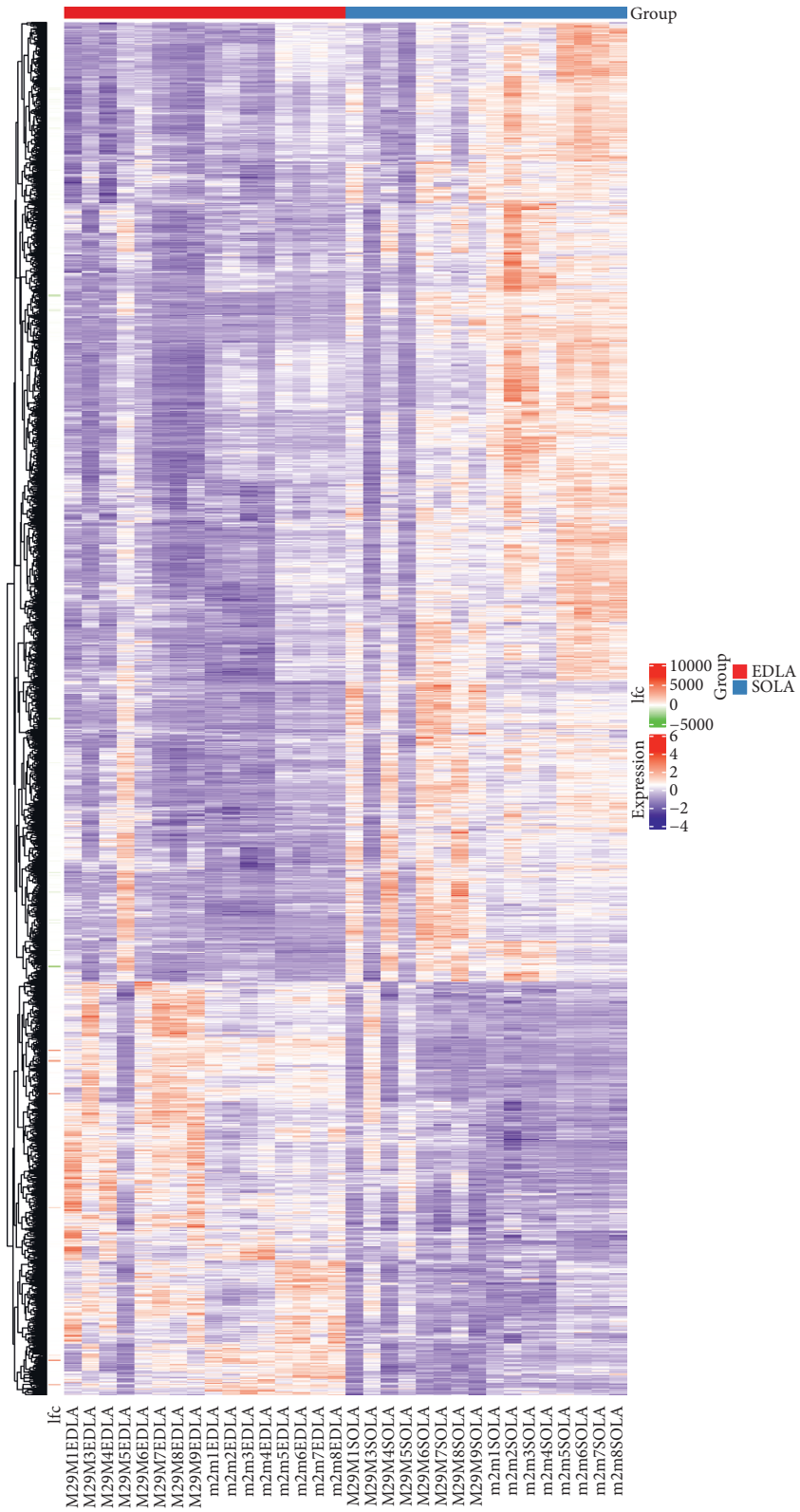

(b)

Figure 1: Continued.

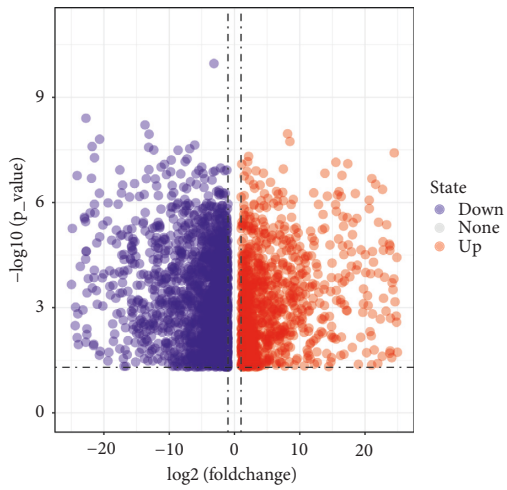

(c)

Figure 1: Continued.

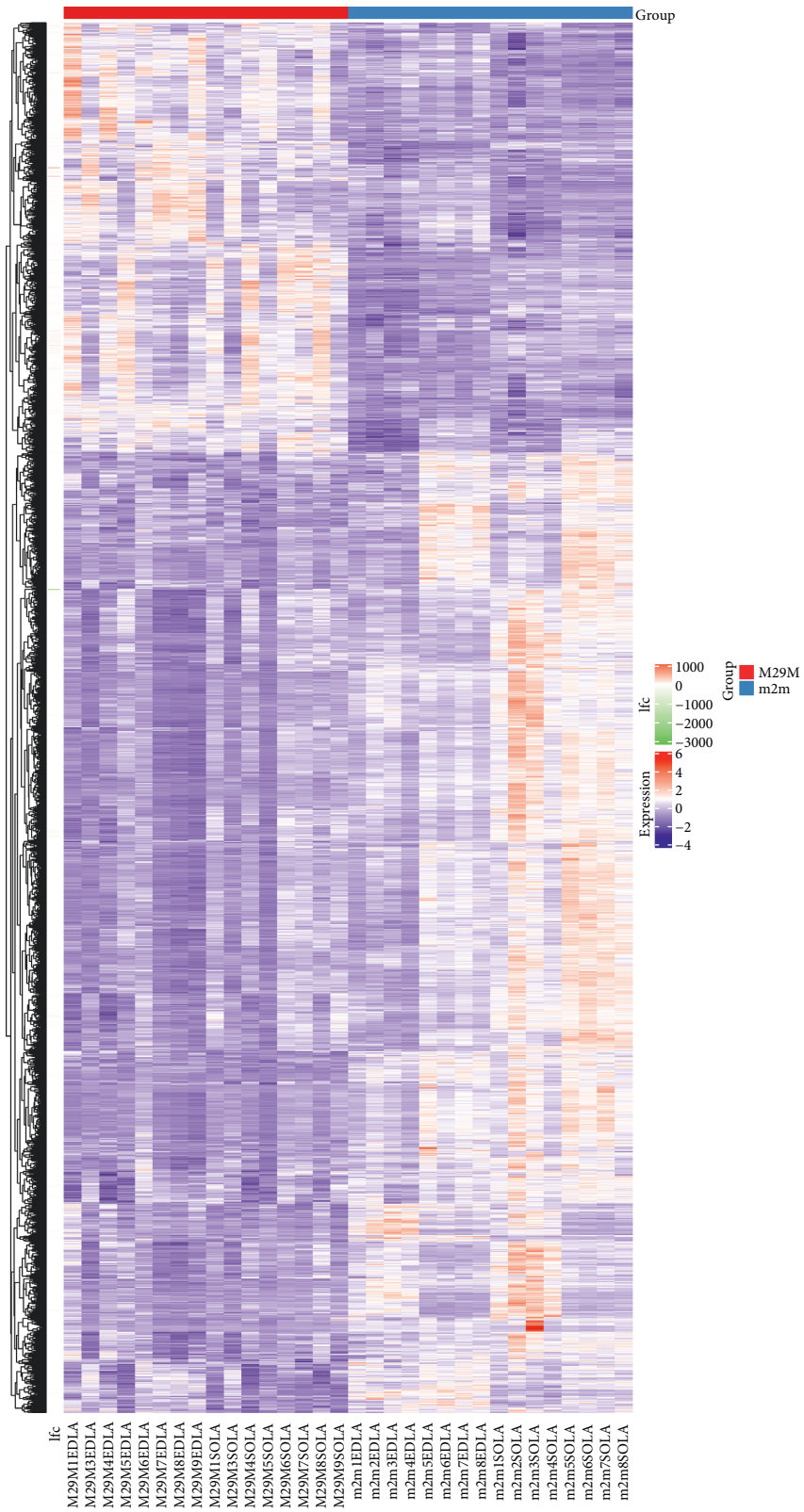

(d)

Figure 1: Continued.

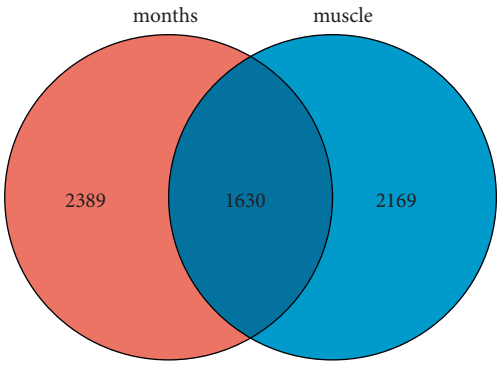

(e)

Figure 1: Results of differential gene expression analysis in different group. (a, b) Differential gene expression results after grouping based on different muscle types. (c, d) Differential gene expression results after grouping based on different monthly ages of mice. (e) DEGs obtained based on monthly age grouping are named months, and DEGs obtained based on muscle type grouping are named muscle. The intersection of the two groups of DEGs was obtained using the Venn diagram.

mouse samples. The differential expression of these genes was compared from two dimensions, and 1630 overlapping genes were obtained.

Further enrichment analysis was used to clarify the role of 1630 DEGs. KEGG enrichment analysis showed that the differential genes were related to Parkinson's disease, Alzheimer's disease, and oxidative phosphorylation. Parkinson's disease (PD) is a progressive dyskinesia. Sarcopenia is common in patients with Parkinson's disease and is associated with more advanced disease stages, higher dyskinesia and nonexercise load, falls, reduced quality of life, and hospitalization. Sarcopenia and Parkinson's disease have multiple common pathways, which may affect each other's prognosis and patients' quality of life [24]. In addition, GO function analysis showed that mitochondrial changes were also an important pathway of muscle atrophy. Previous studies have shown that mitochondrial biosynthesis, mitochondrial respiratory complex subunit expression, mitochondrial respiration, and ATP levels are significantly reduced in aging skeletal muscle [25, 26]. Migliavacca et al. demonstrated for the first time that mitochondrial biological dysfunction is the strongest molecular feature of sarcopenia. Changes in mitochondria include decreased mitochondria, decreased expression and activity of mitochondrial respiratory complexes, and interference with NAD biosynthesis and repair in muscle [27].

In order to further study the gene regulatory factors related to sarcopenia, five key genes were identified by WGCNA and PPI. The expression of CUL3 and COPS5 was significantly correlated with mouse month age and muscle type. CUL3 (Cullin 3) is a key protein of the E3 ubiquitin ligase complex and mediates the proteasomal degradation process [28]. CUL3 regulates a variety of cellular functions, such as antioxidant, cell cycle, protein transport, and signal transduction [29]. CUL3 deficiency increases the expression of cell cycle proteins E and P21, which are associated with abnormal proliferation, DNA damage, and apoptosis [30]. Studies have shown that CUL3 is associated with vascular smooth muscle specificity and may indirectly promote proliferation, migration, and inflammatory response of vascular smooth muscle cells [31]. In contrast, its deletion promotes NO reactivity and leads to atherosclerosis and hypertension [32]. In addition, CUL3 plays a key role in the development and function of the transverse muscle, and it mediates protein homeostasis, with important implications in muscle function [33]. Additional studies have used gene expression and structural analysis to identify CUL3 associated with sarcopenia [34]. Another key gene is COP9 signaling vesicle complex 5 (COPS5), also known as C-Jun activation domain-binding protein-1 (Jab1), a multifunctional protein [35]. COPS5 is involved in the regulation of cellular and developmental processes, such as signal transduction, cell cycle processes, DNA damage response, and tumorigenesis [36], and plays an important role in ubiquitin-mediated protein degradation [37]. Most of the current studies focus on the oncogenic function of COPS5, and its dysregulated activity contributes to the development of cancers, such as breast cancer [38], glioma [39], and prostate cancer [40]. It has been reported that COPS5 usually interacts with proteins or binds to miRNAs to regulate tumor progression [41], and it has also been shown to affect the metastatic potential of cancer cells by inhibiting SNAIL ubiquitination [42]. Regarding the role in muscle function, the results of Velardo et al. showed that COPS5 has an important role in muscle development, maintenance, and regeneration and is associated with the pathogenesis of congenital muscular dystrophy [43].

In order to further understand the functional pathway of the two genes involved in mouse muscle atrophy, CUL3 and COPS5 were analyzed by GSEA. GSEA results showed that CUL3 was related to Parkinson's disease, ECM-receptor interaction, and oxidative phosphorylation. COPS5 is related to the proteasome, protein output, and ubiquitin-mediated proteolysis. Previous studies have shown that the ubiquitin-proteasome system (UPS) is activated during senile muscle atrophy [44]. CUL3 [29] and COPS5 [45] are important members of the ubiquitin-proteasome system, which is consistent with our study. The ubiquitin-

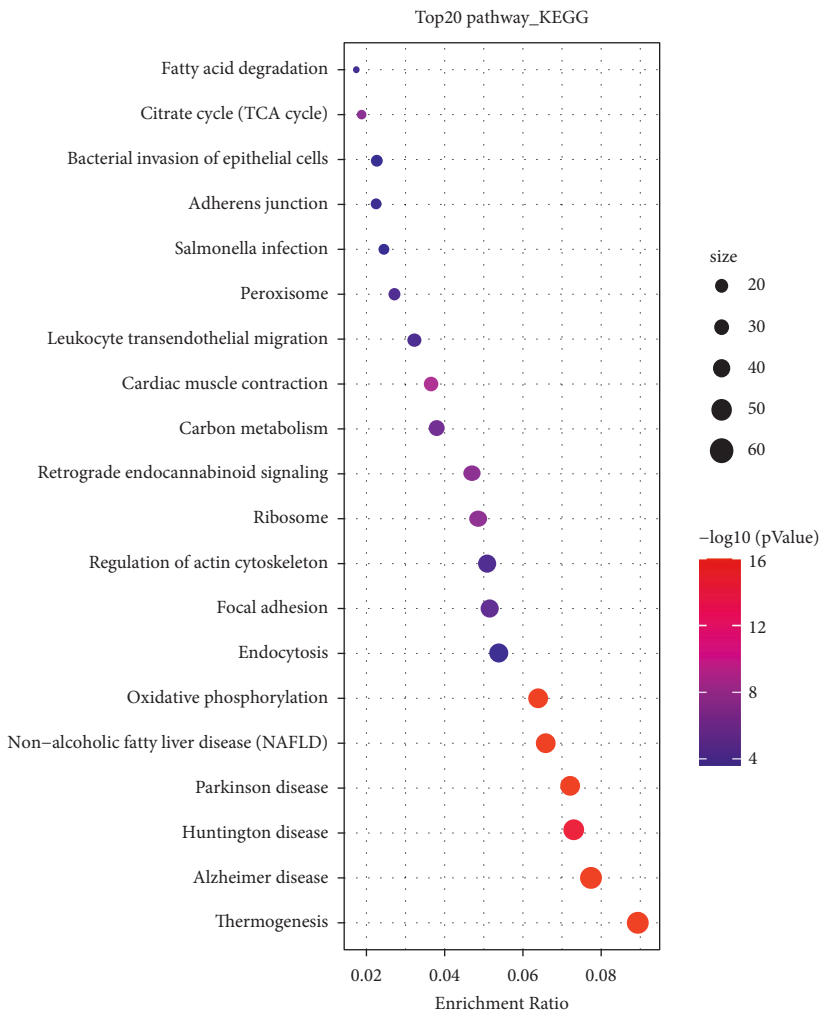

(a)

Figure 2: Continued.

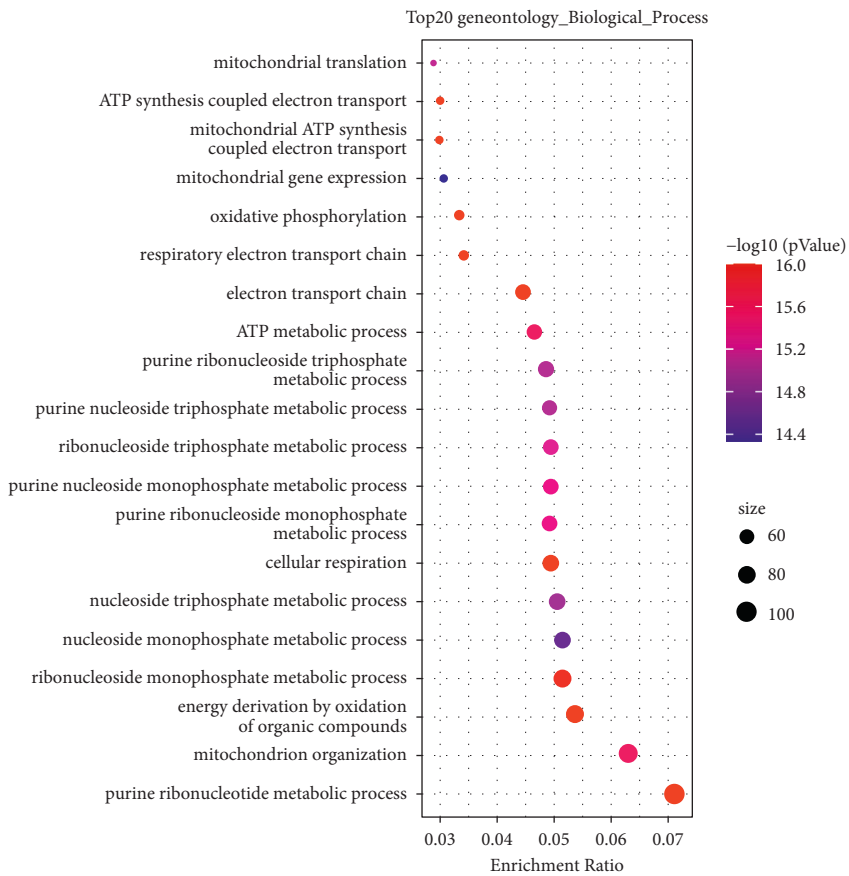

(b)

Figure 2: Continued.

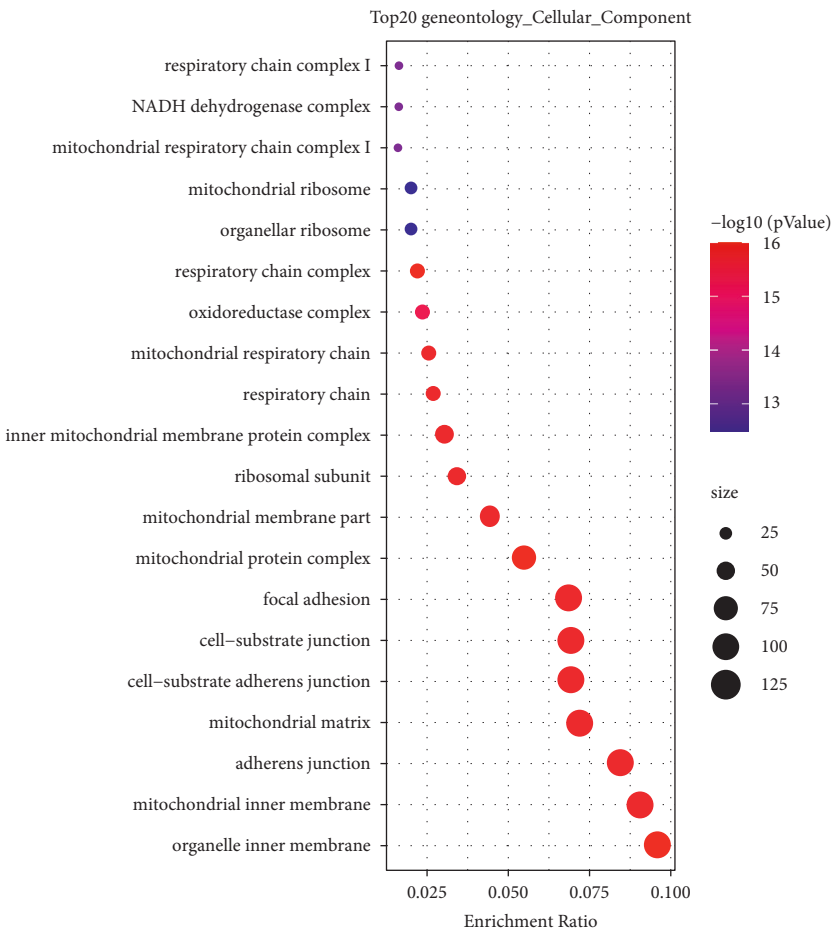

(c)

Figure 2: Continued.

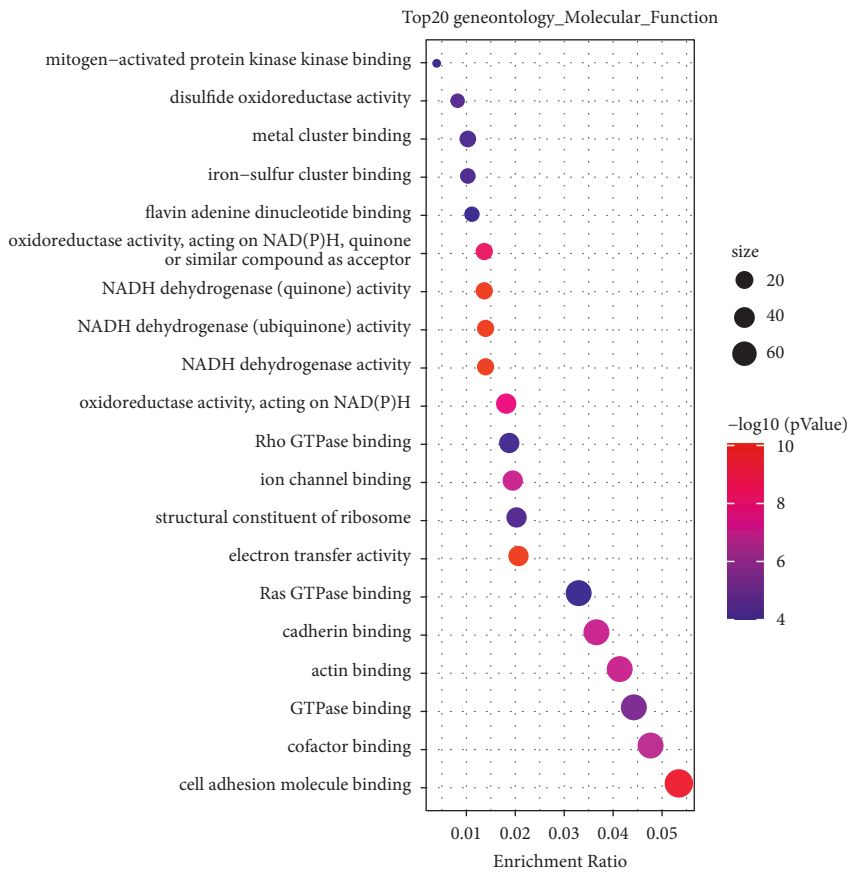

(d)

Figure 2: Results of enrichment analysis of DEGs. (a) Results of the top 20 KEGG pathways. (b–d) Results of the top 20 BP, CC, and MF functions, respectively.

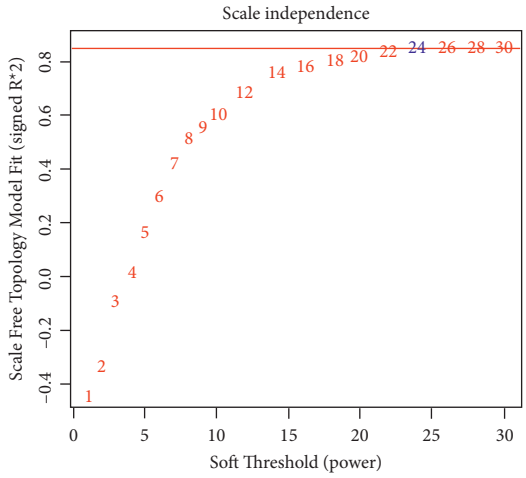

(a)

Figure 3: Continued.

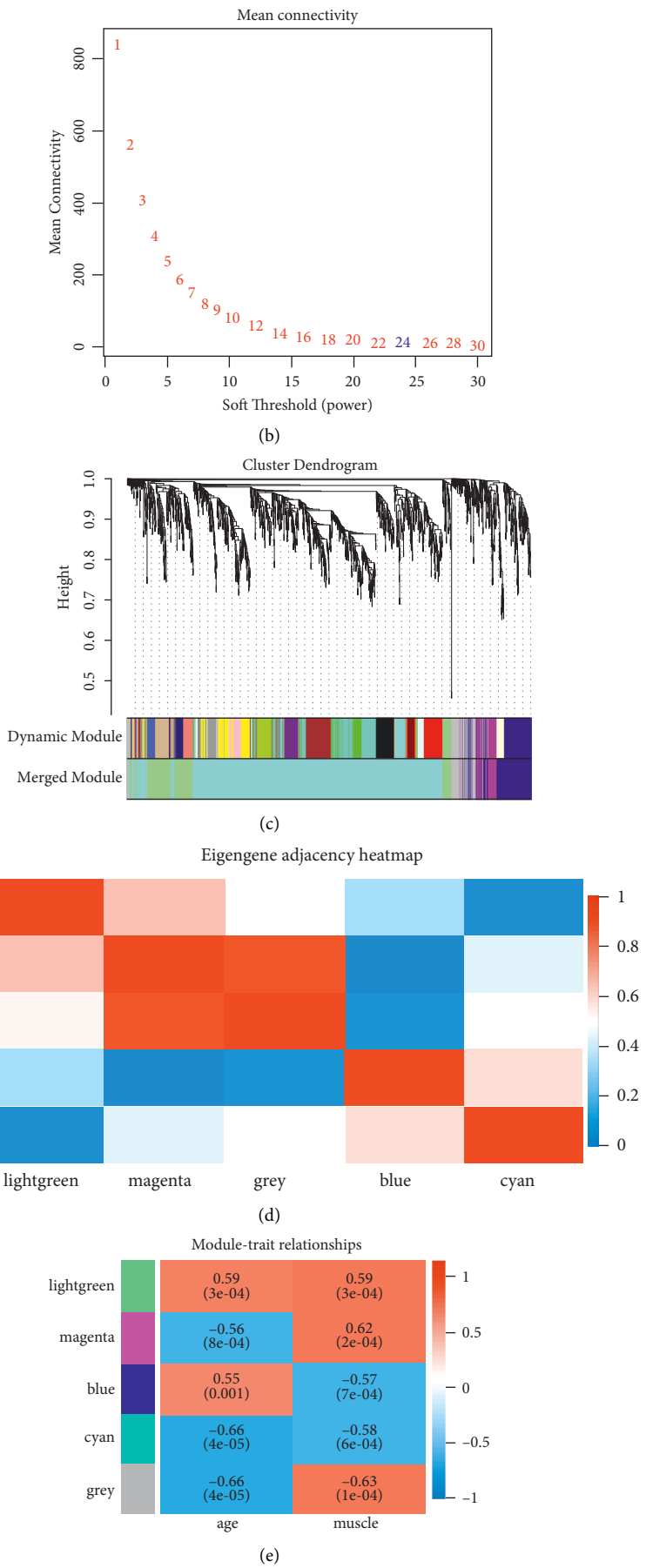

Figure 3: Weighted mouse muscle atrophy gene coexpression. (a, b) T scale-free fit indices and mean connectivity for various soft threshold powers. (c) Dendrogram of overlapping genes based on different index clusters. (d) Neighbor-joining heat map of modular signature genes. (e) Correlation heat map of modular signature genes with different phenotypes of muscle atrophy in mice.

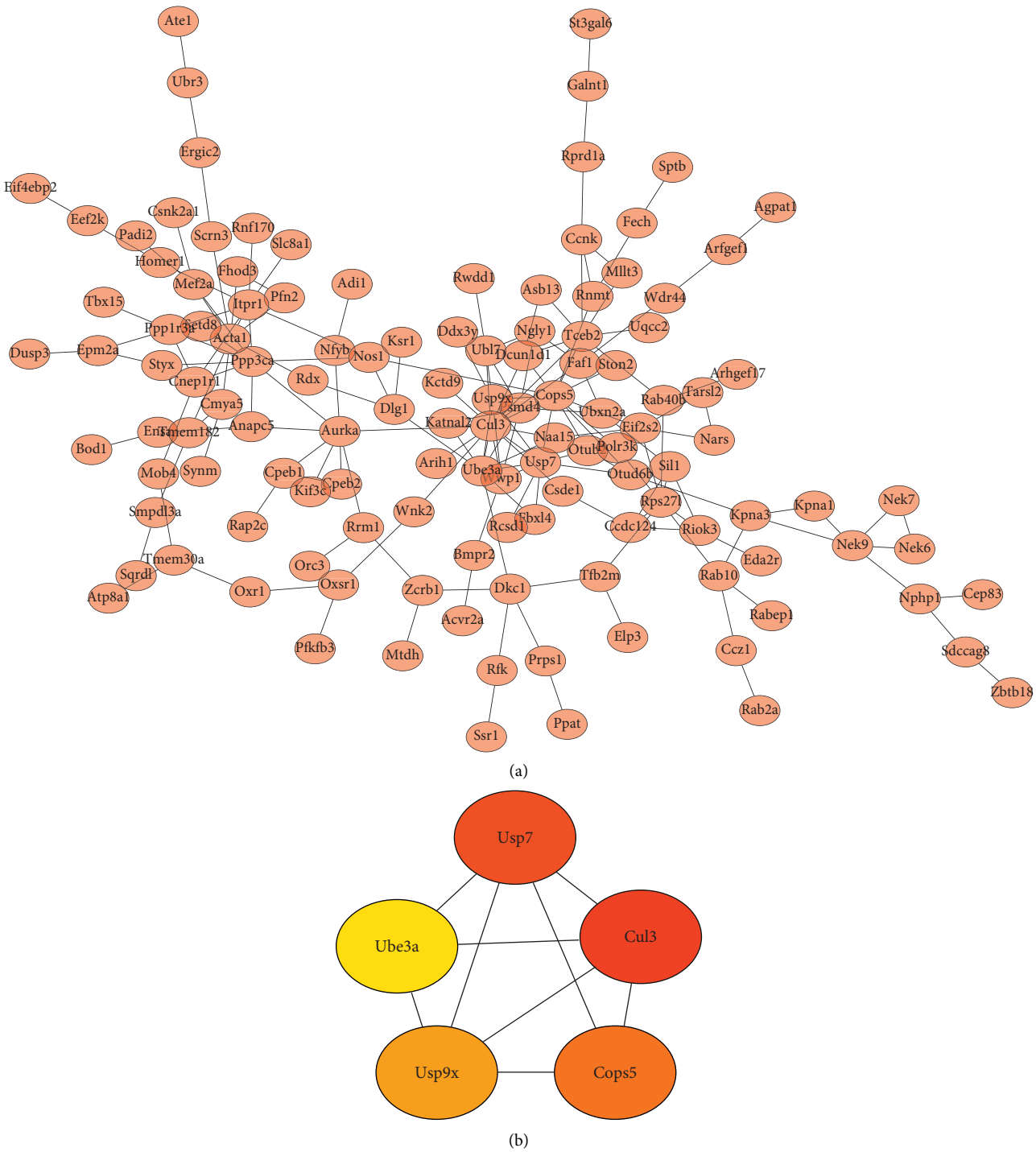

(a)

(b)

Figure 4: PPI results. (a) Map of protein interaction network relationships in the lightgreen module. (b) Top five significant genes.

proteasome pathway is the main protein degradation pathway, and the process is a three-step enzymatic cascade reaction [46]. Furthermore, the E3 ligase of the Cullin family catalyzes the last step, which attaches ubiquitin protein to the target substrate protein [47]. Interestingly, Blondelle et al. in their study showed that the regulation of the Cullin activity is associated with the COP9 signaling vesicle complex [48]. This study is similar to the results of Spearman analysis in the present study, where CUL3 was correlated with COPS5 (cor = 0.73) (Figure 5(a)).

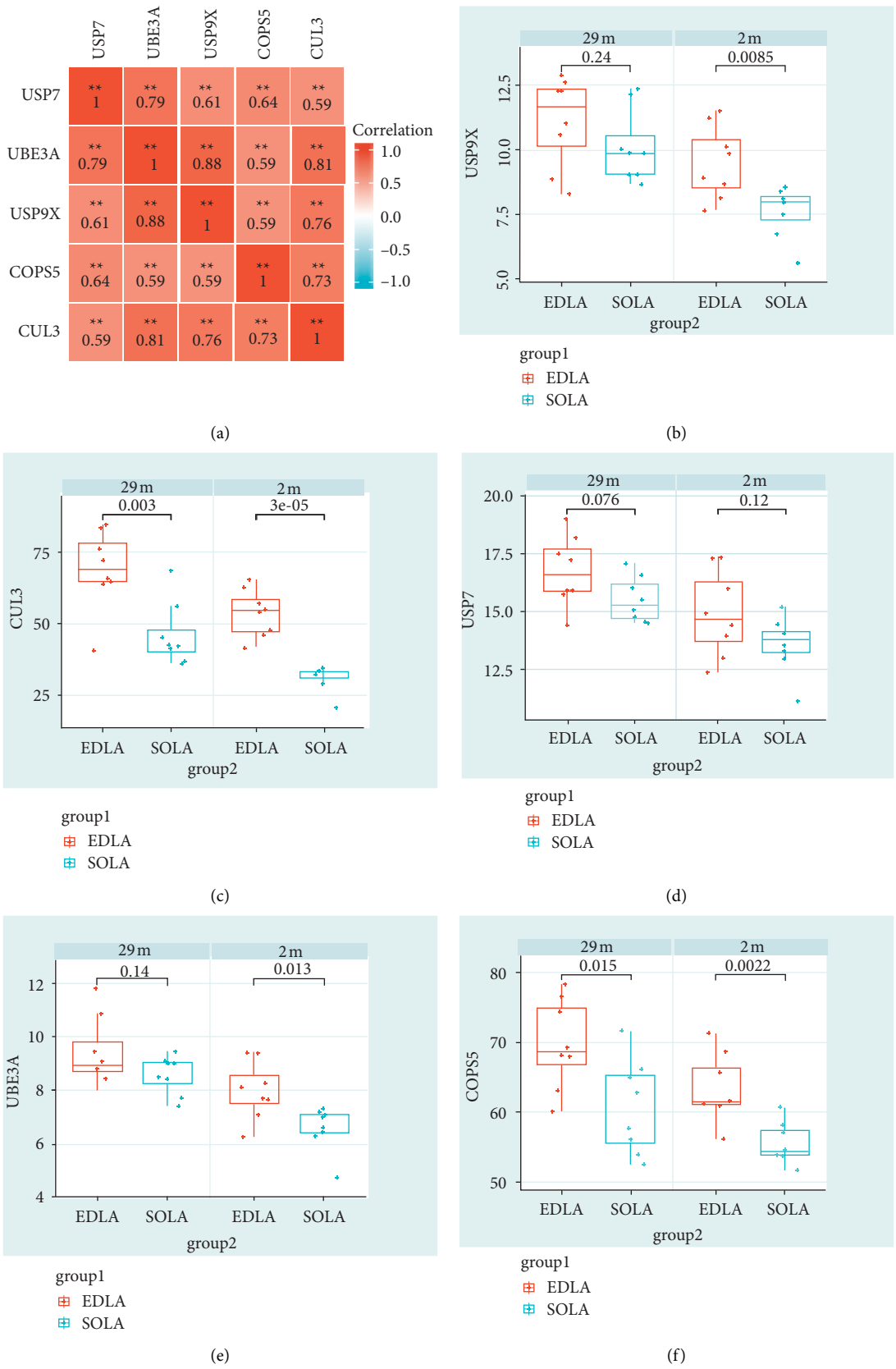

Figure 5: Expression level distribution of pivotal genes. (a) Correlation analysis of expression levels of five pivotal genes, $^{*}P < 0.05$ and $^{**}P < 0.01$. (b–f) The expression levels of USP9X, CUL3, USP7, UBE3A, and COPS5 in different muscle type groups were observed by monthly age grouping, respectively.

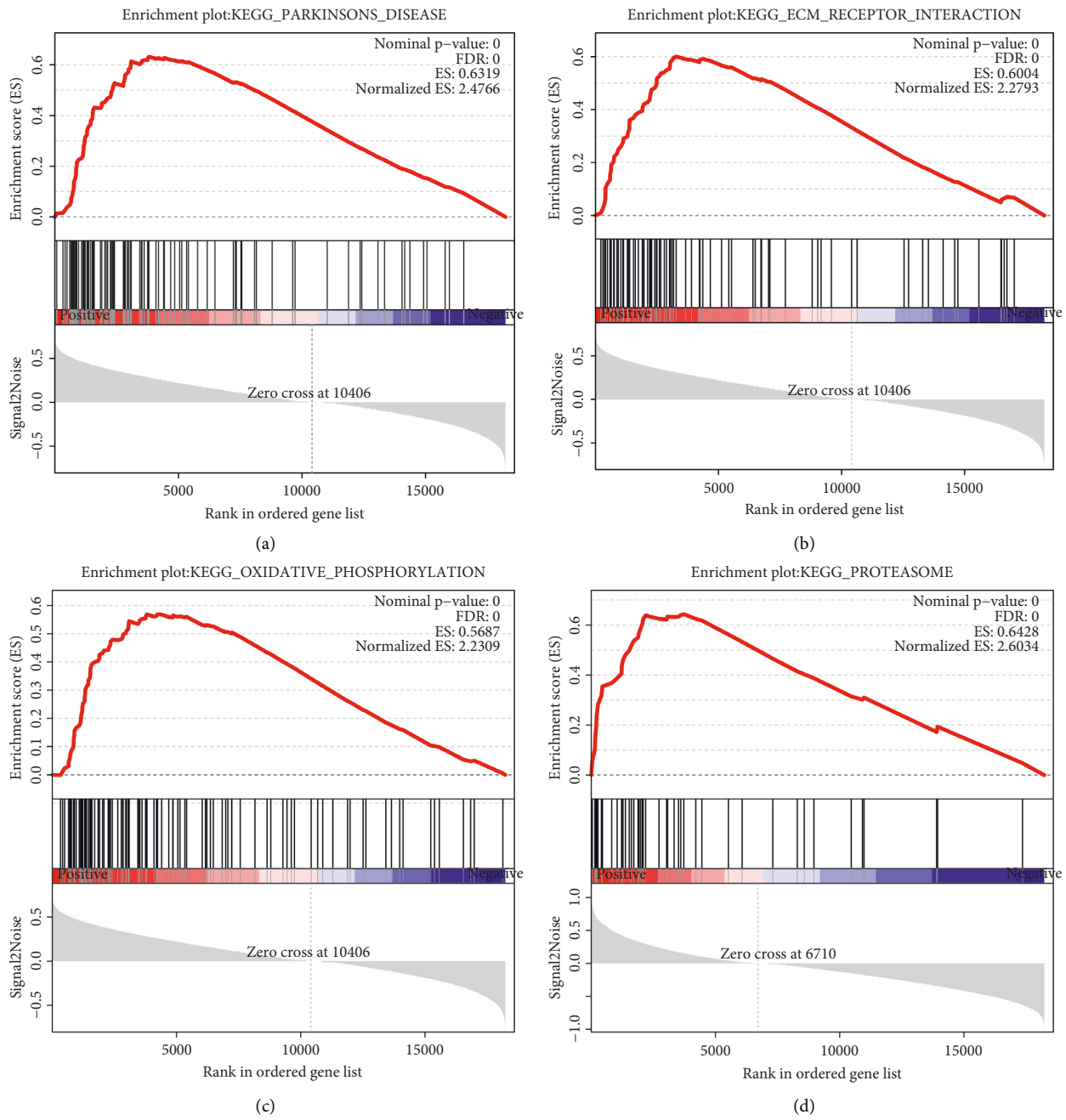

Figure 6: Continued.

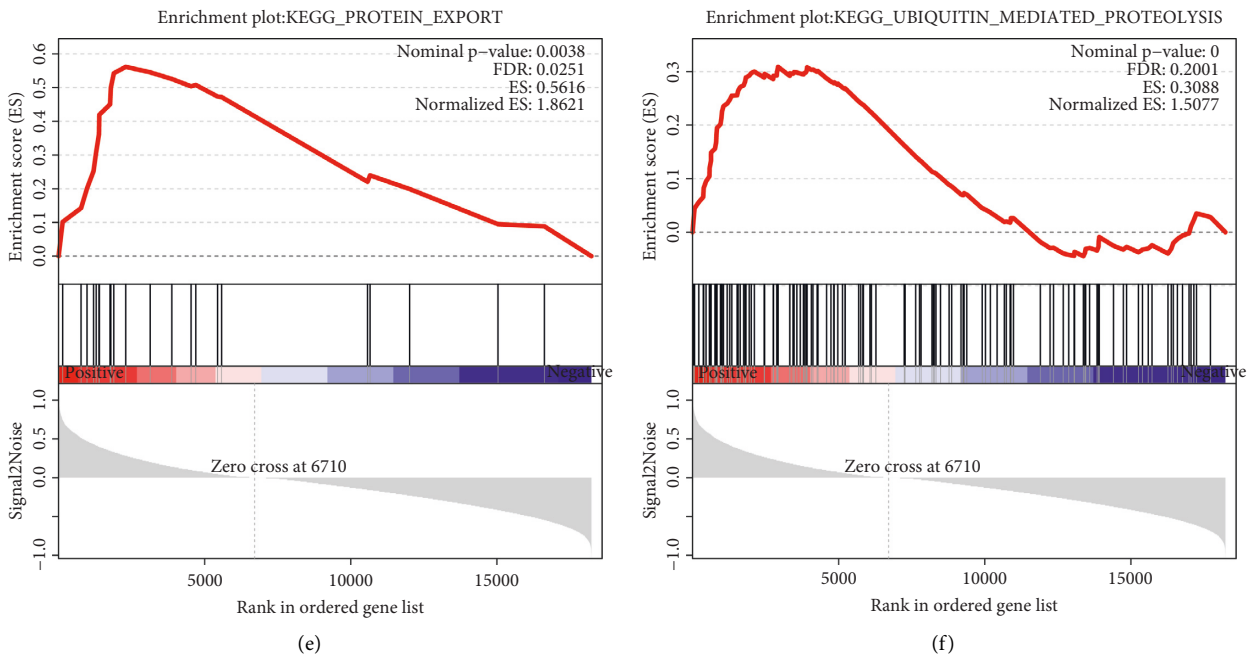

Figure 6: GSEA results of key genes. (a–c) GSEA results of the top three ranked CUL3 in mouse muscle atrophy. (d–f) GSEA results of the top three ranked COPS5 in mouse muscle atrophy.

5. Conclusion

In conclusion, this study identified two new potential genes (CUL3 and COPS5) of muscle atrophy. Furthermore, CUL3 and COPS5 are related to the ubiquitin-proteasome pathway, which may provide useful ideas for the study of the pathogenesis of muscle atrophy. In the future, we will continue to study in vitro and in vivo.

Data Availability

All data generated or analyzed during this study are included in this article.

Disclosure

Qun Xu is the first author.

Conflicts of Interest

The authors declare that they have no conflicts of interest.

Acknowledgments

This research was supported by the National Key R&D Program of China under grant no. 2020YFC2005601 and the National Natural Science Foundation of China under grant no. 81771497.

References

[1] L. Shen, X. Meng, Z. Zhang, and T. Wang, "Physical exercise for muscle atrophy," *Muscle Atrophy*, vol. 1088, pp. 529–545, 2018.

[2] S. H. Lecker, R. T. Jagoe, A. Gilbert et al., "Multiple types of skeletal muscle atrophy involve a common program of changes in gene expression," *The FASEB Journal*, vol. 18, no. 1, pp. 39–51, 2004.

[3] L. Lenchik and R. D. Boutin, "Sarcopenia: beyond muscle atrophy and into the new frontiers of opportunistic imaging, precision medicine, and machine learning," *Seminars in Musculoskeletal Radiology*, Thieme Medical Publishers, New York, NY, USA, 2018.

[4] S. K. Powers, A. J. Smuder, and A. R. Judge, "Oxidative stress and disuse muscle atrophy: cause or consequence?" *Current Opinion in Clinical Nutrition and Metabolic Care*, vol. 15, no. 3, pp. 240–245, 2012.

[5] W. J. Evans, "Skeletal muscle loss: cachexia, sarcopenia, and inactivity," *The American Journal of Clinical Nutrition*, vol. 91, no. 4, pp. 1123S–7S, 2010.

[6] J. Li, M. C. Chan, Y. Yu et al., "miR-29b contributes to multiple types of muscle atrophy," *Nature Communications*, vol. 8, no. 1, p. 15201, 2017.

[7] S. Choi, H.-J. Jeong, H. Kim et al., "Skeletal muscle-specific Prmt1 deletion causes muscle atrophy via deregulation of the PRMT6-FOXO3 axis," *Autophagy*, vol. 15, no. 6, pp. 1069–1081, 2019.

[8] H. Hyatt, R. Deminice, T. Yoshihara, and S. K. Powers, "Mitochondrial dysfunction induces muscle atrophy during prolonged inactivity: a review of the causes and effects," *Archives of Biochemistry and Biophysics*, vol. 662, pp. 49–60, 2019.

[9] M. B. Trevino, X. Zhang, R. A. Standley et al., "Loss of mitochondrial energetics is associated with poor recovery of muscle function but not mass following disuse atrophy," *American Journal of Physiology—Endocrinology and Metabolism*, vol. 317, no. 5, pp. E899–E910, 2019.

[10] R. Qaisar, S. Bhaskaran, R. Ranjit et al., "Restoration of SERCA ATPase prevents oxidative stress-related muscle atrophy and weakness," *Redox Biology*, vol. 20, pp. 68–74, 2019.

[11] W. Choi, J. Lee, J. Lee, K. R. Ko, and S. Kim, "Hepatocyte growth factor regulates the miR-206-HDAC4 cascade to control neurogenic muscle atrophy following surgical denervation in mice," *Molecular Therapy—Nucleic Acids*, vol. 12, pp. 568–577, 2018.

[12] J. T. Ehmsen, R. Kawaguchi, R. Mi, G. Coppola, and A. Höke, "Longitudinal RNA-seq analysis of acute and chronic neurogenic skeletal muscle atrophy," *Scientific Data*, vol. 6, no. 1, p. 179, 2019.

[13] B. Ferrando, M. C. Gomez-Cabrera, A. Salvador-Pascual et al., "Allopurinol partially prevents disuse muscle atrophy in mice and humans," *Scientific Reports*, vol. 8, no. 1, p. 3549, 2018.

[14] Y. Su, D. R. Claflin, M. Huang et al., "Deletion of neuronal CuZnSOD accelerates age-associated muscle mitochondria and calcium handling dysfunction that is independent of denervation and precedes sarcopenia," *International Journal of Molecular Sciences*, vol. 22, no. 19, p. 10735, 2021.

[15] A. C. Thomas, E. M. Wojtys, C. Brandon, and R. M. Palmieri-Smith, "Muscle atrophy contributes to quadriceps weakness after anterior cruciate ligament reconstruction," *Journal of Science and Medicine in Sport*, vol. 19, no. 1, pp. 7–11, 2016.

[16] Z. Li, B. Cai, B. A. Abdalla et al., "LncIRS1 controls muscle atrophy via sponging miR-15 family to activate IGF1-PI3K/AKT pathway," *Journal of Cachexia, Sarcopenia and Muscle*, vol. 10, no. 2, pp. 391–410, 2019.

[17] H. Wang, B. Wang, A. Zhang et al., "Exosome-mediated miR-29 transfer reduces muscle atrophy and kidney fibrosis in mice," *Molecular Therapy*, vol. 27, no. 3, pp. 571–583, 2019.

[18] T. S. Bowen, V. Adams, S. Werner et al., "Small-molecule inhibition of MuRF1 attenuates skeletal muscle atrophy and dysfunction in cardiac cachexia," *Journal of Cachexia, Sarcopenia and Muscle*, vol. 8, no. 6, pp. 939–953, 2017.

[19] Y. Hong, J. H. Lee, K. W. Jeong, C. S. Choi, and H. S. Jun, "Amelioration of muscle wasting by glucagon-like peptide-1 receptor agonist in muscle atrophy," *Journal of Cachexia, Sarcopenia and Muscle*, vol. 10, no. 4, pp. 903–918, 2019.

[20] B. A. Guigni, D. M. Callahan, T. W. Tourville et al., "Skeletal muscle atrophy and dysfunction in breast cancer patients: role for chemotherapy-derived oxidant stress," *American Journal of Physiology—Cell Physiology*, vol. 315, no. 5, pp. C744–C756, 2018.

[21] N. He and H. Ye, "Exercise and muscle atrophy," *Advances in Experimental Medicine and Biology*, vol. 1228, pp. 255–267, 2020.

[22] L. Chen, H. Zhang, M. Chi, Q. Yang, and C. Guo, "Drugs for the treatment of muscle atrophy," *Background and Management of Muscular Atrophy*, vol. 83, 2021.

[23] S. Fochi, G. Giuriato, T. De Simone et al., "Regulation of microRNAs in satellite cell renewal, muscle function, sarcopenia and the role of exercise," *International Journal of Molecular Sciences*, vol. 21, no. 18, p. 6732, 2020.

[24] D. P. Lima, S. B. de Almeida, J. d. C. Bonfadini et al., "Clinical correlates of sarcopenia and falls in Parkinson's disease," *PLoS One*, vol. 15, no. 3, Article ID e0227238, 2020.

[25] A. Bratic and N.-G. Larsson, "The role of mitochondria in aging," *Journal of Clinical Investigation*, vol. 123, no. 3, pp. 951–957, 2013.

[26] K. R. Short, M. L. Bigelow, J. Kahl et al., "Decline in skeletal muscle mitochondrial function with aging in humans," *Proceedings of the National Academy of Sciences*, vol. 102, no. 15, pp. 5618–5623, 2005.

[27] E. Migliavacca, S. K. H. Tay, H. P. Patel et al., "Mitochondrial oxidative capacity and NAD+ biosynthesis are reduced in human sarcopenia across ethnicities," *Nature Communications*, vol. 10, no. 1, p. 5808, 2019.

[28] M. Rapanelli, T. Tan, W. Wang et al., "Behavioral, circuitry, and molecular aberrations by region-specific deficiency of the high-risk autism gene Cul3," *Molecular Psychiatry*, vol. 26, no. 5, pp. 1491–1504, 2021.

[29] Z. Dong, W. Chen, C. Chen et al., "CUL3 deficiency causes social deficits and anxiety-like behaviors by impairing excitation-inhibition balance through the promotion of cap-dependent translation," *Neuron*, vol. 105, no. 3, pp. 475.e6–490.e6, 2020.

[30] T. Saritas, C. A. Cuevas, M. Z. Ferdaus et al., "Disruption of CUL3-mediated ubiquitination causes proximal tubule injury and kidney fibrosis," *Scientific Reports*, vol. 9, no. 1, p. 4596, 2019.

[31] Y. Xiang, L. Li, S. Xia, J. Lv, and X. Li, "Cullin3 (CUL3) suppresses proliferation, migration and phenotypic transformation of PDGF-BB-stimulated vascular smooth muscle cells and mitigates inflammatory response by repressing Hedgehog signaling pathway," *Bioengineered*, vol. 12, no. 2, pp. 9463–9472, 2021.

[32] L. N. Agbor, A. R. Nair, J. Wu et al., "Conditional deletion of smooth muscle cullin-3 causes severe progressive hypertension," *JCI Insight*, vol. 5, no. 14, Article ID 129793, 2019.

[33] J. B. Papizan, A. H. Vidal, S. Bezprozvannaya, R. Bassel-Duby, and E. N. Olson, "Cullin-3–RING ubiquitin ligase activity is required for striated muscle function in mice," *Journal of Biological Chemistry*, vol. 293, no. 23, pp. 8802–8811, 2018.

[34] G. Shafiee, Y. Asgari, A. Soltani, B. Larijani, and R. Heshmat, "Identification of candidate genes and proteins in aging skeletal muscle (sarcopenia) using gene expression and structural analysis," *PeerJ*, vol. 6, p. e5239, 2018.

[35] R. Zhou, Z. Shao, J. Liu et al., "COPS5 and LASP1 synergistically interact to downregulate 14-3-3σ expression and promote colorectal cancer progression via activating PI3K/AKT pathway," *International Journal of Cancer*, vol. 142, no. 9, pp. 1853–1864, 2018.

[36] G. Liu, F. X. Claret, F. Zhou, and Y. Pan, "Jab1/COPS5 as a novel biomarker for diagnosis, prognosis, therapy prediction and therapeutic tools for human cancer," *Frontiers in Pharmacology*, vol. 9, p. 135, 2018.

[37] H. Zhang, A. Zhong, J. Sun et al., "COPS5 inhibition arrests the proliferation and growth of serous ovarian cancer cells via the elevation of p27 level," *Biochemical and Biophysical Research Communications*, vol. 493, no. 1, pp. 85–93, 2017.

[38] B. Wu, Y. Pan, G. Liu et al., "MRPS30-DT knockdown inhibits breast cancer progression by targeting Jab1/Cops5," *Frontiers in Oncology*, vol. 9, p. 1170, 2019.

[39] M. K. Mamidi, W. E. Samsa, D. Danielpour, R. Chan, and G. Zhou, "The transcription co-factor JAB1/COPS5, serves as a potential oncogenic hub of human chondrosarcoma cells in vitro," *American Journal of Cancer Research*, vol. 11, no. 10, pp. 5063–5075, 2021.

[40] D. Danielpour, S. Purighalla, E. Wang, P. M. Zmina, A. Sarkar, and G. Zhou, "JAB1/COPS5 is a putative oncogene that controls critical oncoproteins deregulated in prostate cancer," *Biochemical and Biophysical Research Communications*, vol. 518, no. 2, pp. 374–380, 2019.

[41] S. Jumpertz, T. Hennes, Y. Asare, A. K. Schütz, and J. Bernhagen, "CSN5/JAB1 suppresses the WNT inhibitor DKK1 in colorectal cancer cells," *Cellular Signalling*, vol. 34, pp. 38–46, 2017.

[42] K. Watanabe, S. Yokoyama, N. Kaneto et al., "COP9 signalosome subunit 5 regulates cancer metastasis by deubiquitinating SNAIL," *Oncotarget*, vol. 9, no. 29, pp. 20670–20680, 2018.

[43] D. Velardo, E. Porrello, R. Tonlorenzi et al., "Jab1 in the pathogenesis of merosin deficient congenital muscular dystrophy (MDC1A)," *Neuromuscular Disorders*, vol. 27, p. S108, 2017.

[44] K. Sakuma, W. Aoi, and A. Yamaguchi, "Molecular mechanism of sarcopenia and cachexia: recent research advances," *Pflügers Archiv: European Journal of Physiology*, vol. 469, no. 5-6, pp. 573–591, 2017.

[45] X. C. Zhang, J. Chen, C. H. Su, H. Y. Yang, and M. H. Lee, "Roles for CSN5 in control of p53/MDM2 activities," *Journal of Cellular Biochemistry*, vol. 103, no. 4, pp. 1219–1230, 2008.

[46] Y. T. Kwon and A. Ciechanover, "The ubiquitin code in the ubiquitin-proteasome system and autophagy," *Trends in Biochemical Sciences*, vol. 42, no. 11, pp. 873–886, 2017.

[47] Y. D. Barac, F. Emrich, E. Krutzwakd-Josefson et al., "The ubiquitin-proteasome system: a potential therapeutic target for heart failure," *The Journal of Heart and Lung Transplantation*, vol. 36, no. 7, pp. 708–714, 2017.

[48] J. Blondelle, A. Biju, and S. Lange, "The role of cullin-RING ligases in striated muscle development, function, and disease," *International Journal of Molecular Sciences*, vol. 21, no. 21, p. 7936, 2020.

Hindawi
Evidence-Based Complementary and Alternative Medicine
Volume 2022, Article ID 6088585, 7 pages
https://doi.org/10.1155/2022/6088585

Research Article

Phytochemical Analysis and *In Vitro* and *In Vivo* Pharmacological Evaluation of *Parthenium hysterophorus* Linn

Gul,[1] Abdur Rauf,[2] Imtiaz Ali Khan,[3] Sulaiman Mohammad Alnasser,[4] Syed Uzair Ali Shah,[1] and Md. Mominur Rahman[5]

[1]*Department of Pharmacy, University of Swabi, Anbar 23561, Khyber Pakhtunkhwa, Pakistan*
[2]*Department of Chemistry, University of Swabi, Anbar 23561, Khyber Pakhtunkhwa, Pakistan*
[3]*Department of Entomology, The University of Agriculture, University of Peshawar, Peshawar, Khyber Pakhtunkhwa, Pakistan*
[4]*Department of Pharmacology and Toxicology, Unaizah College of Pharmacy, Qassim University, Unayzah, Saudi Arabia*
[5]*Department of Pharmacy, Faculty of Allied Health Sciences, Daffodil International University, Dhaka 1207, Bangladesh*

Correspondence should be addressed to Abdur Rauf; mashaljcs@yahoo.com and Md. Mominur Rahman; mominur.ph@diu.edu.bd

Received 8 March 2022; Accepted 27 May 2022; Published 17 June 2022

Academic Editor: Atul Kabra

The main aim of this research was to explore *Parthenium hysterophorus* Linn phytochemically and pharmacologically. Phytochemical screening is important for the isolation of active compounds before bulk extraction. The crude extracts and their fractions were screened for enzyme (urease, α-glycosidase, and phosphodiesterase) inhibition assays, *in vivo* analgesic, anti-inflammatory, and sedative effects. Results indicated the presence of steroids, flavonoids, etc. The crude extracts such as methanol, hexane, aqueous, ethyl acetate, chloroform, and butanol exhibited excellent urease inhibitory activities with $IC_{50} = 43.1 \pm 1.24$, 31.9 ± 2.21, 31.9 ± 2.21, 57.3 ± 1.27, 49.2 ± 2.16, and 35.3 ± 1.12, respectively, as compared to standard acetohydroxamic acid (20.3 ± 0.43). The extracts (methanol, hexane, aqueous, ethyl acetate, chloroform, and butanol) also showed promising α-glycosidase potency with $IC_{50} = 13.1 \pm 0.34$, 21.2 ± 1.16, 23.1 ± 0.12, 84.2 ± 2.17, 118.6 ± 3.07, and 840 ± 1.73, respectively against acarbose (840 ± 1.73). The phosphodiesterase activity of the mentioned extracts was also excellent with $IC_{50} = 131.1 \pm 2.41$, 197.2 ± 3.16, 24.2 ± 0.11, 62.4 ± 2.21, 152.4 ± 1.81, and 55.3 ± 2.15, respectively, against the standard (265.5 ± 2.25). Furthermore, butanol (14.96 ± 1.78), ethyl acetate (18.98 ± 1.71), and methanol (16.87 ± 1.00) showed dose-dependent analgesic effects with a maximum inhibition of acetic acid-induced writhes. Whereas, methanolic and butanol extracts exhibited maximum inhibition of inflammation in the carrageenan paw edema test. The aqueous ($p < 0.01$) and butanol ($p < 0.01$) extracts exhibited maximum a sedative effect followed by chloroform ($p < 0.05$), ethyl acetate ($p < 0.05$), and methanolic ($p < 0.05$) fractions as compared to the standard drug. The current research concluded that *Parthenium hysterophorus* Linn has important phytochemical constituents having inhibitory effects on urease, α-glycosidase, and phosphodiesterase enzymes. Furthermore, the plant has analgesic, anti-inflammatory, and sedative effects. The *P. hysterophorus* needs to further be explored for the candidate molecules responsible for the abovementioned activities.

1. Introduction

Parthenium hysterophorus L. (*Asterales*, *Asteraceae*, Linn) is a flowering plant and an aggressive ubiquitous annual herbaceous weed belonging to the family *Asteraceae*. *P. hysterophorus* is commonly known as altamisa, bitter weed, white top, and carrot grass. The flowering of this plant occurs throughout the year [1, 2]. *P. hysterophorus* thrives in Pakistan, America, Africa, Asia, as well as in Australia. It has multi medicinal traditional usage such as for the treatment of fever, neurologic disorders, diarrhea, dysentery, malaria, urinary tract infections, allergic respiratory problems, mutagenicity in humans, and emmenagogue. In addition, *P. hysterophorus* has been employed in traditional medicine as a remedy for inflammation and rheumatism, and as an analgesic in muscular rheumatism [3]. This plant is rich in

active compounds which are responsible for its use in traditional medicine. However, *P. hysterophorus* is not well-explored for its phytochemical constituents. Therefore, research is required for the isolation, purification, and structure determination of active constituents of this plant. *P. hysterophorus* has been reported to contain toxins called sesquiterpene lactones such as the glycoside parthenin [4]. Other phytotoxic compounds or allelochemicals present in this plant are hysterin, ambrosin, and flavonoids such as fumaric acid, quercetagetin 3,7-dimethylether, *p*-coumaric, *p*-hydroxybenzoin, vanillic acid, chlorogenic acid, anisic acid, ferulic acid, and various alcohols [5]. Ether and ethyl acetate fractions of *P. hysterophorus* have led to the isolation of fourteen compounds and some of them having cytotoxic potential [6]. A novel hydroxyproline-rich glycoprotein has been documented from the pollen of *P. hysterophorus* [7]. Another novel sesquiterpenoid, charminarone, has also been previously reported [8–10]. On the basis of the above-mentioned information, there is a need to fully explore the medicinal potential of *P. hysterophorus*, and to extract and isolate more active phytochemicals that rationalize its properties and pharmaceutical applications. The present study is an attempt to evaluate the *in vitro* enzyme (urease, α-glucosidase, and phosphodiesterase) inhibition assays, *in vivo* analgesic, anti-inflammatory, and sedative effects of the various fractions of *P. hysterophorus*.

2. Material and Methods

2.1. Plant Collection and Drying. Plant material of *P. hysterophorus* was collected from various areas of the University of Swabi, Anbar, K.P., Pakistan. The plant specimen was validated by a botanist in the Department of Botany, University of Swabi KP, Pakistan, and voucher specimen NO. BOT.UOS4 was deposited in the said department. The plant material was dried under shade at room temperature and on the ground to obtain a powder for extraction.

2.2. Extraction and Fractionation. The obtained *P. hysterophorus* powder material was subjected to cold extraction using a polar organic solvent such as methanol or ethanol, distilled water, and *n*-hexane. The extract was concentrated by means of a rotary evaporator at a low temperature (50–55°C). This was followed by fractionation using organic solvents of different polarities such as Hexane, $CHCl_3$, EtOAc, and methanol (×3 for each). The extract was then suspended with the minimum amount of water, followed by the addition of different organic solvents starting from nonpolar (*n*-hexane) to more polar ones such as chloroform, dichloromethane, ethyl acetate, and butanol, respectively. Each collected fraction was concentrated under a vacuum by using a rotary evaporator at a low temperature (50–55°C) to obtain a crude fraction. The crude extracts and fractions were subjected to phytochemical screening before bulk extraction. Finally, the obtained crude extracts and fractions were subjected to *in vitro* and *in vivo* biological assays.

2.3. Phytochemical Screening. A phytochemical screening test of extracts/fractions was carried out for identification of active phytochemicals as per reported procedures [11–15].

2.4. In Vitro Enzyme Assays

2.4.1. Urease Inhibition Activity. The urease inhibition activity of the crude extracts and fractions was performed by spectrophotometry in 96-well plates as per the standard method [16]. 5 μL of crude extracts and their fractions (0.5 mM) and 25 μL urease catalyst (1 U/well) were hatched for 15 minutes at 30°C. Then, 55 μL substrate urea (100 mM) was re-brooded at 30°C for 15 minutes. After completion of incubation, 70 μL of alkali reagents (0.1% sodium hypochlorite) and 45 μL of phenol (0.005% w/v, sodium nitroprusside and 1% w/v phenol) were mixed. The incubation of the plates was again performed for 50 minutes at 30°C. The urease screening test was periodically done with continuous urea hydrolysis and ammonia production. The change in absorbance (optical density (OD)) was monitored at 630 nm on an ELISA plate reader (Spectra Max M2, Molecular Devices CA, (USA).

2.4.2. α-Glucosidase Inhibitory Assay. The rat intestinal $(CH_3)_2CO$ (acetone) powder in normal saline (100 : 1; w/v) was sonicated appropriately, and the supernatant was used as a source of basic intestinal α-glucosidase after centrifugation [17]. Shortly, 10 mL of the prepared extract and its isolated fractions of 5 mg/mL in DMSO solution was reconstituted in 100 mL of 100 mM phosphate buffer (pH 6.8) in 96-well microplates. The hatching was done in 50 mL of essential intestinal α-glucosidase for 5 min before 50 mL of substrate (5 mM p-nitrophenyl-a-D-glucopyranoside (p-NPG) was arranged in the similar buffer) was included. The α-glucosidase-mediated conversion of p-NPG into D-glucose and p-nitrophenol at 405 nm was monitored spectrophotometrically every 5 minutes. Singular seats for the screening extract were set up to extract baseline absorbance of the substrate and altered with 50 mL of buffer. The control sample contained 10 mL DMSO alongside screening samples. The percentage of enzyme inhibition was assessed as follows:

$$1 - \left(\frac{B}{A}\right) \times 100, \quad (1)$$

where A speaks to the absorbance of the control exclusive of the prepared extract sample, and B connects to absorbance in the attendance of test samples.

2.4.3. Phosphodiesterase Inhibitory Assay. This enzyme assay was performed using snake venom-derived PDE-1 (Sigma P-4631), adopting already published methods with some modifications [18]. 30 mM Mg-acetate and 33 mM Tris-HCl buffer (pH = 8.8) were mixed as a cofactor with 0.000742 U of enzyme in 96-well plates, then 0.33 mM bis (p-nitrophenyl) phosphate (Sigma N-3002) was added as a substrate. Ethylenediaminetetraacetic acid (EDT, E. Merck, Germany)

was used as a standard drug. The inculcation was achieved for 30 minutes and the enzyme screening was examined at 37°C using a microtiter plate reader spectrophotometer, by the subsequent discharge of *p*-nitrophenol from *p*-nitrophenyl phosphate at 410 nm. All the screening tests were done in triplicate and the initial rates were calculated as the rate of changes in the OD/min (optical density/Min) and then used in the following calculation:

$$\%\,\text{Inhibition} = 100 - \left(\frac{\text{OD testwell}}{\text{OD control}}\right) \times 100. \quad (2)$$

2.5. In Vivo Biological Screening

2.5.1. Analgesic Activity. BALB/c mice of both sexes ($n = 6$) weighing 18–22 g were used. All animals were withdrawn from food 3 hours before the start of the experiment and the mice were distributed in different groups. Among the divided animals, group I was injected with normal saline (10 ml/kg) as the control, while group II was administrated with the standard drug (diclofenac sodium; 10 mg/kg), and the rest of the groups were administered with various extracts and fractions (25, 50, and 100 mg/kg i.p). After administration of 30 min, the animals were treated with 1% acetic acid. Then, the number of abdominal constrictions (writhes) was counted after 5 min of acetic acid injection for the period of 10 minutes as per the usual methods [19].

2.5.2. Anti-Inflammatory Activity. The crude extracts and various fractions of *P. hysterophorus* were also screened for anti-inflammatory activity as per the standard procedure [20]. The animals were divided into different groups of both sexes. Groups I and II were injected with normal saline (10 ml/kg) and diclofenac sodium (10 mg/kg) respectively, while the rest of the groups were administered with extracts/fractions at various doses (25, 50, and 100 mg/kg). After 30 minutes of intraperitoneal treatment, carrageenan (1%, 0.05 ml) was injected subcutaneously into the sub plantar tissue of the hind paw of each mouse. The inflammation was restrained using a plethysmometer (LE 7500 Plan Lab S.L) directly after injection of carrageenan, and then after 1, 2, 3, 4, and 5 hours of carrageenan injection. The regular foot swelling of drug-treated animals, as well as standard, was associated with that of control, and the percent inhibition of edema was calculated using the following formula:

$$\%\,\text{Inhibition} = A - \left(\frac{B}{A}\right) \times 100, \quad (3)$$

where A represents the edema volume of the control and B represents the paw edema volume of the tested group.

2.5.3. Sedative Activity. The crude extracts and various fractions of *P. hysterophorus* were also screened for muscle relaxation activity. For this screening test, a 30 cm long Pyrex glass tube with a 3 cm diameter was used in this study. From the base, the design tube is marked at 20 cm and the animals were screened after 30, 60, and 90 minutes of treatment. Various groups ($n = 5$) were treated with normal saline (10 ml/kg), standard drug, and tested extracts and their fractions (5 and 10 mg/kg i.p). The animals were introduced at one edge of the tube and then permitted to move up to the mark 20 cm from the base. When the treated animals touched the 20 cm mark, the tube was moved straight to the perpendicular position and the animals strained to climb again to the tube with a backward effort. The mouse which failed to reach up to the mark within 30 seconds was considered to have relaxed muscles [20].

3. Results

Phytochemical analysis of *Parthenium hysterophorus* is given in Table 1. The crude extracts and fractions exhibited the presence of various secondary metabolites such as steroids, fatty acids, and terpenoids. These identified phytochemicals are responsible for its urease, α-glucosidase, and phosphodiesterase inhibitory effects.

3.1. In Vitro Enzyme Inhibition Assays

3.1.1. Urease Inhibition. The urease inhibitory activities of this plant are given in Table 2. The crude extracts and various fractions of *Parthenium hysterophorus* showed excellent urease inhibition activity. The polar extracts such as ethyl acetate (87.3%), butanol (84%), and aqueous (81.4%) showed excellent activity with IC_{50} values of 57.3 ± 1.27, 35.3 ± 1.12, and 31.9 ± 2.21, respectively. The inhibitory potential is followed by *n*-hexane (77.4%), methanolic (74.2%), and chloroform (74.2%) fractions which showed moderate activity with IC_{50} values of 39.8 ± 0.36, 43.1 ± 1.24, and 49.2 ± 2.16, respectively. Acetohydroxamic acid (96.3%) is used as a standard urease inhibitor with an IC_{50} value of 20.3 ± 0.43.

3.1.2. α-Glycosidase Inhibition. The α-glycosidase inhibitory activities of this plant are given in Table 3. The crude extracts and different fractions of *P. hysterophorus* showed excellent α-glycosidase inhibition potential. The extracts such as methanolic (94.2%), aqueous (91.4%), and butanol (90.2%) showed excellent activity with IC_{50} values of 13.1 ± 0.34, 23.1 ± 0.12, and 840 ± 1.73, respectively. The inhibitory potential of α-glucosidase was followed by *n*-hexane (84.7%), ethyl acetate (82.7%), and chloroform (76.4%) fractions with IC_{50} values of 840 ± 1.73, 84.2 ± 2.17, and 118.6 ± 3.07, respectively. The standard α-glucosidase inhibitor, acarbose, exhibited percent inhibition (90.2%) with an IC_{50} value of 840 ± 1.73.

3.1.3. Phosphodiesterase Inhibition. The phosphodiesterase inhibitory activities of this plant are given in Table 4. The crude extract and different fractions of *P. hysterophorus* showed excellent phosphodiesterase inhibition potential. The extract such as aqueous (91.4%), butanol (88.4%) and n-hexane (82.7%) showed excellent activity with IC_{50} values of 24.2 ± 0.11, 55.3 ± 2.15, 197.2 ± 3.16, respectively. The inhibitory potential of phosphodiesterase is followed by the methanolic (79%), chloroform (78.4%), and ethyl acetate

Table 1: Phytochemical screening test of extracts and fractions of *P. hysterophorus*.

Phytochemicals	MeOH	Hexane	Aqueous	EtOAc	Chloroform	Butanol
Alkaloids	+	−	+	+	−	+
Tannins	+	−	+	+	−	+
Anthraquinones	−	−	−	−	−	−
Glycosides						
Reducing sugars	+	−	+	−	+	+
Saponins	+	−	+	−	−	+
Flavonoids	+	−	+	+	+	+
Phlobatannins	+	−	+	+	−	+
Steroids	+	+	+	+	+	+
Terpenoids	+	+	+	+	+	+

where MeOH is the methanolic extract and EtOAc is the ethyl acetate fraction.

Table 2: Urease inhibition activity of extracts and fractions of *Parthenium hysterophorus*.

Extract/fractions	Concentrations (μg/mL)	% Inhibition	IC50 (μg)
MeOH	0.2	74.2	43.1 ± 1.24
Hexane	0.2	77.4	39.8 ± 0.36
Aqueous	0.2	81.4	31.9 ± 2.21
Ethyl acetate	0.2	87.3	57.3 ± 1.27
Chloroform	0.2	74.2	49.2 ± 2.16
Butanol	0.2	84.0	35.3 ± 1.12
Acetohydroxamic acid	0.2	96.3	20.3 ± 0.43

Table 3: α-Glucosidase activity of extracts and fractions of *Parthenium hysterophorus*.

	Concentrations (μg/mL)	% inhibition	IC50 (μg)
MeOH	0.2	94.2	13.1 ± 0.34
Hexane	0.2	84.7	21.2 ± 1.16
Aqueous	0.2	91.4	23.1 ± 0.12
Ethyl acetate	0.2	82.7	84.2 ± 2.17
Chloroform	0.2	76.4	118.6 ± 3.07
Butanol	0.2	90.2	840 ± 1.73
Acarbose	0.2	90.2	840 ± 1.73

Table 4: Phosphodiesterase activity of extracts and fractions of *Parthenium hysterophorus*.

Extract/fractions	Concentrations (μM) (μg/mL)	% inhibition	IC50 (μg)
MeOH	0.2	79.0	131.1 ± 2.41
Hexane	0.2	82.7	197.2 ± 3.16
Aqueous	0.2	91.4	24.2 ± 0.11
Ethyl acetate	0.2	76.5	62.4 ± 2.21
Chloroform	0.2	78.4	152.4 ± 1.81
Butanol	0.2	88.4	55.3 ± 2.15
EDTA	0.2	87.9	265.5 ± 2.25

where EDTA is for ethyl amine tetra acetic acid.

(76.5%) with IC_{50} values of 131.1 ± 2.41, 152.4 ± 1.81, and 62.4 ± 2.21, respectively. The standard phosphodiesterase inhibitor, EDTA exhibited 87.9% inhibition with an IC_{50} value of 265.5 ± 2.25.

3.2. In Vivo Activities

3.2.1. Analgesic Effect. The crude extracts and various fractions of *P. hysterophorus* including methanol, hexane, aqueous, ethyl acetate, chloroform, and butanol were assessed for analgesic activity. All the extracts/fractions were tested at 25, 50, and 100 mg/kg and the effects were observed to be dose-dependent. Among the tested extracts, butanol, ethyl acetate, and methanol showed maximum analgesic effect as compared to the standard drug (Table 5). The aqueous, chloroform, and n-hexane fraction of *P. hysterophorus* exhibited a moderate analgesic effect (Table 5).

3.2.2. Anti-Inflammatory Effect. The crude extracts and various fractions were assessed for anti-inflammatory. Among the tested extracts, the methanolic and butanol

Table 5: The analgesic effect of crude extracts and various fractions of *P. hysterophorus*.

Treatment	Dose (mg/kg)	No. of writhing
Normal saline	10 ml/kg	65.77 ± 3.46
Diclofenac sodium	10	17.67 ± 1.14
MeOH	25	51.48 ± 2.45
	50	32.76 ± 1.19
	100	16.87 ± 1.00
Hexane	25	66.85 ± 2.41
	50	48.45 ± 1.17
	100	32.54 ± 1.99
Aqueous	25	60.87 ± 2.67
	50	41.45 ± 1.56
	100	25.45 ± 1.98
Ethyl acetate	25	55.54 ± 2.49
	50	33.76 ± 1.90
	100	18.98 ± 1.71
Chloroform	25	61.45 ± 2.40
	50	42.98 ± 1.14
	100	26.98 ± 1.98
Butanol	25	48.45 ± 2.41
	50	29.98 ± 1.98
	100	14.96 ± 1.78

extracts exhibited maximum inhibition after 3 hours of administration of extracts, as shown in Figure 1. However, the percent inhibition of the standard diclofenac sodium drug was promising throughout 6 hours of the experiment duration.

3.2.3. Sedative Effect. The crude extracts and various fractions of *P. hysterophorus* including methanol, hexane, aqueous, ethyl acetate, chloroform, and butanol were assessed for sedative activity. Among the tested extracts, the aqueous and butanol extracts exhibited maximum sedative effect followed by chloroform, ethyl acetate, and methanolic fractions as compared to the standard drug (Table 6).

4. Discussion

Phytochemicals in medical plants play key roles in their biological potency. Phytochemical analysis plays a significant role in the isolation of new active and rare compounds. The biomedical importance of plants is correlated due to the presence of secondary metabolites. Our plant of interest, *P. hysterophorus,* was collected, processed, and extracted with various solvents to obtain crude extracts and fractions. The crude extracts and fractions exhibited the presence of various secondary metabolites such as steroids, fatty acids, terpenoids alkaloids, tannins, reducing sugars, saponins, flavonoids, and phlorotannins. *P. hysterophorus* is already reported as an ailment for various diseases in the traditional system. The plant is reported to have a diverse nature of compounds including allelochemicals (such as hysterin and ambrosin), flavonoids(such as fumaric acid, quercetagetin 3, 7-dimethylether, *p*-coumaric, *p*-hydroxybenzoin, vanillic acid, chlorogenic acid, anisic acid, and

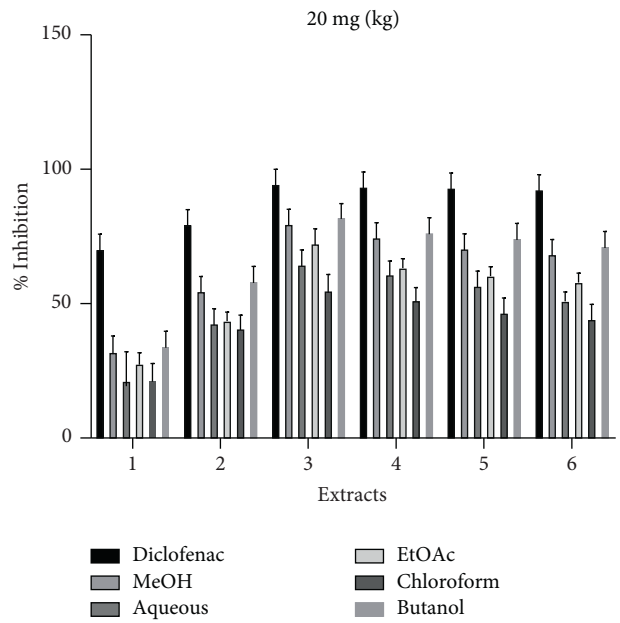

Figure 1: Anti-inflammatory activity of crude extracts/fractions of *P. hysterophorus*.

Table 6: The sedative effect of crude extracts and various fractions of *P. hysterophorus*.

Treatment	Dose	No. of lines crossed
Normal saline	10 ml/kg	126 ± 1.25
Diazepam	0.5 mg/kg	6 ± 0.13***
MeOH	25	110.51 ± 4.23
	50	102.60 ± 3.44
	100	94.68 ± 3.35*
Hexane	25	115.90 ± 4.21
	50	108.69 ± 3.40
	100	100.99 ± 3.30*
Aqueous	25	98.51 ± 4.29
	50	88.63 ± 3.24
	100	80.61 ± 3.14***
Ethyl acetate	25	107.51 ± 3.99
	50	97.61 ± 3.29
	100	89.66 ± 3.00**
Chloroform	25	105.55 ± 4.34
	50	94.65 ± 3.20
	100	83.69 ± 3.10**
Butanol	25	100.54 ± 4.200
	50	90.69 ± 3.23
	100	81.65 ± 3.13***

where, $P < 0.05^{*}$, $P < 0.03^{**}$, and $P < 0.01^{***}$.

ferulic acid), and various alcohols [5]. A novel hydroxyproline-rich glycoprotein has been documented from the pollen of *P. hysterophorus* [7]. Another novel sesquiterpenoid, charminarone, has also been previously reported [8–10].

The extracts and fractions of *P. hysterophorus* were screened for in vitro selective enzyme inhibition assays including urease, α-glucosidase, and phosphodiesterase. The ethyl acetate (87.3%), butanol (84%), and aqueous

(81.4%) fractions of *P. hysterophorus* exhibited maximum inhibition of urease enzyme compared to other fractions, however, exhibited less activity than the standard acetohydroxamic acid (96.3%). Urease is a metalloenzyme found in bacteria and plants. The urease inhibitors are important in the conditions associated with ureolytic bacteria [21]. Furthermore, the urease inhibitor is effective against *H pylori* infections [22]. In agriculture, urease inhibitors are associated with the proper utilization of urea fertilizers and modifying the nitrogen cycle [23]. Furthermore, α-glucosidase inhibition by various fractions of *P. hysterophorus* highlighted its importance for controlling hyperglycemia in diabetic patients [24, 25].

The phosphodiesterase inhibition by the fractions of *P. hysterophorus* is worth noting. Phosphodiesterase (PDE) has more than 40 isoforms, further subdivided into eleven families. These enzymes (present in each cell) hydrolyze the intercellular second messengers, cyclic nucleotide adenosine-3′, 5′- cyclic monophosphate (cAMP), and guanosine-3′, 5′-cyclic monophosphate (cGMP), thus altering cell response [24]. The PDEs are considered potential targets for combating various diseases including Alzheimer's disease, erectile dysfunction, and asthma [26]. The PDE isoforms expressed in cardiovascular systems and CNS are targeted in the treatment of pulmonary hypertension and cardiovascular disorders [27].

The acetic acid-induced writhing test is used to examine the preliminary analgesic properties of *P. hysterophorus* extracts and fractions [28]. The acetic acid causes the generation of pain mediators, thereby resulting in the constriction of the abdominal muscles [28, 29]. Our data exhibited promising analgesic effects in the butanol, ethyl acetate, and methanol extracts *P. hysterophorus*, whereas aqueous, chloroform, and *n*-hexane fractions exhibited moderate analgesic activity. Therefore, the phytochemical constituents of *P. hysterophorus* may play a role in inhibiting the release of pain-stimulating mediators such as prostaglandins (PGs), bradykinin, and histamine [30, 31]. Among these mediators, PGs are mostly responsible for the induction of pain. The selected plant probably inhibits cyclooxygenase, and thus, blocks the production of PGs and other intracellular cascades leading to pain, inflammation, and pyrexia.

The traction and chimney screening tests are common tools for the *in vivo* assessment of the skeleton muscle relaxation potential of substances [28]. In our findings, the aqueous and butanol extracts exhibited maximum sedative effect followed by chloroform, ethyl acetate, and methanolic fractions as compared to the standard drug, diazepam. The sedative and muscle relaxant effect suggested that the chemical constituents of this plant keep the anion neuronal channels open, especially the chloride channels which leads to central nervous system depression. The induction of anion influx is mostly related to the stimulation of GABA (gamma-aminobutyric acid) receptors, thereby hyperpolarizing the neuronal membrane via more chloride influx [32]. It is also suggested that the extracts or fractions might be accelerating the action of GABA neurotransmitters which are responsible for sedation and muscle relaxant effect.

5. Conclusion

It is concluded that crude extracts and various fractions showed the presence of active phytochemicals such as steroids, alkaloids, and terpenoids. The polar extracts and fractions exhibited excellent enzyme inhibition potency, thereby signifying the inhibition potential of urease, α-glucosidase, and phosphodiesterase by its phytochemical constituents. The sedative, anti-inflammatory, and analgesic potential of plants are also validated experimentally. Based on our data, we can conclude that *P. hysterophorus* could be a potential source of new, less toxic, safe, and more effective candidate drugs for pharmaceutical industries, thereby decreasing the economic burden for the therapy of different diseases involving the targets such as urease, α-glucosidase, and phosphodiesterase.

Data Availability

All data are available in the text.

Conflicts of Interest

The authors declare that they have no conflicts of interest.

Acknowledgments

The authors acknowledge the Pakistan Science Foundation Project NO. PSF/NSLP/KP-UoS (737) for providing research funds for this work.

References

[1] R. K. Meena, B. Dutt, R. Kumar, and K. R. Sharma, "Phytochemistry of congress grass (*Parthenium hysterophorus* L.) and harmful and beneficial effect on human and animals: a review," *International Journal of Chemical Studies*, vol. 5, no. 4, pp. 643–647, 2017.

[2] S. Patel, "Harmful and beneficial aspects of *Parthenium hysterophorus:* an update," *3 Biotech*, vol. 1, no. 1, pp. 1–9, 2011.

[3] A. I. Maishi, P. K. Shoukat Ali, S. A. Chaghtai, and G. Khan, "A proving of *Parthenium hysterophorus*, L," *British Homeopathic Journal*, vol. 87, no. 01, pp. 17–21, 1998.

[4] A. Rauf, A. Khan, N. Uddin et al., "Preliminary phytochemical screening, antimicrobial and antioxidant activities of *Euphorbia milli*," *Pakistan Journal of Pharmaceutical Sciences*, vol. 27, no. 4, pp. 947–951, 2014.

[5] H. C. Evans, "Parthenium hysterophorus. a review of its weed status and the possibilities for biological control," *Biocontrol News and Information*, vol. 18, pp. 89–98, 1997.

[6] M.-H. Wang, J.-J. Gan, W.-H. Chen, and Y.-L. Guan, "Chemical constituents of *Parthenium hysterophorus*," *Chemistry of Natural Compounds*, vol. 56, no. 3, pp. 556–558, 2020.

[7] H. Lata, V. K. Garg, and R. K. Gupta, "Sequestration of nickel from aqueous solution onto activated carbon prepared from *Parthenium hysterophorus* L," *Journal of Hazardous Materials*, vol. 157, no. 2-3, pp. 503–509, 2008.

[8] N. Gupta, B. M. Martin, D. D. Metcalfe, and P. V. S. Rao, "Identification of a novel hydroxyproline-rich glycoprotein as the major allergen in Parthenium pollen," *The Journal of*

Allergy and Clinical Immunology, vol. 98, no. 5, pp. 903–912, 1996.

[9] A. Joshi, R. K. Bachheti, A. Sharma, and R. Mamgain, "*Parthenium hysterophorus*. L. (asteraceae): a boon or curse? (a review)," *Oriental Journal of Chemistry*, vol. 32, no. 3, pp. 1283–1294, 2016.

[10] A. Ramos, R. Rivero, A. Visozo, J. Piloto, and A. García, "Parthenin, a sesquiterpene lactone of *Parthenium hysterophorus* L. is a high toxicity clastogen," *Mutation Research*, vol. 514, no. 1-2, pp. 19–27, 2002.

[11] N. R. Farnsworth, "Biological and phytochemical screening of plants," *Journal of Pharmaceutical Sciences*, vol. 55, no. 3, pp. 225–276, 1966.

[12] J. R. Shaikh and M. Patil, "Qualitative tests for preliminary phytochemical screening: an overview," *International Journal of Chemical Studies*, vol. 8, no. 2, pp. 603–608, 2020.

[13] S. C. Chhabra, F. C. Uiso, and E. N. Mshiu, "Phytochemical screening of Tanzanian medicinal plants. I," *Journal of Ethnopharmacology*, vol. 11, no. 2, pp. 157–179, 1984.

[14] A. Doss, "Preliminary phytochemical screening of some Indian medicinal plants," *Ancient Science of Life*, vol. 29, no. 2, pp. 12–16, 2009.

[15] O. A. Aiyegoro and A. I. Okoh, "Preliminary phytochemical screening and in vitro antioxidant activities of the aqueous extract of *Helichrysum longifolium* DC," *BMC Complementary and Alternative Medicine*, vol. 10, no. 1, p. 21, 2010.

[16] A. Hameed, M. Al-Rashida, M. Uroos et al., "A patent update on therapeutic applications of urease inhibitors (2012–2018)," *Expert Opinion on Therapeutic Patents*, vol. 29, no. 3, pp. 181–189, 2019.

[17] F. Shaheen, M. Ahmad, S. Nahar Khan et al., "New α-glucosidase inhibitors and antibacterial compounds from *Myrtus communis* L," *European Journal of Organic Chemistry*, vol. 10, pp. 2371–2377, 2006.

[18] D. Saleheen, S. Bukhari, S. R. Haider et al., "Association of phosphodiesterase 4D gene with ischemic stroke in a Pakistani population," *Stroke*, vol. 36, no. 10, pp. 2275–2277, 2005.

[19] N. Muhammad, R. Lal Shrestha, A. Adhikari et al., "First evidence of the analgesic activity of govaniadine, an alkaloid isolated from *Corydalis govaniana* Wall," *Natural Product Research*, vol. 29, no. 5, pp. 430–437, 2015.

[20] N. Muhammad, M. Saeed, and S. N. Gilani, "Analgesic and anti-inflammatory profile of n-hexane fraction of viola betonicifolia," *Tropical Journal of Pharmaceutical Research*, vol. 11, no. 6, pp. 963–969, 2013.

[21] N. Muhammad, M. Saeed, H. Khan, and I. Haq, "Evaluation of *n*-hexane extract of viola betonicifolia for its neuropharmacological properties," *Journal of Natural Medicines*, vol. 67, pp. 1–8, 2013.

[22] L. V. Modolo, A. X. de Souza, L. P. Horta, D. P. Araujo, and A. de Fatima, "An overview on the potential of natural products as ureases inhibitors: a review," *Journal of Advanced Research*, vol. 6, no. 1, pp. 35–44, 2015.

[23] J. T. Zhou, C. L. Li, L. H. Tan et al., "Inhibition of *Helicobacter pylori* and its associated urease by palmatine: investigation on the potential mechanism," *PLoS One*, vol. 12, no. 1, Article ID e0168944, 2017.

[24] T. Hara, J. Nakamura, N. Koh, F. Sakakibara, N. Takeuchi, and N. Hotta, "An importance of carbohydrate ingestion for the expression of the effect of α-glucosidase inhibitor in NIDDM," *Diabetes Care*, vol. 19, no. 6, pp. 642–647, 1996.

[25] E. M. Kawakami, D. M. Oosterhuis, J. L. Snider, and M. Mozaffari, "Physiological and yield responses of field-grown cotton to application of urea with the urease inhibitor NBPT and the nitrification inhibitor DCD," *European Journal of Agronomy*, vol. 43, pp. 147–154, 2012.

[26] S. Uckert, P. Hedlund, E. Waldkirch et al., "Interactions between cGMP-and cAMP-pathways are involved in the regulation of penile smooth muscle tone," *World Journal of Urology*, vol. 22, no. 4, pp. 261–266, 2004.

[27] J. Prickaerts, P. R. A. Heckman, and A. Blokland, "Investigational phosphodiesterase inhibitors in phase I and phase II clinical trials for Alzheimer's disease," *Expert Opinion on Investigational Drugs*, vol. 26, no. 9, pp. 1033–1048, 2017.

[28] M. M. Rahman, F. Islam, A. Parvez et al., "Citrus limon L.(lemon) seed extract shows neuro-modulatory activity in an in vivo thiopental-sodium sleep model by reducing the sleep onset and enhancing the sleep duration," *Journal of Integrative Neuroscience*, vol. 21, no. 1, p. 42, 2022.

[29] S. Bawazeer, M. Ibrar, N. Ikram et al., "*In vivo* antinociceptive and muscle relaxant activity of leaf and bark of *Buddleja asiatica* L," *Pakistan Journal of Pharmaceutical Sciences*, vol. 29, no. 5, pp. 1509–1512, 2016.

[30] J. Zhao, F. Fang, L. Yu, G. Wang, and L. Yang, "Anti-nociceptive and anti-inflammatory effects of *Croton crassifolius* ethanol extract," *Journal of Ethnopharmacology*, vol. 142, no. 2, pp. 367–373, 2012.

[31] I. D. Duarte, M. Nakamura, and S. H. Ferreira, "Participation of the sympathetic system in acetic acid-induced writhing in mice," *Brazilian Journal of Medical and Biological Research*, vol. 21, no. 2, pp. 341–343, 1988.

[32] H. Khan, M. Saeed, A. U. H. Gilani, M. A. Khan, A. Dar, and I. Khan, "The antinociceptive activity of Polygonatum verticillatumrhizomes in pain models," *Journal of Ethnopharmacology*, vol. 127, no. 2, pp. 521–527, 2010.

Hindawi
Evidence-Based Complementary and Alternative Medicine
Volume 2022, Article ID 6798377, 7 pages
https://doi.org/10.1155/2022/6798377

Research Article

The Protective Effect of Ginsenoside Rg1 on Apoptosis in Human Ankle Joint Traumatic Arthritis Chondrocytes

Zhiqiang Xu,[1] Xue Li,[2] Guodong Shen,[2] Yunxuan Zou,[2] Hongning Zhang,[2] Kangyong Yang,[2] and Yongzhan Zhu[2]

[1]*Orthopaedics Center, Foshan Hospital of Traditional Chinese Medicine, Guangzhou University of Chinese Medicine, Foshan 528000, China*
[2]*8th Department of Orthopaedics, Foshan Hospital of Traditional Chinese Medicine, Guangzhou University of Chinese Medicine, Foshan 528000, China*

Correspondence should be addressed to Yongzhan Zhu; lixue8132581@163.com

Received 31 December 2021; Revised 15 February 2022; Accepted 17 February 2022; Published 21 April 2022

Academic Editor: Atul Kabra

The ankle biomechanics is easily changed due to the acute injury of the tissue around the ankle joint and the damage of the ankle joint structure, such as ankle instability and joint surface imbalance. When the mechanical load of the ankle changes, it can cause ankle regeneration and remodeling processes such as cartilage loss, bone remodeling, and degenerative changes. The aim of this study was to investigate the effect and mechanism of ginsenoside Rg1 against interleukin-1β (IL-1β)-induced apoptosis in human articular chondrocytes (HACs). The apoptosis model of HAC cells was established by IL-1β induction, and then the HAC cells were cultured with different concentrations of Rg1. The protective effect of Rg1 on HAC cell apoptosis was investigated by detecting the changes of apoptosis and activity of PI3K/Akt/mitochondrial signaling pathway. The results showed that a specific concentration of Rg1 could promote the proliferation of IL-1β-induced HAC cells and inhibit apoptosis. At the same time, Rg1 treatment with specific concentration can reduce the content of reactive oxygen species (ROS) and malondialdehyde (MDA) in HACs and improve the related expression of mitochondrial membrane potential (MMP). Furthermore, qRT-PCR and western blot results showed that Rg1 could improve the low expression of Bcl-2 and inhibit the high expression of Bax, caspase-3, caspase-8, caspase-9, FasL, AIF, and Cyto c in IL-1β-induced cells. In summary, Rg1 can inhibit IL-1β-induced apoptosis of HAC cells by decreasing the activity of PI3K/Akt/mitochondrial signaling pathway, and Rg1 has a protective effect on apoptosis of HAC cells.

1. Introduction

Traumatic arthritis is followed by joint trauma; clinical pain and dysfunction signs often lag behind the initial injury for years or decades, accounting for about 12% of all types of osteoarthritis (OA) [1]. Ankle sprains are the most common sports-related injuries, involving the lateral collateral ligament complex in 85% of cases [2]. Any trauma to damage the surface of ankle can lead to the occurrence of ankle traumatic arthritis; the most common traumatic causes are considered to be intra-ankle fractures resulting in cartilage damage and ligament instability [3–5]. Apoptosis is considered to be one of the main causes of the loss of joint cartilage cells [6]. Apoptosis is designed to maintain environmental stability in the individual body, a process of independent and orderly cell death that is controlled by genes, regulated by a variety of cytokines and signaling pathways [7].

Cartilage protective drugs, which are nonsteroidal anti-inflammatory drugs, are the main drugs used to treat traumatic arthritis of human ankle joints [8, 9]. But their clinical effect of preventing or improving OA disease is not obvious [10]. Chinese medicine gained popularity in recent years for its potential therapeutic effects and low side effects [11, 12]. At present, ginseng saponin has been shown to have antagonistic apoptosis in many cells [13]. Gong et al. have found that ginsenoside Rg1 protected β-amyloid-induced apoptosis of primary cultured rat hippocampal neurons by

increasing the Bcl-2/Bax ratio and inhibiting caspase-3 activation [14]. Hashimoto et al. then reported that ginseng saponins can inhibit the activation of PC12 cell line caspase-3 by activating the Akt and ERK1/2 signaling pathways and ultimately inhibit its apoptosis [15]. It can be seen that Rg1 does inhibit apoptosis, thus protecting related cells. In recent years, ginsenoside Rg1 has also been studied in osteoarthritis. Rg1 can treat both osteoarthritis and anterior cruciate ligament transection in rats. Rg1 can inhibit the inflammatory response of chondrocytes in vitro and reduce articular cartilage damage in rats. Rg1 has good research significance in the treatment of osteoarthritis. However, the mechanism of Rg1 in the treatment of osteoarthritis needs further study.

Mitochondria are susceptible parts of various damage factors, and the change of mitochondrial membrane permeability is a key step in the survival process of cells [16]. Caspase is an evolutionarily conservative family of cysteine protease, and the signaling pathway of relying on caspase is the primary route of apoptosis [17, 18]. We suspect that Rg1 may inhibit the apoptosis of human articular chondrocytes (HACs) by affecting the PI3K/Akt/mitochondrial signaling pathway, ultimately reducing the production of inflammatory factors.

In this study, the IL-1 β-induced HAC apoptosis model was used to determine the protective effect of Rg1 on HAC apoptosis through PI3K/Akt/mitochondrial signaling pathway.

2. Materials and Methods

2.1. Culture and Identification of HAC. The knee cartilage of healthy volunteers was cut under sterile conditions. The knee cartilage was cut into 0.5–1 mm^3 particles on a superclean workbench. It was digested about 2 hours with trypsin and washed twice with D-Hanks solution [19]. Then, the 10× cartilage volume of 0.2% II-type collagen enzyme was added to digest the cartilage overnight. The next day, the raw fluid was removed by centrifuge to obtain the cells and the media were added. The cells were moved into 100 mm cell culture dish and incubated at 37°C. The fluid was changed 2 to 3 times a week. The cells were digested 3 min with 0.05% trypsin containing EDTA when it near fusion. The cells were subcultured for 3-4 generations to obtain the human articular chondrocytes (HACs). All volunteers signed informed consent before surgery. Meanwhile, the study has been approved by the Ethics Committee of Foshan City Hospital of the Guangzhou University of Chinese Medicine.

2.2. Immunofluorescence Detection. HAC cells were inoculated in Petri dishes with cover glass slides for further subculture. After the cells developed into a monolayer, the cover glass was removed and washed twice with PBS buffer. 4% paraformaldehyde was added and fixed for 4 h and then washed for 3 times with PBS. Sealing solution was added and sealed for 30 min and then washed with PBS for 3 times. The anti-collagen II antibody (GB14073; Servicebio, Wuhan, China) was added at the dilution of 1 : 300 and incubated overnight and then washed with PBST for 3 times. Cy3-labeled secondary antibody (GB21401; Servicebio, Wuhan, China) was added at the dilution of 1 : 500 and incubated at room temperature for 1 h without light and then rinsed with PBST for 3 times. Fluorescence microscopy was performed, and the luminescence was excited at 570 nm.

2.3. CCK-8 Assay. HACs were grown in 96-well microplates. The CCK-8 solution (PH687; DOJINDO, Japan) was then added to the medium and incubated at 37°C for 4 h. Cell viability was measured using Multiskan FC (Thermo Scientific, USA).

2.4. Flow Cytometry. Annexin V-FITC/PI (KL602, DOJINDO, Japan) staining was used to determine the number of apoptotic cells. In simple terms, 5 μL PI and 10 μL annexin V-FITC solutions were added to 200 μL binding buffer, followed by cells resuspension and reaction for 10 min at 25°C in the dark. The apoptosis cells were analyzed using flow cytometry (BD, USA).

2.5. Reactive Oxygen Species (ROS). HAC cells were added with different concentrations of Rg1 solution and incubated in a cell incubator at 37°C in the dark. The collected cells were added with trypsin 10 μL and 1 mL PBS buffer and incubated. The cells were centrifuged at 4600g for 5 min. The supernatant was taken and centrifuged at 4,100g for 10 min. The supernatant was discarded, the precipitation was collected, and 200 μL PBS was added to resuspend the mitochondrial extract. The instructions of the ROS test kit (BB-47051; BestBio, China) were followed. An appropriate amount of DCFH-DA solution was added to the mitochondria suspension and then incubated at 37°C in darkness for 15 min. The excitation wavelength was set at 488 nm, and the emission wavelength was set at 525 nm. The fluorescence intensity of ROS was measured using a fluorescence spectrophotometer.

2.6. Malondialdehyde (MDA) Activity. HAC cells were collected and evaluated for MDA activity using a commercial ELISA kit (MSK, Wuhan). The blank control well was set. The 50 μL sample was taken out and added into the sample well. 50 μL detection antibody was added, and the reaction well was sealed with a sealing plate membrane and incubated in an incubator at 37°C for 2 h. The reaction solution was disposed, and 300 μL washing solution was added, washed 5 times repeatedly. Substrates A and B 50 μL were added to each well and incubated at 37°C for 15 min in the dark. The 50 μL stop solution was added and shook well. The OD value at 450 nm was determined by using an enzyme plate analyzer.

2.7. Mitochondrial Membrane Potential (MMP) Assay. The MMP kit (Beyotime, Haimen, China) was used to detect MMP in cells. HAC cells in 6-well plates were routinely cultured, washed with PBS, and resuspended. The cells were cultured in 500 μL JC-1 working solution at 37°C for 20 min

and washed with PBS twice. MMP ratios of cells were analyzed using a flow cytometer system (BD, USA).

2.8. qRT-PCR. The mRNA expression of gene was detected by RT-PCR. The total RNA was extracted by using the Total RNA Extraction Kit (TIANGEN, Beijing, China) and then reversely transcribed into cDNA. The corresponding reaction system was configured to conduct PCR on cDNA. The reaction conditions were as follows: preheating at 95°C for 3 min, 95°C for 1 min, 60°C for 30 seconds, 72°C for 1 min, a total of 35 cycles.

2.9. Western Blot. Cells were collected and cultured in cell culture plates. Total proteins were extracted from the cells for gel electrophoresis and membrane transfer. The target protein was detected by anti-Cyto c (1 : 1000), caspase-9 (1 : 1000), Bcl-2 (1 : 500), and FasL (1 : 1000) (Abcam, USA) antibodies. HRP-labeled secondary antibody (1 : 1000; Santa Cruz, USA) was combined with primary antibody and cultured at 25°C for 1 h. The bands were detected using an infrared imaging system (LI-COR Biosciences, Nebraska, USA).

2.10. Statistical Analysis. GraphPad 8.0 software was used to analyze the data, and the mean ± standard deviation was used for all analyses. ANOVA was used to analyze the differences between groups, with $P < 0.05$ regarded as significant. All experiments were repeated three times.

3. Results

3.1. Culture and Identification of HAC. Primary cells generally adhered early and gradually extended to the surrounding after adherence, tiling into a polygon or short shuttle shape (Figure 1(a)). After cultivating for about 1 week, 80% of the cells were nearly confluent, at which time they could be digested and passaged. The shape of the third-generation cells was similar to the primary cells, evenly distributed (Figure 1(b)) and can produce cartilage-specific matrix, which was conducive to the maintenance and recovery of chondrocyte phenotype (Figure 1(c)). The expression of collagen type 2 in HAC cells was observed by immunofluorescence assay, and the cells were cultured well (Figure 1(d)).

3.2. Rg1 Promotes the Proliferation of HAC. There was no significant difference between the groups at 24 h ($P > 0.05$), and there was significant difference in cell proliferation promotion between the groups at 48 h and 72 h (Figure 2). Moreover, the high dose of Rg1 (100 μg/mL) exhibited an increase in cell viability between the groups at 48 h and 72 h. This indicates that the appropriate concentration of Rg1 obviously promotes the proliferation of HAC, and the high concentration of Rg1 obviously promote the cell proliferation with the culturing time.

3.3. Rg1 Inhibits Apoptosis of IL-1β-Induced HAC. We used the culture of IL-1β (10 μg/L) as an experimental concentration to induce HAC for 24 h and then treated the HAC with different concentrations of Rg1. Figure 3 shows the result of HAC being tested by a flow cytometer. The rate of apoptosis cells in the IL-1β+0 μg/mL Rg1 group was significantly higher than that of the control group ($P < 0.05$). The apoptosis rate of Rg1 treatment group was markedly lower than that of the IL-1β group and was in a concentration-dependent manner.

3.4. Effect of Rg1 on HAC Cell Mitochondrial Signaling Pathways. In order to further clarify the protective effect of Rg1 on mitochondrial apoptosis, we detected the levels of ROS and MDA in cells of different treatment groups. The results of the fluorescence spectrophotometer showed that the ROS content in IL-1β-induced cells was significantly increased ($P < 0.001$). The ROS contents in the IL-1β+(10, 50, 100 μg/mL Rg1) groups were significantly lower than that in the IL-1β group (Figure 4(a)). In addition, the MMP test results showed that the MMP was significantly decreased in the IL-1β group, but the inhibition was reversed with the increase of Rg1 concentration (Figure 4(b)). The results showed that MDA content in IL-1β -induced cells was significantly increased, and increased Rg1 concentration could effectively reduce MDA content in IL-1β -induced cells (Figure 4(c)). To further explore how Rg1 inhibits mitochondrial pathway apoptosis, qRT-PCR and western blot analysis showed that IL-1β-induced cells reduced Bcl-2 expression and increased the expression of Bax, caspase-3, caspase-8, caspase-9, FasL, AIF, and Cyto c expressions (all $P < 0.01$) (Figures 4(d) and 4(e)). Mitochondrial apoptosis induced by IL-1β can be ameliorated by treatment with Rg1.

4. Discussion

Recent studies have found that Rg1 has a higher medicinal effect because of its antiapoptosis effect in a variety of cells. Gong et al. observed that in the neurons of the hippocampus, Rg1 has antagonistic amyloid-induced apoptosis, which can be used as a neuroprotector [14]. Yan et al.'s study found that Rg1 had a protective effect on β-amyloid-induced epithelial apoptosis [20]. In our present study, we found that the use of different concentrations of Rg1 pretreatment of HAC of IL-1β showed that the apoptosis rate of HAC was significantly lower than that of the IL-1β group, indicating that Rg1 did have an effect in suppressing HAC apoptosis.

The signaling pathway mechanism for the effect of Rg1 on the apoptosis of cartilage cells is not yet known. Studies have shown that blocking the PI3K/Akt/mitochondrial signaling pathway can reduce the apoptosis of IL-1β-induced cartilage cells in cartilage cells [21, 22]. Mitochondrial function plays an important role in the process of apoptosis [23]. Bcl-2 family protein is the main protein for mitochondrial pathways to regulate apoptosis, while Bcl-2 and Bax are the most representative inhibitory apoptosis and promoter proteins in the Bcl-2 family, respectively [24, 25]. Caspase-3 is the most important promoter of apoptosis, downstream of the apoptosis-affiliated reaction, resulting in cell death [26]. The Fas/FasL system is one of the leading signal transduction pathways for

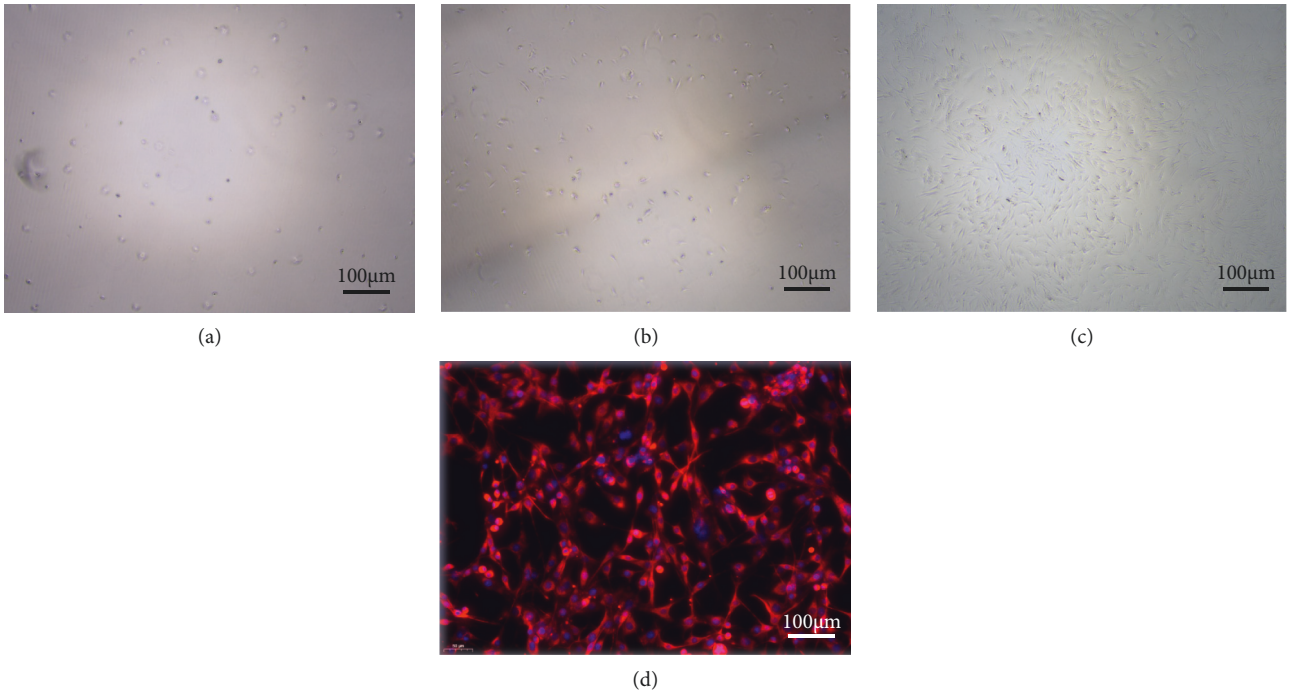

Figure 1: Culture and identification of HAC. (a) The primary cells of HAC. (b) The third-generation cells of HAC. (c) The third-generation cells of HAC adherent growth (200×). (d) Detection of type 2 collagen in HAC by immunofluorescence.

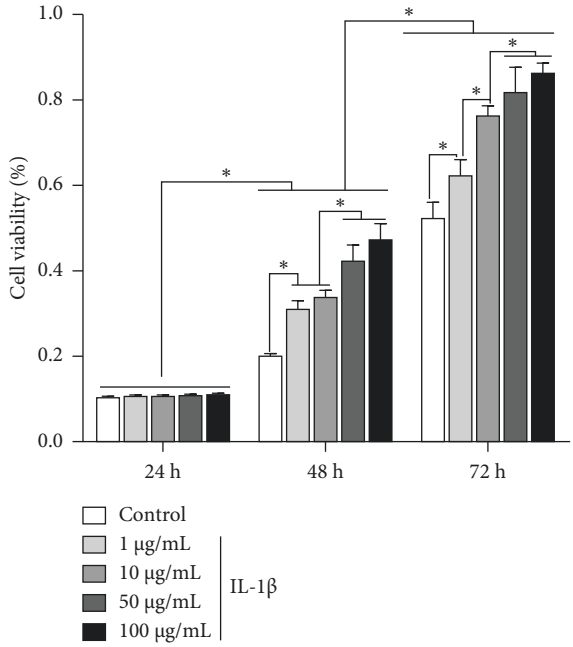

Figure 2: Rg1 promotes the proliferation of HAC. The cell viability was evaluated by MTT assay (*$p < 0.05$).

mediated apoptosis. Most cell procedural deaths are involved in the Fas/FasL system [27]. AIF is present in mitochondrial gap and can reduce the damage caused by oxidation stress to cell membranes and DNA by removing free radicals in cells through the redox reaction, thereby preventing apoptosis and acting as anti-cell apoptosis [28]. In this study, ROS and MDA content in IL-1β-induced HAC cells were significantly reduced by Rg1 treatment at different concentrations. In addition, high concentrations of Rg1 treatment increased the decrease of MMP in IL-1β-induced cells. Furthermore, qRT-PCR and western blot results showed that Rg1 increased the Bcl-2 downregulation and the expression of Bax, caspase-3, caspase-8, caspase-9, FasL, AIF, and Cyto c in IL-1β-induced cells. Huang et al. also confirmed that ginsenoside Rg1 can block

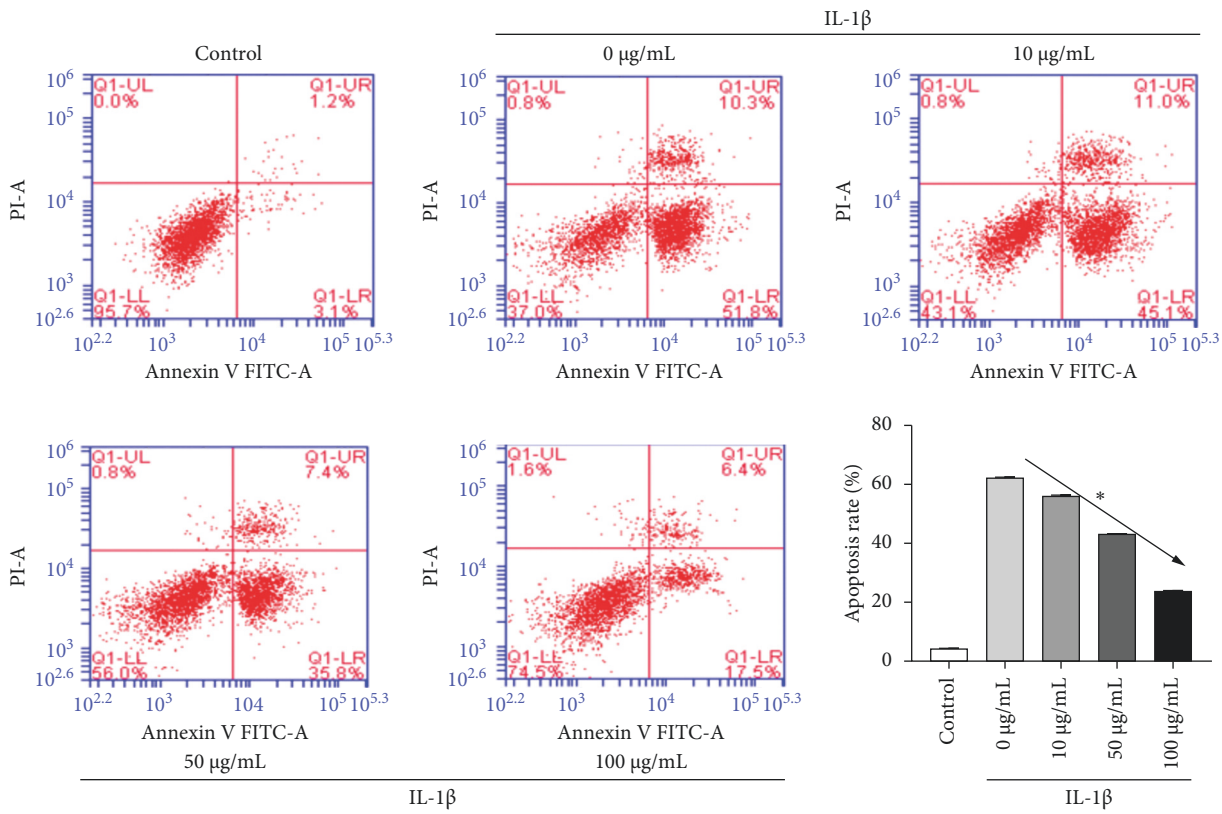

Figure 3: Rg1 inhibits apoptosis of IL-1β-induced HAC. After the chondrocytes were treated with IL-1β or different concentrations of Rg1, apoptosis was detected by flow cytometry ($^{*}p < 0.05$).

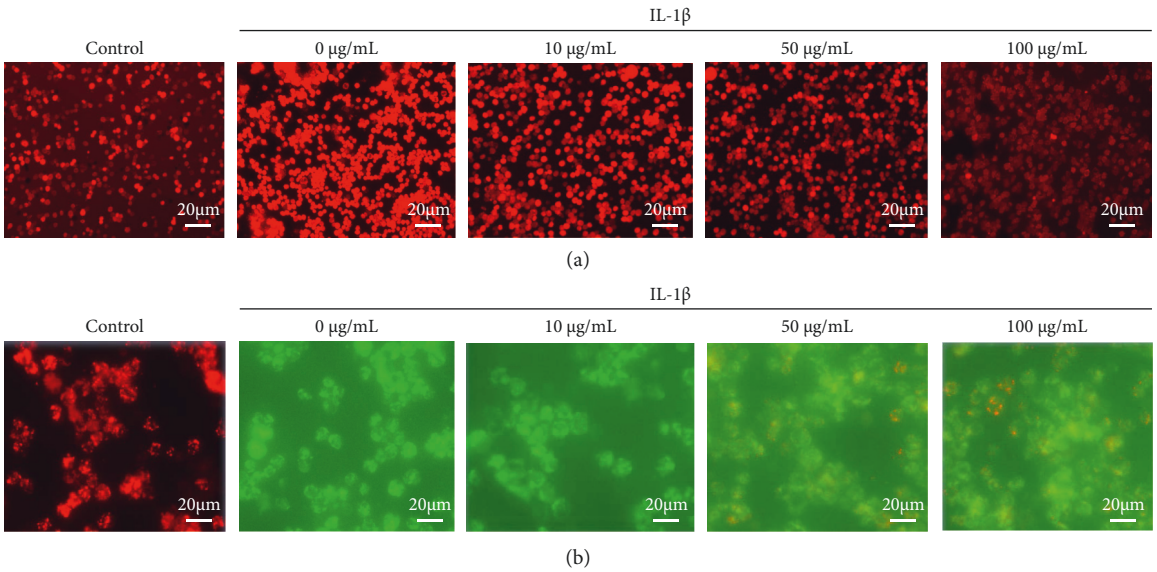

Figure 4: Continued.

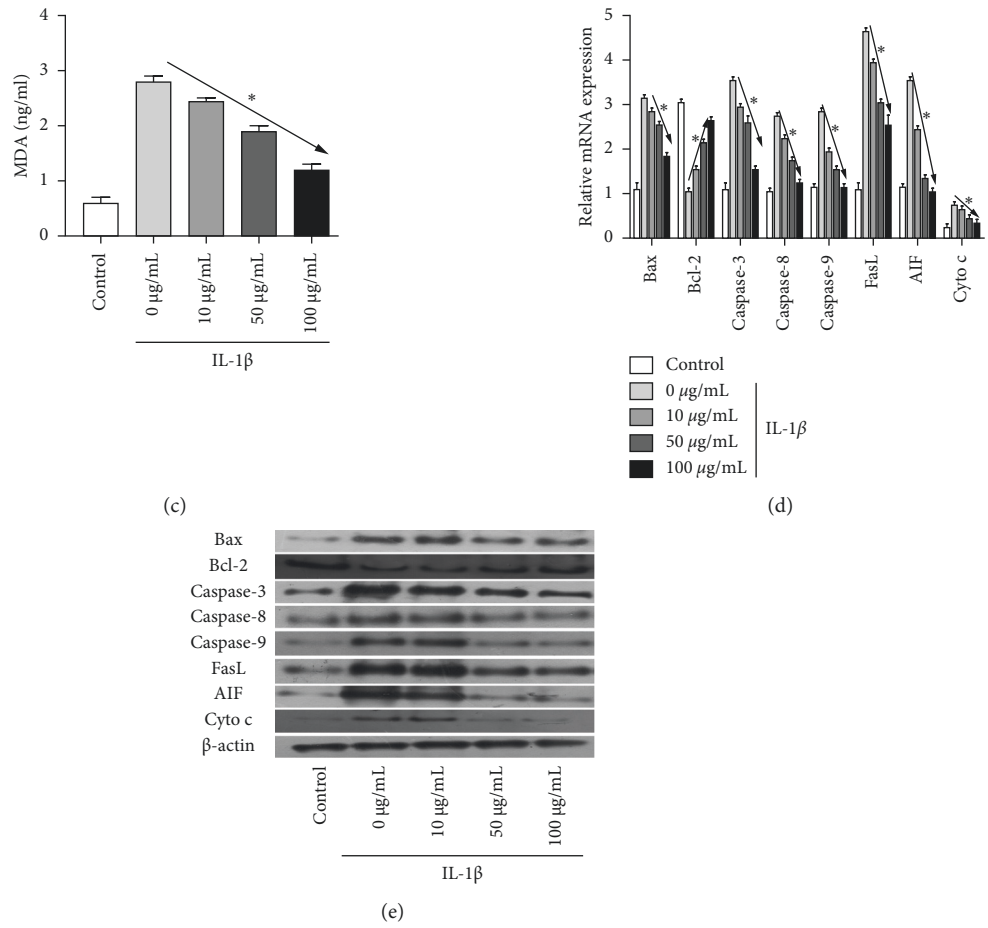

Figure 4: Effect of Rg1 on HAC cell mitochondrial signaling pathways. (a) The relative intensity of ROS was evaluated by cellular immunofluorescence. (b) The variation of MMP was evaluated by JC-1. (c) The content of MDA was evaluated by ELISA assay. (d) The Bax, Bcl-2, caspase-3, caspase-8, caspase-9, FasL, AIF, and Cyto c mRNA expressions were evaluated by qRT-PCR. (e) The Bax, Bcl-2, caspase-3, caspase-8, caspase-9, FasL, AIF, and Cyto c protein expressions were evaluated by western blot. Values with different letters within the same column differ significantly ($^*p < 0.05$).

caspase-3 release and protect rat chondrocytes from IL-1β-induced mitochondrial activated cell apoptosis through the PI3K/Akt signaling pathway [29]. This study is consistent with Huang's study that the PI3K/Akt signaling pathway plays a significant role in osteoarthritis. In the future, we can explore more treatments for osteoarthritis from the PI3K/Akt signaling pathway and mitochondrial activation pathway.

There are some shortcomings in our experiment. We have only conducted an in vitro experimental study of the effects of Rg1 inhibiting HAC apoptosis, and evidence of in vivo experiments is needed to further determine that Rg1 has inhibited HAC apoptosis.

5. Conclusion

In summary, we found that Rg1 may regulate IL-1β-induced HAC apoptosis through the PI3K/Akt/mitochondrial signaling pathway. Our results provide reliable evidence that Rg1 regulates the PI3K/Akt/mitochondrial signaling pathway in human ankle traumatic arthritis and strongly support Rg1 as a promising drug target for the treatment of ankle traumatic arthritis.

Data Availability

The data used to support this research are included within this manuscript.

Conflicts of Interest

The authors declare that they have no conflicts of interest.

Authors' Contributions

Zhiqiang Xu and Xue Li contributed equally to this study.

Acknowledgments

This paper was supported by the Foshan Self-Funded Science and Technology Foundation (2018AB001571).

References

[1] A. C. Thomas, T. Hubbard-Turner, E. A. Wikstrom, and R. M. Palmieri-Smith, "Epidemiology of posttraumatic

osteoarthritis," *Journal of Athletic Training*, vol. 52, no. 6, pp. 491–496, 2017.

[2] A. Iqbal, E. Mcloughlin, D. Beale, S. L. James, and R. Botchu, "A rare pattern of ligamentous injury of the ankle: a case report and review of the literature," *The Journal of Foot and Ankle Surgery*, vol. 60, no. 4, pp. 870–872, 2021.

[3] E. Feria-Arias, K. Boukhemis, C. Kreulen, and E. Giza, "Foot and ankle injuries in soccer," *American Journal of Orthopedics*, vol. 47, no. 10, 2018.

[4] W. Yan, X. Meng, J. Sun, H. Yu, and Z. Wang, "Intelligent localization and quantitative evaluation of anterior talofibular ligament injury using magnetic resonance imaging of ankle," *BMC Medical Imaging*, vol. 21, no. 1, p. 130, 2021.

[5] E. C. Nwankwo, L. A. Labaran, V. Athas, S. Olson, and S. B. Adams, "Pathogenesis of posttraumatic osteoarthritis of the ankle," *Orthopedic Clinics of North America*, vol. 50, no. 4, pp. 529–537, 2019.

[6] C. M. Thomas, C. J. Fuller, C. E. Whittles, and M. Sharif, "Chondrocyte death by apoptosis is associated with cartilage matrix degradation," *Osteoarthritis and Cartilage*, vol. 15, no. 1, pp. 27–34, 2007.

[7] A. Ramachandran, M. Madesh, and K. A. Balasubramanian, "Apoptosis in the intestinal epithelium: its relevance in normal and pathophysiological conditions," *Journal of Gastroenterology and Hepatology*, vol. 15, no. 2, pp. 109–120, 2000.

[8] J. F. Dickson and R. F. Willkens, "Nonsteroidal anti-inflammatory drugs in the treatment of rheumatoid arthritis," *Clinical Immunotherapeutics*, vol. 2, no. 3, pp. 185–191, 1994.

[9] P. A. Rochon, J. H. Gurwitz, R. W. Simms et al., "A study of manufacturer-supported trials of nonsteroidal anti-inflammatory drugs in the treatment of arthritis," *Archives of Internal Medicine*, vol. 154, no. 2, pp. 157–163, 1994.

[10] A. Boffa, D. Previtali, G. Di Laura Frattura, F. Vannini, C. Candrian, and G. Filardo, "Evidence on ankle injections for osteochondral lesions and osteoarthritis: a systematic review and meta-analysis," *International Orthopaedics*, vol. 45, no. 2, pp. 509–523, 2021.

[11] N. N. Zhang, P. Bu, H. H. Zhu, and W. G. Shen, "Inhibitory effects of scutellaria barbatae D. Don on tumor angiogenesis and its mechanism," *Chinese Journal of Cancer*, vol. 24, no. 12, pp. 1459–1463, 2005.

[12] Z. H. Xu, Y. Y. Gao, H. T. Zhang, K. F. Ruan, and F. Yi, "Progress in experimental and clinical research of the diabetic retinopathy treatment using traditional Chinese medicine," *The American journal of Chinese medicine*, vol. 46, no. 7, pp. 1421–1447, 2018.

[13] T. K. Milugo, L. K. Omosa, J. O. Ochanda et al., "Antagonistic effect of alkaloids and saponins on bioactivity in the quinine tree (*Rauvolfia caffra* sond.): further evidence to support biotechnology in traditional medicinal plants," *BMC Complementary and Alternative Medicine*, vol. 13, no. 1, pp. 285–294, 2013.

[14] L. Gong, S.-L. Li, H. Li, and L. Zhang, "Ginsenoside Rg1 protects primary cultured rat hippocampal neurons from cell apoptosis induced by β-amyloid protein," *Pharmaceutical Biology*, vol. 49, no. 5, pp. 501–507, 2011.

[15] R. Hashimoto, J. Yu, H. Koizumi, Y. Ouchi, and T. Okabe, "Ginsenoside Rb1 prevents MPP+-Induced apoptosis in PC12 cells by stimulating estrogen receptors with consequent activation of ERK1/2, Akt and inhibition of SAPK/JNK, p38 MAPK," *Evidence-based Complementary and Alternative Medicine*, vol. 2012, Article ID 693724, 8 pages, 2012.

[16] P. Grover, H. Shi, M. Baumgartner, C. J. Camacho, and T. E. Smithgall, "Fluorescence polarization screening assays for small molecule allosteric modulators of ABL kinase function," *PLoS One*, vol. 10, no. 7, Article ID e0133590, 2015.

[17] N. A. Thornberry, "The caspase family of cysteine proteases," *British Medical Bulletin*, vol. 53, no. 3, pp. 478–490, 1997.

[18] S. Koszinowski, K. Buss, K. Kaehlcke, and K. Krieglstein, "Signaling via the transcriptionally regulated activin receptor 2B is a novel mediator of neuronal cell death during chicken ciliary ganglion development," *International Journal of Developmental Neuroscience*, vol. 41, no. 1, pp. 98–104, 2015.

[19] J. Liu, L. Cao, X. Gao et al., "Ghrelin prevents articular cartilage matrix destruction in human chondrocytes," *Biomedicine & Pharmacotherapy*, vol. 98, pp. 651–655, 2018.

[20] J. Yan, Q. Liu, Y. Dou et al., "Activating glucocorticoid receptor-ERK signaling pathway contributes to ginsenoside Rg1 protection against β-amyloid peptide-induced human endothelial cells apoptosis," *Journal of Ethnopharmacology*, vol. 147, no. 2, pp. 456–466, 2013.

[21] B.-S. Pan, Y.-K. Wang, M.-S. Lai, Y.-F. Mu, and B.-M. Huang, "Cordycepin induced MA-10 mouse leydig tumor cell apoptosis by regulating p38 MAPKs and PI3K/AKT signaling pathways," *Scientific Reports*, vol. 5, no. 1, pp. 13372–13380, 2015.

[22] Y. Safdari, M. Khalili, M. A. Ebrahimzadeh, Y. Yazdani, and S. Farajnia, "Natural inhibitors of PI3K/AKT signaling in breast cancer: emphasis on newly-discovered molecular mechanisms of action," *Pharmacological Research*, vol. 93, pp. 1–10, 2015.

[23] J. Yuan and B. A. Yankner, "Apoptosis in the nervous system," *Nature*, vol. 407, no. 6805, pp. 802–809, 2000.

[24] Y. Shi, "A structural view of mitochondria-mediated apoptosis," *Nature Structural Biology*, vol. 8, no. 5, pp. 394–401, 2001.

[25] C. Tan, P. J. Dlugosz, J. Peng et al., "Auto-activation of the apoptosis protein Bax increases mitochondrial membrane permeability and is inhibited by bcl-2," *Journal of Biological Chemistry*, vol. 281, no. 21, pp. 14764–14775, 2006.

[26] J. Ribera, V. Ayala, and J. E. Esquerda, "c-Jun-like immunoreactivity in apoptosis is the result of a crossreaction with neoantigenic sites exposed by caspase-3-mediated proteolysis," *Journal of Histochemistry & Cytochemistry*, vol. 50, no. 7, pp. 961–972, 2002.

[27] D. L. Eizirik and T. Mandrup-Poulsen, "A choice of death - the signal-transduction of immune-mediated beta-cell apoptosis," *Diabetologia*, vol. 44, no. 12, pp. 2115–2133, 2001.

[28] B. Schumacher, J. H. Hoeijmakers, and G. A. Garinis, "Sealing the gap between nuclear DNA damage and longevity," *Molecular and Cellular Endocrinology*, vol. 299, no. 1, pp. 112–117, 2009.

[29] Y. Huang, D. Wu, and W. Fan, "Protection of ginsenoside Rg1 on chondrocyte from IL-1β-induced mitochondria-activated apoptosis through PI3K/Akt signaling," *Molecular and Cellular Biochemistry*, vol. 392, no. 1-2, pp. 249–257, 2014.

Hindawi
Evidence-Based Complementary and Alternative Medicine
Volume 2022, Article ID 7495867, 9 pages
https://doi.org/10.1155/2022/7495867

Research Article

In Vivo Anti-Inflammatory, Analgesic, Sedative, Muscle Relaxant Activities and Molecular Docking Analysis of Phytochemicals from *Euphorbia pulcherrima*

Abdullah S. M. Aljohani,[1] **Fahad A. Alhumaydhi**,[2] **Abdur Rauf**,[3] **Essam M. Hamad**,[4] **and Umer Rashid**[5]

[1]*Department of Veterinary Medicine, College of Agriculture and Veterinary Medicine, Qassim University, Buraydah, Saudi Arabia*
[2]*Department of Medical Laboratories, College of Applied Medical Sciences, Qassim University, Buraydah, Saudi Arabia*
[3]*Department of Chemistry, University of Swabi, Anbar, Anbar, Khyber Pakhtunkhwa, Pakistan*
[4]*Department of Food Science & Human Nutrition, College of Agriculture and Veterinary Medicine, Qassim University, Buraydah, Saudi Arabia*
[5]*Department of Chemistry, COMSATS University Islamabad, Abbottabad Campus, Abbottabad 22060, Pakistan*

Correspondence should be addressed to Abdullah S. M. Aljohani; jhny@qu.edu.sa and Abdur Rauf; abdurrauf@uoswabi.edu.pk

Received 15 December 2021; Accepted 30 March 2022; Published 13 April 2022

Academic Editor: Rohit Sharma

Euphorbia pulcherrima is an important medicinal plant that is used in a traditional system for its curative properties such as analgesic potency, antipyretic, anti-inflammatory, sedation potential, and antidepressant and cure of diseases such as skin diseases. This study deals with the isolation of two flavonoids namely spinacetin (1) and patuletin (2) from chloroform fraction of *Euphorbia pulcherrima*. The isolated compound spinacetin (1) and patuletin (2) were screened for *in vivo* anti-inflammatory, analgesic, sedative, and muscle relaxant effects. Compounds 1 and 2 were assessed against hot plate-induced noxious stimuli at various doses which showed excellent ($p < 0.05$) analgesic effect in a dose-dependent manner. The muscle relaxant activity was determined by traction and inclined screening model, both compounds showed significant muscle relaxant activity with time. The sedative potential of isolated compounds 1 and 2 was determined by the open field model, both compounds showed good sedation ($p < 0.05$) at 20 mg/kg. The anti-inflammatory potential of compound 1 was recorded by histamine-induced paw edema and carrageen paw edema model, and in both models, compounds 1 and 2 showed strong effect at 20 mg/kg. Binding orientations, binding energy values, and computed inhibition constants (Ki) values revealed that the studied compounds have a good to excellent inhibition potential against μ-opioid receptors and COX-2.

1. Introduction

Medicinal plants are a key source of various classes of secondary metabolites [1]. The medicinal importance of plants is correlated due to the presence of natural products. There are several bioactive natural products isolated and are major constituents of the modern medicinal system [1]. Many plants are investigated for new drug discovery because the drugs prepared from plants are more effective and have no toxicity. Many medicinal plants have several biomedical applications such as Alzheimer's diseases [2], neurodegenerative [3], depressive [3], and metabolic disorders [4] as well as promote health and prevent disease [5].

Euphorbia pulcherrima is a member of the family Euphorbiaceae. Euphorbiaceae is also known as spurge or Euphorbias family. Euphorbiaceae is the largest flowering family among the Anthophyta. This family comprises 5000 species and 300 genera throughout the globe. All members of this family are a key and rich source of bioactive natural products. Members of this family are distributed in Saudi Arabia, Pakistan, and India. Different species of this genus is famous for its folk usage for the cure of various ailments.

These species contain latex which is a rich source of bioactive secondary metabolites [6]. This genus comprises diterpenoids and other compounds which his documented for excellent anticancer and other properties [7]. For example, the essential oil isolated from *E. hirta* is used for the treatment of asthma and is also used as a mosquito repellent. Various phytochemicals including phytosterols, triterpenes, tannins, flavonoids, and polyphenols have been isolated from various parts of *E. hirta* [8]. Dry roots of *E. kansui* herbal remedy are used for the cure of ascites, edema, and cancer [8]. Various parts of dhudi (*E. hirta*) also comprise saponins, alkaloids, and flavonoids. *E. hirta* is employed for curing several ailments such as kidney stones, bronchial ailments, gastrointestinal problems, respiratory disease, and diabetes [9].

Euphorbia pulcherrima is also known as poinsettia or Christmas flower and is distributed on the Pacific coast of America as well as Mexico and Guatemala. *E. pulcherrima* is also found in various countries of Asia and Nepal [10]. The aerial part of *Euphorbia pulcherrima* is used in the traditional system for the treatment of ailments such as normal/slow transit constipation, skin disease, and rise of milk secretion in nursing mothers. Also, *E. pulcherrima* documented for various in vitro and in vivo biological activities [11]. Some species of Euphorbiaceae has been documented for numerous pharmacological potential such as central nervous system, inflammation, fever, neuropharmacological, and hypnotic [12]. Flavonoids isolated from *Euphorbia pulcherrima* have reported moulting properties with *Spodoptera littoralis* [13]. Flavonoids documented from other plants have been reported for anti-inflammation, analgesic, phosphodiesterase, and antidiarrheal activities [14–16].

Based on extensive pharmacological applications on the family Euphorbiacea, there looks to be unsatisfactory information on *E. pulcherrima*. The current finding aimed at the isolation of flavonoids namely spinacetin (1) and patuletin (2) and their in vivo pharmacological potential.

2. Materials and Methods

2.1. Collection of Plant. *Euphorbia pulcherrima* plant materials were collected in July 2015 from the botanical garden of the University of Peshawar, Peshawar Khyber Pakhtunkhwa, Pakistan. The collected plant sample was recognized by Prof. Dr. Barkatullah, Botany Department, Peshawar University, Khyber Pakhtunkhwa. The voucher specimen number (PUP545)/UOP was retained at the herbarium of the mentioned department.

2.2. Extraction and Isolation. The collected plant material was dried in shade, converted to powder, and then assessed to cold extraction with a polar solvent (methanol) for 20 days as per the reported method [17]. The extract obtained was filtered and then concentrated at reduced pressure and low through the rota evaporator. The crude extract 189 g was subjected to fractionation with various polarity solvents such as n-hexane, chloroform, ethyl acetate, and butanol. All fractions were subjected to think layer chromatography among which chloroform contain a maximum number of phytochemicals which was subjected for chromatographic analysis. Among chloroform fraction, 24.27 gm has exposed to column chromatographic analysis on silica gel and then eluted with a mixture of hexane and EtOAc (100 : 00 to 50 : 50). The column chromatography afforded 243 subfractions (AF1-TO AF243). The subfraction was combined based on TLC profile which yields ten subfactions (AFF1-AFF10). Among which AFF7 was subjected to repeated column chromatography on silica gel, eluting with hexane and EtOAc (40 : 60) which afforded compound 1 (1.62 g) and compound 2 (1.73 g). The chemical structure of isolated constituents 1 and 2 was identified by advanced spectroscopic analysis and comparing the spectral and physical data with reported data [18–20].

2.3. Animals. In vivo biological screening of compounds was performed by using Balb/c mice of both sexes having weight (24–27 g). The animals were housed in standard laboratory conditions, providing *ad libitum* water and food. The biological test was performed at the Department of Veterinary Medicine, College of Agriculture and Veterinary Medicine, Qassim University, Buraydah, Saudi Arabia, and University of Swabi, Pakistan, according to standard methods. The in vivo test involving animals was approved by local ethical committees (21-16-04, Committee of Research Ethics, Deanship of Scientific Research, Qassim University) and (UOS/Pharm-650, Department of Pharmacy, University of Swabi, KPK, Pakistan).

2.4. Anti-Inflammatory Screening. The isolated flavonoids spinacetin (1) and patuletin (2) were assessed for anti-inflammatory screening with carrageen paw edema and histamine-induced edema procedure as per the published procedure [21]. The mice were divided into various groups each group comprise six animals. The distributed groups of animals consist of negative control (10 mL/saline) and positive control (diclofenac; loratadine; 5 mg/kg). Tested groups of divided animals were treated with isolated flavonoids spinacetin (1) and patuletin (2) (5, 10, 15, and 20 mg/kg). Exactly after 30 minutes of the intraperitoneal administration, 1% of carrageen (0.05 mL) and histamine (0.1 mL) were transdermally administered in the right paw of each mice. The inflammation of PW was observed for each tested mice for six hours after injection of carrageen and histamine with the help of a plethysmometer. The anti-inflammatory of both tested flavonoids (1 and 2) was calculated with the help of the following formula:

$$\%\,\text{effect} = \left(\frac{A - B}{A}\right) \times 100, \quad (1)$$

where A is the paw edema of the control and B is the paw edema of tested flavonoids.

2.5. Analgesic Activity. The isolated flavonoids spinacetin (1) and patuletin (2) were also subjected to analgesic screening according to our published procedure [21]. In this model, all animals were distributed to various groups, and each group

consists of six mice. Among the entire groups, only one group of mice was administered with normal saline (10 mL/kg) as a control for statistical calculation, and one group was administered with tramadol (5 mg/kg). The remaining groups of animals were treated with isolated flavonoids spinacetin (1) and patuletin (2) (5, 10, 15, and 20 mg/kg). The analgesic effect of tested compounds was identified through a hot-plate analgesiometer according to the reported method [21]. After 30 minutes of sample administration, every group of mice was screened for analgesic potential through hot plate and the exact time of the latency was observed in seconds. The percentage analgesic effect was identified as per the standard method [22].

2.6. Sedative Activity. The isolated flavonoids spinacetin (1) and patuletin (2) were also screened for sedation properties [23]. All animals were divided into various groups and each group consists of 6 animals. Among the entire group, the control was administered with 0.5 mg/kg of diazepam. The sedative potential of flavonoids spinacetin (1) and patuletin (2) was performed as per the reported method. According to this procedure, after 30 minutes of administration, every group of animals should be placed in a special design box containing lines, the line crossed by every mouse observed. Amount tested groups of animals, that group of animals with the delayed movement was considered as a sedative while the rest of groups of mice which crossed more lines were considered none sedative.

2.7. Muscle Relaxant Screening

2.7.1. Inclined Plane Method. The isolated flavonoids spinacetin (1) and patuletin (2) were also screening for muscle relaxant potential in an include plane procedure as per the published method [23]. Include plane model composed 2 plywood boards linked to each other among which one side of the plywood board shaped the base and the other side of the plywood board was connected to the base at almost 65 degrees. All animals were divided into various groups, and each group consists of 6 animals. Animals of a different group in this screening were treated with standard (diazepam; 1 mg/kg), normal saline (10 mL/kg), and isolated flavonoids spinacetin (1) and patuletin (2) (5, 10, 15, and 20 mg/kg). After treatment of all samples including spinacetin (1) and patuletin (2), standard, and saline with various time intervals (30, 60, and 90 minutes), the animals was observed to fall or not for around 30 seconds on putting on the upper part of an inclined plane.

2.7.2. Traction Method. The isolated flavonoids spinacetin (1) and patuletin (2) were also screened for muscle relaxant potential by using the traction model [23]. This model comprises a metal wire cover with rubber, where ends of this metal wire were tightly stretched and reinforced with stands and were kept about 60 to 70 cm above the bench. To screen all samples, the animals were distributed into fourteen groups and each group comprises 5 animals. Among the groups, one group received distilled water, one received diazepam which was considered as a negative and positive group. The remaining groups of animals were administered with spinacetin (1) and patuletin (2) in various doses such as 5, 10, 15, and 20 mg/kg i.p. The muscle relaxation properties were observed for all groups of animals at various time intervals, i.e., 30, 60, and 90 minutes. Every mouse in this assay was suspended on the metal wire from hind legs, and the floppy time was recorded for nearly 5 seconds. This failure of mice to hang in the metal wire in less than 5 sec indicated the presence of muscle relaxant property for spinacetin (1) and patuletin (2).

2.8. Toxicological Profile. The purified spinacetin (1) and patuletin (2) was screened for toxicological study as per reported method [23]. All animals were distributed into respective groups, each group comprising six animals. The purified spinacetin (1) and patuletin (2) were administered to various groups of animals at doses 10, 20, 100, and 200 mg/kg. The tested animals were kept under observation for 2 days. The mortality was calculated from the number of dead and surviving animals of each group.

2.9. Statistical Analysis. The results of anti-inflammatory, analgesic, sedative, and muscle relaxant screening are represented as the mean ± standard error of the mean (SEM) to identify the significant difference in all tested animals. The results achieved were evaluated to one-way analysis of variance (ANOVA). The analysis was done with help of Dunnett's multiple assessment screening using GraphPad Prism 5.

3. Molecular Docking

The isolated spinacetin (1) and patuletin (2) were docked in the binding site of COX-2 and opioid receptors by using Molecular Operating Environment (MOE) software (201.2016.0802) and AutoDock (v 4.0) [22, 24]. Online database of biological macromolecules RCSB PDB was used to download three-dimensional (3D) crystal structures of selected proteins. The accession codes of these proteins are 1CX2 for COX-2, 4COF for μ-opioid receptor, and 5C1M for $GABA_A$ receptor.

Next, we performed validation of docking protocol by using the redock method. All the native ligands were extracted and docked into the binding site of their respective proteins. A comparison between redocked conformation and experimental confirmation showed a root mean square deviation with a limit (<2.0 Å).

2D structures of isolated compounds were drawn in ChemDraw and then exported to the MOE and AutoDock. The structures were saved in a 3D format in MOL2 (for AutoDock) and molecular database (.mdb) format for MOE, and saved as 3D structures. Preparation of downloaded proteins was performed by using our previously reported methods [25]. For each compound, we set the default parameters for docking simulations. Finally, 3D and 2D

analysis of each docked pose was performed by using MOE and a discovery studio visualizer [25].

4. Results

4.1. Characterization of Spinacetin (1) and Patuletin (2). Spinacetin (1) and patuletin (2) were purified from chloroform soluble fraction of *E. pulcherrima* through chromatographic analysis. The structure of spinacetin (1) and patuletin (2) (Figure 1) was characterized by advanced nuclear magnetic resonance spectroscopy and mass spectrometry.

4.2. Anti-Inflammatory Effect. The results of spinacetin (1) and patuletin (2) showed that it exhibited 35.22 and 46.00% attenuation in carrageenan-induced paw edema model which reached a maximum of 79.22 and 89.01% after 3rd hours at 20 mg/kg and remain good in the 5th hours. Both tested compounds showed mild effect at 5, 10, and 15 mg/kg as compared to 20 mg/kg. Diclofenac sodium was used as a positive control in this investigation which showed outstanding effect as compared to spinacetin (1) and patuletin (2) (Figure 2).

Likewise in the histamine paw edema model, spinacetin (1) and patuletin (2; 20 mg/kg) exhibited 76.45 and 91.45% activity for the initial phase (at the 1st hrs) while 78.33 and 94.00% (after 2nd hrs) and continues up to 3rd hours. Spinacetin (1) and patuletin (2) exhibited excellent activity as compared to loratadine (Figure 3).

4.3. Analgesic Effect. Spinacetin (1) and patuletin (2) isolated from *E. pulcherrima* exhibited promising ($p < 0.001$) central analgesic potency at tested doses (5, 10, 15, and 20 mg/kg) as represented in Table 1. Spinacetin (1) and patuletin (2) increase the latency time from the start of treatment of compounds (1 and 2) and sustained a promising increase ($p < 0.001$) up to 120 minutes. Both tested compounds exhibited lower effects at low tested doses.

4.4. Sedative Effect. Sedative potentials of spinacetin (1) and patuletin (2) are given in Table 2. Spinacetin (1) and patuletin (2) showed promising ($p < 0.001$) sedation effect at tested doses (5, 10, 15, and 20 mg/kg) in dose-dependent manner. Patuletin (2) exhibited significant ($p < 0.001$) activity at 20 mg/kg, as represented by hindering the mobility of animals in a distinct box.

4.5. Muscle Relaxant Effect. Spinacetin (1) and patuletin (2) isolated from *E. pulcherrima* were also screened for muscle relaxant effect on inclined plan and traction model, which showed promising muscle relaxant potential (Table 3). Spinacetin (1) and patuletin (2) exhibited significant effects in the dose- and time-dependent manner. Both tested compounds possess good activity in both models. The effect of both compounds was excellent from the start of the experiment against the standard drug.

4.6. Toxicological Study. The purified spinacetin (1) and patuletin (2) was screened for toxicological study in the higher doses 10, 20, 100, and 200 mg/kg. Spinacetin (1) and patuletin (2) was administered to the animals intraperitoneally (i.p). The tested animals were kept for 2 days under observation. The number of surviving and dead animals was recorded. All groups of treated animals survived all tested doses. Interestingly, spinacetin (1) and patuletin (2) was found safe at all tested doses.

4.7. Docking Studies on μ-Opioid and $GABA_A$ Receptors. We have performed the docking simulations on GABAA receptors as well as on μ-opioid receptors. The accession codes for the downloaded proteins from the protein data bank are 5C1M for μ-opioid and 4COF for GABA receptors. After the validation of the docking protocols, we docked spinacetin (1) and patuletin (2) into the binding sites of the downloaded and prepared targets.

Three-dimensional (3D) interaction plots of isolated compounds show that spinacetin (1) forms a hydrogen bond interaction with Gln64. The phenyl ring of the compound forms π-π interactions with Tyr62. His54 forms with the phenyl ring (Figure 4(a)), while patuletin (2) forms two hydrogen bond interactions and one p-π interaction. Asn41 and Gln64 forms hydrogen bond interactions, and Tyr62 forms p-π interactions (Figure 4(b)).

Three-dimensional (3D) and two-dimensional (2D) interaction plots of the isolated compounds in the binding site of μ-opioid (5C1M) are shown in Figure 5. The phenyl ring of spinacetin (1) established two p-π interactions with His54 and Tyr148 (Figure 5(a)). Patuletin (2) forms hydrogen bond interactions with Gln124 and Asn127, while chromen-4-one ring forms bifurcated π-π interactions with His54 and Trp318 (Figure 5(b)).

We docked isolated compounds into the binding site of COX-2 isoform (PDB Id: 1CX2). 3D/2D interaction plots of the studied compounds are shown in Figure 6. It can be observed from these interaction plots that both compounds interact with the amino acid residues (His90, Gln192, Ser353, and Arg531) present in the selectivity pocket of the COX-2. The hydroxyl groups of compounds 1 and 2 form hydrogen bond interactions with selectivity pocket residues His90, Ser353, and Arg513. Ile517 also establishes a hydrogen bond with the hydroxyl group of compound 1 (Figures 6(a) and 6(b)).

Furthermore, we performed the docking studies by using the AutoDock 4.0 software. The purpose is to compute the inhibition constant (Ki) of the isolated compounds against the tested targets. The binding energy values computed via MOE and AutoDock and Ki values computed via AutoDock are listed in Tables 4-5.

5. Discussion

E. pulcherrima is employed for multimedicinal usage for the central analgesic potency, antipyretic, anti-inflammatory, sedation potential, and antidepressant and for the cure of skin diseases. Due to the diverse biological potential, the

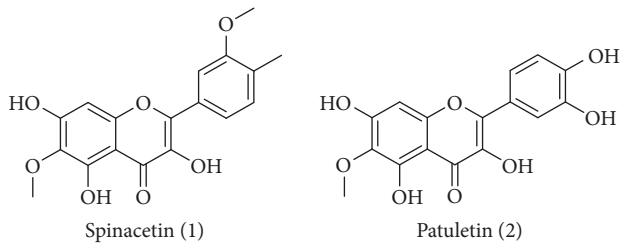

Figure 1: Chemical structures of spinacetin (1), patuletin (2) isolated from *E. pulcherrima*.

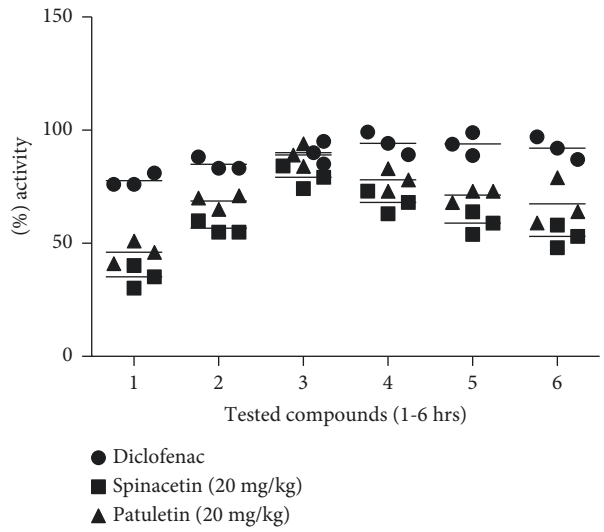

Figure 2: Anti-inflammatory effect of spinacetin (1) and patuletin (2; 20 mg/kg) of the *E. pulcherrima* on carrageenan paw in mice. The obtained results are shown as ±SEM for six groups of animals. The analysis of data was induced paw edema in mice. The achieved results are shown as ±SEM for 6 groups of animals. The calculation was performed by ANOVA followed by Dunnett's test.

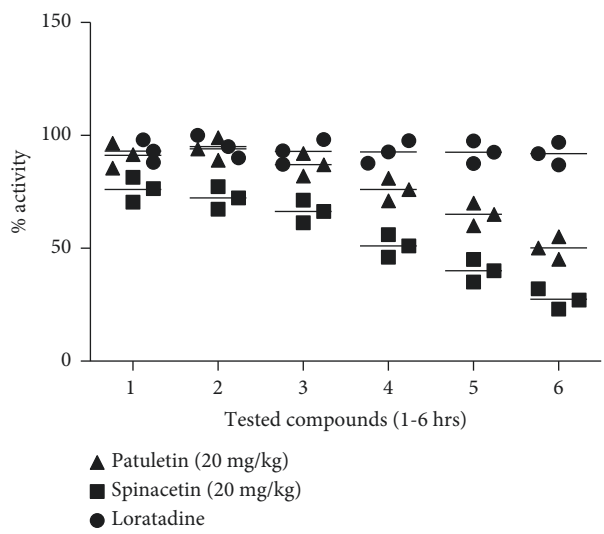

Figure 3: Anti-inflammatory effect of spinacetin (1) and patuletin (2; 20 mg/kg) of *E. pulcherrima* on histamine-induced paw edema in mice. The achieved results are shown as ±SEM for 6 groups of animals. The calculation was performed by ANOVA followed by Dunnett's test.

isolation and structure determination of secondary metabolites followed by in vivo biological screening is important to identify the secondary metabolites responsible for the diverse biological application. In this finding, compounds 1 and 2 were isolated and screened for analgesia, muscle relaxation, sedative, and anti-inflammatory properties.

Prostaglandin is an important product of arachidonic acid by cyclooxygenase enzyme. Majority of the cyclooxygenase enzyme inhibitors are recognized as active painkillers, also as anti-inflammatory agents [26, 27]. It is a big challenge for a researcher to discover new potent and less or nontoxic inhibitors. Spinacetin (1) and patuletin (2) also attenuated inflammation in both tested models, i.e., carrageenan and histamine. Carrageenan paws edema model consists of two phases: the initial phase edema is recognized to the local release of histamine serotonin and bradykinins while the further phase is due to overproduction of PG [27]. In the tested model, spinacetin (1) and patuletin (2) exhibited significant analgesic activity against the standard drug.

The muscle relaxant effect of spinacetin (1) and patuletin (2) in both models that is inclined plan and traction model was analysed as per well-established methods. Spinacetin (1) and patuletin (2) exhibited a strong muscle relaxant effect. In both tested models, the relaxation of muscle was assessed after 30, 60, and 90 minutes of treatment of spinacetin (1) and patuletin (2). An outstanding muscle relaxant effect was observed after 60 minutes of spinacetin (1) and patuletin (2) administration at a higher dose.

Similarly, spinacetin (1) and patuletin (2) were also evaluated for their sedative properties which showed excellent activity. The sedative activity of these secondary metabolites has been recognized with their antihistaminic potential [28]. The antihistaminic potential may be similar to H1 receptor blocker, i.e., pheniramine which has an excellent sedative potential; thus, our screen compounds (1 and 2) have outstanding sedative potential. From our outstanding results, we recommend researchers for comprehensive and detailed screening as leading molecules for curing various diseases. The excellent anti-inflammatory, analgesic, sedative, and muscle relaxant potential of spinacetin (1) and patuletin (2) provide a strong scientific background for folkloric use of *E. pulcherrima* for treatment of various diseases.

To further support the in vitro result findings, we performed molecular docking analysis on the selected target receptors. First of all, docking simulations were performed on GABAnergic and μ-opioid targets. Both isolated compounds showed interactions with the amino acid residues of the studied targets. μ-Opioid receptor (μOR) and membrane proteins are considered as key therapeutic targets for pain. The binding of ligands to the target identifies the responses which are resulted into the activation of signaling pathway. A number of crystal structures have been solved for μOR that enable the drug discovery scientists to design a new ligand. Insights into the binding pattern of native agonist BU72 (PDB 5C1M) revealed that it interacts with His54, Asp147, and Tyr148 *via* hydrogen bond interactions. Here, in our study, the phenyl ring of spinacetin (1) established π-π

Table 1: Analgesic effect of compounds (1 and 2) isolated from *E. pulcherrima*.

Group	Dose (mg/kg)	Time in minutes			
		30	60	90	120
Normal saline	10 mL	9.25 ± 0.07	9.24 ± 0.08	9.25 ± 0.15	9.23 ± 0.11
Tramadol	10	25.00 ± 0.08***	26.28 ± 0.07***	25.50 ± 0.06***	25.70 ± 0.11***
Compound 1	5	11.55 ± 0.30	12.90 ± 0.43	12.80 ± 0.35	12.77 ± 0.40
	10	14.98 ± 0.98	15.55 ± 0.21	15.30 ± 0.45	15.20 ± 0.46
	15	17.32 ± 0.40	18.90 ± 0.33	18.30 ± 0.43	18.20 ± 0.49
	20	20.00 ± 0.33	21.03 ± 0.23	20.88 ± 0.32	20.80 ± 0.55
Compound 2	5	13.66 ± 0.10	14.96 ± 0.18	14.80 ± 0.20	14.60 ± 0.45
	10	16.90 ± 0.39	17.55 ± 0.23	17.36 ± 0.43	17.31 ± 0.55
	15	19.80 ± 0.21	20.93 ± 0.27	20.88 ± 0.40	20.59 ± 0.40
	20	22.98 ± 0.60	23.84 ± 0.73	23.70 ± 0.80	23.65 ± 0.90

The recorded results are represented as the mean ± SEM of all animals' tolerance to thermal stimuli in seconds.

Table 2: Effect of compounds (1 and 2) isolated from *E. pulcherrima* (locomotive activity).

Sample	Dose (mg/kg)	No. of lines crossed
Control	5 mL	129.35 ± 3.24
Diazepam	0.5	9.32 ± 0.45***
Compound 1	5	70.54 ± 1.01
	10	65.87088
	15	54.76 ± 0.66**
	20	44.87 ± 0.98**
Compound 2	5	66.21 ± 1.06
	10	57.91 ± 1.00**
	15	46.98 ± 0.97**
	20	37.66 ± 0.93***

The recorded results are represented as the mean ± SEM of all animals' tolerance to thermal stimuli in seconds.

Table 3: Muscle relaxant effect of compounds (1 and 2) isolated from *E. pulcherrima*.

Group	Dose (mg/kg)	Inclined plane test (% effect)			Traction test (effect)		
		30 mints	60 mints	90 mints	30 mints	60 mints	90 mints
Distilled water	10 mL	0.00 ± 0	0.00 ± 0	0.00 ± 0	0.00 ± 0	0.00 ± 0	0.00 ± 0
Diazepam	1	100 ± 0.00	100 ± 0.00	100 ± 0.00	100 ± 0.00	100 ± 0.00	100 ± 0.00
Compound 1	5	25.32 ± 1.44	29.90 ± 1.37	31.66 ± 1.20	26.61 ± 1.32	27.22 ± 1.00	26.09 ± 1.33
	10	30.22 ± 1.40	34.65 ± 1.33	36.98 ± 1.34	31.88 ± 1.34	32.67 ± 1.03	31.07 ± 1.20
	15	40.23 ± 1.35	47.09 ± 1.32	48.67 ± 1.18	41.34 ± 1.09	42.34 ± 1.04	41.22 ± 1.18
	20	46.09 ± 1.36	52.00 ± 1.28	53.99 ± 1.23	47.32 ± 1.05	48.23 ± 1.06	47.23 ± 1.23
Compound 2	5	30.21 ± 1.23	36.87 ± 1.45	37.32 ± 1.02	31.11 ± 1.09	32.034 ± 1.00	31.98 ± 1.32
	10	36.09 ± 1.67	43.34 ± 1.32	45.23 ± 1.07	37.23 ± 1.23	38.012 ± 1.34	37.56 ± 1.07
	15	47.03 ± 1.40	55.13 ± 1.22	57.45 ± 1.44	48.87 ± 1.09	49.03 ± 1.09	47.66 ± 1.23
	20	55.08 ± 1.33	63.11 ± 1.00	64.98 ± 1.76	56.32 ± 1.23	58.02 ± 1.23	56.76 ± 1.02

The recorded results are represented as the mean ± SEM of all animals' tolerance to thermal stimuli in seconds.

interactions with His54 and Tyr148, while the chromen-4-one ring of patuletin (2) forms bifurcated π-π interactions with His54 and Trp318.

The computed binding energy values by using MOE and AutoDock revealed that both compound bind to GABAa receptor with almost same affinity. However, compound 1 showed slight more affinity when bound with μOR. We moved further and computed the inhibition constant (Ki) of these compounds. Hence, we used AutoDock to calculate the Ki values of the compounds. Both compounds showed good inhibition constant against μOR. The Ki values are in low micromolar range (Table 4), while for GABA receptors, the compounds exhibited moderate Ki values.

In the next step, we studied the inflammation pathway *via* COX-2 inhibition. Carrageenan-induced paw edema model is considered as COX-2-dependent model of inflammation. Spinacetin (1) exhibited excellent Ki value in submicromolar concentration (Ki = 0.631 μM). Binding pose revealed that the isolated compound is more oriented towards the additional or the selectivity pocket of COX-2 and established significant hydrogen bond interactions with the key amino acid residues (His90, Gln192, and Arg513).

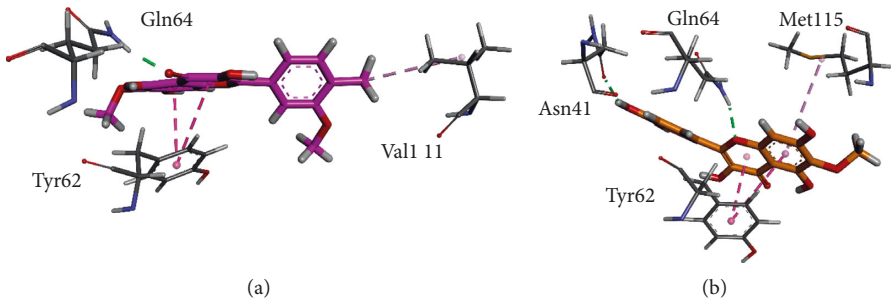

Figure 4: The 3D interaction plots of spinacetin (1) and patuletin (2) into the binding site of GABA (PDB Id: 4COF). (a) Spinacetin (pink) and (b) patuletin (orange).

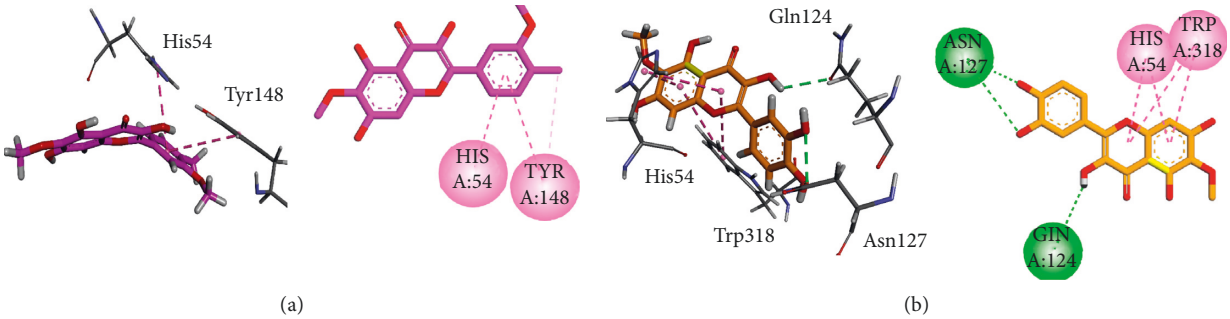

Figure 5: The 3D and 2D interaction plots of spinacetin (1) and patuletin (2) into the binding site of μ-opioid (5C1M). (a) Spinacetin (pink) and (b) patuletin (orange).

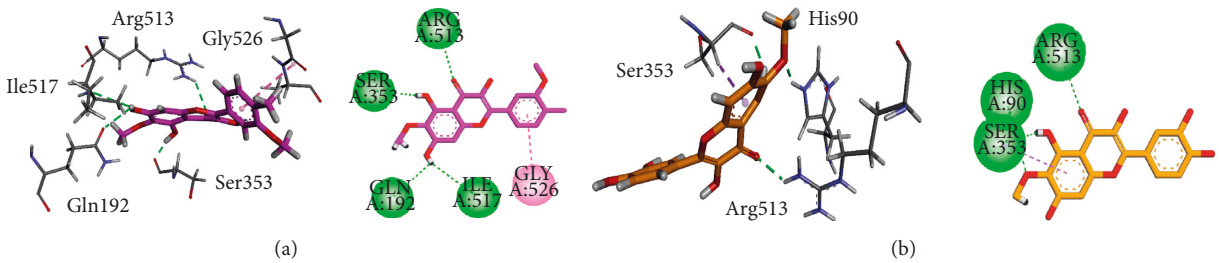

Figure 6: The 3D and 2D interaction plots of isolated compounds into the binding site of COX-2 (PDB Id: 1CX2). (a) Spinacetin (pink) and (b) patuletin (orange).

Table 4: Binding energy and inhibition constant of the spinacetin (1) and patuletin (2) calculated by AutoDock into the binding site of μ-opioid and $GABA_A$ receptors.

Compound no.	GABAA receptor (PDB Id: 4COF)			μ-opioid receptor (PDB Id: 5C1M)		
	MOE	AutoDock		MOE	AutoDock	
	BE (kcal/mol)	BE (kcal/mol)	Ki (μM)	BE (kcal/mol)	BE (kcal/mol)	Ki (μM)
1	−5.8221	−6.49	17.44	−7.1978	−7.89	4.84
2	−5.8935	−6.33	22.82	−6.7992	−7.11	6.19

Table 5: Binding energy and inhibition constant of the isolated spinacetin (1) and patuletin (2) calculated by AutoDock into the binding site of COX-2 receptors.

Compound no.	COX-2 (PDB Id: 1CX2)		
	MOE	AutoDock	
	BE (kcal/mol)	BE (kcal/mol)	Ki (μM)
1	−7.7702	−8.46	0.631
2	−6.8761	−7.86	1.74

6. Conclusions

It is concluded that spinacetin (1) and patuletin (2) isolated from *E. pulcherrima* showed excellent anti-inflammatory, analgesic, sedative, and muscle relaxant effects. Thus, our current research provides a scientific rationale to the traditional use of *E. pulcherrima* for the cure of various diseases. Furthermore, spinacetin (1) and patuletin (2) are outdating candidates for detailed research study to find its clinical application. Compounds 1 and 2 showed excellent ($p < 0.05$) analgesic effect in a dose-dependent manner. The muscle relaxant activity results showed significant muscle relaxant activity with time, while sedative potential of compounds under study showed good sedation ($p < 0.05$) at 20 mg/kg. Moreover, the anti-inflammatory potential of compounds determined *via* histamine-induced paw edema and carrageen paw edema model showed strong effect at 20 mg/kg. Inhibition constants (Ki) values computed *via* the AutoDock software revealed that these compounds have a good to excellent inhibition potential against GABA and COX-2, while binding orientation and interaction plots also showed binding affinities the studied targets. The excellent anti-inflammatory, analgesic, sedative, and muscle relaxant potential of spinacetin (1) and patuletin provides a strong scientific background for folkloric use of *E. pulcherrima* for treatment of various diseases.

Data Availability

The spectroscopic data of isolated compounds (1–3) are available on request to the contact authors. The graphical abstract is given in supplementary data.

Conflicts of Interest

There are no potential conflicts of interest associated to this project.

Authors' Contributions

All authors contributed equally to this project.

Acknowledgments

The authors gratefully acknowledge Qassim University, represented by the Deanship of Scientific Research, for the financial support for this research under the number 10263-cavm-3-1-2020 during the academic year 1441 AH/2020 AD.

Supplementary Materials

Graphical abstract illustrating the in vivo anti-inflammatory, analgesic, sedative, and muscle relaxant activities and molecular docking analysis of phytochemicals from *Euphorbia pulcherrima*. (*Supplementary Materials*)

References

[1] P. Pant, S. Pandey, and S. Dall'Acqua, "The influence of environmental conditions on secondary metabolites in medicinal plants: a literature review," *Chemistry and Biodiversity*, vol. 18, Article ID e2100345, 2021.

[2] U. Ghani, M. Naeem, H. Rafeeq et al., "A novel approach towards nutraceuticals and biomedical applications," *Scholars International Journal of Biochemistry*, vol. 2, no. 10, pp. 245–252, 2019.

[3] G. Ratheesh, L. Tian, J. R. Venugopal et al., "Role of medicinal plants in neurodegenerative diseases," *Biomanufacturing Reviews*, vol. 2, pp. 1–16, 2017.

[4] D. Patel, R. Kumar, D. Laloo, and S. Hemalatha, "Diabetes mellitus: an overview on its pharmacological aspects and reported medicinal plants having antidiabetic activity," *Asian Pacific Journal of Tropical Biomedicine*, vol. 2, no. 5, pp. 411–420, 2012.

[5] D. Tungmunnithum, A. Thongboonyou, A. Pholboon, and A. Yangsabai, "Flavonoids and other phenolic compounds from medicinal plants for pharmaceutical and medical aspects: an overview," *Medicines*, vol. 5, no. 3, p. 93, 2018.

[6] H. A. Rehman, Z. Yousaf, M. Rashid et al., "Phytochemical relationship of Euphorbia helioscopia and Euphorbia pulcherrima with Lactuca sativa," *Natural Product Research*, vol. 28, no. 20, pp. 1725–1731, 2014.

[7] J. Gao, Q.-B. Chen, Y.-Q. Liu, X.-L. Xin, A. Yili, and H. A. Aisa, "Diterpenoid constituents of *Euphorbia macrorrhiza*," *Phytochemistry*, vol. 122, pp. 246–253, 2016.

[8] M. Ogunlesi, W. Okiei, E. Ofor, and A. E. Osibote, "Analysis of the essential oil from the dried leaves of *Euphorbia hirta* Linn (Euphorbiaceae), a potential medication for asthma," *African Journal of Biotechnology*, vol. 8, p. 24, 2009.

[9] S. Kumar and D. Kumar, "Evaluation of antidiabetic activity of *Euphorbia hirta* Linn.instreptozotocin induced diabetic mice," *Indian Journal of Natural Products and Resources*, vol. 1, pp. 200–203, 2010.

[10] K. K. Singh, G. P. Rauniar, H. Sangraula, and H. Sangraula, "Experimental study of neuropharmacological profile of *Euphorbia pulcherrima* in mice and rats," *Journal of Neurosciences in Rural Practice*, vol. 3, no. 3, pp. 311–319, 2012.

[11] B. L. Dunn, T. Cavins, and C. Goad, "Effect of applying calcium chloride and three milk supplements to poinsettia 'prestige red'," *Journal of Plant Nutrition*, vol. 39, no. 1, pp. 45–50, 2016.

[12] B. Ahmad, N. Ali, S. Bashir, M. I. Choudhary, S. Azam, and I. Khan, "Parasiticidal, antifungal and antibacterial activities of OnosmagriffithiiVatke," *African Journal of Biotechnology*, vol. 8, pp. 5084–5087, 2009.

[13] S. Khafagy, N. Nazmi, N. A. Salam, and A. S. Eldin, "Steroid, triterpenoid, and flavonoid constituents of *Euphorbia pulcherrima* Villd. Leave," *Acta Pharmaceutica Jugoslavica*, vol. 30, pp. 103–107, 1980.

[14] J. Gonzalez-Gallego, S. Sánchez-Campos, and M. J. Tunon, "Anti-inflammatory properties of dietary flavonoids," *Nutrición hospitalaria*, vol. 22, pp. 287–293, 2007.

[15] S. Humayun and M. Ibrar, "Evaluation of anti-inflammatory and analgesic activity from *Vitex negundo* Linn," *Journal of Biodiversity and Environmental Sciences*, vol. 4, pp. 164–172, 2014.

[16] E. Tadesse, E. Engidawork, T. Nedi, and G. Mengistu, "Evaluation of the anti-diarrheal activity of the aqueous stem extract of *Lantana camara* Linn (Verbenaceae) in mice," *BMC Complementary and Alternative Medicine*, vol. 17, pp. 190–198, 2017.

[17] A. Beretz, M. Joly, J. Stoclet, and R. Anton, "Inhibition of 3′,5′-AMP phosphodiesterase by biflavonoids and xanthones," *Planta Medica*, vol. 36, no. 7, pp. 193–195, 1979.

[18] J. B. Harborne, V. H. Heywood, and L. King, "Evolution of yellow flavonols in flowers of anthemideae," *Biochemical Systematics and Ecology*, vol. 4, no. 1, pp. 1–4, 1976.

[19] D. M. Smith, C. W. Glennie, and J. B. Harborne, "Identification of eupalitin, eupatolitin and patuletin glycosides in ipomopsis aggregata," *Phytochemistry*, vol. 10, no. 12, pp. 3115–3120, 1971.

[20] M. M. Khan, I. Khan, and A. Rauf, "Phytochemical Investigation and biological screening of Euphorbia pulcherrima and Micromeria biflora," PhD thesis, http://prr.hec.gov.pk/jspui/handle/123456789/14967, Higher Education Commission, Islamabad, Pakistan, 2020.

[21] N. Muhammad, M. Saeed, and H. Khan, "Antipyretic, analgesic and anti-inflammatory activity of *Viola betonicifolia* whole plant," *BMC Complementary and Alternative Medicine*, vol. 12, pp. 1–8, 2012.

[22] S. Hussain, F. Ullah, M. Ayaz et al., "In silico, cytotoxic and antioxidant potential of novel ester, 3-hydroxyoctyl-5-trans-docosenoate isolated from *Anchusa arvensis* (L.) m. bieb. against hepg-2 cancer cells," *Drug Design, Development and Therapy*, vol. 13, pp. 4195–4205, 2019.

[23] N. Muhammad, M. Saeed, H. Khan, A. Adhikari, and K. M. Khan, "Muscle relaxant and sedative-hypnotic activities of extract of *Viola betonicifoliain* animal models supported by its isolated compound, 4-hydroxy coumarin," *Journal of Chemistry*, vol. 2013, Article ID 326263, 6 pages, 2013.

[24] A. Ahmad, F. Ullah, A. Sadiq et al., "Comparative cholinesterase, α-glucosidase inhibitory, antioxidant, molecular docking, and kinetic studies on potent succinimide derivatives," *Drug Design, Development and Therapy*, vol. 14, pp. 2165–2178, 2020.

[25] A. Sadiq, M. H. Mahnashi, B. A. Alyami, Y. S. Alqahtani, A. O. Alqarni, and U. Rashid, "Tailoring the substitution pattern of pyrrolidine-2,5-dione for discovery of new structural template for dual COX/LOX inhibition," *Bioorganic Chemistry*, vol. 112, Article ID 104969, 2021.

[26] M. A. Khan, H. Khan, S. Khan, T. Mahmood, P. M. Khan, and A. Jabar, "Anti-inflammatory, analgesic and antipyretic activities of *Physalis minima* Linn," *Journal of Enzyme Inhibition and Medicinal Chemistry*, vol. 24, no. 3, pp. 632–637, 2009.

[27] G. R. Donald, P. D. Fernandes, and F. Boylan, "Antinociceptive activity of *Zanthoxylum piperitum* DC. Essential oil," *Evidence-Based Complementary and Alternative Medicine*, vol. 2016, Article ID 3840398, 8 pages, 2016.

[28] S. Naeem, S. N. Ali, A. Qayoom, H. Muhammad, U. Haroon, and S. Nisar, "Charge transfer complexes of antihistamines with curcumin: spectrophotometric determination in pharmaceutical formulations," *Journal of the Chemical Society of Pakistan*, vol. 40, p. 904, 2018.

Hindawi
Evidence-Based Complementary and Alternative Medicine
Volume 2022, Article ID 6159874, 14 pages
https://doi.org/10.1155/2022/6159874

Review Article

Quality of Evidence Supporting the Role of Curcuma Longa Extract/Curcumin for the Treatment of Osteoarthritis: An Overview of Systematic Reviews

Wenqiang Chen,[1] Hongshuo Shi,[1] Pin Deng,[2] Zhenguo Yang,[3] Wenbin Liu,[3] Lu Qi,[3] Chengda Dong,[4] Guomin Si,[5] Dong Guo,[6] and Lei Wang[3]

[1]*College of Traditional Chinese Medicine, Shandong University of Traditional Chinese Medicine, Jinan, China*
[2]*The Third Affiliated Hospital of Beijing University of Chinese Medicine, Beijing, China*
[3]*The Second Affiliated Hospital of Shandong University of Traditional Chinese Medicine, Jinan, China*
[4]*First Clinical Medical College, Shandong University of Traditional Chinese Medicine, Jinan, China*
[5]*Department of Traditional Chinese Medicine, Provincial Hospital Affiliated to Shandong First Medical University, Jinan, China*
[6]*Center for Faculty Development, Shandong University of Traditional Chinese Medicine, Jinan, China*

Correspondence should be addressed to Lei Wang; wlyywm@163.com

Received 2 January 2022; Revised 16 February 2022; Accepted 12 March 2022; Published 31 March 2022

Academic Editor: Jelena Zivkovic

Background. Well known for its good anti-inflammatory effect, curcuma longa extract (CLE)/curcumin (C) has a potential effect on osteoarthritis (OA), and a large number of researchers have completed several systematic reviews/meta-analyses (SRs/MAs) in this research area. However, the methodological and evidentiary quality of these SRs/MAs need to be further evaluated, and whether these findings provide reliable evidence for clinicians remains controversial. *Methods*. Two researchers collected data from seven databases for SRs/MAs that are about randomized controlled trials (RCTs) on CLE/C for OA. Assessment was made for the SRs/MAs included in this article by means of the Assessment System for Evaluating Methodological Quality 2 (AMSTAR-2), the Risk of Bias in Systematic (ROBIS) scale, the list of Preferred Reporting Items for Systematic Reviews and Meta-Analyses (PRISMA), and the Grading of Recommendations Assessment, Development, and Evaluation (GRADE) system. *Results*. Nine published SRs/MAs were included in our study. According to the results of the AMSTAR-2 assessment, only one SR/MA was assessed as high quality. According to the ROBIS evaluation results, only 2 SRs/MAs have a low risk of bias. According to the results of the PRISMA checklist assessment, only 2 SRs/MAs studies fully reported the checklist, while other studies had reporting flaws. According to GRADE, a total of 59 effect sizes extracted from the included SRs/MAs were evaluated, among which no effect size was rated as high. *Conclusions*. CLE/C may be an effective and safe complementary treatment for OA. However, further standard SRs/MAs and RCTs are needed to provide an evidence-based medical rationale for this.

1. Introduction

Osteoarthritis (OA) is a global inflammatory joint disease. It is one of the main causes of joint disability [1]. With the combined effects of aging, rising obesity rate, and the increase in the number of joint injuries, OA has become an increasingly common disease on a worldwide scale, and a global estimate indicates that the affected population has reached 250 million. [2, 3]. Pain, joint stiffness or deformity, and even terminal disability are commonly reported as typical symptoms of OA in studies around the world [4, 5]. However, most current drug therapies focus only on pain relief and symptomatic treatment, including the use of nonsteroidal anti-inflammatory drugs (NSAIDs), intra-articular injection of glucocorticoids and opioids [6]. However, gastrointestinal discomfort and dose dependence are common problems with these drugs [7, 8]. In addition, total knee arthroplasty (TKA) is mainly used to treat severe KOA,

which has a high complication rate [9]. Therefore, it is necessary to explore a safer treatment for OA.

OA used to be considered a degenerative cartilage disease, but now, this concept has been transformed into a complex disease that affects the entire joint [10]. It is now recognized that OA involves mechanical, inflammatory, and metabolic factors, rather than a simple "wear and tear" disease. Inflammation plays a greater role in the pathogenesis of OA than previously recognized, and OA is now regarded as a low-grade inflammatory disease that affects all tissues of the joint, including cartilage degeneration, bone remodeling, osteophytes, and synovitis [11]. In view of the fact that inflammation may play a key role in the pathogenesis and progression of osteoarthritis, it may be a good idea to develop new treatments for OA from this perspective.

Recently, curcuma longa extract (CLE, an anti-inflammatory and antioxidant preparation) has been used in traditional Chinese medicine and Ayurveda to treat arthritis and has thus become an attractive treatment option for improving the joint condition of OA patients [12]. Often used as an alternative medicine or dietary supplement, turmeric is typically an extract that is standardized to 80–95% curcuminoids, which include curcumin (C), demethoxylated curcumin (DMC), and didemethoxylated curcumin (BDMC), among which C [13] is the most active ingredient in turmeric and is "generally regarded as safe" by the US FDA [14]. In addition, the CLE alone has anti-inflammatory properties similar to NSAIDs [15]. It has been shown that CLE affects the signal transduction of proinflammatory cytokines by influencing the activity of NF-κB, such as interleukin, phospholipase A2, 5-lipoxygenase, and COX-2 [16].

Many systematic reviews/meta-analyses (SRs/MAs) have been conducted to evaluate the potential therapeutic benefits of CLE/C for patients with OA. However, the conclusions are inconsistent due to the defects of the quality and methods of the preliminary research studies. The systematic review is a novel tool for solving specific and key issues related to policies and practices [17]. The purpose is to combine the evidence from multiple SRs/MAs to form a practical document that can be used to guide healthcare professionals and decision-makers [18]. The purpose of our research is to use a systematic overview to critically evaluate the scientific quality of related SRs/MAs in the CLE/C treatment of OA.

2. Materials and Methods

2.1. Protocol Registration. This overview protocol has been registered with the INPLASY website (Registration number: INPLASY202220063).

2.2. Research Methods. The SR/MA overview is based on the guidelines specified in Cochrane Handbook [19], the Preferred Reporting Project for System Reviews and Meta-Analyses (PRISMA) statement (Supplementary file 1) [20], and the overview of high-quality methods [21, 22].

2.3. Development of Inclusion and Exclusion Criteria

2.3.1. Literature Inclusion Criteria

(i) Study Design: This overview only includes SRs/MAs from randomized controlled trials (RCTs) of CLE/C in the treatment of OA.

(ii) Study Participants: Subjects who have been clinically or radiologically diagnosed with OA according to national or international standards, regardless of gender, race, or age.

(iii) Study Intervention: The intervention method was CLE/C; the control group was treated with conventional treatment (CT) or placebo.

(iv) Study Outcome Measures: Western Ontario and McMaster University Arthritis Index Score (WOMAC), visual analog scale (VAS), adverse reactions, and other outcome measures, including the use of rescue drugs, incidence of withdrawal from treatment due to adverse events, the use of rescue drugs, walking distance, and analgesic discontinuation rate.

2.3.2. Exclusion Criteria. Duplicate publications, other overviews, conference abstracts, narrative reviews, and network meta-analysis were excluded.

2.4. Search Strategy. Two researchers (WQ-C and HS-S) independently conducted a literature search. The search was carried out with 7 databases including PubMed, Embase, Cochrane Library, CNKI, Wanfang Database, Chongqing VIP, and Chinese Biological Medicine (CBM) Database from its establishment until December 1, 2021. The search strategy adopts a combination of MeSH terms and free words. We searched the above databases with the following key terms: curcuma longa extract, curcumin, osteoarthritis, systematic reviews, and meta-analysis. We also manually searched the references of related articles. The specific search strategy was modified according to different databases. Supplementary file 2 provided the search strategy.

2.5. Eligibility Assessment and Data Extraction. Two researchers (WQ-C and P-D) independently performed literature screening. After deleting duplicate content, researchers read the title and abstract to find potential SRs/MAs based on the inclusion and exclusion criteria. Then, full-text articles were obtained for further screening to determine their eligibility. Afterwards, two researchers (ZG-Y and WB-L) independently extracted data using a standardized data extraction form. The following specific characteristics are extracted from each SR/MA: first author, the year of publication, country, the number of included studies, sample size, treatment intervention, control intervention, quality assessment methods, results, and main conclusions.

2.6. SRs/MAs Quality Assessment. Quality assessment of included SRs/MAs was performed independently by two researchers (Q-L and CD-D).

2.6.1. Assessment of Methodological Quality. The Assessment System for Evaluating Methodological Quality 2 (AMSTAR-2) [23] scale was used to assess the methodological quality of the included SRs/MAs. It consists of 16 items, 7 of which are critical areas (2, 4, 7, 9, 11, 13, and 15). Each item was assessed and rated as "yes," "partially yes," or "no."

2.6.2. Assessment of Risk of Bias. The risk of bias of the included SRs/MAs was assessed by the risk of bias in systematic (ROBIS) scale [24]. The scale was completed in 3 stages to assess the overall risk of bias. The results are assessed and rated as "low," "unclear," or "high."

2.6.3. Assessment of Reporting Quality. The list of PRISMA was used to assess the quality of each SR/MA report based on the following aspects: (a) title, (b) summary, (c) introduction, (d) method, (e) result, (f) discussion, and (g) funding. It consists of 27 items, with a focus on reporting methods and results in a meta-analysis. Based on the completeness of the project information report, each project is assessed and rated as "yes" (full report), "partial yes" (partial report), or "no" (no report).

2.6.4. Assessment of Quality of Evidence. The GRADE scale was used to assess the quality of the evidence of the included SRs/MAs from five aspects: research limitations, inconsistencies, indirectness, imprecision, and publication bias [25].

2.7. Data Synthesis and Presentation. In this overview, a narrative synthesis was used. The characteristics and results of each SR/MA and the assessment results of AMSTAR 2, PRISMA, ROBIS, and GRADE were reported in the form of a list.

3. Results

3.1. Results on Literature Search and Screening. A total of 71 articles were retrieved from seven literature databases, and 21 duplicate articles were deleted. We filtered by the title and abstract of the literature and finally obtained 9 literature studies for full-text screening. After evaluation according to the inclusion and exclusion criteria, we finally obtained 9 literature studies [26, 27] included for study. Figure 1 shows the screening flow chart.

3.2. Description of Included SRs/MAs. Nine SRs/MAs [26, 27] published from 2016 to 2021 were included, and all the included papers were SR and MA. Of these published SRs/MAs, five were from China [27–31], and the remaining four were from the United States [26], the United Kingdom [32], Australia [33], and South Korea, respectively [34]. Among them, 8 SRs/MAs [26, 28–34] were published in English and one [27] was published in Chinese. All SRs/MAs contained a total of 28 RCTs, and the number of RCTs included in each SR/MA ranged from 5 to 15, and the total number of individuals in the included RCTs for a single SR/MA ranged from 599 to 1,621. The intervention rendered to the treatment group was curcuma longa extract or curcumin, and the control group was treated with CT or placebo, and CT modalities include painkillers and NSAIDs. In terms of quality assessment scales, all the literature adopted the Cochrane risk of bias standard. The details of the SRs/MAs included are shown in Table 1.

3.3. Summary of the Results of the Included Studies. The result indicators extracted from the included studies are listed in Table 2.

3.3.1. Efficacy and Safety of CLE/C for OA (Compared with Placebo Group) (Table 2(a))

(1) Pain. All SRs/MAs [26–34] have reported that CLE/C could significantly alleviate the pain of OA patients compared with placebo. Among them, 2 SRs/MAs [26, 33] gave a direct quantitative report that CLE/C could significantly relieve pain. Seven SRs/MAs [27–32, 34] reported that CLE/C could significantly reduce the VAS score of OA patients. Two SRs/MAs [29, 31] reported that CLE/C could significantly reduce the pain score of the WOMAC scale in patients with OA.

(2) Function. Nine SRs/MAs [26–34] reported that CLE/C could significantly improve the joint function of patients with OA. Among them, 2 SRs/MAs [26, 33] gave a direct quantitative report that CLE/C could significantly improve the joint function of patients with OA, and 5 of the SRs/MAs [27, 29, 30, 32, 34] reported that CLE/C could significantly improve the WOMAC scale for patients with OA. Two SRs/MAs both reported that CLE/C could significantly reduce the physical score [29, 31] and stiffness score [29, 31] of the WOMAC scale in patients with OA compared with placebo. In addition, 2 SRs/MAs reported that CLE/C could significantly improve the walking distance [27] and Lequesne pain-function index (LPFI) [32] of patients with OA, respectively.

(3) Adverse events. Seven SRs/MAs [26–31, 33] reported the occurrence of adverse events in CLE/C compared with placebo, none of which was statistically significant. Two SRs/MAs [26, 33] reported that, compared with placebo, there was no significant difference in the use of rescue drugs during the treatment with CLE/C. A SR/MA [26] reported that CLE/C was not statistically significant in the incidence of withdrawal from treatment due to adverse events compared with placebo.

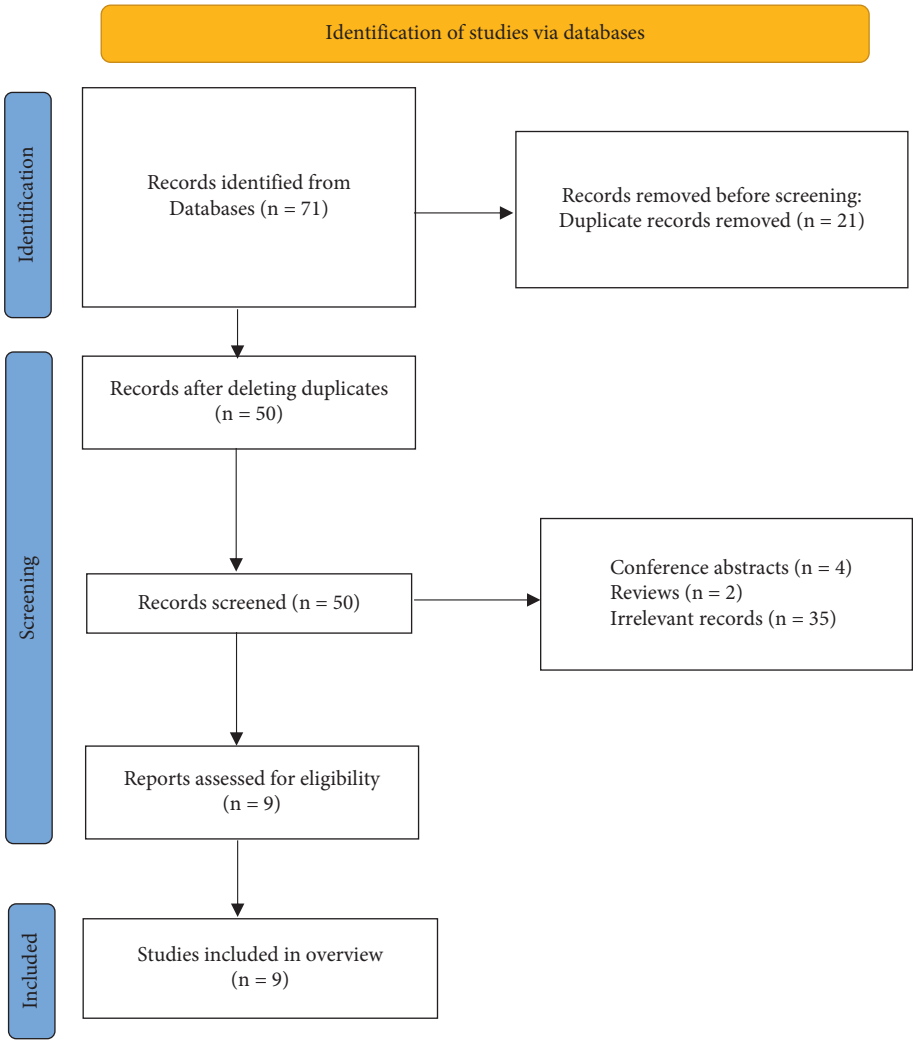

Figure 1: The flowchart of the screening process.

3.3.2. Efficacy and Safety of CLE/C for OA (Compared with CT) (Table 2(b))

(1) Pain. Five SRs/MAs [26–28, 31, 33] reported the effects of CLE/C on pain in patients with OA compared with NSAIDs, and 2 SRs/MAs [31, 33] indicated that CLE/C had similar effects on pain relief compared with NSAIDs. In addition, a SR/MA [27] showed that NSAIDs were superior to CLE/C in reducing pain in patients with OA.

(2) Function. Seven SRs/MAs [26–28, 30–34] reported the improvement of joint function between CLE/C and CT in patients with OA. One SR/MA [34] reported that CLE/C exhibited no statistical significance in the improvement of joint function compared with analgesics. The results of the other 6 SRs/MAs [26–28, 30–33] also showed that CLE/C was equivalent to NSAIDs in improving joint function. One SR/MA [27] reported that there was no difference between CLE/C and NSAIDs in improving walking distance.

(3) Adverse events. Six SRs/MAs [26–28, 30–33] reported the occurrence of adverse events in CLE/C compared with NSAIDs. Among them, the results of 4 SRs/MAs [26, 27, 31, 33] showed that patients using CLE/C had a lower incidence of adverse events. Two SRs/MAs [26, 33] reported no difference between CLE/C and NSAIDs in the use of rescue drugs. A SR/MA [26] reported that CLE/C has a lower incidence of withdrawal due to adverse events than NSAIDs.

3.4. Results on SRs/MAs Quality Assessment

3.4.1. Methodological Quality Assessment. The AMSTAR-2 assessment breakdown for each review is shown in Table 3. Only one SR/MA was of high quality [29]. Since more than one key item was missing in the remaining SRs/MAs, their quality was rated very low. The method restriction came from the following items: item 2 (only 2 SRs/MAs [26, 29] had registered in the protocol), item 7 (only 2 SRs/MAs provided a research exclusion list), and item 15 (the 4 SRs/MAs [26, 27, 30, 32] did not conduct publication bias studies or discuss their impact on SR/MA).

Table 1: Characteristics of the included SRs/MAs.

Author, year (country)	Trials (subjects)	Intervention group	Control group	Quality assessment	Main results
Raveendhara R. 2018 (USA) [26]	7 (769)	Curcumin	CT, placebo	Cochrane	Curcumin compounds can be a valuable supplement to the pharmacological treatment of OA in relieving pain, improving physical function, and reducing the risk of adverse events.
James W. Daily 2016 (South Korea) [34]	8 (892)	Curcumin, curcuma longa extract	CT, placebo	Cochrane	Compared with placebo, turmeric/curcumin can significantly reduce the VAS and WOMAC scores of OA patients. Compared with analgesics, the VAS scores of turmeric/curcumin and the control group were not significantly different, and there was no significant difference in the occurrence of adverse events.
An-Fang Hsiao 2021 (China) [28]	11 (1,258)	Curcumin	CT, placebo	Cochrane	Curcumin compounds were significantly better than the control drugs in the VAS score and WOMAC pain score, and there was no significant difference in the occurrence of adverse events.
Igho J. ONAKPOYA 2017 (UK) [32]	7 (797)	Curcumin	CT, placebo	Cochrane	Compared with placebo, curcuma longa extract has obvious effect in relieving pain and improving physical function. However, compared with NSAIDs, curcuma longa extract cannot improve stiffness and has less pain relief effect for patients with knee OA.
Zhiqiang Wang 2021 (Australia) [33]	10 (1,810)	Curcuma longa extract	CT, placebo	Cochrane	Compared with placebo, curcuma longa extract has obvious effect in relieving pain and improving physical function. However, compared with NSAIDs, curcuma longa extract has a higher level of safety for patients with knee OA.
Wenli Dai 2021 (China) [29]	10 (783)	Curcuma longa extract	Placebo	Cochrane	Compared with placebo, curcuma longa extract is more beneficial in relieving pain and improving the symptomatic OA, and there is no difference in the risk of adverse reactions.
Jian Wu 2019 (China) [30]	5 (599)	Curcumin, curcuma longa extract	CT, placebo	Cochrane	Curcumin can effectively treat patients with OA, improve WOMAC score and VAS score, and curcumin has no more side effects than ibuprofen.
Liuting Zeng 2021 (China) [31]	15 (1,621)	Curcumin, curcuma longa extract	CT, placebo	Cochrane	Both curcuma longa extract and curcumin can relieve pain and joint stiffness in patients with OA, improve joint function, and will not increase the occurrence of adverse events.
Weiyan Gong 2017 (China) [27]	6 (606)	Curcumin, curcuma longa extract	CT, placebo	Cochrane	Curcumin has the effect of treating OA without increasing gastrointestinal side effects

3.4.2. Risk of Bias of the Included SRs/MAs. The risk of bias for all SRs/MAs [26, 29] in the first stage and Domain 1 of the ROBIS evaluation was assessed as low risk. In Domain 2, 6 SRs/MAs [26, 27, 29, 30, 32, 33] were assessed as low risk. In Domain 3, 8 SRs/MAs [26, 28–34] were assessed as low risk of bias and only 2 SRs/MAs [28, 29] were assessed as low risk of bias in Domain 4. In Phase 3, 7 SRs/MAs [26, 28–31, 33, 34] had a low risk of bias. The evaluation details of the included SRs/MAs on the ROBIS scale are shown in Table 4.

3.4.3. Report Quality. The results of the PRISMA inventory evaluation are shown in Table 5. Among the 27 items, 24 items had a "yes" response rate of more than 70%, which showed that the report was relatively complete. However, there were some reporting deficiencies in other projects. Items 5 (protocol and registration) was inadequately reported (the "yes" response rate is less than 50%).

3.4.4. Evidence Quality. Table 6 shows the results of GRADE evaluation including SR/MA-related effect sizes. The 9 SRs/MAs included 59 effect sizes related to the efficacy and safety of CLE/C for OA. In the evaluation results based on the effect sizes, 19 were rated as medium, 20 low, and 20 very low in terms of the quality of evidence. Publication bias ($n = 42$) was the most common downgrading factor, followed by imprecision ($n = 38$), inconsistency ($n = 23$), risk of bias ($n = 22$), and imprecision ($n = 0$).

4. Discussion

CLE/C may be a complementary treatment for OA, which is a common disease in the elderly. At the same time, more and

Table 2: Summary of evidence.

Author, year (country)	Outcomes	Studies (participants)	Relative effect (95% CI)	Heterogeneity
(a) (CLE/C vs placebo)				
Raveendhara R. 2018 (USA) [26]	Pain	5 (331)	SMD: −0.81 (−1.25, −0.37)*	$I2 = 71\%$
	Function	3 (232)	SMD: −0.48 (−0.74, −0.22)*	$I2 = 0\%$
	The use of rescue drugs	3 (141)	RR: 0.65(0.48, 1.05)	$I2 = 74\%$
	Incidence of withdrawal from treatment due to adverse events	4 (288)	RR: 0.90 (0.21, 3.79)	$I2 = 14\%$
	Adverse events	3 (247)	RR: 2.22 (0.94, 5.26)	$I2 = 0\%$
James W. Daily 2016 (South Korea) [34]	VAS	3 (104)	MD: −2.04 (−2.85, −1.24)*	$I2 = 27\%$
	WOMAC scale	3 (122)	MD: −15.36 (−26.9, −3.77)*	$I2 = 91\%$
An-Fang Hsiao 2021 (China) [28]	VAS	7 (501)	SMD: −2.073 (−4.339, 0.194)	$I2 = 96.6\%$
	Adverse events	6 (527)	Or: 1.115 (0.548, 2.271)	$I2 = 0\%$
Igho J. ONAKPOYA 2017 (UK) [32]	VAS	5 (366)	SMD: −3.30(−4.99,−2.01)*	$I2 = 97\%$
	WOMAC scale	3 (167)	SMD: −4.42 (−6.66, −2.19)*	$I2 = 93\%$
	LPFI	2 (107)	MD: −2.69 (−3.48,−1.90)*	$I2 = 0\%$
Zhiqiang Wang 2021 (Australia) [33]	Pain	12 (1,071)	SMD = −0.82 (−1.17, −0.47)*	$I2 = 86.23\%$
	Function	10 (973)	SMD = −0.75 (−1.18, −0.33)*	$I2 = 90.05\%$
	Adverse events	8 (791)	RD: 0.00 (−0.06,0.06)	$I2 = 31.85\%$
	The use of rescue drugs	7 (300)	RD: −0.13 (−0.24,−0.01)*	$I2 = 54.36\%$
	Analgesic discontinuation rate	4 (154)	RD: 0.36 (0.1, 0.61)*	$I2 = 87.06\%$
Wenli Dai 2021 (China) [29]	VAS	8 (569)	MD: −2.21 (−3.15, −1.28)*	$I2 = 94\%$
	WOMAC scale	5 (377)	MD: −11.93 (−16.63, −7.23)*	$I2 = 81\%$
	WOMAC (pain) scale	5 (377)	MD: −1.94 (−2.80, −1.09)*	$I2 = 76\%$
	WOMAC (physical) scale	5 (377)	MD: −6.45 (−9.10,−3.80)*	$I2 = 83\%$
	WOMAC (stiffness) scale	5 (377)	MD: −0.53 (−0.95, −0.11)*	$I2 = 77\%$
	Adverse events	7 (623)	RR: 1.08 (0.69, 1.70)	$I2 = 19\%$
Jian Wu 2019 (China) [30]	WOMAC scale	3 (146)	SMD: −1.30 (−1.66, −0.94)*	$I2 = 37\%$
	VAS	2 (98)	SMD: −1.65 (−2.11, −1.19)*	$I2 = 0\%$
	Adverse events	2 (113)	RR:1.46 (0.57, 3.77)	$I2 = 0\%$
Liuting Zeng 2021 (China) [31]	VAS	6 (381)	MD: −11.55 (−14.3, −9.06)*	$I2 = 69\%$
	WOMAC (pain) scale	4 (315)	SMD: −0.66 (−0.88, −0.43)*	$I2 = 34\%$
	WOMAC (physical) scale	4 (315)	SMD: −0.79 (−1.27, −0.31)*	$I2 = 75\%$
	WOMAC (stiffness) scale	4 (315)	SMD: −0.35 (−0.57, −0.12)*	$I2 = 26\%$
	Adverse events	6 (629)	RR: 1.18 (0.71, 1.94)	$I2 = 25\%$

Table 2: Continued.

Author, year (country)	Outcomes	Studies (participants)	Relative effect (95% CI)	Heterogeneity
Weiyan Gong 2017 (China) [27]	VAS	2 (82)	SMD: −0.69 (−0.99, −0.40)*	$I2 = 48.4\%$
	WOMAC scale	2 (82)	SMD: −1.44 (−1.91, −0.96)*	$I2 = 0\%$
	Adverse events	2 (152)	Or: 1.5 (0.65, 3.44)	$I2 = 0\%$
	Walking distance	1 (48)	MD: 202.0 (187.56, 216.44)*	NA
(b) (CLE/C vs CT)				
Raveendhara R. 2018 (USA) [26]	Pain (vs NSAIDs)	2 (422)	SMD: −0.05 (−0.41, 0.31)*	$I2 = 60\%$
	Function (vs NSAIDs)	1 (331)	SMD: −0.02 (−0.24, 0.19)	NA
	The use of rescue drugs (vs NSAIDs)	2 (422)	RR 2.46 (0.48, 12.52)	$I2 = 60\%$
	Incidence of withdrawal from treatment due to adverse events (vs NSAIDs)	2 (474)	RR: 0.22 (0.05, 0.99)*	$I2 = 0\%$
	Adverse events (vs NSAIDs)	2 (467)	RR: 0.74 (0.60, 0.91)*	$I2 = 0\%$
James W. Daily 2016 (South Korea) [34]	WOMAC scale (vs painkillers)	5 (625)	MD: −1.89 (−4.13,0.35)	$I2 = 94\%$
An-Fang Hsiao 2021 (China) [28]	VAS (vs NSAIDs)	2 (256)	SMD: −0.329 (−0.540, −0.117)*	$I2 = 0\%$
	Adverse events (vs NSAIDs)	3 (623)	Or: 0.524 (0.121, 2.279)	$I2 = 63.2\%$
Igho J. ONAKPOYA 2017 (UK) [32]	WOMAC scale (vs NSAIDs)	1 (331)	MD: −0.03 (−0.03, 0.09)	NA
Zhiqiang Wang 2021 (Australia) [33]	Pain (vs NSAIDs)	5 (648)	SMD = −0.09 (−0.30, 0.12)	$I2 = 34.97\%$
	Function (vs NSAIDs)	3 (477)	SMD = −0.14 (−0.36, 0.09)	$I2 = 20.02\%$
	Adverse events (vs NSAIDs)	3 (571)	RD: −0.12 (−0.24, −0.01)*	$I2 = 42.74\%$
Jian Wu 2019 (China) [30]	The use of rescue drugs (vs NSAIDs)	2 (443)	RD: 0.02 (−0.01, 0.04)	$I2 = 0.01\%$
	WOMAC scale (vs NSAIDs)	1 (331)	SMD: −0.06 (−0.28, 0.15)	NA
	Adverse events (vs NSAIDs)	2 (159)	RR:0.81 (0.63, 1.05)	$I2 = 0\%$
Liuting Zeng 2021 (China) [31]	VAS (vs NSAIDs)	2 (230)	MD: −0.34 (−1.25, 0.57)	$I2 = 0\%$
	WOMAC (pain) scale (vs NSAIDs)	1 (331)	SMD: 0.04 (−0.18, 0.25)	NA
	WOMAC (physical) scale (vs NSAIDs)	1 (331)	SMD: 0.07 (−0.14, 0.29)	NA
	WOMAC (stiffness) scale (vs NSAIDs)	1 (331)	SMD: 0.07 (−0.17, 0.27)	NA
	Adverse events (vs NSAIDs)	3 (561)	RR: 0.55 (0.34, 0.88)*	$I2 = 70\%$
Weiyan Gong 2017 (China) [27]	VAS (vs NSAIDs)	1 (112)	MD: 13.00 (8.162,17.838)*	NA
	WOMAC scale (vs NSAIDs)	1 (331)	MD: 0.13 (−0.302, 0.562)	NA
	Walking distance (vs NSAIDs)	2 (360)	MD: −1.17 (−19.7, 17.37)	$I2 = 0\%$
	Adverse events (vs NSAIDs)	3 (491)	Or: 0.55 (0.38, 0.81)*	$I2 = 75.3\%$

Note. *The 95% confidence interval does not cross the invalid line.

more related SRs/MAs have been carried out. This overview summarizes the available evidence to comprehensively assess the efficacy of CLE/C for the treatment of OA.

4.1. Summary of the Main Findings. This overview incorporated 9 SR/MAs published between 2016 and 2021, 8(8/9, 88.9%) of which were published in the past 5 years, indicating that an increasing attention has been paid to the effectiveness and safety of CLE/C treatment of OA in recent years.

Based on the results of the AMSTAR-2 evaluation in this overview, only one methodological quality of SR/MA was evaluated as high, and the other methodological qualities were very low, and especially in items 2 (protocol registration, 2/9, 22.2%), 7 (exclusion list, 1/9, 11.1%), and 15 (publication bias, 55.6%). Only 2 SRs/MAs were registered for the protocol. Protocol registration is very important when conducting each SR/MA and should be carried out at the time of topic selection, which helps reduce the potential for selective reporting bias and ensures that each SR/MA is conducted in a more accurate manner [35]. Only 2 SRs/MAs provided a complete list of excluded literature, increasing publication bias. Providing a list of excluded literature can provide strong evidence of the accuracy and rigor of the literature screening process. In addition, publication of biased assessments may reduce the veracity of the final results. In this overview, we used the ROBIS scale to evaluate the risk of bias for the included SRs/MAs. Among them, incomplete literature retrieval and insufficient evaluation of publication bias are the main factors leading to a high risk of bias. Similar to the results of the AMSTAR-2 evaluation, the

Table 3: Result of the AMSTAR-2 assessments.

Author, year (country)	Q1	Q2	Q3	Q4	Q5	Q6	Q7	Q8	Q9	Q10	Q11	Q12	Q13	Q14	Q15	Q16	Quality
Raveendhara R. 2018 (USA) [26]	Y	Y	Y	Y	Y	Y	N	Y	Y	Y	Y	Y	Y	Y	N	Y	VL
James W. Daily 2016 (South Korea) [34]	Y	PY	Y	PY	Y	Y	N	Y	Y	Y	Y	Y	Y	N	Y	Y	VL
An-Fang Hsiao 2021 (China) [28]	Y	PY	Y	PY	Y	Y	N	Y	Y	Y	Y	Y	Y	Y	Y	Y	VL
Igho J. ONAKPOYA 2017 (UK) [32]	Y	PY	Y	Y	Y	Y	Y	Y	Y	Y	Y	Y	N	Y	N	Y	VL
Zhiqiang Wang 2021 (Australia) [33]	Y	PY	Y	Y	Y	Y	N	Y	Y	Y	Y	Y	Y	Y	Y	Y	VL
Wenli Dai 2021 (China) [29]	Y	Y	Y	Y	Y	Y	Y	Y	Y	Y	Y	Y	Y	Y	Y	Y	H
Jian Wu 2019 (China) [30]	Y	PY	Y	Y	Y	Y	N	Y	Y	Y	Y	Y	Y	Y	N	Y	VL
Liuting Zeng 2021 (China) [31]	Y	PY	Y	PY	Y	Y	N	Y	Y	Y	Y	Y	Y	Y	Y	Y	VL
Weiyan Gong 2017 (China) [27]	Y	PY	Y	Y	Y	Y	N	Y	Y	Y	Y	N	N	N	N	N	VL

Note. Y, yes; PY, partial yes; N, no; VL, very low; L, low; H, high.

Table 4: Results of the ROBIS assessments

Author, year (country)	Phase 1		Phase 2			Phase 3
	Assessing relevance	Domain 1: Study eligibility criteria	Domain 2: Identification and selection of studies	Domain 3: Collection and study appraisal	Domain 4: Synthesis and findings	Risk of bias in the review
Raveendhara R. 2018 (USA) [26]	√	√	√	√	×	√
James W. Daily 2016 (South Korea) [34]	√	√	×	√	×	√
An-Fang Hsiao 2021 (China) [28]	√	√	×	√	√	√
Igho J. ONAKPOYA 2017 (UK) [32]	√	√	√	√	×	×
Zhiqiang Wang 2021 (Australia) [33]	√	√	√	√	×	√
Wenli Dai 2021 (China) [29]	√	√	√	√	√	√
Jian Wu 2019 (China) [30]	√	√	√	√	×	√
Liuting Zeng 2021 (China) [31]	√	√	×	√	×	√
Weiyan Gong 2017 (China) [27]	√	√	√	×	×	×

Note: √, low risk; ×, high risk.

Table 5: Results of the PRISMA checklist.

Section/ topic	Items	Raveendhara R. 2018 (USA) [26]	James W. Daily 2016 (South Korea) [34]	An-Fang Hsiao 2021 (China) [28]	Igho J. ONAKPOYA 2017 (UK) [32]	Zhiqiang Wang 2021 (Australia) [33]	Wenli Dai 2021 (China) [29]	Jian Wu 2019 (China) [30]	Liuting Zeng 2021 (China) [31]
Title	Q1. Title	Y	Y	Y	Y	Y	Y	Y	Y
Abstract	Q2. Structured summary	Y	Y	Y	Y	Y	Y	Y	Y
Introduction	Q3. Rationale	Y	Y	Y	Y	Y	Y	Y	Y
	Q4. Objectives	Y	Y	Y	Y	Y	Y	Y	Y

Table 5: Continued.

Section/ topic	Items	Raveendhara R. 2018 (USA) [26]	James W. Daily 2016 (South Korea) [34]	An-Fang Hsiao 2021 (China) [28]	Igho J. ONAKPOYA 2017 (UK) [32]	Zhiqiang Wang 2021 (Australia) [33]	Wenli Dai 2021 (China) [29]	Jian Wu 2019 (China) [30]	Liuting Zeng 2021 (China) [31]
Methods	Q5. Protocol and registration	Y	N	N	N	N	Y	N	N
	Q6. Eligibility criteria	Y	Y	Y	Y	Y	Y	Y	Y
	Q7. Information sources	Y	Y	Y	Y	Y	Y	Y	Y
	Q8. Search	N	N	Y	Y	Y	N	N	Y
	Q9. Study selection	Y	Y	Y	Y	Y	Y	Y	Y
	Q10. Data collection process	Y	Y	Y	Y	Y	Y	Y	Y
	Q11. Data items	Y	Y	Y	Y	Y	Y	Y	Y
	Q12. Risk of bias in individual studies	Y	Y	Y	Y	Y	Y	Y	Y
	Q13. Summary measures	Y	Y	Y	Y	Y	Y	Y	Y
	Q14. Synthesis of results	Y	Y	Y	Y	Y	Y	Y	Y
	Q15. Risk of bias across studies	N	Y	Y	Y	Y	Y	Y	Y
	Q16. Additional analyses	Y	Y	Y	Y	Y	Y	Y	Y
Results	Q17. Study selection	Y	Y	Y	Y	Y	Y	Y	Y
	Q18. Study characteristics	Y	Y	Y	Y	Y	Y	Y	Y
	Q19. Risk of bias within studies	Y	Y	Y	Y	Y	Y	Y	Y
	Q20. Results of individual studies	Y	Y	Y	Y	Y	Y	Y	Y
	Q21. Synthesis of results	Y	Y	Y	Y	Y	Y	Y	Y
	Q22. Risk of bias across studies	N	Y	Y	N	Y	Y	Y	Y
	Q23. Additional analysis	Y	Y	Y	Y	Y	Y	Y	Y
Discussion	Q24. Summary of evidence	Y	Y	Y	Y	Y	Y	Y	Y
	Q25. Limitations	Y	Y	Y	Y	Y	Y	Y	Y
	Q26. Conclusions	Y	Y	Y	Y	Y	Y	Y	Y
Funding	Q27. Funding	Y	Y	Y	Y	Y	Y	Y	Y

Note. Y, yes; N, no.

Table 6: Results of evidence quality.

Author, year (country)	Outcomes	Studies (participants)	Limitations	Inconsistency	Indirectness	Imprecision	Publication bias	Quality
A (CLE/C vs placebo)								
Raveendhara R. 2018 (USA) [26]	Pain	5 (331)	0	0	0	0	−1④	Moderate
	Function	3 (232)	0	0	0	0	−1④	Moderate
	The use of rescue drugs	3 (141)	−1①	0	0	−1③	−1④	Very low
	Incidence of withdrawal from treatment due to adverse events	4 (288)	0	0	0	−1③	−1④	Low
	Adverse events	3 (247)	0	0	0	−1③	−1④	Low
James W. Daily 2016 (South Korea) [34]	VAS	3 (104)	0	0	0	−1③	0	Moderate
	WOMAC scale	3 (122)	0	−1②	0	−1③	0	Low
An-Fang Hsiao 2021 (China) [28]	VAS	7 (501)	0	−1②	0	−1③	−1④	Very low
	Adverse events	6 (527)	0	0②	0	−1③	0	Moderate
Igho J. ONAKPOYA 2017 (UK) [32]	VAS	5 (366)	−1①	−1②	0	0	−1④	Very low
	WOMAC scale	3 (167)	−1①	−1②	0	−1③	−1④	Very low
	LPFI	2 (107)	−1①	0	0	−1③	−1④	Very low
Zhiqiang Wang 2021 (Australia) [33]	Pain	12 (1,071)	0	−1②	0	0	−1④	Low
	Function	10 (973)	0	−1②	0	0	−1④	Low
	Adverse events	8 (791)	0	0	0	−1③	−1④	Low
	The use of rescue drugs	7 (300)	0	0	0	0	−1④	Moderate
	Analgesic discontinuation rate	4 (154)	0	−1②	0	−1③	−1④	Very low
Wenli Dai 2021 (China) [29]	VAS	8 (569)	0	−1②	0	0	0	Moderate
	WOMAC scale	5 (377)	0	−1②	0	0	0	Moderate
	WOMAC (pain) scale	5 (377)	0	−1②	0	0	0	Moderate
	WOMAC (physical) scale	5 (377)	0	−1②	0	0	0	Moderate
	WOMAC (stiffness) scale	5 (377)	0	−1②	0	0	0	Moderate
	Adverse events	7 (623)	0	0	0	−1③	0	Moderate
Jian Wu 2019 (China) [30]	WOMAC scale	3 (146)	0	0	0	−1③	−1④	Low
	VAS	2 (98)	0	0	0	−1③	−1④	Low
	Adverse events	2 (113)	0	0	0	−1③	−1④	Low
Liuting Zeng 2021 (China) [31]	VAS	6 (381)	−1①	0	0	0	0	Moderate
	WOMAC (pain) scale	4 (315)	−1①	0	0	0	−1⑤	Low
	WOMAC (physical) scale	4 (315)	−1①	−1②	0	0	0	Low
	WOMAC (stiffness) scale	4 (315)	−1①	0	0	0	0	Moderate
	Adverse events	6 (629)	−1①	0	0	−1③	0	Low
Weiyan Gong 2017 (China) [27]	VAS	2 (82)	−1①	0	0	−1③	−1④	Very low
	WOMAC scale	2 (82)	−1①	0	0	−1③	−1④	Very low
	Adverse events	2 (152)	−1①	0	0	−1③	−1④	Very low
	Walking distance	1 (48)	−1①	−1②	0	−1③	−1④	Very low

Table 6: Continued.

Author, year (country)	Outcomes	Studies (participants)	Limitations	Inconsistency	Indirectness	Imprecision	Publication bias	Quality
B (CLE/C vs CT)								
Raveendhara R. 2018 (USA) [26]	Pain (vs NSAIDs)	2 (422)	0	0	0	−1③	−1④	Low
	Function (vs NSAIDs)	1 (331)	0	−1②	0	−1③	−1④	Very low
	The use of rescue drugs (vs NSAIDs)	2 (422)	0	0	0	−1③	−1④	Low
	Incidence of withdrawal from treatment due to adverse events (vs NSAIDs)	2 (474)	0	0	0	0	−1④	Moderate
	Adverse events (vs NSAIDs)	2 (467)	0	0	0	0	−1④	Moderate
James W. Daily 2016 (South Korea) [34]	WOMAC scale (vs painkillers)	5 (625)	0	−1②	0	−1③	0	Low
An-Fang Hsiao 2021 (China) [28]	VAS (vs NSAIDs)	2 (256)	0	0	0	0	−1⑤	Moderate
	Adverse events (vs NSAIDs)	3 (623)	0	0	0	−1③	0	Moderate
Igho J. ONAKPOYA 2017 (UK) [32]	WOMAC scale (vs NSAIDs)	1 (331)	0	−1②	0	−1③	−1④	Very Low
Zhiqiang Wang 2021 (Australia) [33]	Pain (vs NSAIDs)	5 (648)	0	0	0	−1③	−1④	Low
	Function vs NSAIDs)	3 (477)	0	0	0	−1③	−1④	Low
	Adverse events (vs NSAIDs)	3 (571)	0	0	0	0	−1④	Moderate
	The use of rescue drugs (vs NSAIDs)	2 (443)	0	0	0	−1③	−1④	Low
Jian Wu 2019 (China) [30]	WOMAC scale (vs NSAIDs)	1 (331)	0	−1②	0	−1③	−1④	Very low
	Adverse events (vs NSAIDs)	2 (159)	0	0	0	−1③	−1④	Low
Liuting Zeng 2021 (China) [31]	VAS (vs NSAIDs)	2 (230)	−1①	0	0	−1③	0	Low
	WOMAC (pain) scale (vs NSAIDs)	1 (331)	−1①	−1②	0	−1③	−1④	Very low
	WOMAC (physical) scale (vs NSAIDs)	1 (331)	−1①	−1②	0	−1③	−1④	Very low
	WOMAC (stiffness) scale (vs NSAIDs)	1 (331)	−1①	0	0	−1③	−1④	Very low
	Adverse events (vs NSAIDs)	3 (561)	−1①	0	0	0	0	Moderate
Weiyan Gong 2017 (China) [27]	VAS (vs NSAIDs)	1 (112)	−1①	−1②	0	−1③	−1④	Very low
	WOMAC scale (vs NSAIDs)	1 (331)	−1①	−1②	0	−1③	−1④	Very low
	Walking distance (vs NSAIDs)	2 (360)	−1①	0	0	−1③	−1④	Very low
	Adverse events (vs NSAIDs)	3 (491)	−1①	−1②	0	0	−1④	Very low

Note. ①The included studies have a large bias in methodology such as randomization, allocation concealment, and blinding. ②The confidence interval overlaps less, or the I2 value of the combined results was larger. ③The sample size from the included studies does not meet the optimal sample size or the 95% confidence interval crosses the invalid line. ④The funnel chart is asymmetry. ⑤Fewer studies were included, and their results were all positive, which may result in a large publication bias.

evaluation using the PRISMA checklist found that only 2 SRs/MAs completed the program registration.

The quality of the evidence is based on the GRADE system. Among the 59 effect sizes, no one was rated as high in terms of the quality of evidence. Publication bias is the most common downgrading factor, followed by imprecision, inconsistency, risk of bias, and imprecision. Further analysis revealed a lack of publication bias analysis or the presence of publication bias for the effect sizes included in the SRs/MAs included in this overview. In addition, the insufficient number of RCTs included in the publication bias assessment of the relevant effect size is a potential reason for the missing publication bias assessment. When assessing the quality of evidence for a relevant effect size, the insufficient number of study populations included in that effect size is also a significant contributor to the low quality of the final evidence. Descriptive analysis shows that CLE/C is an effective treatment for OA and may be safer than CT. Due to the low methodological and evidentiary quality of the included RCTs, conclusions from the inclusion of SRs/MAs may differ from real-world outcomes and caution should be exercised when recommending CLE/C as a complementary intervention for OA.

4.2. Implications for Future Research. Various aspects of each SR/MA included were assessed using AMSTAR-2, PRISMA, ROBIS, and GRADE with the aim of facilitating future standardization of SRs/MAs. Researchers conducting SRs/MAs should register or publish study protocols in advance to minimize the risk of bias and ensure the credibility of SRs/MAs results and should provide a list of excluded literature with explanations to ensure transparency and minimize publication bias. In future RCTs, it is important to increase the sample size of the study in a reasonable way to increase the credibility of the evidence. In addition, a complete evaluation of publication bias will also increase the accuracy of the meta-analysis results. With the development of evidence-based complementary and alternative medicine, it is hoped that researchers will continue to promote the standardization of related single RCTs in the future. Well-designed and strictly implemented RCTs can minimize or avoid bias. This is the gold standard for evaluating interventions [36].

4.3. Strengths and Limitations. As far as we know, our study is the first overview of SRs/MAs on the use of CLE/C in the treatment of OA, which can provide a comprehensive evidence reference for clinical practice. In addition, the evaluation process of AMSTAR-2, PRISMA, ROBIS, and GRADE revealed the obvious limitations of SRs/MAs and RCT, which may help guide high-quality research in the future. However, we found that the methodological quality of most of the included SRs/MAs was poor, a limitation that also prevented our study from drawing firm conclusions about the use of CLE/C for OA.

5. Conclusion

According to the available published evidence, CLE/C may be effective and safe for the treatment of OA. However, due to the generally low quality of methodologies, reports, and evidence in the included SRs/MAs, clinicians should approach this finding with caution in their practice.

Data Availability

The datasets analyzed during the current study are available from the corresponding author on reasonable request.

Disclosure

Wenqiang Chen and Hongshuo Shi are the co-first authors.

Conflicts of Interest

The authors declare no conflicts of interest.

Authors' Contributions

WL, GD, and SGM participated in the research design. DP, LWB, SHS, YZG, and CWQ conducted a literature search and screened data extraction. CWQ and SHS analyzed the data, did a statistical analysis, and wrote a manuscript. LWB, QL, DCD, and SHS participated in the correction of the manuscript. All authors reviewed the manuscript. All authors read and approved the final version of the manuscript.

Acknowledgments

This study was supported by Shandong Provincial Natural Science Foundation of China (ZR2021MH2) and Shandong Traditional Chinese Medicine Science and Technology Development Program (2019-0234)

Supplementary Materials

The SR/MA overview is based on the guidelines specified in Cochrane Handbook [19], the Preferred Reporting Project for System Reviews and Meta-Analyses (PRISMA) statement (Supplementary file 1) [20], and the overview of high-quality methods [21, 22]. Supplementary file 2 provided the search strategy. (*Supplementary Materials*)

References

[1] L. Busija, L. Bridgett, S. R. M. Williams et al., "Osteoarthritis," *Best Practice & Research Clinical Rheumatology*, vol. 24, no. 6, pp. 757–768, 2010.

[2] D. J. Hunter and S. Bierma-Zeinstra, "Osteoarthritis," *The Lancet*, vol. 393, no. 10182, pp. 1745–1759, 2019.

[3] A. Litwic, M. H. Edwards, E. M. Dennison, and C. Cooper, "Epidemiology and burden of osteoarthritis," *British Medical Bulletin*, vol. 105, no. 1, pp. 185–199, 2013.

[4] M. C. Hochberg, L. Yerges-Armstrong, M. Yau, and B. D. Mitchell, "Genetic epidemiology of osteoarthritis," *Current Opinion in Rheumatology*, vol. 25, no. 2, pp. 192–197, 2013.

[5] J. Riegger and R. E. Brenner, "Pathomechanisms of post-traumatic osteoarthritis: chondrocyte behavior and fate in a precarious environment," *International Journal of Molecular Sciences*, vol. 21, no. 5, p. 1560, 2020.

[6] M. Gao, C. Chen, Q. Zhang, J. Bian, L. Qin, and L. Bao, "Research progress on the antiosteoarthritic mechanism of action of natural products," *Evidence-based Complementary and Alternative Medicine*, vol. 2021, pp. 1–17, 2021.

[7] D. H. Solomon, M. E. Husni, P. A. Libby et al., "The risk of major NSAID toxicity with celecoxib, ibuprofen, or naproxen: a secondary analysis of the PRECISION trial," *The American Journal of Medicine*, vol. 130, no. 12, pp. 1415–1422, 2017, e4.

[8] F. K. L. Chan, J. Y. L. Ching, Y. K. Tse et al., "Gastrointestinal safety of celecoxib versus naproxen in patients with cardiothrombotic diseases and arthritis after upper gastrointestinal bleeding (CONCERN): an industry-independent, double-blind, double-dummy, randomised trial," *The Lancet*, vol. 389, no. 10087, pp. 2375–2382, 2017.

[9] R. Gunaratne, D. N. Pratt, J. Banda, D. P. Fick, R. J. K. Khan, and B. W. Robertson, "Patient dissatisfaction following total knee arthroplasty: a systematic review of the literature," *The Journal of Arthroplasty*, vol. 32, no. 12, pp. 3854–3860, 2017.

[10] S. Glyn-Jones, A. J. R. Palmer, R. Agricola et al., "Osteoarthritis," *The Lancet*, vol. 386, no. 9991, pp. 376–387, 2015.

[11] M. Millerand, F. Berenbaum, and C. Jacques, "Danger signals and inflammaging in osteoarthritis," *Clinical & Experimental Rheumatology*, vol. 37, no. 120, pp. 48–56, 2019.

[12] S. Srivastava, A. K. Saksena, S. Khattri, S. Kumar, and R. S. Dagur, "Curcuma longa extract reduces inflammatory and oxidative stress biomarkers in osteoarthritis of knee: a four-month, double-blind, randomized, placebo-controlled trial," *Inflammopharmacology*, vol. 24, no. 6, pp. 377–388, 2016.

[13] T. Appelboom, N. Maes, and A. Albert, "A new curcuma extract (flexofytol) in osteoarthritis: results from a Belgian real-life experience," *The Open Rheumatology Journal*, vol. 8, no. 1, pp. 77–81, 2014.

[14] Turmeric, *Drugs and Lactation Database (LactMed)*National Library of Medicine (US), Bethesda, MD, USA, 2021.

[15] B. Kocaadam and N. Şanlier, "Curcumin, an active component of turmeric (Curcuma longa), and its effects on health," *Critical Reviews in Food Science and Nutrition*, vol. 57, no. 13, pp. 2889–2895, 2017.

[16] S. M. Plummer, K. A. Holloway, M. M. Manson et al., "Inhibition of cyclo-oxygenase 2 expression in colon cells by the chemopreventive agent curcumin involves inhibition of NF-κB activation via the NIK/IKK signalling complex," *Oncogene*, vol. 18, no. 44, pp. 6013–6020, 1999.

[17] O. Onasanya, G. Iyer, E. Lucas, D. Lin, S. Singh, and G. C. Alexander, "Association between exogenous testosterone and cardiovascular events: an overview of systematic reviews," *Lancet Diabetes & Endocrinology*, vol. 4, no. 11, pp. 943–956, 2016.

[18] M. Wang, M. Jia, W. Q. DU et al., "Overview of systematic reviews/Meta-analysis of Xingnaojing Injection in treatment of intracerebral hemorrhage," *Zhongguo Zhongyao Zazhi*, vol. 46, no. 18, pp. 4633–4643, 2021.

[19] J. T. J. C. J Higgins, *Cochrane Handbook for Systematic Reviews of Interventions*, John Wiley & Sons, Chichester (UK), 2nd edition, 2019.

[20] D. Moher, A. Liberati, J. Tetzlaff, D. G. Altman, and PRISMA Group, "Preferred reporting items for systematic reviews and meta-analyses: the PRISMA statement," *BMJ*, vol. 339, no. jul21 1, Article ID b2535, 2009.

[21] N. Liu, T. Zhang, J. Sun et al., "An overview of systematic reviews of Chinese herbal medicine for alzheimer's disease," *Frontiers in Pharmacology*, vol. 12, Article ID 761661, 2021.

[22] M. Shen, J. Huang, and T. Qiu, "Quality of the evidence supporting the role of acupuncture for stable Angina pectoris: an umbrella review of systematic reviews," *Frontiers in Cardiovascular Medicine*, vol. 8, Article ID 732144, 2021.

[23] B. J. Shea, B. C. Reeves, G. Wells et al., "AMSTAR 2: a critical appraisal tool for systematic reviews that include randomised or non-randomised studies of healthcare interventions, or both," *BMJ*, vol. 358, Article ID j4008, 2017.

[24] P. Whiting, J. Savović, J. P. T. Higgins et al., "ROBIS: a new tool to assess risk of bias in systematic reviews was developed," *Journal of Clinical Epidemiology*, vol. 69, pp. 225–234, 2016.

[25] D. Atkins, D. Best, P. A. Briss et al., "Grading quality of evidence and strength of recommendations," *BMJ*, vol. 328, no. 7454, p. 1490, 2004.

[26] R. R. Bannuru, M. C. Osani, F. Al-Eid, and C. Wang, "Efficacy of curcumin and Boswellia for knee osteoarthritis: systematic review and meta-analysis," *Seminars in Arthritis and Rheumatism*, vol. 48, no. 3, pp. 416–429, 2018.

[27] W. Gong and S. Zhang, "Meta analysis of curcumin in the treatment of arthritis," *Chinese Journal of Antibiotics*, vol. 42, no. 01, pp. 79–83, 2017.

[28] A.-F. Hsiao, Y.-C. Lien, I.-S. Tzeng, C.-T. Liu, S.-H. Chou, and Y.-S. Horng, "The efficacy of high- and low-dose curcumin in knee osteoarthritis: a systematic review and meta-analysis," *Complementary Therapies in Medicine*, vol. 63, Article ID 102775, 2021.

[29] W. Dai, W. Yan, X. Leng, J. Chen, X. Hu, and Y. Ao, "Effectiveness of Curcuma longa extract versus placebo for the treatment of knee osteoarthritis: a systematic review and meta-analysis of randomized controlled trials," *Phytotherapy Research*, vol. 35, no. 11, pp. 5921–5935, 2021.

[30] J. Wu, M. Lv, and Y. Zhou, "Efficacy and side effect of curcumin for the treatment of osteoarthritis: a meta-analysis of randomized controlled trials," *Pakistan Journal of Pharmaceutical Sciences*, vol. 32, no. 1, pp. 43–51, 2019.

[31] L. Zeng, G. Yu, W. Hao, K. Yang, and H. Chen, "The efficacy and safety of Curcuma longa extract and curcumin supplements on osteoarthritis: a systematic review and meta-analysis," *Bioscience Reports*, vol. 41, no. 6, Article ID BSR20210817, 2021.

[32] I. J. Onakpoya, E. A. Spencer, R. Perera, and C. J. Heneghan, "Effectiveness of curcuminoids in the treatment of knee osteoarthritis: a systematic review and meta-analysis of randomized clinical trials," *International Journal of Rheumatic Diseases*, vol. 20, no. 4, pp. 420–433, 2017.

[33] Z. Wang, A. Singh, G. Jones et al., "Efficacy and safety of turmeric extracts for the treatment of knee osteoarthritis: a systematic review and meta-analysis of randomised controlled trials," *Current Rheumatology Reports*, vol. 23, no. 2, p. 11, 2021.

[34] J. W. Daily, M. Yang, and S. Park, "Efficacy of turmeric extracts and curcumin for alleviating the symptoms of joint arthritis: a systematic review and meta-analysis of randomized

clinical trials," *Journal of Medicinal Food*, vol. 19, no. 8, pp. 717–729, 2016.

[35] L. Stewart, D. Moher, and P. Shekelle, "Why prospective registration of systematic reviews makes sense," *Systematic Reviews*, vol. 1, no. 1, p. 7, 2012.

[36] D. Moher, S. Hopewell, K. F. Schulz et al., "CONSORT 2010 explanation and elaboration: updated guidelines for reporting parallel group randomised trials," *International Journal of Surgery*, vol. 10, no. 1, pp. 28–55, 2012.

Hindawi
Evidence-Based Complementary and Alternative Medicine
Volume 2022, Article ID 7562569, 12 pages
https://doi.org/10.1155/2022/7562569

Research Article

Toxicity, Anti-Inflammatory, and Antioxidant Activities of Cubiu (*Solanum sessiliflorum*) and Its Interaction with Magnetic Field in the Skin Wound Healing

Jéssica Franco Dalenogare,[1] Marina de Souza Vencato,[2] Greice Franciele Feyh dos Santos Montagner,[1] Thiago Duarte,[1] Marta Maria Medeiros Frescura Duarte,[1] Camila Camponogara,[3] Sara Marchesan Oliveira,[3] Marcelo Leite da Veiga,[2] Maria Izabel de Ugalde Marques da Rocha,[2] Maria Amália Pavanato,[1] and Liliane de Freitas Bauermann[1]

[1]*Department of Physiology and Pharmacology, Federal University of Santa Maria, Santa Maria, Brazil*
[2]*Department of Morphology, Federal University of Santa Maria, Santa Maria, Brazil*
[3]*Department of Biochemistry, Federal University of Santa Maria, Santa Maria, Brazil*

Correspondence should be addressed to Liliane de Freitas Bauermann; lgfbauermann@gmail.com

Received 15 August 2021; Revised 23 December 2021; Accepted 12 February 2022; Published 10 March 2022

Academic Editor: Rohit Sharma

Cubiu, an Amazonian fruit, is widely used as food and popular treatment for pathologies that present an inflammatory pattern, such as skin wound healing. However, there is still no confirmation in the scientific literature about the safety profile, as well as the anti-inflammatory, antioxidant, and healing actions of cubiu. This study is divided into two experimental protocols using Wistar rats. Thus, the first objective (protocol 1) of this study was to evaluate the toxicity of an oral administration of cubiu extract at different doses for 28 days. The macroscopic and microscopic analyses of the liver and kidney were performed, and the following analysis was determined in plasma: glutamic oxaloacetic transaminase, glutamic pyruvic transaminase, gamma-glutamyl transpeptidase, glucose, triglycerides, total cholesterol, urea, creatinine, and uric acid. After, we conducted the second protocol aimed to establish the potential antioxidant and anti-inflammatory capacity of cubiu and its interaction with magnetic field in skin wound healing. On days 3, 7, and 14 of treatment, skin and blood samples were collected and analyzed: the oxidative stress biomarkers (reactive substances to thiobarbituric acid, nonprotein thiols, superoxide dismutase, catalase, and glutathione S-transferase), myeloperoxidase enzymatic activity, and cytokines levels (interleukin 1, interleukin 6, interleukin 10, and tumor necrosis factor-alpha). The cubiu has shown to be safe and nontoxic. Both cubiu and magnetic field promoted decreased levels of proinflammatory and prooxidant biomarkers (interleukin 1, interleukin 6, tumor necrosis factor-alpha, and reactive substances to thiobarbituric acid), as well as increased levels of anti-inflammatory and antioxidant biomarkers (interleukin 10, nonprotein thiols, and superoxide dismutase), with greater potential when treatments are used in association. Thus, cubiu promotes antioxidant and anti-inflammatory action in skin wound healing, while also improving results of the conventional treatment for skin healing (magnetic field) when used in association.

1. Introduction

Solanum sessiliflorum (Dunal) is a Solanaceae native of the Amazon Basin, currently found throughout the Brazilian, Ecuadorian, Colombian, and Venezuelan Amazonian territory. Its fruit, called cubiu in Portuguese, also known as "apple/peach tomato, is widely used as food, and it can be used in numerous ways such as juices, sweets, jellies, and consumed in natura [1]. Furthermore, cubiu is very nutritious and rich in iron, niacin, citric acid, and pectin. Thus,

cubiu presents compounds considered adjuvants for health promotion, such as fibers, minerals, and bioactive compounds like phenolic acids [2].

Amazonian people commonly employ cubiu as a remedy or cosmetic. In their traditional medicine system, cubiu is used because of its hypoglycemic, hypolipidemic, and antioxidant properties to treat diabetes and skin wound healing [3–5]. However, no studies have investigated the anti-inflammatory properties of cubiu, considering the inflammatory profile of the pathologies traditionally treated with this plant. Moreover, the in vivo antioxidant potential of cubiu is scarcely approached in scientific literature. Cubiu also could be a suitable alternative for use in combination with magnetic fields. Therapy with magnetic fields is used for skin wound healing, but its systemic performance in the oxidative and inflammatory profile is controversial in the scientific literature. Considering these data, an investigation of magnetic fields associated with antioxidants was suggested [6, 7]. Among these substances, there are natural antioxidants, primarily contained in plants. As previously mentioned, cubiu is commonly used for its antioxidant properties [8] and also popularly used for skin wound healing. Therefore, we believe to be pertinent to elucidate the effects of cubiu combined with magnetic field therapy.

Thus, the first objective of the present study was to evaluate the oral toxicity of cubiu. After completing this objective, the potential antioxidant and anti-inflammatory capacities of cubiu and its interaction with magnetic fields in an in vivo model of skin healing were analyzed.

2. Materials and Methods

2.1. Cubiu Extract Preparation. Cubiu samples were purchased in the Municipal Market Adolfo Lisboa-Manaus city, Amazonas, Brazil. Botanic specialist Eduardo Vellez Marin (CRBio 09112-03) confirmed the fruits to be *Solanum sessiliflorum* Dunal. This research is part of a project previously authorized by the Brazil Environmental Ministry to assess the components of genetic patrimony in national territory (no. 010547/2013-4) according to Brazilian legislation (no. 2186-16). The cubiu samples were registered in the Management of Genetic Patrimony Council, Brazil (CGEN, process number A6723EB).

The fresh fruits of cubiu weighed 147 ± 38 g. The preparation of the cubiu extract included washing and peeling the fruits, as well as grinding the pulp with small seeds in a mixer for 5 min and then extracting with 70% absolute ethanol (neon, commercial-03467; São Paulo, SP, Brazil). After extraction, the product obtained was filtered, evaporated, lyophilized, and was stored in a −20 degrees freezer [9]. Subsequently, the lyophilized cubiu extract was diluted daily in saline and administered via oral gavage for oral administration. The use of fresh fruit followed institutional, national, and international guidelines and legislation. The cubiu extract phytochemical characterization is demonstrated in the study by Montagner et al. [9].

2.2. Experimental Animals. Male Wistar rats (90 days of life, weighing 150 g) were obtained from the Central Animal Facility of the Federal University of Santa Maria (UFSM) and were maintained during the experimental protocol at the Animal Facility of the Physiology Department (UFSM), under controlled environmental conditions ($23^{\circ}C \pm 1$), 12-hour light/dark cycle, and food and water provided ad libitum. This research was conducted following the Animal Research: Reporting of In Vivo Experiments (ARRIVE guidelines) and the internationally accepted guidelines on animal welfare (EEC Directive 1986; 86/609/EEC) and in agreement with national and institutional rules. The experimental protocol was approved by the Ethics Committee on Animal Use of the Federal University of Santa Maria, registration no. 119/2013.

2.3. Protocol 1: Toxicity Evaluation of Cubiu Extract by Dose-Response Curve. A curve was proposed for different doses of the cubiu extract diluted in saline and administrated by oral gavage for 28 days ($n = 3$ animals per group, total = 12 animals). This allowed verifying the toxicity of the cubiu extract and the most adequate or beneficial dose for protocol 2. Tested doses of cubiu extract were 25 mg/kg, 50 mg/kg, 100 mg/kg, and 150 mg/kg per rat body weight. This protocol had a control group that received only saline. The toxicity was performed according to OECD guideline 407 (OECD, 2008) [10] with slight modifications.

2.3.1. Biochemical Analyses. Plasma analyses of glutamic oxaloacetic transaminase (GOT), glutamic pyruvic transaminase (GPT), gamma-glutamyl transpeptidase (GGT), glucose, triglycerides, total cholesterol, urea, creatinine, and uric acid were performed using a commercial kit (Bioclin®), according to manufacturer's instructions. These analyses were processed in an automatic biochemical analyzer (Mindray BS-120®). The results were expressed in UI/l (GOT, GPT), U/l (GAMA GT), mg/dl (triglycerides, total cholesterol, urea, creatinine, and uric acid), and g/dl (glucose).

2.3.2. Morphological Analyses. Organs were evaluated macroscopically regarding preservation of organ architecture, presence of hemorrhage, and any aspects associated with degeneration, in addition to, shape, size, color, and general appearance. After euthanasia, the samples were fixed in 10% buffered formalin and embedded in histological paraffin for light microscopic examination after removal. Sections (6 μm thick) were stained using the hematoxylin and eosin method. Two independent observers performed double-blind analysis. For liver samples, following criteria were evaluated: presence of inflammatory infiltrate, cellular degeneration or necrosis, congestion or dilatation of the central vein or liver sinusoids, and presence of sinusoidal vacuolization. For kidney samples, evaluated criteria were dilatation of Bowman's capsule, dilatation of subcapsular space, dilatation of proximal and distal convoluted tubules, and glomerular and tubular degeneration [11].

2.3.3. Oxidative Status. Evaluation of oxidative status was conducted in homogenized hepatic and renal tissue. To homogenize tissue samples, 9 mL of sodium phosphate buffer 0.3M (KCl 140 mM, pH 7.4) was used per gram of tissue. Phenylmethylsulfonyl fluoride (PMSF) was added at the concentration of 100 nM diluted with isopropanol, 10 μl of PMSF per mL of buffer. Homogenization was performed for 60 seconds in ULTRA-TURRAX at 0–4°C. Centrifugation of homogenate was carried in refrigerated equipment for 10 minutes at 3000 rpm (1100 g).

(1) Total Protein Determination. Protein content in the homogenate was evaluated using the method described by Lowry et al. [12]. Results were expressed in mg/ml.

(2) Thiobarbituric Acid Reactive Substances (TBARS) Determination. The TBARS method was carried in accordance with Buege and Aust [13]. Results were expressed as nmoles of TBARS/mg of protein.

(3) Quantification of Nonprotein Sulfhydryl Groups. Quantification of nonprotein sulfhydryl (NPSH) was accomplished following Ellman [14]. Individual absorbance values were interpolated with glutathione standard curve and expressed as μg of glutathione/g of protein.

(4) Antioxidant Enzymatic Activities. Catalase (CAT) activity was verified through the method described by Boveris and Chance [15], and results were expressed as nmoles/mg of protein. Superoxide dismutase (SOD) activity was evaluated as described by Boveris and Cadenas [16]. Results were expressed as units of SOD/mg of protein. Enzymatic activity of glutathione S-transferase (GST) was performed according to Habig et al. [17], and results were expressed in μmoles/min per mg of protein.

2.4. Protocol 2: Experimental Wound Healing Design. At the beginning of the experimental protocol (day 0), to induce the wound healing process along with inflammation and oxidative unbalance, a patch of the skin of 1 cm^2 was removed from all animals. Each animal was anesthetized with the association of ketamine (75 mg/kg) and xylazine (10 mg/kg) administrated intraperitoneally [18]. After that, animals were immobilized at a surgical table, and procedure was conducted using surgical scissors and tweezers. Wounds were cut circularly in the middle of the upper back of each animal, about 20 mm from the base of the skull and normalized [19]. After this surgical procedure, total animals ($n = 72$) were separated into four groups:

Control group: animals that did not receive any treatment, only saline by oral gavage and simulation of exposition to the magnetic field ($n = 18$)

Group treated with cubiu: animals treated with the ingestion by oral gavage of 50 mg/kg of cubiu extract ($n = 18$)

Group treated with magnetic field: animals treated by the exposition to the magnetic field ($n = 18$)

Group treated with magnetic field + cubiu: animals treated with the ingestion by oral gavage of 50 mg/kg of cubiu extract and exposition to the magnetic field ($n = 18$)

The 50 mg/kg cubiu extract dose used in the experiment was chosen according to results of toxicity studies. The pulsed magnetic field used in this experiment was a pulsed one, with a flux density of 2 mT, constant intervals between pulses (1, 5 s), frequency of 60 Hz, and 30 minutes of exposition per day, which was chosen based on the literature [20–22]. Treatments were performed once daily. On days 3, 7, and 14 after surgery, the animals ($n = 6$ per group) were euthanized to proceed with the collection of blood and skin samples [23, 24]. Figure 1 shows the experimental procedures of protocols 1 and 2.

2.4.1. Inflammatory Cytokines. Skin and plasma determination of interleukin 1 (IL-1), interleukin 6 (IL-6), interleukin 10 (IL-10), and tumor necrosis factor-alpha (TNF-α) were evaluated using the ELISA kit (eBioscience, San Diego, EUA), according to the manufacturer's instructions. Hemocysteine levels were assayed using an IMMULITE analyzer (Diagnostic Products Corporation, Los Angeles, California). Results are expressed in pg/ml.

2.4.2. Leukocyte Infiltration Marker. Skin samples were collected to evaluate the myeloperoxidase activity (MPO) to estimate inflammatory cell infiltration in the skin after injury. The activity of this enzyme was used as a marker of neutrophil infiltration [25, 26]. First, tissue samples were homogenized with a motor-driven homogenizer in 300 μl of acetate buffer (8 mM, pH 5.4) containing 0.5% HTAB (45 s at 0°C). The homogenate was then centrifuged at 11000 ×g at 4°C for 20 min, and supernatants were stored at −4°C. To evaluate MPO activity, 10 μl of supernatant was incubated with 200 μl of acetate buffer (8 mM, pH 5.4) and 20 μl of TMB (18.4 mM) at 37°C for 3 min. The reaction was stopped with 30 μl of acetic acid in a cold bath, and the enzyme activity value was assessed colorimetrically at 630 nm using a microplate reader. Results were expressed as optical density (OD)/mg of protein.

2.4.3. Determination of Oxidative Status. Fresh homogenized hepatic and dermal tissues (skin). TBARS and NPSH levels and SOD, CAT, and GST activities were determined as described in Sections 2.3.3

2.5. Statistical Analysis. For the first protocol, homogeneity of variances among different tested concentrations was verified with Levene's test and one-way ANOVA, followed by Tukey's post hoc test. For the second protocol, homogeneity of variances was evaluated in the same way, and a three-way ANOVA was performed followed by Tukey. The software used for this analysis was software Statistica® 7.0. The significance level (α) adopted was ≤ 0.05.

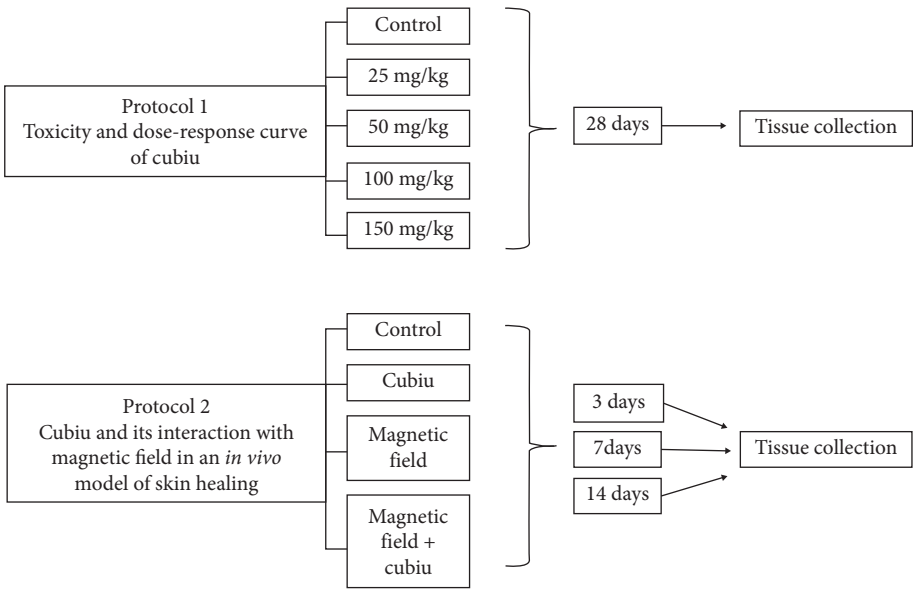

Figure 1: Schematic demonstration of the experimental procedures of protocols 1 and 2.

3. Results

3.1. Oral Toxicity Evaluation of Cubiu Extract. Initially, cubiu extract daily oral administration toxicity was evaluated through a dose-response curve for 28 days. No changes in GOT, GPT, GGT, glucose, triglycerides, total cholesterol, urea, and uric acid levels were observed between the groups that received different doses of cubiu extract in comparison to the control group (Table 1). Regarding creatinine levels, animals treated with cubiu extract at a dose of 100 mg/kg had their levels increased when compared to the animals treated with 25 mg/kg of cubiu extract.

The second objective of the experiments conducted in protocol 1 was to determine, among the studied doses, the one with the greatest beneficial potential in the face of oxidative status. Table 2 provides the oxidative/antioxidant biomarkers in the liver, in which no change was observed in levels of TBARS, NPSH, and GST between the groups that received the different doses of cubiu extract compared to the control group. As for the enzymatic activity of SOD, an increase was observed in the groups treated with 25 mg/kg, 50 mg/kg, and 150 mg/kg of cubiu extract compared to the control group. In addition, the group treated with 100 mg/kg of cubiu extract presented reduced SOD activity compared to the groups treated with 25 mg/kg and 150 mg/kg of cubiu extract. The enzymatic activity of CAT was increased in the group treated with 25 mg/kg of cubiu extract compared to the control group and compared to the groups treated with 100 mg/kg and 150 mg/kg of cubiu extract.

For the renal biomarkers of oxidative stress (Table 2), it was evident that enzymatic activity of SOD was increased in the groups treated with 25 mg/kg, 50 mg/kg, and 100 mg/kg of cubiu extract compared to the control group. Furthermore, the enzymatic activity of CAT was increased in the group treated with 50 mg/kg of cubiu extract compared to the control group.

The morphological analysis showed no macroscopic or histological changes in hepatic and renal structures between the groups that received different doses of cubiu extract (25, 50, 100, and 150 mg/kg) compared to the control group (Figure 2).

Following the presented data, the dose of cubiu extract chosen for continuity of the other experimental protocols was 50 mg/kg.

3.2. Inflammatory Biomarkers in the Skin and Plasma. The results of inflammatory markers in the skin are given in Table 3 and in the plasma are given in Table 4. Levels of proinflammatory cytokines IL-1 and IL-6, in the skin and plasma, were decreased in all experimental groups on the 3rd day in comparison to the control group of the respective time. Also, on 3rd day, the TNF-α levels decreased in the skin and plasma in groups treated with magnetic field and with magnetic field + cubiu. On days 7 and 14, the group treated with magnetic field and the group treated with magnetic field + cubiu had decreased IL-1, IL-6, and TNF-α skin and plasma levels when compared to the control group. Additionally, on the 14th day, the group treated with cubiu had decreased IL-6 plasma levels when compared to the control group.

Furthermore, among the treatments, it was observed that in the skin, on day 3, the group treated with magnetic field and cubiu combination significantly reduced IL-1, IL-6, and TNF-α levels when compared to the group treated with cubiu or magnetic field separately. On the 7th day, the group treated with magnetic field + cubiu presented a reduction in IL-1 levels when compared to the group treated only with cubiu. On day 14, the group treated with the magnetic field and cubiu combination had reduced levels of IL-1 when compared to the groups treated with cubiu or magnetic field separately, and the group treated with magnetic field + cubiu presented a decrease in IL-6 and TNF-α levels when

Table 1: Biochemical parameters of rats after 28-day treatment with cubiu extract.

	Control	25 mg/kg	50 mg/kg	100 mg/kg	150 mg/kg
GOT (UI/l)	151.02 ± 36.00	179.83 ± 16.72	159.75 ± 31.11	151.90 ± 15.14	172.27 ± 11.71
GPT (UI/l)	132.98 ± 9.04	108.83 ± 12.30	147.82 ± 7.63	117.26 ± 17.12	123.96 ± 16.06
GAMA GT (U/l)	28.73 ± 3.19	25.14 ± 1.56	34.83 ± 5.97	34.47 ± 3.29	24.77 ± 5.53
Glucose (g/dl)	100.54 ± 12.64	140.35 ± 17.12	121.79 ± 8.91	141.43 ± 9.01	105.22 ± 20.75
Triglycerides (mg/dl)	125.92 ± 14.37	108.33 ± 28.09	110.18 ± 21.35	108.33 ± 23.29	78.70 ± 2.44
Total cholesterol (mg/dl)	87.61 ± 21.96	88.57 ± 24.41	58.09 ± 11.23	116.18 ± 9.94	73.33 ± 20.88
Urea (mg/dl)	52.06 ± 3.07	44.95 ± 3.69	43.24 ± 4.93	46.37 ± 2.05	44.38 ± 3.84
Creatinine (mg/dl)	0.57 ± 0.004	0.53 ± 0.06^{D}	0.55 ± 0.02	0.73 ± 0.05^{B}	0.60 ± 0.01
Uric acid (mg/dl)	1.43 ± 0.31	0.79 ± 0.13	1.17 ± 0.40	1.46 ± 0.40	0.95 ± 0.24

Values are represented as the mean ± standard error. Different capital letters indicate significant differences between treatments ($p < 0.05$). The capital letters "B" corresponds to the group 50 mg/kg and letter "D" corresponds to the group 150 mg/kg. GOT, glutamic oxaloacetic transaminase; GPT, glutamic pyruvic transaminase; GAMA GT, gamma-glutamyl transpeptidase.

compared to the group treated only with cubiu. Additionally, IL-6 levels reduced in the group treated with magnetic field compared to the group treated with cubiu.

In plasma, among the treatments, it was observed that, on the 3rd day, the group treated with the magnetic field and cubiu combination had decreased levels of IL-1, IL-6, and TNF-α when compared to the group treated with cubiu or with magnetic field separately. On days 7 and 14, the group treated with magnetic field + cubiu presented a decrease in IL-1 and Il-6 levels compared to the group treated only with cubiu. Also, on the 14th day, TNF-α levels decreased in the group treated with magnetic field + cubiu compared to the group treated only with cubiu.

IL-10 anti-inflammatory cytokine levels in the skin and plasma were increased in the group treated with magnetic field and the group treated with magnetic field + cubiu on the 3rd day in comparison to the control group of the respective time. On the 7th day, the group treated with magnetic field + cubiu presented increased levels of IL-10 in comparison to the control group. On day 14, all treatments (cubiu, magnetic field, and magnetic field + cubiu) had higher levels of IL-10 when compared to the control group. Furthermore, among the treatments, it was observed that in the skin and plasma, on day 3, the group treated with magnetic field + cubiu had increased IL-10 levels in comparison to the group treated only with cubiu. On day 7, the group treated with the magnetic field and cubiu combination had increased IL-10 levels compared to the group treated with cubiu or with magnetic field separately.

Regarding the changes in IL-1, IL-6, and TNF-α proinflammatory cytokines skin and plasma levels over time, reductions were generally observed in all experimental groups. In relation to IL-10 anti-inflammatory cytokine skin and plasma levels over time, increases were generally observed in all experimental groups, corresponding to what was physiologically expected.

3.3. Leukocyte Infiltration Markers in the Skin. Results in myeloperoxidase activity are shown in Figure 3. On the 3rd day, it was evident that all treatments (cubiu, magnetic field, and magnetic field + cubiu) decreased the myeloperoxidase enzymatic activity in comparison to the control group. In addition, over time, a decrease in enzymatic activity of myeloperoxidase was observed in the control group. The group treated with cubiu, and the group treated with magnetic field + cubiu presented a decrease in myeloperoxidase activity on the 14th day compared to the 3rd day. Also, the magnetic field group demonstrated a reduction in myeloperoxidase activity on the 14th day compared to the 7th day.

3.4. Oxidative Status in the Skin. Table 5 provides the results concerning oxidative status biomarkers in the skin. It was observed that the levels of TBARS were reduced in all treatments (cubiu, magnetic field, and magnetic field + cubiu) compared to the control group on the 3rd day of treatment. On the 14th day, the group treated with magnetic field had reduced TBARS levels when compared to the control group.

NPSH levels were increased in the group treated with magnetic field + cubiu on the 14th day compared to the control group. In addition, changes over time were observed; the control group and the group treated with cubiu had reduced NPSH levels on day 7 when compared to the respective group on days 3 and 14. The group treated with magnetic field and the group treated with magnetic field + cubiu increased NPSH levels on the 14th day compared to the 3rd day and 7th day.

As for SOD activity, it was observed that the group treated with magnetic field + cubiu had its activity increased on the 14th day in relation to the control group. Also, changes were observed over time. In the control group, there was a reduction in SOD activity on day 7 compared to day 3, a reduction in the group treated with magnetic field on day 7 in comparison to days 3 and 14, and an increase in the group treated with magnetic field + cubiu on the 14th day compared to the 7th day.

CAT activity increased in the group treated with cubiu and the group treated with magnetic field + cubiu on the 14th day compared to the 7th day. Enzyme GST activity demonstrated an increase on the 14th day compared to the 3rd and 7th days in all treated groups (cubiu, magnetic field, and magnetic field + cubiu), as well as in the control group.

4. Discussion

Cubiu is widely used for food and traditional medicine [1, 2]. Therefore, it is important to check the safety of cubiu

Table 2: Biomarkers of oxidative status in the liver and kidney after 28-day treatment with cubiu extract.

	Liver					Kidney				
	Control	25	50	100	150	Control	25	50	100	150
TBARS	0.91 ± 0.24	0.83 ± 0.21	0.81 ± 0.13	0.80 ± 0.12	1.20 ± 0.13	0.72 ± 0.04	1.71 ± 0.51	1.40 ± 0.37	1.30 ± 0.37	0.74 ± 0.08
NPSH	4.06 ± 0.14	3.99 ± 0.71	3.32 ± 0.44	2.87 ± 0.16	4.10 ± 0.59	1.81 ± 0.20	2.07 ± 0.21	2.06 ± 0.26	1.83 ± 0.26	1.61 ± 0.19
SOD	4.58 ± 0.41	$9.29 \pm 0.31^{*C}$	$8.03 \pm 0.63^{*}$	6.64 ± 0.39^{AD}	$9.78 \pm 1.06^{*C}$	5.34 ± 0.21	$7.69 \pm 0.53^{*}$	$7.17 \pm 0.14^{*}$	$8.02 \pm 0.77^{*}$	6.47 ± 0.41
CAT	3.14 ± 0.33	$5.56 \pm 0.81^{*CD}$	3.61 ± 0.51	3.47 ± 0.45^{A}	2.96 ± 0.22^{A}	1.14 ± 0.07	1.27 ± 0.20	$1.78 \pm 0.16^{*}$	1.67 ± 0.21	1.31 ± 0.10
GST	6.94 ± 1.12	11.50 ± 1.23	9.06 ± 1.30	6.67 ± 1.00	8.65 ± 2.93	1.16 ± 0.09	1.25 ± 0.22	1.08 ± 0.12	1.34 ± 0.24	1.17 ± 0.04

Values are represented as the mean ± standard error. *Significant differences from the control group ($p < 0.05$). Different capital letters indicate significant differences between treatments ($p < 0.05$). The capital letter "A" corresponds to the group 25 mg/kg, "B" corresponds to the group 50 mg/kg, "C" corresponds to the group 100 mg/kg, and letter "D" corresponds to the group 150 mg/kg. TBARS, thiobarbituric acid reactive substances (μmol/mg protein); SPSH, nonprotein thiols (nmol/mg protein); SOD, superoxide dismutase (SOD units/mg protein); CAT, catalase (ρmol/mg protein); GST, glutathione S-transferase (ρmol/min/mg protein).

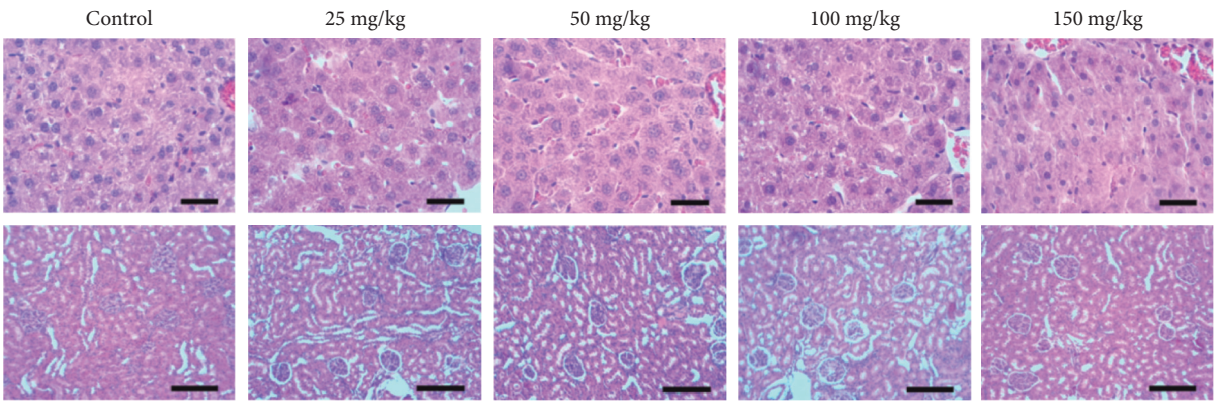

Figure 2: Photomicrography of the liver (L) and photomicrography of the kidney (K) of the Wistar rats in the control group, groups treated with 25 mg/kg of cubiu extract, 50 mg/kg of cubiu extract, 100 mg/kg of cubiu extract, and 150 mg/kg of cubiu extract. Bar = 20 micrometers in the liver's photomicrography and 100 micrometers in the kidney's photomicrography.

Table 3: Inflammatory biomarkers in the skin.

Time	Treatments	IL-1	IL-6	TNF-α	IL-10
3 day	Control	$90.67 \pm 0.84^{++\ +++}$	$99.17 \pm 1.14^{++\ +++}$	$105.33 \pm 1.69^{++\ +++}$	$20.25 \pm 1.22^{++\ +++}$
	Cubiu	$84.00 \pm 0.36^{*\,bcC}$	$89.67 \pm 0.67^{*\,bcC}$	101.67 ± 1.26^{bcC}	26.70 ± 1.65^{cC}
	Magnetic field	$82.83 \pm 0.60^{*\,bcC}$	$89.00 \pm 1.39^{*\,bcC}$	$95.67 \pm 1.28^{*\,bcC}$	$30.28 \pm 2.05^{*\,c}$
	Magnetic field + cubiu	$71.33 \pm 0.88^{*\,ABc}$	$75.83 \pm 1.40^{*\,ABc}$	$82.83 \pm 1.58^{*\,ABc}$	$36.01 \pm 1.64^{*\,Ac}$
7 day	Control	$76.40 \pm 1.50^{+\ +++}$	$81.33 \pm 0.84^{+\ +++}$	$88.17 \pm 0.48^{+\ +++}$	$33.15 \pm 0.90^{+\ +++}$
	Cubiu	74.33 ± 1.11^{acC}	79.33 ± 1.65^{ac}	85.00 ± 1.15^{ac}	31.89 ± 0.82^{cC}
	Magnetic field	$70.50 \pm 0.84^{*\,ac}$	$73.50 \pm 1.34^{*\,ac}$	$79.67 \pm 0.84^{*\,ac}$	31.35 ± 1.05^{cC}
	Magnetic field + cubiu	$68.20 \pm 1.77^{*\,Ac}$	$73.17 \pm 1.60^{*\,c}$	$80.67 \pm 1.58^{*\,c}$	$40.49 \pm 1.77^{*\,ABc}$
14 day	Control	$58.80 \pm 1.24^{+\ ++}$	$70.50 \pm 0.72^{+\ ++}$	$77.00 \pm 1.24^{+\ ++}$	$47.12 \pm 1.37^{+\ ++}$
	Cubiu	55.20 ± 1.24^{abC}	64.75 ± 2.50^{abBC}	72.17 ± 1.74^{abC}	$55.54 \pm 1.26^{*\,ab}$
	Magnetic field	$53.00 \pm 0.51^{*\,abC}$	$57.20 \pm 1.46^{*\,aAb}$	$67.17 \pm 1.64^{*\,ab}$	$60.20 \pm 0.73^{*\,ab}$
	Magnetic field + cubiu	$46.50 \pm 1.19^{*\,aAbB}$	$53.17 \pm 1.01^{*\,aAb}$	$62.83 \pm 1.64^{*\,aAb}$	$60.92 \pm 0.95^{*\,ab}$

Values are represented as the mean ± standard error. *Significant differences from the control group at the same time ($p < 0.05$). Different capital letters indicate significant differences between treatments at the same time ($p < 0.05$). Different lowercase letters indicate significant differences between times at the same treatment ($p < 0.05$). The capital letters "A" corresponds to the group cubiu, "B" corresponds to the group MF, and "C" corresponds to the group MF + cubiu. The lowercase letters "a" corresponds to the time 3rd day of the respective group, "b" corresponds to the time 7th day of the respective group, and "c" corresponds to the time 14th day of the respective group. To demonstrate the significant difference between the control groups of different times are used: +control 3rd day, ++control 7th day, and +++control 14th day.

Table 4: Inflammatory biomarkers in plasma.

Time	Treatments	IL-1	IL-6	TNF-α	IL-10
3 day	Control	$150.33 \pm 1.43^{++\ +++}$	$165.50 \pm 2.08^{++\ +++}$	$175.67 \pm 2.88^{++\ +++}$	$18.83 \pm 1.14^{++\ +++}$
	Cubiu	$139.33 \pm 0.71^{*\,bcC}$	$149.33 \pm 1.23^{*\,bcC}$	170.00 ± 2.07^{bcC}	24.83 ± 1.54^{cC}
	Magnetic field	$137.17 \pm 1.01^{*\,bcC}$	$148.00 \pm 1.98^{*\,bcC}$	$159.50 \pm 2.39^{*\,bcC}$	$28.17 \pm 1.90^{*\,c}$
	Magnetic field + cubiu	$117.67 \pm 1.89^{*\,ABc}$	$128.60 \pm 1.69^{*\,ABc}$	$139.17 \pm 2.50^{*\,ABc}$	$33.50 \pm 1.52^{*\,Ac}$
7 day	Control	$127.50 \pm 2.17^{+\ +++}$	$135.83 \pm 1.40^{+\ +++}$	$147.50 \pm 0.76^{+\ +++}$	$30.83 \pm 0.83^{+\ +++}$
	Cubiu	123.00 ± 1.57^{acC}	132.00 ± 2.76^{acC}	141.67 ± 1.54^{ac}	29.67 ± 0.76^{cC}
	Magnetic field	$115.33 \pm 1.80^{*\,ac}$	$124.60 \pm 1.72^{*\,ac}$	$133.50 \pm 1.73^{*\,ac}$	29.17 ± 0.98^{cC}
	Magnetic field + cubiu	$112.50 \pm 2.95^{*\,Ac}$	$121.67 \pm 2.69^{*\,Ac}$	$134.67 \pm 2.64^{*\,c}$	$37.67 \pm 1.65^{*\,ABc}$
14 day	Control	$99.50 \pm 2.26^{+\ ++}$	$117.83 \pm 1.11^{+\ ++}$	$128.17 \pm 1.94^{+\ ++}$	$43.83 \pm 1.28^{+\ ++}$
	Cubiu	91.50 ± 1.84^{abC}	$106.00 \pm 3.99^{*\,abC}$	120.50 ± 2.88^{abC}	$51.67 \pm 1.17^{*\,ab}$
	Magnetic field	$87.83 \pm 1.01^{*\,ab}$	$95.40 \pm 2.52^{*\,ab}$	$112.00 \pm 2.65^{*\,ab}$	$56.00 \pm 0.68^{*\,ab}$
	Magnetic field + cubiu	$80.17 \pm 2.85^{*\,aAb}$	$88.67 \pm 1.73^{*\,aAb}$	$105.00 \pm 2.65^{*\,aAb}$	$56.67 \pm 0.88^{*\,ab}$

Values are represented as the mean ± standard error. *Significant differences from the control group at the same time ($p < 0.05$). Different capital letters indicate significant differences between treatments at the same time ($p < 0.05$). Different lowercase letters indicate significant differences between times at the same treatment ($p < 0.05$). The capital letters "A" corresponds to the group cubiu, "B" corresponds to the group MF, and "C" corresponds to the group MF + cubiu. The lowercase letters "a" corresponds to the time 3rd day of the respective group, "b" corresponds to the time 7th day of the respective group, and "c" corresponds to the time 14th day of the respective group. To demonstrate a significant difference between the control groups of different times are used: +control 3rd day, ++control 7th day, and +++control 14th day.

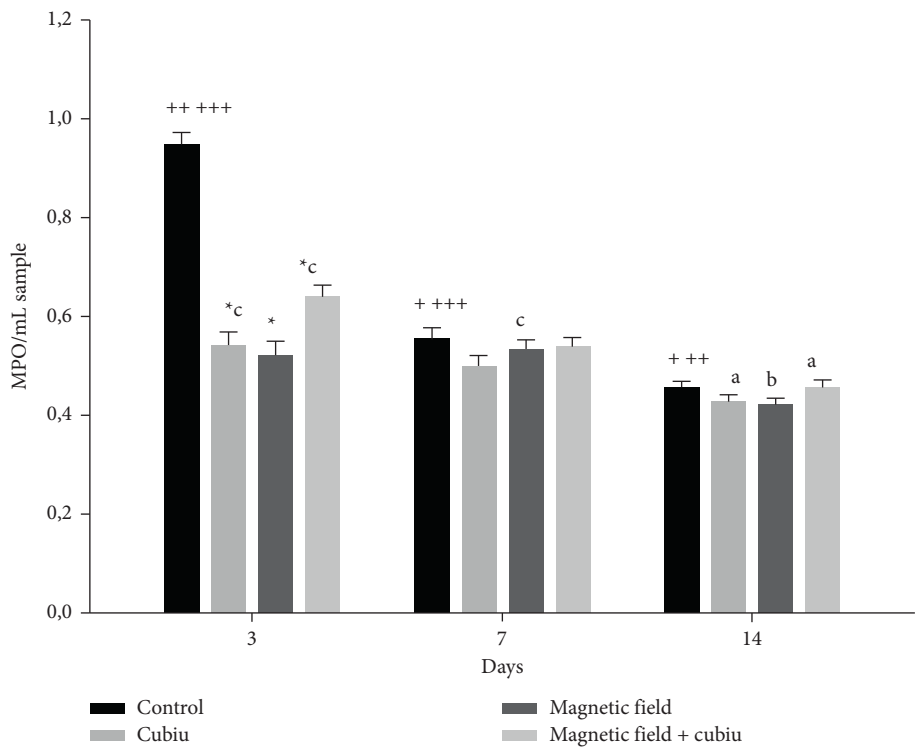

Figure 3: Graphical representation of myeloperoxidase activity. The results were expressed as optical density (OD)/mg of protein. *Significant differences from the control group at the same time. Lowercase letters indicate significant differences between times at the same treatment. The letters "a" corresponds to the group cubiu, "b" corresponds to the group MF, and "c" corresponds to the group MF + cubiu. To demonstrate a significant difference between the control groups of different times are used $^{+}$ for the control 3rd day, $^{++}$ for the control 7th day, and $^{+++}$ for the control 14th day.

Table 5: Biomarkers of oxidative stress in the skin.

Time	Treatments	TBARS	NPSH	SOD	CAT	GST
3 day	Control	2.80 ± 0.16	$16.7 \pm 1.55^{++}$	$4.93 \pm 0.25^{++}$	4.48 ± 0.46	$2.19 \pm 0.23^{+++}$
	Cubiu	$1.78 \pm 0.07^{*}$	16.1 ± 1.09^{b}	4.19 ± 0.29	4.56 ± 0.62	1.82 ± 0.44^{c}
	Magnetic field	$1.73 \pm 0.16^{*}$	14.7 ± 0.94^{c}	4.42 ± 0.37^{b}	4.43 ± 0.53	0.85 ± 0.06^{c}
	Magnetic field + cubiu	$1.81 \pm 0.12^{*}$	15.8 ± 1.23^{bc}	3.93 ± 0.40	3.34 ± 0.37	1.17 ± 0.38^{c}
7 day	Control	2.17 ± 0.11	$10.9 \pm 0.44^{++++}$	$2.91 \pm 0.10^{+}$	2.84 ± 0.21	$1.79 \pm 0.15^{+++}$
	Cubiu	2.02 ± 0.12	10.7 ± 0.79^{ac}	3.40 ± 0.25	2.90 ± 0.24^{c}	2.35 ± 0.52^{c}
	Magnetic field	1.52 ± 0.12	10.4 ± 0.32^{c}	2.86 ± 0.23^{ac}	3.13 ± 0.40	1.57 ± 0.25^{c}
	Magnetic field + cubiu	1.93 ± 0.15	10.7 ± 0.70^{ac}	2.76 ± 0.24^{c}	3.16 ± 0.30^{c}	1.55 ± 0.07^{c}
14 day	Control	2.81 ± 0.07	$17.2 \pm 1.10^{++}$	3.77 ± 0.24	3.95 ± 0.32	$5.25 \pm 0.44^{+\ ++}$
	Cubiu	2.36 ± 0.08	18.1 ± 1.28^{b}	3.92 ± 0.14	4.77 ± 0.31^{b}	4.70 ± 0.35^{ab}
	Magnetic field	$1.52 \pm 0.12^{*}$	21.3 ± 1.70^{ab}	4.88 ± 0.39^{b}	3.93 ± 0.42	4.14 ± 0.19^{ab}
	Magnetic field + cubiu	2.39 ± 0.17	$23.0 \pm 1.24^{*\,ab}$	$5.43 \pm 0.42^{*\,b}$	5.00 ± 0.43^{b}	5.31 ± 0.26^{ab}

Values are represented as the mean ± standard error. *Significant differences from the control group at the same time ($p < 0.05$). Different capital letters indicate significant differences between treatments at the same time ($p < 0.05$). Different lowercase letters indicate significant differences between times at the same treatment ($p < 0.05$). The capital letters "A" corresponds to the group cubiu, "B" corresponds to the group MR, and "C" corresponds to the group MR + cubiu. The lowercase letters "a" corresponds to the time 3rd day of the respective group, "b" corresponds to the time 7th day of the respective group, and "c" corresponds to the time 14th day of the respective group. To demonstrate a significant difference between the control groups of different times are used: $^{+}$control 3rd day, $^{++}$control 7th day, and $^{+++}$control 14th day. TBARS, thiobarbituric acid reactive substances (μmol/mg protein); SPSH, nonprotein thiols (nmol/mg protein); SOD, superoxide dismutase (SOD units/mg protein); CAT, catalase (ρmol/mg protein); GST, glutathione S-transferase (ρmol/min/mg protein).

toxicity. Experimental results regarding the toxicity of daily oral administration of cubiu extract evaluated through a dose-response curve for 28 days demonstrated the safety of cubiu extract. Biochemical parameters indicated that the extract did not present toxicity at any dose evaluated in this study. Furthermore, macroscopic and microscopic (histology) assessments of the liver and kidney, considered indispensable for toxicological analysis, evidenced that tested doses preserved the normal structure of these organs. In agreement with our results, Hernandes et al. [27] reported safe use of cubiu due to the absence of genotoxic and cytotoxic effects.

The dose of 50 mg/kg was chosen for the second protocol in this study; it did not present toxicity, and it revealed benefits to oxidative status, increasing the enzymatic activity of SOD in the liver and increasing enzymatic activity of SOD and CAT in the kidney.

After choosing cubiu extract dose, we followed a standardized wound healing model in the second protocol, also operating as an induction model for inflammatory and oxidative unbalance in the second protocol. This choice finds legitimacy in literature [19]. Magnetic fields have testified wound healing effects [28, 29], and *Solanum sessiliflorum* has its popular use as a wound healing, but there is no scientific confirmation [30].

In a wound healing model, it is important to conduct evaluations at the 3rd, 7th, and 14th day of treatment after injury induction. This strategy is very important to estimate the effect of treatments at each of the different phases of the wound healing process, divided into three distinguished but overlapping stages [31]. The first phase is the inflammatory phase, marked by the presence of inflammatory cells and mediators, occurring 0–3 days after initial injury. The next phase is known as proliferation, characterized by the presence of fibroblasts and synthesis of the extracellular matrix. This phase takes place from 3rd to 7th day. The last phase is tissue remodeling, marked by the reorganization of the extracellular matrix and maturation of collagen fibers. Didactically, remodeling happens from 7th to 14th days, but it can persist for months [31, 32].

It is well known that wound healing treatments operate mainly at the first stage of healing, the inflammatory phase, contributing to repair due to anti-inflammatory and antioxidant properties of drugs [29]. Eventhough magnetic fields are described in the literature as a treatment for skin wound healing, their contribution to systemic inflammatory and oxidant profile is still controversial. Depending on the application parameters such as time and intensity, magnetic fields can be prooxidant or antioxidant, as well as be anti-inflammatory or promote inflammation in other tissues [33–36]. Considering that, it has been suggested that the systemic use of antioxidant substances along with magnetic fields should be investigated [6, 7]. Therefore, we analyzed the action of these treatments not only on the skin but also on plasma to evaluate the response towards the systemic inflammatory profile.

Observing the results from all treatments proposed on the inflammatory profile, it was evidenced that all treatments, isolated (cubiu or magnetic field) and combined (magnetic field + cubiu), demonstrated anti-inflammatory activity, and the anti-inflammatory action is increased with the combination of cubiu and magnetic field. Treatments were able to reduce the levels of proinflammatory cytokines and increase the levels of anti-inflammatory cytokine (IL-10), both on the skin and plasma. Inflammatory cytokines are mediators present during the wound healing process. They can act by increasing the spread of the inflammatory process, as is the case of IL-1, IL-6, and TNF-α, and they can also act by reducing and controlling the inflammatory process, as is the case of IL-10 [32].

Thus, an increase in the levels of proinflammatory cytokines during healing ends up delaying this healing process, in addition to causing damage at the systemic level, as is the case of serious injuries or infections, in which there may be hemodynamic and metabolic changes, organ damage, and even compromised life. In this context, anti-inflammatory cytokines act by containing and controlling the inflammatory process [37].

The action of the magnetic field in the reduction of proinflammatory cytokines is justified by its action mechanism that acts on the modulation of adenosine and its receptors A_{2A} and A_3ARs, increasing the expression of these, which are capable of suppressing high levels of proinflammatory cytokines [38]. Also, the anti-inflammatory activity of cubiu can be based on the bioactive compounds present in its composition. The cubiu extract used in this study had its phytochemical characterization previously published in [9], evidencing the presence of phenolic compounds in its composition.

In agreement, Rodrigues et al. [39] demonstrated through HPLC-MS that cubiu extract constituted mainly of phenolic compounds, such as chlorogenic acid, specially 5-caffeoylquinic acid. Also, other species of *Solanum*, such as *Solanum lycocarpum*, has phenolic compounds, including caffeoylquinic acids in its composition, to which antioxidant and anti-inflammatory capacities exerted by Solanaceae were attributed [40]. The anti-inflammatory activity exerted by phenolic compounds has as its mechanism of action the ability to inhibit enzymes that are related to inflammation, such as prostaglandin synthetase, lipoxygenase, and cyclooxygenase [41]. In addition, chlorogenic acid interferes with the leukocyte response to chemokines, preventing their interaction with the adhesion molecules involved in cell migration, thus inhibiting cell adhesion and controlling and reducing the inflammatory process [42].

In relation to cell migration, this research also explored the effect of treatment towards the enzymatic activity of myeloperoxidase. This enzyme is known as a biomarker for neutrophil infiltrations [43]. Our results demonstrated that all treatments reduced the activity of myeloperoxidase on the 3rd day, which corresponds to the inflammatory phase of the wound healing process. It indicates that treatments promoted a reduction in neutrophilic infiltration, reinforcing anti-inflammatory properties of magnetic field and cubiu. This corroborates previous results of the present study regarding the determination of cytokines, which demonstrated reduced levels of proinflammatory cytokines and increased levels of anti-inflammatory cytokines for treated groups.

During the wound healing process, intimately related to inflammation, reactive oxygen species (ROS) and reactive nitrogen species (RNS) are released, which play a defensive role, especially against potential microbial invasion, and act on cell signaling in the healing process. However, when the excessive formation of reactive species overcomes the body's antioxidant capacity, a condition known as oxidative stress is generated. Oxidative stress can lead to damage on the cell membrane, lipids, proteins, and DNA and may culminate in cellular death [44–46]. Also, oxidative stress acts on the propagation of the inflammatory response because the

production of inflammatory enzymes such as cyclooxygenase (COX) and lipoxygenase is stimulated from lipid peroxidation and induces leukocytes to release proinflammatory cytokines [47]. Thus, it is well described how oxidative stress is closely related to the pathogenesis of nonhealing wounds. Therefore, excess in reactive species must be avoided because it slows down the healing process [48, 49].

Results demonstrate that treatments proved to maintain oxidative balance with safety, manifesting a clear antioxidant potential. That becomes evident with the reduction of TBARS (biomarker for lipoperoxidation) in the skin, promoted by all treatments on day 3. The decrease of these substances in inflammatory phase is very positive, considering the great influence of reactive species in this period [49]. Thus, all treatments showed protection against lipoperoxidation.

On day 14, treatment with magnetic field reduced TBARS and treatment with magnetic field + cubiu increased NPSH and SOD levels in the skin. Therefore, treatments positively improved the antioxidant defense system. Differences throughout time are expected as part of the natural wound healing process, both for oxidative and inflammatory profile, as the quantification of analyses oscillates towards balance. Again, the combination of magnetic field + cubiu revealed positive results. It is known that magnetic fields promote exchanges with the biomagnetic potential of the organism, thus being able to activate enzymatic reactions [50, 51]. The action of magnetic fields in oxidative balance can occur through the cellular signaling mechanism, such as the extracellular signal-regulated kinase pathways [52]. Also, the antioxidant activity of cubiu can be attributed to the presence of phenolic compounds in its composition, which are known for their antioxidant and chelant properties [53].

Thereby, the results from this study allow us to affirm that cubiu can be used safely, not demonstrating toxicity at the researched doses and during the period of administration. We evidenced that isolated (only magnetic field or cubiu) or combined treatments (magnetic field + cubiu) manifested anti-inflammatory and antioxidant properties, improving all stages of the wound healing process, especially the inflammatory phase. The association of the treatments has better results than when used alone.

5. Conclusion

This research revealed that cubiu extract demonstrated safety and absence of toxicity at the administrated doses during the time of treatment adopted in our protocol. It also enlightened that the proposed treatments provided decreased levels of proinflammatory cytokines, increased levels of anti-inflammatory cytokines, and reduced activity of myeloperoxidase. Concerning stress biomarkers, treatments reduced TBARS levels and increased enzymatic activity of SOD and NPSH levels. Therefore, cubiu promotes antioxidant and anti-inflammatory actions in skin wound healing and increases the results of conventional treatment for skin healing (magnetic field) when used in association.

Data Availability

The data generated or analyzed during this study are included within this article.

Additional Points

After the conclusions obtained in this study, we now intend to develop a nanostructured topical application of the cubiu and thus test its performance in skin wound healing.

Conflicts of Interest

The authors declare that they have no conflicts of interest.

Acknowledgments

This work was supported by CAPES—Coordenação de Aperfeiçoamento de Pessoal de Nível Superior (88882.428091/2019-01).

References

[1] F. E. Argote, D. P. Vargas, and H. S. Villada, "Investigación de mercado sobre el grado de aceptación de mermelada de cocona en sibundoy, putumayo," *Revista Guillermo de Ockham*, vol. 11, no. 2, pp. 197–206, 2013.

[2] C. Colodel, R. M. d. G. Bagatin, T. M. Tavares, and C. L. d. O. Petkowicz, "Cell wall polysaccharides from pulp and peel of cubiu: a pectin-rich fruit," *Carbohydrate Polymers*, vol. 174, pp. 226–234, 2017.

[3] D. F. d. Silva Filho, L. K. O. Yuyama, J. P. L. Aguiar, M. C. Oliveira, and L. H. P. Martins, "Caracterização e avaliação do potencial agronômico e nutricional de etnovariedades de cubiu (*Solanum sessiliflorum* dunal) da amazônia," *Acta Amazonica*, vol. 35, no. 4, pp. 399–405, 2005.

[4] D. F. da Sila Filho, J. S. de Andrade, C. R. Clement, F. M. Machado, and H. Noda, "Correlações fenotípicas, genéticas e ambientais entre descritores morfológicos e químicos em frutos de cubiu (*Solanum sessiliflorum* dunal) da amazônia1," *Acta Amazonica*, vol. 29, pp. 503–511, 1999.

[5] A. R. Schuelter, A. K. Grunvald, A. T. Amaral Jnior et al., "In vitro regeneration of cocona (*Solanum sessiliflorum*, *solanaceae*) cultivars for commercial production," *Genetics and Molecular Research*, vol. 8, no. 3, pp. 963–975, 2009.

[6] A. M. Ceyhan, V. B. Akkaya, Ş. C. Güleçol, B. M. Ceyhan, F. Özgüner, and W. Chen, "Protective effects of β-glucan against oxidative injury induced by 2.45 GHz electromagnetic radiation in the skin tissue of rats," *Archives of Dermatological Research*, vol. 304, no. 7, pp. 521–527, 2012.

[7] S. Ghodbane, A. Lahbib, M. Ammari, M. S. H. Abdelmelek, and H. Abdelmelek, "Does static magnetic field-exposure induced oxidative stress and apoptosis in rat kidney and muscle? effect of vitamin E and selenium supplementations," *General Physiology and Biophysics*, vol. 34, no. 1, pp. 23–32, 2015.

[8] J. Tauchen, L. Bortl, L. Huml et al., "Phenolic composition, antioxidant and anti-proliferative activities of edible and medicinal plants from the peruvian amazon," *Revista Brasileira de Farmacognosia*, vol. 26, no. 6, pp. 728–737, 2016.

[9] G. F. F. d. S. Montagner, F. Barbisan, P. C. Ledur et al., "In vitro biological properties of *Solanum sessiliflorum* (dunal), an

amazonian fruit," *Journal of Medicinal Food*, vol. 23, no. 9, pp. 978–987, 2020.

[10] OECD, *Test No. 407: OECD Guidelines for the Testing of Chemicals: Repeated dose 28-Day Oral Toxicity Study in Rodents*, OECD, Paris, France, 2008.

[11] R. De Lima, C. G. Guex, A. R. H. Da Silva et al., "Acute and subacute toxicity and chemical constituents of the hydroethanolic extract of *Verbena litoralis* kunth," *Journal of Ethnopharmacology*, vol. 224, pp. 76–84, 2018.

[12] O. Lowry, M. Rosebrough, A. Farr, and R. Randal, "Protein measurement with the folin phenol reagent," *Journal of Biological Chemistry*, vol. 193, no. 1, p. 265, 1951.

[13] J. A. Buege and S. D. Aust, "Microsomal lipid peroxidation," *Methods in Enzymology*, vol. 52, pp. 302–310, 1978.

[14] G. L. Ellman, "Tissue sulfhydryl groups," *Archives of Biochemistry and Biophysics*, vol. 82, no. 1, pp. 70–77, 1959.

[15] A. Boveris and B. Chance, "The mitochondrial generation of hydrogen peroxide: general properties and effect of hyperbaric oxygen," *Biochemical Journal*, vol. 134, no. 3, pp. 707–716, 1973.

[16] A. Boveris and E. Cadenas, *Superoxide Dismutase*, L. W. Oberley, Ed., Iowa City, IA, USA, 1982.

[17] W. H. Habig, M. J. Pabst, and W. B. Jakoby, "Glutathione S-transferases," *Journal of Biological Chemistry*, vol. 249, no. 22, pp. 7130–7139, 1974.

[18] S. B. Damy, R. S. Camargo, R. Chammas, and L. F. P. d. Figueiredo, "Aspectos fundamentais da experimentação animal—aplicações em cirurgia experimental," *Revista da Associação Médica Brasileira*, vol. 56, no. 1, pp. 103–111, 2010.

[19] G. Bertolino, A. de Freitas Braga, K. de Oliveira Lima do Couto Rosa, L. C. de Brito Junior, and J. E. de Araujo, "Macroscopic and histological effects of magnetic field exposition in the process of tissue reparation in wistar rats," *Archives of Dermatological Research*, vol. 298, no. 3, pp. 121–126, 2006.

[20] V. Manni, A. Lisi, D. Pozzi et al., "Effects of extremely low frequency (50 Hz) magnetic field on morphological and biochemical properties of human keratinocytes," *Bioelectromagnetics*, vol. 23, no. 4, pp. 298–305, 2002.

[21] M. Matic, B. Lazetic, M. Poljacki, V. Djuran, A. Matic, and Z. Gajinov, "Influence of different types of electromagnetic fields on skin reparatory processes in experimental animals," *Lasers in Medical Science*, vol. 24, no. 3, pp. 321–327, 2009.

[22] A. Goraca, E. Ciejka, and A. Piechota, "Effects of extremely low frequency magnetic field on the parameters of oxidative stress in heart," *Journal of Physiology and Pharmacology: An Official Journal of the Polish Physiological Society*, vol. 61, pp. 333–338, 2010.

[23] R. Jangde, S. Srivastava, M. R. Singh, and D. Singh, "In vitro and in vivo characterization of quercetin loaded multiphase hydrogel for wound healing application," *International Journal of Biological Macromolecules*, vol. 115, pp. 1211–1217, 2018.

[24] M. He, L. Sun, X. Fu, S. P. McDonough, and C.-C. Chu, "Biodegradable amino acid-based poly (ester amine) with tunable immunomodulating properties and their in vitro and in vivo wound healing studies in diabetic rats' wounds," *Acta Biomaterialia*, vol. 84, pp. 114–132, 2019.

[25] K. Suzuki, H. Ota, S. Sasagawa, T. Sakatani, and T. Fujikura, "Assay method for myeloperoxidase in human polymorphonuclear leukocytes," *Analytical Biochemistry*, vol. 132, no. 2, pp. 345–352, 1983.

[26] S. Lloret and J. J. Moreno, "Effects of an anti-inflammatory peptide (antiflammin 2) on cell influx, eicosanoid biosynthesis and oedema formation by arachidonic acid and tetradecanoyl phorbol dermal application," *Biochemical Pharmacology*, vol. 50, no. 3, pp. 347–353, 1995.

[27] L. C. Hernandes, A. F. Aissa, M. R. d. Almeida et al., "In vivo assessment of the cytotoxic, genotoxic and antigenotoxic potential of maná-cubiu (*Solanum sessiliflorum* dunal) fruit," *Food Research International*, vol. 62, pp. 121–127, 2014.

[28] J. Carruthers and A. Carruthers, "Commentary: electromagnetic radiation and wound healing," *Dermatologic Surgery*, vol. 38, no. 3, pp. 451–453, 2012.

[29] A. Patruno, A. Ferrone, E. Costantini et al., "Extremely low-frequency electromagnetic fields accelerates wound healing modulating MMP-9 and inflammatory cytokines," *Cell Proliferation*, vol. 51, no. 2, Article ID e12432, 2018.

[30] Instituto Nacional de Pesquisas da Amazonia, "Cubiu," in . 2017, http://www.inpa.gov.br/cpca/areas/cubiu.html.

[31] A. C. D. O. Gonzalez, T. F. Costa, Z. D. A. Andrade, and A. R. A. P. Medrado, "Wound healing-a literature review," *Anais Brasileiros de Dermatologia*, vol. 91, no. 5, pp. 614–620, 2016.

[32] A. Stunova and L. Vistejnova, "Dermal fibroblasts-A heterogeneous population with regulatory function in wound healing," *Cytokine & Growth Factor Reviews*, vol. 39, pp. 137–150, 2018.

[33] F. Ortiz, B. I. Fernández-Gil, A. Guerra-Librero, L. C. López, D. Acuña-Castroviejo, and G. Escames, "Preliminary evidence suggesting that nonmetallic and metallic nanoparticle devices protect against the effects of environmental electromagnetic radiation by reducing oxidative stress and inflammatory status," *European Journal of Integrative Medicine*, vol. 8, no. 5, pp. 835–840, 2016.

[34] M. Emre, S. Cetiner, S. Zencir, I. Unlukurt, I. Kahraman, and Z. Topcu, "Oxidative stress and apoptosis in relation to exposure to magnetic field," *Cell Biochemistry and Biophysics*, vol. 59, no. 2, pp. 71–77, 2011.

[35] M. Glinka, S. Gawron, A. Sieroń, K. Pawłowska-Góral, G. Cieślar, and K. Sieroń, "Impact of static magnetic field on the antioxidant defence system of mice fibroblasts," *BioMed Research International*, vol. 2018, Article ID 5053608, 8 pages, 2018.

[36] A. G. Canseven, S. Coskun, and N. Seyhan, "Effects of various extremely low frequency magnetic fields on the free radical processes, natural antioxidant system and respiratory burst system activities in the heart and liver tissues," *Indian Journal of Biochemistry & Biophysics*, vol. 45, pp. 326–331, 2008.

[37] C. S. R. Oliveira, R. Sakata, A. Issy, and L. Gerola, "Citocinas e a dor," *Revista Brasileira de Anestesiologia*, vol. 61, pp. 255–265, 2011.

[38] K. Varani, F. Vincenzi, A. Ravani et al., "Adenosine receptors as a biological pathway for the anti-inflammatory and beneficial effects of low frequency low energy pulsed electromagnetic fields," *Mediators of Inflammation*, vol. 2017, Article ID 2740963, 11 pages, 2017.

[39] E. Rodrigues, L. R. B. Mariutti, and A. Z. Mercadante, "Carotenoids and phenolic compounds from *Solanum sessiliflorum*, an unexploited amazonian fruit, and their scavenging capacities against reactive oxygen and nitrogen species," *Journal of Agricultural and Food Chemistry*, vol. 61, no. 12, pp. 3022–3029, 2013.

[40] M. G. Morais, A. A. Saldanha, J. P. Costa Rodrigues et al., "Chemical composition, antioxidant, anti-inflammatory and antinociceptive activities of the ethanol extract of ripe fruits of

Solanum lycocarpum st. hil. (solanaceae)," *Journal of Ethnopharmacology*, vol. 262, Article ID 113125, 2020.

[41] E. P. Gutierrez-Grijalvahttps, J. D. L. Ambriz-Pérez, N. Leyva-López, and B. Heredia, "Phenolic compounds: natural alternative in inflammation treatment: a review," *Cogent Food & Agriculture*, vol. 2, pp. 1–14, 2016.

[42] W.-C. Chang, C.-H. Chen, M.-F. Lee, T. Chang, and Y.-M. Yu, "Chlorogenic acid attenuates adhesion molecules upregulation in IL-1β-treated endothelial cells," *European Journal of Nutrition*, vol. 49, no. 5, pp. 267–275, 2010.

[43] P. Martin and R. Nunan, "Cellular and molecular mechanisms of repair in acute and chronic wound healing," *British Journal of Dermatology*, vol. 173, no. 2, pp. 370–378, 2015.

[44] R. Sharma and N. Martins, "Telomeres, DNA damage and ageing: potential leads from ayurvedic rasayana (anti-ageing) drugs," *Journal of Clinical Medicine*, vol. 9, pp. 1–7, 2020.

[45] R. Sharma, K. Kuca, E. Nepovimova, A. Kabra, M. Rao, and P. Prajapati, "Traditional ayurvedic and herbal remedies for Alzheimer's disease: from bench to bedside," *Expert Review of Neurotherapeutics*, vol. 19, no. 5, pp. 359–374, 2019.

[46] R. Sharma, N. Martins, A. Chaudhary et al., "Adjunct use of honey in diabetes mellitus: a consensus or conundrum?" *Trends in Food Science & Technology*, vol. 106, pp. 254–274, 2020.

[47] S. Biswas, R. Das, and E. Ray Banerjee, "Role of free radicals in human inflammatory diseases," *AIMS Biophysics*, vol. 4, no. 4, pp. 596–614, 2017.

[48] M. Wlaschek and K. Scharffetter-Kochanek, "Oxidative stress in chronic venous leg ulcers," *Wound Repair and Regeneration*, vol. 13, no. 5, pp. 452–461, 2005.

[49] N.-Y. Park and Y. Lim, "Short term supplementation of dietary antioxidants selectively regulates the inflammatory responses during early cutaneous wound healing in diabetic mice," *Nutrition & Metabolism*, vol. 8, no. 1, p. 80, 2011.

[50] U. Warnke, "Grundlagen zu magnetisch induzierten physiologischen effecten," *Terapiewoche*, vol. 20, pp. 4609–4616, 1980.

[51] M. Glinka, A. Sieroń, E. Birkner, and G. Cieślar, "Influence of extremely low-frequency magnetic field on the activity of antioxidant enzymes during skin wound healing in rats," *Electromagnetic Biology and Medicine*, vol. 32, no. 4, pp. 463–470, 2013.

[52] T. Mert, "Pulsed magnetic field treatment as antineuropathic pain therapy," *Reviews in the Neurosciences*, vol. 28, no. 7, pp. 751–758, 2017.

[53] A. Yashin, Y. Yashin, X. Xia, and B. Nemzer, "Antioxidant activity of spices and their impact on human health: a review," *Antioxidants*, vol. 6, no. 3, p. 70, 2017.

Hindawi
Evidence-Based Complementary and Alternative Medicine
Volume 2022, Article ID 4284893, 12 pages
https://doi.org/10.1155/2022/4284893

Research Article

Herbal Formula Modified Bu-Shen-Huo-Xue Decoction Attenuates Intervertebral Disc Degeneration via Regulating Inflammation and Oxidative Stress

Jialiang Lin,[1,2,3] **Jionghui Gu**,[4] **Dongwei Fan**,[1,2,3] **and Weishi Li**[1,2,3]

[1]*Department of Orthopaedics, Peking University Third Hospital, Beijing 100191, China*
[2]*Beijing Key Laboratory of Spinal Disease Research, Beijing, China*
[3]*Engineering Research Center of Bone and Joint Precision Medicine, Ministry of Education, Beijing, China*
[4]*Department of Ultrasound, The First Affiliated Hospital, College of Medicine, Zhejiang University, Hangzhou 310003, China*

Correspondence should be addressed to Dongwei Fan; fdw@bjmu.edu.cn and Weishi Li; puh3liweishi@163.com

Received 18 August 2021; Revised 15 November 2021; Accepted 6 December 2021; Published 2 February 2022

Academic Editor: Rohit Sharma

Objective. This study aims to clarify the potential mechanism of modified Bu-Shen-Huo-Xue decoction (MBSHXD) in treating intervertebral disc degeneration (IDD) with methods of network pharmacology and molecular docking. *Methods*. An MBSHXD and IDD-related common target gene set was established through TCMSP, UniProt, and two disease gene databases. GO and KEGG enrichment analysis and protein-protein interaction (PPI) networks were performed through the R platform and STRING to discover the potential mechanism. Molecular docking between the active ingredients and the core genes is used to calculate the binding energy. *Results*. A total of 147 active ingredients and 79 common genes (including 10 core genes, TNF, VEGFA, IL6, MAPK3, AKT1, MAPK8, TP53, JUN, MMP9, and CXCL8) were identified. The results of GO and KEGG enrichment analysis showed that MBSHXD plays an essential role in regulating inflammation and oxidative stress. The meaningful pathways are the AGE-RAGE signaling pathway in diabetic complications, the IL-17 signaling pathway, the TNF signaling pathway, the PI3K-Akt signaling pathway, the MAPK signaling pathway, and apoptosis. In addition, the PPI network and molecular docking further demonstrated the roles that nine bioactive ingredients of MBSHXD play in IDD treatment through their interference with core target proteins. *Conclusion*. This study reveals that MBSHXD has the characteristics of a "multi-component, multi-target, and multi-pathway" in the treatment of IDD by regulating inflammation and oxidative stress, and network pharmacology may provide a feasible method to verify the molecular mechanism of MBSHXD for IDD by combining with molecular docking.

1. Introduction

As a common symptom, low back pain is the leading cause of years living with disability [1]. It is reported that up to 40% of low back pain is associated with intervertebral disc degeneration (IDD) [2]. IDD is a highly prevalent degenerative spinal disorder that manifests as pain, numbness, and even paralysis of the lower limbs. The discomfort caused by IDD brings great pain and inconvenience to life and work of patients. However, except for nonsteroidal anti-inflammatory drugs (NSAIDs) to relieve acute pain, no effective drugs against IDD are currently available.

In recent years, traditional Chinese medicine (TCM), as an essential branch of complementary and alternative medicine, has received increasing attention for its role in various diseases [3–5]. Modified Bu-Shen-Huo-Xue decoction (MBSHXD), which adds or reduces several herbs based on Bu-Shen-Huo-Xue decoction, is a traditional Chinese herbal recipe that was widely used in elderly patients for fractures therapy in ancient times. MBSHXD consists of the following 9 medicinal herbs: *Radix Rehmanniae Preparata, Cortex Eucommiae, Radix Aconiti Lateralis Preparata, Fructus Lycii, Fructus Corni, Semen Persicae, Flos Carthami, Rhizoma Dioscoreae, and Radix Glycyrrhizae.*

According to TCM, MBSHXD has the effects of nourishing the kidney, promoting blood circulation, and strengthening the bones. Recent studies have shown that MBSHXD may delay the progression of degenerative diseases of the musculoskeletal system, including osteoarthritis and IDD [6, 7]. Zhu et al. [7] reported that MBSHXD could inhibit the calcification of the cartilage endplate in gerbils during the process of aging. However, its underlying mechanisms are still unclear.

Network pharmacology, an emerging and interdisciplinary research approach, is based on traditional pharmacology, bioinformatics, chemoinformatics, and network biology [8, 9]. The development of network pharmacology promotes the transition from the era that a drug fits into the specific target to the generation of mapping the polypharmacology network onto the human disease-gene network [10–12]. Due to the complexity of its composition and function, the clinical application of TCM is distinctly hampered. Fortunately, network pharmacology could be a valuable tool for analyzing and constructing a "drug-target-disease" interaction network to reveal the molecular mechanisms of action between mutiherbs and the disease [13–15]. Recent studies have confirmed that network pharmacology can help develop TCM applications for the treatment of other diseases or the development of new drugs [16–19] and provide biochemical principles to manage current pandemic diseases, such as COVID-19 [20]. This study aims to clarify the potential mechanism of MBSHXD in the treatment of IDD. The flowchart of our research is shown in Figure 1.

2. Materials and Methods

2.1. Active Ingredients and Target Genes in MBSHXD. We got the active ingredients of each herb in MBSHXD through the Traditional Chinese Medicine Systems Pharmacology (TCMSP) database (https://tsmspw.com) [21]. The oral bioavailability (OB) ≥ 30% and drug-likeness (DL) ≥ 0.18 were set as filtration conditions. Next, the potential target proteins of the selected active ingredients were mined in the DrugBank database (http://www.drugbank.ca) [22].Then, we utilized the UniProt database (https://www.uniprot.org/) [23] to obtain the unique corresponding gene names and to establish the MBSHXD target gene set.

2.2. The Related Target of IDD. IDD-related targets were obtained through retrieving GeneCards (https://www.genecards.org) [24] and Online Mendelian Inheritance in Man (OMIM) (https://omim.org, update November 25, 2020) [25] using the keywords "intervertebral disc degeneration." GeneCards is a comprehensive, user-friendly database that provides information of all annotated and predicted human genes, and we screened for targets with a relevance score ≥10 [26]. The OMIM database provides an organized description of human genes and phenotypes and the relationships between them and is a comprehensive, authoritative, and timely resource for research [25]. Finally, the results of the two databases were summarized, integrated, and deduplicated, and then 1595 potential targets were obtained, and all targets were standardized in the UniProt database (https://www.uniprot.org/) [23].

2.3. Network Visualization and Enrichment Analysis. A common gene set between MBSHXD targets and IDD-related genes was built by the Venn diagram. According to a common gene set, we identified the active components corresponding to each gene and constructed an "active ingredient-common target gene network" using Cytoscape 3.7.2 software [27]. In addition, we have established a "disease-core genes–active ingredients–herbs" network.

The biological functions of genes were revealed in three different aspects, including biological processes (BPs), cell components (CCs), and molecular functions (MFs), by gene ontology (GO) enrichment analysis. The Kyoto Encyclopedia of Genes and Genomes (KEGG) is a database resource for understanding high-level functions and utilities of the biological system, such as cells, organisms, and ecosystems, from molecular-level information. We used the clusterProfiler package of the R platform for GO and KEGG functional enrichment analysis [28].

2.4. Protein-Protein Interaction (PPI) Network Construction and Core Gene Selection. The common genes of MBSHXD targets and IDD-related genes were used to build a PPI network through the STRING database (https://www.string-db.org/) [29]. In this database, we set the organism as "*Homo sapiens*" and a confidence score >0.4. In the same way, the PPI network of IDD targets was also established. The PPI network of the common target was imported into the Cytoscape software to make it visible. A cytoHubba plugin [30] was used to identify the top 10 core genes by a method of maximal clique centrality (MCC). In addition, the cluster analysis was performed for the IDD targets PPI network by using the MCODE plugin in Cytoscape software [31]. The parameter conditions are as follows: a node score cutoff = 0.2, k core = 2, maximum depth = 100, and a degree cutoff = 2 [32].

2.5. Molecular Docking. The 3D structures of the proteins encoded by the core genes and the 2D structures of active ingredients were downloaded from the RSCB PDB database (https://www.rcsb.org/) and PubChem database (https://pubchem.ncbi.nlm.nih.gov/), respectively. The energy of the molecular ligand was optimized using the MM2 calculation method and derived using the ChemBio 3D software. The receptor protein was dehydrated and small-molecule ligand was removed with PyMOL 2.4.0 software. The AutoDock tool performed hydrogenation of proteins and active ingredients. Finally, AutoDock Vina was used to calculate the binding energy between the receptor protein and active components [33].

3. Result

3.1. Screening of Candidate Targets and Active Ingredients. The MBSHXD contained the following 9 main herbs: *Radix Rehmanniae Preparate* (Shudihuang), *Cortex Eucommiae*

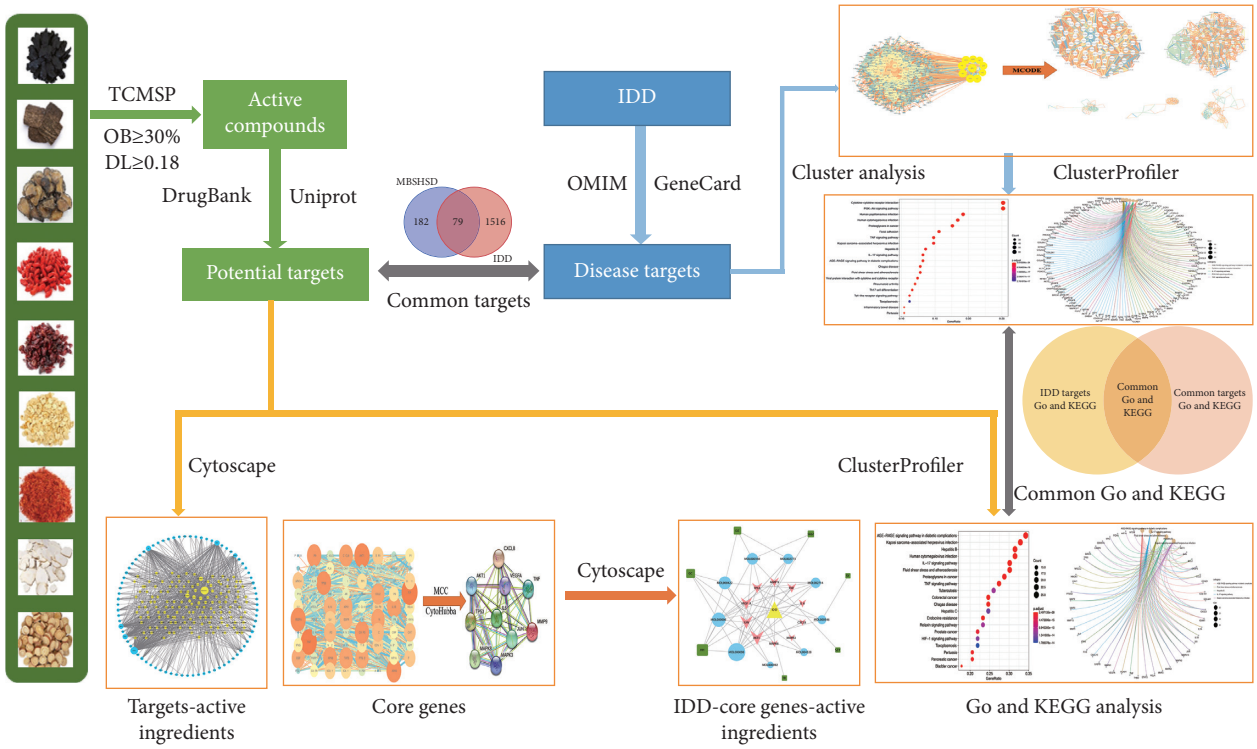

Figure 1: Flowchart to explore the possible mechanism of modified Bushen Huoxue decoction against intervertebral disc degeneration (IDD).

(Duzhong), *Radix Aconiti Lateralis Preparate* (Fuzi), *Fructus Lycii* (Gouqizi), *Fructus Corni* (Shanzhuyu), *Semen Persicae* (Taoren), *Flos Carthami* (Honghua), *Rhizoma Dioscoreae* (Shangyao), and *Radix Glycyrrhiza* (Ganzao). A total of 244 active ingredients of MBSHXD were obtained through searching TCMSP (Supplementary Table 1). Based on the active ingredients, we acquired 299 targets, which were protein names coded by genes (Supplementary Table 2). Then, after converting the gene symbols by the UniProt database, 261 drug targets were gained (Supplementary Table 3). In addition, a total of 1595 IDD-related genes were obtained from the two abovementioned disease gene databases. By intersecting the targets of MBSHXD and IDD, 79 common target genes were acquired, corresponding to which there were 147 active components (Supplementary Table 4, Figure 2(a)).

3.2. Common Targets-Active Ingredients Network. A network of common targets-active ingredients with 226 nodes and 904 edges was visualized using Cytoscape software (Figure 2(b)).

3.3. PPI Network Construction of IDD Target. A protein-protein interaction network was established using the STRING database, which showed complex relationships between the proteins encoded by IDD genes (Figure 3). We selected 10 genes (AKT1, IL6, TP53, VEGFA, TNF, FN1, EGFR, EGF, MAPK3, and MYC) whose largest degree was demonstrated on the right. The PPI network was imported into the Cytoscape software for further cluster analysis and visualization with the MCODE plugin. Finally, the top five clusters were selected from 32 clusters based on their MCODE score (Figure 3 and Table 1). In addition, we performed GO functional enrichment and KEGG pathway analysis on the IDD target genes contained in these 5 clusters. Among the 291 genes, we acquired 3088 BPs, 93 CCs, 135 MFs, and 151 KEGG pathways with P value less than or equal to 0.05 (Supplementary Table 5). Then, Figure 4 shows the top 10 for GO functional enrichment and the top 20 for KEGG pathway analysis.

The biological processes of IDD may be mainly related to the inflammatory response and the exogenous pathways of apoptosis, such as leukocyte migration, extracellular matrix (ECM) organization, extracellular structure organization, and extrinsic apoptotic signaling pathways. The molecular functions of IDD would be related to cytokine activity, cytokine receptor binding, and signaling receptor activator activity. The cellular components associated with IDD might activate the collagen-containing ECM, endoplasmic reticulum lumen, and external side of the plasma membrane (Figure 4). Meanwhile, the results of KEGG indicated that the main pathways were related to cytokine-cytokine receptor interaction, the PI3K-Akt signaling pathway, and the TNF signaling pathway (Figure 4).

3.4. Enrichment Analysis of Common Genes. To further explore the interactions between common target genes and the mechanisms by which MBSHXD may treat IDD, GO enrichment analysis and KEGG pathway enrichment were performed using the R platform. We acquired a total of 2114

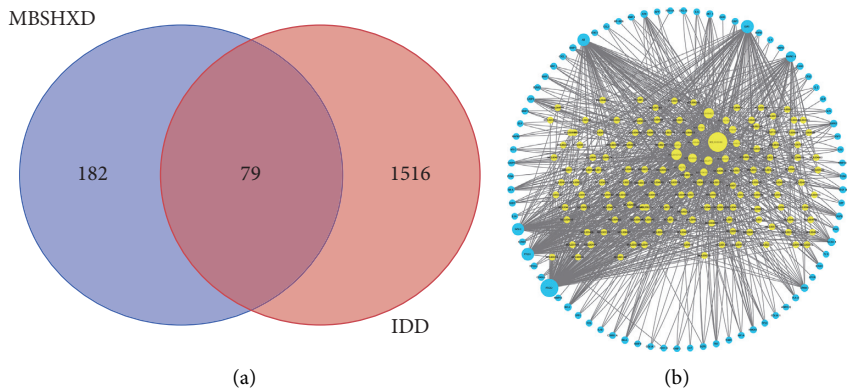

Figure 2: Construction of common gene-active ingredients network. (a) Venn diagram. (b) Common targets-active ingredients network. Yellow nodes represent the common targets of IDD and modified Bushen Huoxue decoction; blue nodes represent the active ingredients related to the common targets. The line between two nodes represents the interaction; the size of each node represents the number of connections.

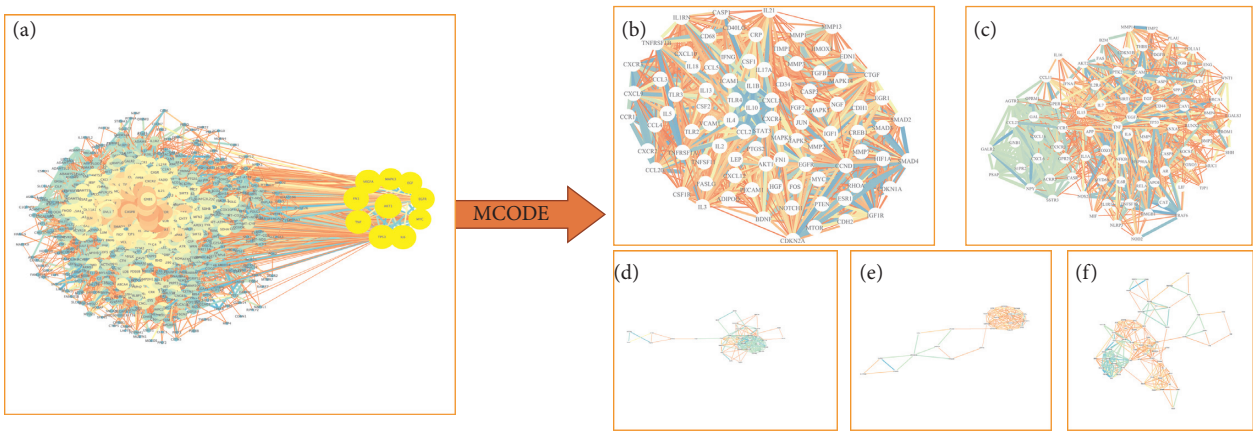

Figure 3: Protein-protein interaction (PPI) network and cluster analysis of the IDD targets. (a) PPI network of IDD targets. The 10 genes with the largest degree values are shown on the right with yellow nodes. (b–f) The top 5 cluster graphs of the IDD targets from its PPI network.

Table 1: The top 5 cluster information of the IDD targets from its network.

Cluster	Score	Nodes	Edges
1	61.506	90	2737
2	23.952	84	994
3	9.091	34	150
4	8.762	22	92
5	8.4	61	252

entries about biological processes. The top 10 are shown in Figure 5, among which 4 items were related to oxidative stress. By analyzing the results of the cellular component, we found that the target genes mainly acted in the membrane raft, membrane microdomain, and membrane region. The main molecular functions of common targets were cytokine activity, cytokine receptor binding, signaling receptor activator activity, and receptor-ligand activity. Simultaneously, the top 20 pathways were selected to investigate the possible mechanism of MBSHXD on the disease (Figure 5). The most meaningful pathways of common targets are the AGE-RAGE signaling pathway in diabetic complications, the TNF signaling pathway, and apoptosis. All the results of the enrichment analysis are listed in Supplementary Table 6.

3.5. PPI Network of Common Target and Core Genes. Firstly, we inputted 79 common genes into the STRING to construct the PPI network (Figure 6). To further obtain the core genes of the MBSHXD treatment for IDD, the obtained PPI network was imported into the software through the cytoHubba plugin with the MCC method. Finally, the top 10 genes were identified as core genes (TNF, VEGFA, IL6, MAPK3, AKT1, MAPK8, TP53, JUN, MMP9, and CXCL8). Fortunately, there are six genes (TNF, VEGFA, IL6, MAPK3, AKT1, and TP53) that overlap with the critical genes for IDD. In addition, we found that the PPI network for 10 core genes all had a node degree of 9 (Figure 6).

3.6. Selection of Critical Enrichment Analysis. After comparing and analyzing the KEGG enrichment of the disease targets and common targets of MBSHXD and IDD, we found 138 overlapping KEGG pathways (Supplementary

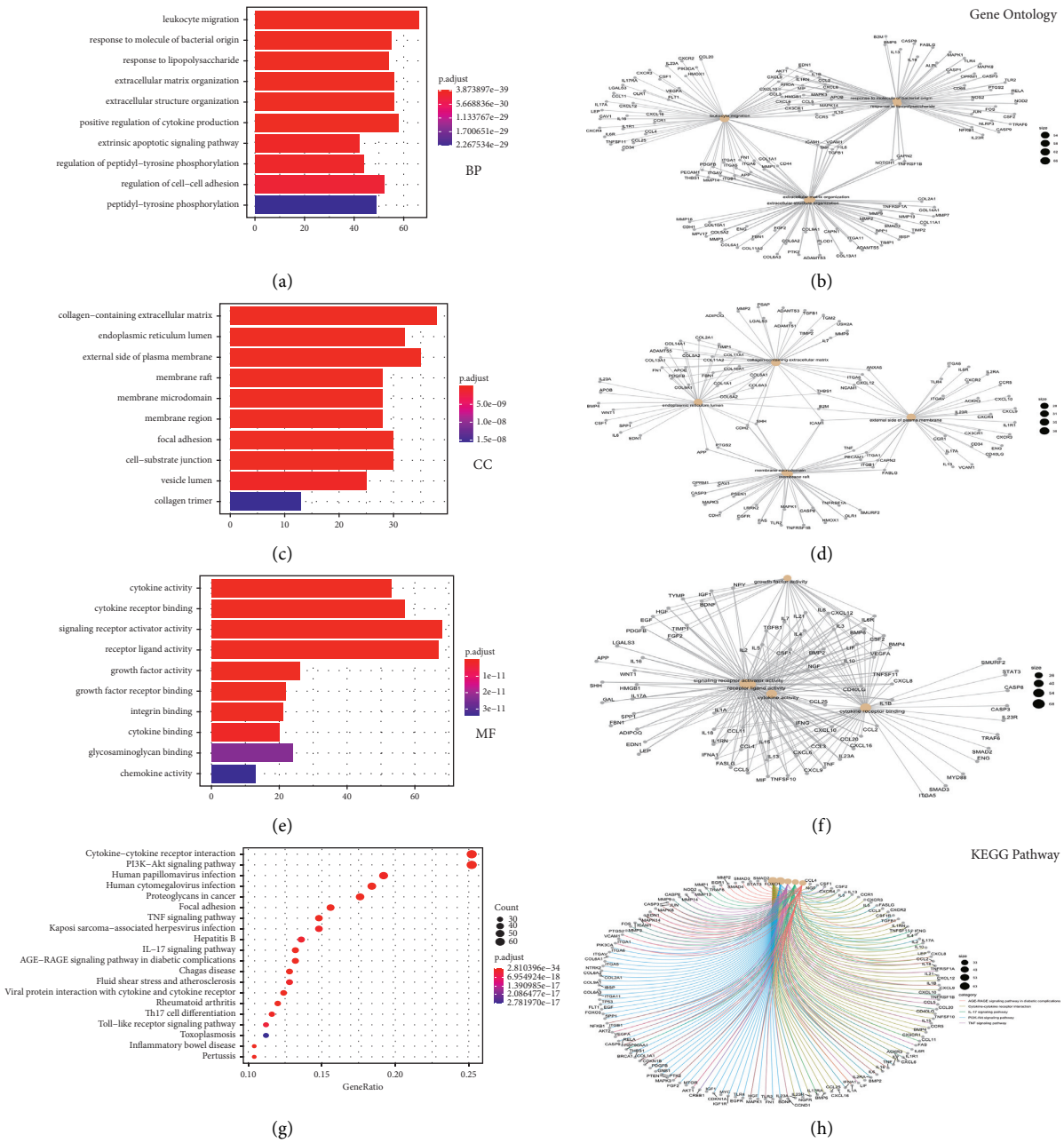

Figure 4: GO (including BP, MF, and CC) and KEGG analysis of IDD-related genes. (a, c, d) The top 10 significantly GO (BP, MF, and CC) enriched terms are arranged according to the adjusted P value. (b, e, f) Subnetwork showing the top five terms and related genes. (g) The 20 pathways with the lowest adjusted P values. The darker the color, the smaller the adjusted P value. The larger the circle, the greater the number of target genes in the term. (h) Subnetwork showing the top five KEGG pathways and related genes.

Table 7). To further screen these pathways, we sorted them according to the proportion of genes and compared the potentially related IDD pathways in PubMed with the abovementioned ways. Finally, 9 relatively related IDD pathways were obtained. Table 2 shows the basic information of the 9 pathways that may be relevant for IDD.

3.7. Disease-Core Genes-Active Ingredients-Herbs Network. According to the 10 core genes, we found the corresponding seven herbs and nine active components. The disease-core genes-active ingredients-herbs network is demonstrated in Figure 7. The 9 active components are sorted by degree as follows: quercetin (MOL000098), luteolin (MOL000006), kaempferol (MOL000422), beta-sitosterol (MOL000358), baicalein (MOL002714), beta-carotene (MOL002773), diosgenin (MOL000546), naringenin (MOL004328), and formononetin (MOL000392). The basic information of the nine active components in MBSHXD is listed in Table 3. Quercetin (MOL000098) was the essential active compound with the largest degree, which may play a key role in IDD treatment by MBSHXD.

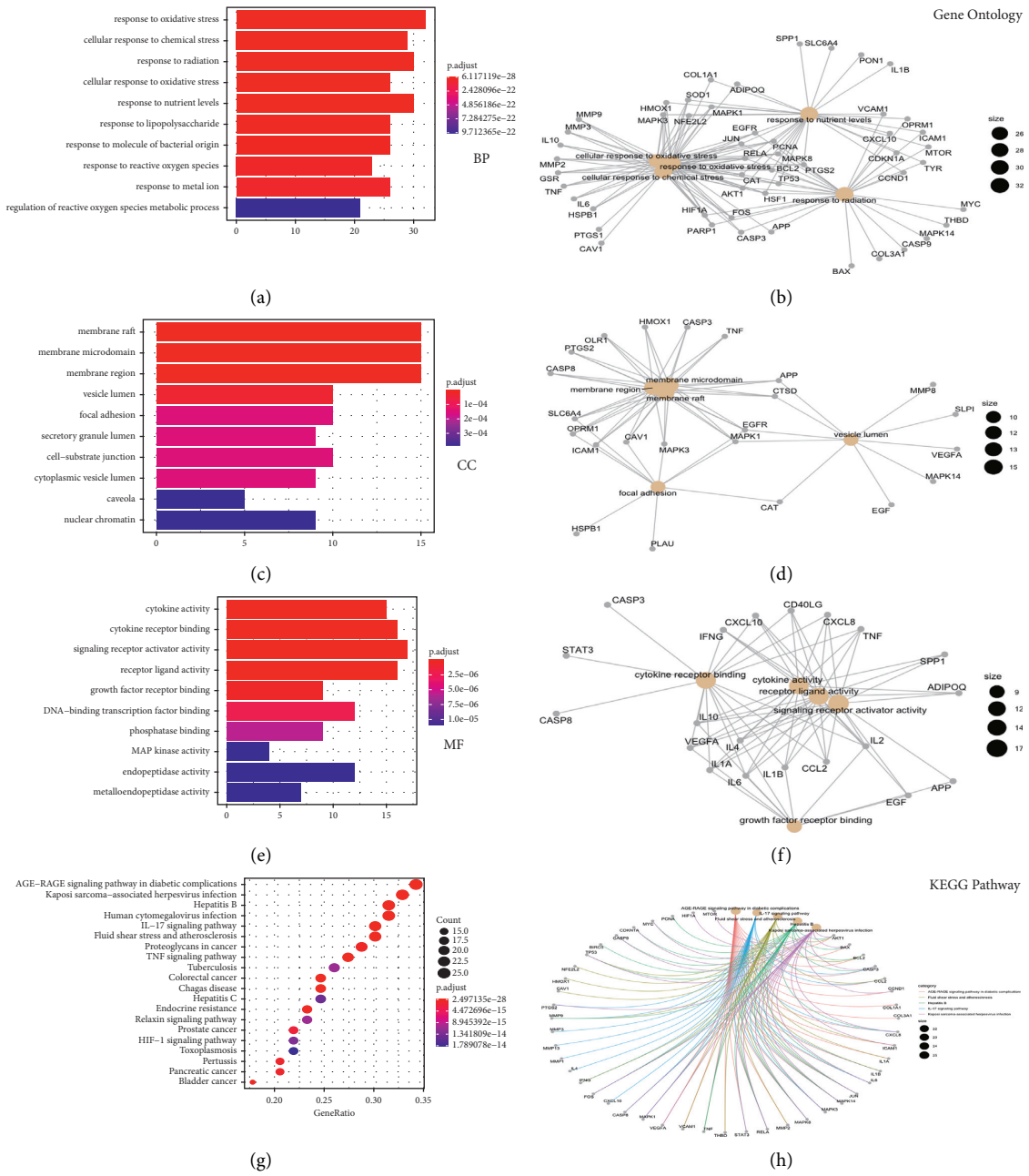

Figure 5: GO (including BP, MF, and CC) and KEGG analysis of common genes. (a, c, d) The top 10 significantly GO (BP, MF, and CC) enriched terms are arranged according to the adjusted P value. (b, e, f) Subnetwork showing the top five terms and related genes. (g) The 20 pathways with the lowest adjusted P values. The darker the color, the smaller the adjusted P value. The larger the circle, the greater the number of target genes in the term. (h) Subnetwork showing the top five KEGG pathways and related genes.

3.8. Molecular Docking Verified Active Ingredients and Core Genes Encoding Proteins. Ten key genes were used as receptor proteins, and nine active compounds were used as ligands for molecular docking verification. The details of 10 receptor proteins are listed in Table 4, and Figure 8 shows these results [34]. Binding energy, which is the criterion to judge stability, less than −5.0 kcal/mol was considered relatively stable between proteins and small-molecule compounds. As we expected, the binding energies between the active ingredients and the core genes were all less than −5.0 kcal/mol, indicating that all active compounds can easily enter the active pocket of proteins coded by core genes and bind stably. We selected 4 proteins and small molecules with the highest binding energy for demonstration (Figure 9).

4. Discussion

IDD is a widespread degenerative disease of the spine. With the increasing aging of society, the incidence of IDD has been on the rise in recent years and tends to be younger. The incidence rate of cervical, thoracic, and lumbar diseases

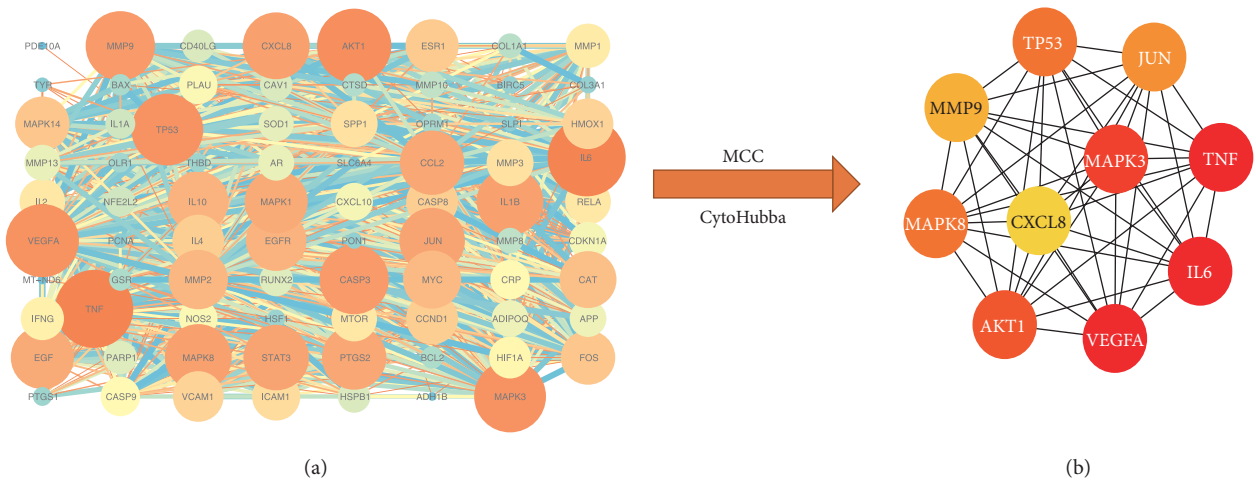

Figure 6: Confirmation of core genes. (a) Visualization of seventy-nine common targets protein-protein interaction (PPI) network with 79 nodes and 1487 edges. (b) PPI network of the core genes.

Table 2: The enriched 9 possible related pathways for IDD.

ID	Description	KEGG index enriched by IDD targets		KEGG index enriched by common targets		
		p. adjust	Count	p. adjust	Count	Count of active ingredients
Hsa04933	AGE-RAGE signaling pathway in diabetic complications	$4.08E-24$	33	$2.4971E-28$	25	125
Hsa04657	IL-17 signaling pathway	$5.06E-25$	33	$3.4116E-24$	22	243
Hsa04668	TNF signaling pathway	$5.71E-27$	37	$9.6621E-20$	20	245
Hsa04151	PI3K-Akt signaling pathway	$1.19E-29$	63	$7.355E-10$	19	47
Hsa04210	Apoptosis	$1.32E-11$	24	$2.0176E-14$	17	66
Hsa04010	MAPK signaling pathway	$6.74E-15$	40	$3.2112E-10$	16	54
Hsa05206	MicroRNAs in cancer	$1.83E-08$	31	$3.389E-08$	16	188
Hsa05010	Alzheimer's disease	$2.69E-06$	30	$3.3702E-07$	16	257
Hsa05215	Prostate cancer	$6.98E-17$	26	$2.1985E-15$	16	127

caused by IDD is up to 80%, which has become a major global health problem [35]. At present, the interventions for IDD mainly include the use of pain relievers or surgical treatment [36, 37]. However, there is still a lack of effective nonsurgical treatments for IDD, making the exploration of novel and effective nonsurgical treatments for IDD a focus of research in degenerative spinal disorders. Notably, TCM has been used for more than 2,000 years to treat various diseases, including IDD [38]. TCM mainly focuses on expelling wind and cold, tonifying the liver and kidney in the treatment of IDD, supplemented by tonifying the spleen and replenishing qi, promoting blood circulation, and dredging collaterals [39–41]. MBSHXD, which comes from the ancient Chinese literature "Shangke Dacheng," consists of 9 Chinese herbs, which are as follows: Shudihuang, Duzhong, Fuzi, Gouqi, Shanzhuyu, Taoren, Honghua, Shanyao, and Gancao [42]. It was demonstrated that MBSHXD could promote the proliferation of nucleus pulposus (NP) cells and remodel the ECM during IDD [43]. However, due to the complex composition and comprehensive action of MBSHXD, the specific mechanism of its treatment for IDD is still unclear, so we decided to use an approach of network pharmacology to reveal it and lay a foundation for further studies.

We used Cytoscape software to reconstruct the PPI network of common genes obtained from the STRING database and got 10 core genes (TNF, VEGFA, IL6, MAPK3, AKT1, MAPK8, TP53, JUN, MMP9, and CXCL8) of MBSHXD against IDD by the MCC algorithm. These core target proteins are involved in multiple signaling pathways such as inflammation, immunity, metabolism, and proliferation-related signaling pathways. Studies have confirmed that the process of IDD can be delayed by inhibiting the TNF-α-induced inflammatory response and reducing the expression of inflammatory cytokines, including IL-6 [44, 45]. It is worth noting that TP53 was found to be potentially involved in the progression of IDD by analyzing the microarray datasets of GSE19943, GSE15227, and GSE34095 [46]. Akt1 is a serine/threonine protein kinase that is involved in inflammation and cell metabolism through a wide variety of signaling pathways such as PI3K-Akt and MAPK signaling. Wang et al. found that the degeneration of NP cells was ameliorated by regulating the ITGA2/PI3K/Akt signaling pathway [47]. Moreover, Zhan et al. found that the degree of intervertebral disc degeneration was related to the loss of vascular buds and the downregulation of VEGFA and its receptors [48].

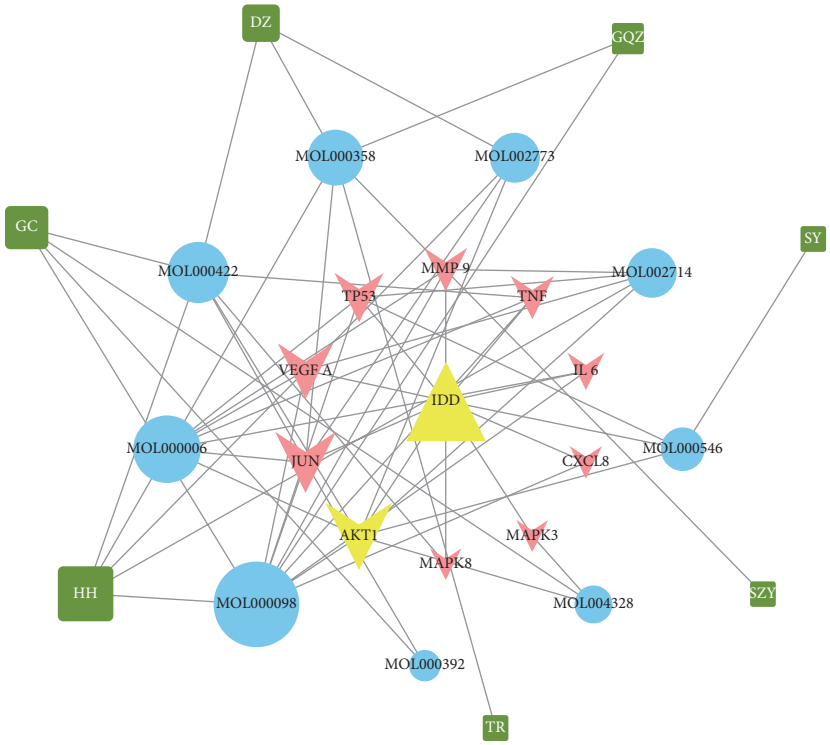

Figure 7: IDD-core gene-active ingredient-herb network. Red triangle nodes represent disease, pink arrow-like nodes represent core genes, blue circle nodes represent the active ingredients related to the core genes, and the green square nodes represent herbs. The size of each node was set according to its degree value.

Table 3: Basic information of the nine active components in MBSHXD.

Molecule ID	Molecule name	PubChem CID	OB (%)	DL	Source (herb name)	Targeted core genes
MOL000098	Quercetin	5280343	46.43	0.28	Duzhong, Gouqizi, Honghua, Gancao	AKT1, CXCL8, IL6, JUN, MMP9, TNF, TP53, VEGFA
MOL000006	Luteolin	5280445	36.16	0.25	Honghua	TNF, MMP9, IL6, VEGFA, TP53, JUN, AKT1
MOL000422	Kaempferol	5280863	41.88	0.24	Duzhong, Honghua, Gancao	TNF, MAPK8, JUN, AKT1
MOL000358	Beta-sitosterol	222284	26.91	0.75	Duzhong, Gouqizi, Shanzhuyu, Taoren, Honghua	JUN
MOL002714	Baicalein	5281605	33.52	0.21	Honghua	MMP9, VEGFA, TP53, AKT1
MOL002773	Beta-carotene	5280489	37.18	0.58	Duzhong, Honghua	VEGFA, JUN, AKT1,
MOL000546	Diosgenin	99474	80.88	0.81	Shanyao	VEGFA, TP53, AKT1
MOL004328	Naringenin	932	59.29	0.21	Gancao	MAPK3, AKT1
MOL000392	Formononetin	5280378	69.67	0.21	Gancao	JUN

Table 4: Detailed information of the 10 core targets.

Protein	PDB ID	Relevant citation
TNF	7KP9	DOI: 10.1038/s41467-020-20828-3
VEGFA	4DEQ	DOI: 10.1074/jbc.M111.331140
ILA	1ALU	DOI: 10.1093/emboj/16.5.989
MAPK3	6GES	DOI: 10.1016/j.chembiol.2019.02.021
AKT1	6S9W	DOI: 10.1002/anie.201909857
MAPK8	4L7F	DOI: 10.1016/j.bmcl.2013.06.087
TP53	7DHZ	DOI: 10.1016/j.ccell.2020.11.013
JUN	1JUN	DOI: 10.1074/jbc.271.23.13663
MMP9	5CUH	DOI: 10.1016/j.ejmech.2016.01.053
CXCL8	1IKL	DOI: 10.1021/bi00040a008

According to our "disease-core genes–active ingredients–herbs" network, nine bioactive compounds between the 10 core genes and the corresponding active compounds in MBSHXD were identified. Furthermore, three hub ingredients, quercetin, luteolin, and kaempferol, were selected, and they targeted the largest number of core genes. In vitro experiments showed that quercetin ameliorated the progression of IDD by suppressing the expression of senescence associated secreted phenotype factors and improving the senescence phenotype of NP cells via the Nrf2/NF-κB axis [49]; luteolin, a natural flavonoid, has anti-inflammatory and anticatabolic effects [50]; kaempferol has been reported

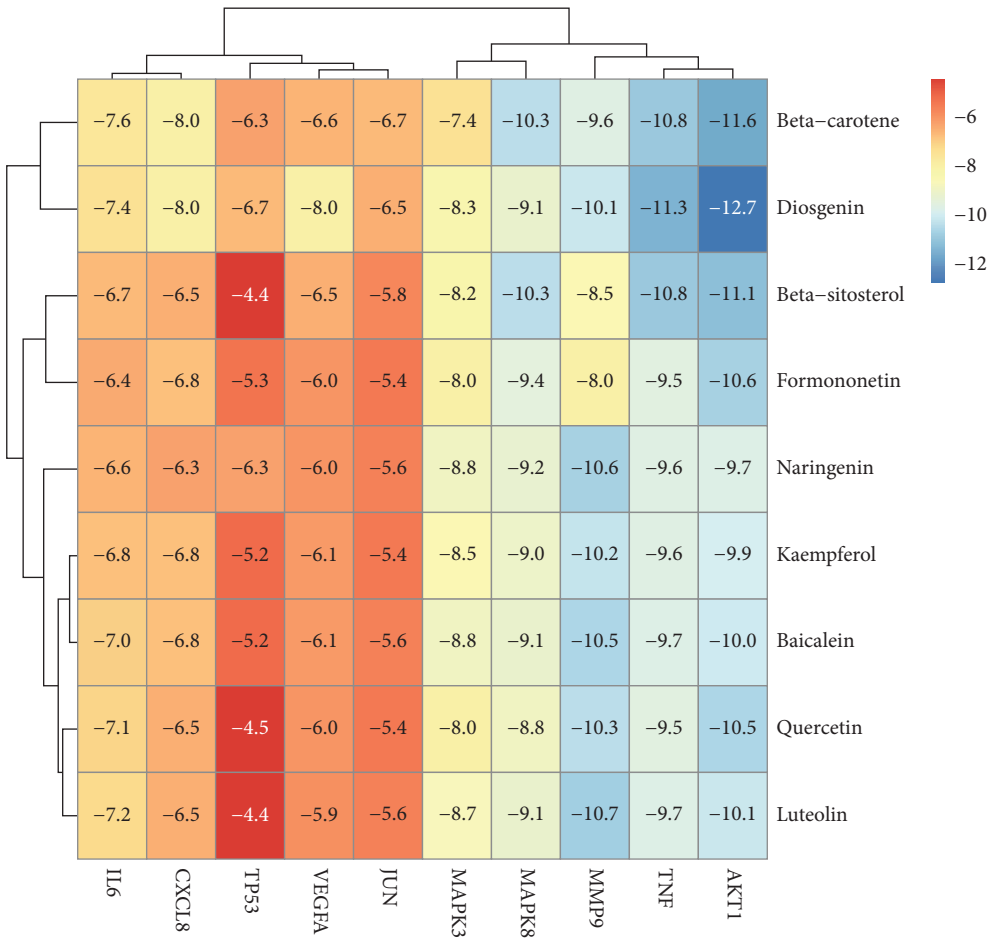

Figure 8: Heat map of molecular docking between 10 core genes and 9 active ingredients [34].

to regulate osteogenesis/adipogenesis balance and inhibit inflammation in bone mesenchymal stem cells to slow the progression of IDD [51]. These compounds are the material basis of MBSHXD in the treatment of IDD.

Based on the ten core genes and their corresponding core compounds, molecular docking was performed to demonstrate the binding energy between proteins and small-molecule compounds, which all showed good binding affinity. The abovementioned molecular docking results were presented in the form of a heat map by using R software. In addition, the software package ClusterProfiler was used for enrichment analysis of GO and KEGG pathways. The results of two enrichment analyses of GO and KEGG were compared with the IDD-related pathways searched in PubMed. We speculated that the therapeutic effect of MBSHXD in IDD may be related to its anti-inflammatory and anti-oxidative stress effects, which inhibit apoptosis and senescence of NP cells. Indeed, inflammation, ECM degradation, and senescence of NP cells are thought to be the main pathogenic mechanisms of IDD [52, 53]. The abovementioned mechanisms mainly involve the AGE-RAGE signaling pathway in diabetic complications, the IL-17 signaling pathway, the TNF signaling pathway, the PI3K-Akt signaling pathway, the MAPK signaling pathway, and apoptosis. It has been reported that the PI3K-Akt pathway is involved in the proliferation, apoptosis, senescence, and ECM metabolism of NP cells and is significantly associated with NP degeneration. It is considered as an essential signaling pathway involved in IDD [54–56]. TNF and IL-17 pathways play a synergistic role in IDD progression, mainly by promoting the release of inflammatory mediators, the apoptosis of NP cells, and the degradation of ECM [57–59]. In addition, the MAPK pathway is thought to primarily mediate the inflammatory response of NP cells to TNF-α stimulation [60]. Illien–Jünger et al. [61] suggested AGE accumulation is related to endochondral ossification, which may induce hypertrophy and osteogenic differentiation of intervertebral disc cells through the AGE/RAGE axis. More importantly, the accumulation of AGEs is closely associated with oxidative stress, which may lead to alterations in the oxidative microenvironment of NP and, in turn, contribute to IDD. Thus, targeted clearance of AGEs may be a promising direction to noninvasively slow down the progression of IDD.

However, our study also has some limitations. For example, the results of this study lacked validation by in vitro experiments, while further external validation in animals should be performed. In addition, the database we selected may not be comprehensive enough, and the active ingredients and related genes screened through the database may have been missed.

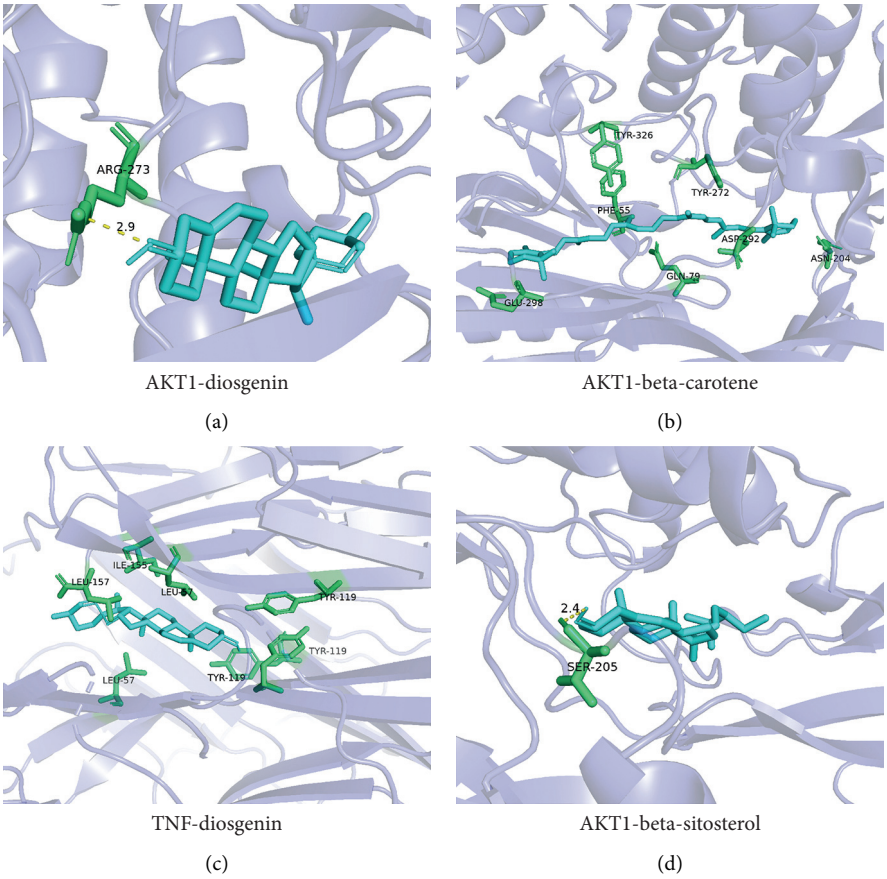

Figure 9: Molecular docking of "bioactive compound-hub gene." (a) AKT1 to Diosgenin; (c) TNF to Diosgenin; (b) AKT1 to betacarotene; and (d) AKT1 to betasitosterol.

In conclusion, we reveal that MBSHXD has the characteristics of "multi-component, multi-target, and multi-pathway" in IDD treatment based on network pharmacology and molecular docking. MBSHXD retards the progression of IDD by regulating the antioxidant stress and inflammatory response, which inhibits apoptosis and senescence of NP cells. The primary mechanism is related to 9 core bioactive components, 10 core genes, and 9 related pathways. This study may inspire novel treatment strategies for IDD and inform future research.

Data Availability

The data used to support the findings of this study are included within the article.

Conflicts of Interest

The authors declare that they have no conflicts of interest.

Supplementary Materials

Supplementary Table 1: ingredients of each herb contained in MBSHXD. Supplementary Table 2: known therapeutic targets correspond to the active ingredients. Supplementary Table 3: the target protein corresponds to the gene name from UniPort. Supplementary Table 4: the common targets and corresponding active components. Supplementary Table 5: detailed information of GO and KEGG enrichment analysis for IDD-related targets. Supplementary Table 6: detailed information of GO and KEGG enrichment analysis for common targets. Supplementary Table 7: detailed information of overlapping KEGG pathways. (*Supplementary Materials*)

References

[1] D. Hoy, L. March, P. Brooks et al., "The global burden of low back pain: estimates from the global burden of disease 2010 study," *Annals of the Rheumatic Diseases*, vol. 73, no. 6, pp. 968–974, 2014.

[2] B. I. Martin, R. A. Deyo, S. K. Mirza et al., "Expenditures and health status among adults with back and neck problems," *JAMA*, vol. 299, no. 6, p. 656, 2008.

[3] Y. Wu, F. Zhang, K. Yang et al., "SymMap: an integrative database of traditional Chinese medicine enhanced by symptom mapping," *Nucleic Acids Research*, vol. 47, no. D1, pp. D1110–D1117, 2019.

[4] J. Wu, B. Sun, L. Hou et al., "Prospective: evolution of Chinese medicine to treat COVID-19 patients in China," *Frontiers in Pharmacology*, vol. 11, Article ID 615287, 2020.

[5] X. Zhang, Y. Yang, F. Zhang et al., "Traditional Chinese medicines differentially modulate the gut microbiota based on their nature (Yao-Xing)," *Phytomedicine: International*

Journal of Phytotherapy and Phytopharmacology, vol. 85, Article ID 153496, 2021.

[6] W. Liu, Y.-h. Wu, X.-y. Liu, B. Xue, W. Shen, and K. Yang, "Metabolic regulatory and anti-oxidative effects of modified bushen huoxue decoction (补肾活血方) on experimental rabbit model of osteoarthritis," *Chinese Journal of Integrative Medicine*, vol. 19, no. 6, pp. 459–463, 2013.

[7] L. G. Zhu, P. Zhang, Q. H. Song et al., "Preliminary study of intervention in effect of Bushen Huoxue recipe on calcification of lumbar vertebra cartilage endplate of the aging gerbils," *Zhongguo gu Shang = China Journal of Orthopaedics and Traumatology*, vol. 30, no. 10, p. 926, 2017.

[8] A. L. Hopkins, "Network pharmacology: the next paradigm in drug discovery," *Nature Chemical Biology*, vol. 4, no. 11, pp. 682–690, 2008.

[9] S. I. Berger and R. Iyengar, "Network analyses in systems pharmacology," *Bioinformatics*, vol. 25, no. 19, pp. 2466–2472, 2009.

[10] A. L. Hopkins, "Network pharmacology," *Nature Biotechnology*, vol. 25, no. 10, pp. 1110-1111, 2007.

[11] E. Guney, J. Menche, M. Vidal, and A.-L. Barábasi, "Network-based in silico drug efficacy screening," *Nature Communications*, vol. 7, no. 1, p. 10331, 2016.

[12] M. Kibble, N. Saarinen, J. Tang, K. Wennerberg, S. Mäkelä, and T. Aittokallio, "Network pharmacology applications to map the unexplored target space and therapeutic potential of natural products," *Natural Product Reports*, vol. 32, no. 8, pp. 1249–1266, 2015.

[13] X.-M. Wu and C.-F. Wu, "Network pharmacology: a new approach to unveiling Traditional Chinese Medicine," *Chinese Journal of Natural Medicines*, vol. 13, no. 1, pp. 1-2, 2015.

[14] Z. Zhou, B. Chen, S. Chen et al., "Applications of network pharmacology in traditional Chinese medicine research," *Evidence-based Complementary and Alternative Medicine*, vol. 2020, Article ID 1646905, 7 pages, 2020.

[15] S. Li, T. P. Fan, W. Jia, A. Lu, and W. Zhang, "Network pharmacology in traditional Chinese medicine," *Evidence-based Complementary and Alternative Medicine*, vol. 2014, Article ID 138460, 2 pages, 2014.

[16] N. Choudhary and V. Singh, "A census of P. longum's phytochemicals and their network pharmacological evaluation for identifying novel drug-like molecules against various diseases, with a special focus on neurological disorders," *PLoS One*, vol. 13, no. 1, Article ID e0191006, 2018.

[17] N. Choudhary, S. Choudhary, A. Kumar, and V. Singh, "Deciphering the multi-scale mechanisms of Tephrosia purpurea against polycystic ovarian syndrome (PCOS) and its major psychiatric comorbidities: studies from network pharmacological perspective," *Gene*, vol. 773, Article ID 145385, 2021.

[18] D. Shah, M. Gandhi, A. Kumar, N. Cruz-Martins, R. Sharma, and S. Nair, "Current insights into epigenetics, noncoding RNA interactome and clinical pharmacokinetics of dietary polyphenols in cancer chemoprevention," *Critical Reviews in Food Science and Nutrition*, vol. 1, 2021.

[19] N. Choudhary and V. Singh, "Insights about multi-targeting and synergistic neuromodulators in Ayurvedic herbs against epilepsy: integrated computational studies on drug-target and protein-protein interaction networks," *Scientific Reports*, vol. 9, no. 1, Article ID 10565, 2019.

[20] D.-h. Zhang, X. Zhang, B. Peng et al., "Network pharmacology suggests biochemical rationale for treating COVID-19 symptoms with a Traditional Chinese Medicine," *Communications Biology*, vol. 3, no. 1, p. 466, 2020.

[21] J. Ru, P. Li, J. Wang et al., "TCMSP: a database of systems pharmacology for drug discovery from herbal medicines," *Journal of Cheminformatics*, vol. 6, no. 13, p. 13, 2014.

[22] D. S. Wishart, Y. D. Feunang, A. C. Guo et al., "DrugBank 5.0: a major update to the DrugBank database for 2018," *Nucleic Acids Research*, vol. 46, no. D1, pp. D1074–D1082, 2018.

[23] "UniProt: a hub for protein information," *Nucleic Acids Research*, vol. 43, p. D204, 2015.

[24] M. Rebhan, V. Chalifa-Caspi, J. Prilusky, and D. Lancet, "GeneCards: integrating information about genes, proteins and diseases," *Trends in Genetics*, vol. 13, no. 4, p. 163, 1997.

[25] J. S. Amberger, C. A. Bocchini, F. Schiettecatte, A. F. Scott, and A. Hamosh, "OMIM.org: Online mendelian inheritance in man (OMIM®), an online catalog of human genes and genetic disorders," *Nucleic Acids Research*, vol. 43, p. D789, 2015.

[26] G. Stelzer, N. Rosen, I. Plaschkes et al., "The GeneCards suite: from gene data mining to disease genome sequence analyses," *Current protocols in bioinformatics*, vol. 54, pp. 1–33, 2016.

[27] P. Shannon, A. Markiel, O. Ozier et al., "Cytoscape: a software environment for integrated models of biomolecular interaction networks," *Genome Research*, vol. 13, no. 11, pp. 2498–2504, 2003.

[28] G. Yu, L.-G. Wang, Y. Han, and Q.-Y. He, "clusterProfiler: an R package for comparing biological themes among gene clusters," *OMICS: A Journal of Integrative Biology*, vol. 16, no. 5, pp. 284–287, 2012.

[29] D. Szklarczyk, A. L. Gable, D. Lyon et al., "STRING v11: protein-protein association networks with increased coverage, supporting functional discovery in genome-wide experimental datasets," *Nucleic Acids Research*, vol. 47, no. D1, pp. D607–D613, 2019.

[30] C. H. Chin, S. H. Chen, H. H. Wu, C. W. Ho, M. T. Ko, and C. Y. Lin, "cytoHubba: identifying hub objects and sub-networks from complex interactome," *BMC Systems Biology*, vol. 8, no. 4, p. S11, 2014.

[31] S. Gu, Y. Xue, Y. Zhang et al., "An investigation of the mechanism of rapid relief of ulcerative colitis induced by five-flavor Sophora flavescens enteric-coated capsules based on network pharmacology," *Combinatorial Chemistry & High Throughput Screening*, vol. 23, no. 3, pp. 239–252, 2020.

[32] J. L. Deng, Y. H. Xu, and G. Wang, "Identification of potential crucial genes and key pathways in breast cancer using bioinformatic analysis," *Frontiers in Genetics*, vol. 10, p. 695, 2019.

[33] O. Trott and A. J. Olson, "AutoDock Vina: improving the speed and accuracy of docking with a new scoring function, efficient optimization, and multithreading," *Journal of Computational Chemistry*, vol. 31, no. 2, pp. 455–61, 2010.

[34] L. Wang, J. Lin, and W. Li, "Pharmacological mechanism of danggui-sini formula for intervertebral disc degeneration: a network pharmacology study," *BioMed Research International*, vol. 2021, Article ID 5165075, 12 pages, 2021.

[35] A. B. Dario, M. L. Ferreira, K. M. Refshauge, T. S. Lima, J. R. Ordoñana, and P. H. Ferreira, "The relationship between obesity, low back pain, and lumbar disc degeneration when genetics and the environment are considered: a systematic review of twin studies," *The Spine Journal*, vol. 15, no. 5, pp. 1106–1117, 2015.

[36] M.-l. Ji, H. Jiang, X.-j. Zhang et al., "Preclinical development of a microRNA-based therapy for intervertebral disc degeneration," *Nature Communications*, vol. 9, no. 1, p. 5051, 2018.

[37] M. Minetama, M. Kawakami, M. Teraguchi et al., "Therapeutic advantages of frequent physical therapy sessions for patients with lumbar spinal stenosis," *Spine (Phila Pa 1976)*, vol. 45, no. 11, p. E639, 2020.

[38] L. Zhu, C. Yu, X. Zhang et al., "The treatment of intervertebral disc degeneration using Traditional Chinese Medicine," *Journal of Ethnopharmacology*, vol. 263, Article ID 113117, 2020.

[39] S.-H. Feng, F. Xie, H.-Y. Yao, G.-B. Wu, X.-Y. Sun, and J. Yang, "The mechanism of Bushen Huoxue decoction in treating intervertebral disc degeneration based on network pharmacology," *Annals of Palliative Medicine*, vol. 10, no. 4, pp. 3783–3792, 2021.

[40] T. Li, S. Wang, S. Zhang et al., "Evaluation of clinical efficacy of silver-needle warm acupuncture in treating adults with acute low back pain due to lumbosacral disc herniation: study protocol for a randomized controlled trial," *Trials*, vol. 20, no. 1, p. 470, 2019.

[41] K. Zhao, M. Chen, T. Liu et al., "Rhizoma drynariae total flavonoids inhibit the inflammatory response and matrix degeneration via MAPK pathway in a rat degenerative cervical intervertebral disc model," *Biomedicine & Pharmacotherapy*, vol. 138, Article ID 111466, 2021.

[42] H.-H. Xu, S.-M. Li, R. Xu, L. Fang, H. Xu, and P.-J. Tong, "Predication of the underlying mechanism of Bushenhuoxue formula acting on knee osteoarthritis via network pharmacology-based analyses combined with experimental validation," *Journal of Ethnopharmacology*, vol. 263, Article ID 113217, 2020.

[43] S. Yang, L. Li, L. Zhu et al., "Bu-Shen-Huo-Xue-Fang modulates nucleus pulposus cell proliferation and extracellular matrix remodeling in intervertebral disk degeneration through miR-483 regulation of Wnt pathway," *Journal of Cellular Biochemistry*, vol. 120, no. 12, pp. 19318–19329, 2019.

[44] S. Wang, J. Wei, J. Shi et al., "Follistatin-like 1 attenuation suppresses intervertebral disc degeneration in mice through interacting with TNF-α and smad signaling pathway," *Oxidative Medicine and Cellular Longevity*, vol. 2021, Article ID 6640751, 13 pages, 2021.

[45] H. Cui, X. Du, C. Liu et al., "Visfatin promotes intervertebral disc degeneration by inducing IL-6 expression through the ERK/JNK/p38 signalling pathways," *Adipocyte*, vol. 10, no. 1, pp. 201–215, 2021.

[46] J. He, R. Xue, S. Li et al., "Identification of the potential molecular targets for human intervertebral disc degeneration based on bioinformatic methods," *International Journal of Molecular Medicine*, vol. 36, no. 6, pp. 1593–1600, 2015.

[47] D. Wang, Y. Chen, S. Cao et al., "Cyclic mechanical stretch ameliorates the degeneration of nucleus pulposus cells through promoting the ITGA2/PI3K/AKT signaling pathway," *Oxidative Medicine and Cellular Longevity*, vol. 2021, Article ID 6699326, 11 pages, 2021.

[48] J. W. Zhan, S. Q. Wang, M. S. Feng et al., "Effects of axial compression and distraction on vascular bud and VEGFA expression in the vertebral endplate of an ex vivo rabbit spinal motion segment culture model," *Spine (Phila Pa 1976)*, vol. 46, no. 7, p. 421, 2021.

[49] Z. Shao, B. Wang, Y. Shi et al., "Senolytic agent Quercetin ameliorates intervertebral disc degeneration via the Nrf2/NF-κB axis," *Osteoarthritis and Cartilage*, vol. 29, no. 3, pp. 413–422, 2021.

[50] J. Fei, B. Liang, C. Jiang, H. Ni, and L. Wang, "Luteolin inhibits IL-1β-induced inflammation in rat chondrocytes and attenuates osteoarthritis progression in a rat model-flammation in rat chondrocytes and attenuates osteoarthritis progression in a rat model," *Biomedicine & Pharmacotherapy*, vol. 109, pp. 1586–1592, 2019.

[51] J. Zhu, H. Tang, Z. Zhang et al., "Kaempferol slows intervertebral disc degeneration by modifying LPS-induced osteogenesis/adipogenesis imbalance and inflammation response in BMSCs," *International Immunopharmacology*, vol. 43, pp. 236–242, 2017.

[52] C. Feng, H. Liu, M. Yang, Y. Zhang, B. Huang, and Y. Zhou, "Disc cell senescence in intervertebral disc degeneration: causes and molecular pathways," *Cell Cycle*, vol. 15, no. 13, pp. 1674–1684, 2016.

[53] F. Wang, F. Cai, R. Shi, X.-H. Wang, and X.-T. Wu, "Aging and age related stresses: a senescence mechanism of intervertebral disc degeneration," *Osteoarthritis and Cartilage*, vol. 24, no. 3, pp. 398–408, 2016.

[54] Z. Liao, R. Luo, G. Li et al., "Exosomes from mesenchymal stem cells modulate endoplasmic reticulum stress to protect against nucleus pulposus cell death and ameliorate intervertebral disc degeneration in vivo," *Theranostics*, vol. 9, no. 14, pp. 4084–4100, 2019.

[55] Y. Wang, R. Zuo, Z. Wang et al., "Kinsenoside ameliorates intervertebral disc degeneration through the activation of AKT-ERK1/2-Nrf2 signaling pathway," *Aging*, vol. 11, no. 18, pp. 7961–7977, 2019.

[56] Y. Xi, J. Ma, and Y. Chen, "PTEN promotes intervertebral disc degeneration by regulating nucleus pulposus cell behaviors," *Cell Biology International*, vol. 44, no. 2, pp. 583–592, 2020.

[57] J. Zhang, X. Wang, H. Liu et al., "TNF-α enhances apoptosis by promoting chop expression in nucleus pulposus cells: role of the MAPK and NF-κB pathways," *Journal of Orthopaedic Research*, vol. 37, no. 3, pp. 697–705, 2019.

[58] L. Miguélez-Rivera, S. Pérez-Castrillo, M. L. González-Fernández et al., "Immunomodulation of mesenchymal stem cells in discogenic pain," *The Spine Journal*, vol. 18, no. 2, p. 330, 2018.

[59] X.-G. Liu, H.-W. Hou, and Y.-L. Liu, "Expression levels of IL-17 and TNF-α in degenerated lumbar intervertebral discs and their correlation," *Experimental and Therapeutic Medicine*, vol. 11, no. 6, pp. 2333–2340, 2016.

[60] G. Wang, K. Huang, Y. Dong et al., "Lycorine suppresses endplate-chondrocyte degeneration and prevents intervertebral disc degeneration by inhibiting NF-κB signalling pathway," *Cellular Physiology and Biochemistry*, vol. 45, no. 3, pp. 1252–1269, 2018.

[61] S. Illien-Jünger, O. M. Torre, W. F. Kindschuh, X. Chen, D. M. Laudier, and J. C. Iatridis, "AGEs induce ectopic endochondral ossification in intervertebral discs," *European Cells and Materials*, vol. 32, p. 257, 2016.

Hindawi
Evidence-Based Complementary and Alternative Medicine
Volume 2022, Article ID 5105545, 12 pages
https://doi.org/10.1155/2022/5105545

Research Article

Wu-Teng-Gao External Treatment Improves Th17/Treg Balance in Rheumatoid Arthritis

Xueming Yao,[1] Qiuyi Wang,[1] Changming Chen,[1] Ping Zeng,[1] Lei Hou,[1] Jing Zhou,[1] Ying Huang,[1,2] and Wukai Ma[1]

[1]*Department of Rheumatology and Immunology, The Second Affiliated Hospital of Guizhou University of Traditional Chinese Medicine, Guiyang 550001, China*
[2]*Guizhou Medical University, Beijing Road, Guiyang, Guizhou Province 550004, China*

Correspondence should be addressed to Ying Huang; 40741698@qq.com and Wukai Ma; fsmymwk@163.com

Received 28 October 2021; Accepted 14 December 2021; Published 21 January 2022

Academic Editor: Atul Kabra

Rheumatoid arthritis (RA) represents the consequence of an immune response of the body's immune system attacking healthy cells. This chronic inflammatory disorder has complicated pathogenesis. Traditional Chinese medicine (TCM) is well recognized as an effective therapy in treating RA and has been widely applied for centuries. Wu-Teng-Gao (WTG) is used as a representative natural herb formula in RA treatment in China, while its mechanisms are to be fully clarified. The present study attempted to explore mechanisms of WTG on RA treatment in a network pharmacological approach and verified using experiments in vitro. Following the establishment of a rat model of collagen-induced arthritis (CIA), WTG was applied externally on the metapedes of rats. HE staining was subsequently performed to visualize the pathological changes of synovium and bone. Simultaneously, flow cytometry was conducted to detect the cell ratio of T helper 17 (Th17) and Regulatory T cells (Treg) in splenic lymphocytes. Additionally, ELISA, qRT-PCR, and Western blot assays were adopted to determine expressions of RA-related factors in joints and serum. Results of network pharmacological analysis suggested that Th17 cell differentiation might serve as a potential signaling pathway of WTG therapy for RA. Animal experiments demonstrated that WTG ameliorated the articular inflammation and effectively inhibited the destruction of articular cartilage, and decreased Th17 and Treg cell ratios in CIA rats. Furthermore, WTG also greatly suppressed relevant levels of inflammatory cytokines (IL-17, TNF-α, IL-1, and IL-6) and RNAKL, whereas it elevated expressions of anti-inflammatory cytokines IL-10 and TGF-β. Our results confirmed that WTG might improve the imbalance of Th17/Treg cells in CIA animals through differentiation regulation, thus alleviating joint inflammation and bone destruction.

1. Introduction

Rheumatoid Arthritis (RA) has been well recognized as a systemic and chronic autoimmune disorder. The principal characteristics include the proliferation of synovial cells, infiltration of inflammatory cells, as well as destruction in articular cartilage and bones, thus resulting in joint deformity and disability [1]. The RA pathogenesis is intricate and unclear, which can be triggered by genetic factors, environmental factors, and aberrant immune systems [2]. As one subset of T cells [3], Th17 cells play an essential role in proinflammation, and when in excess, such cells contribute to autoimmunity and tissue damage. The other subset of T cells is Treg cells, which are antagonistic, and once they fail, the same diseases occur [3]. The Th17/Treg ratio is lower in healthy control than that of RA patients, especially the active RA patients [4]. Th17/IL-17 axis is of great significance in local inflammation and bone destruction of RA joints [5, 6]. Exosomes contain multiple proteins and nucleic acids, which are involved in T cell activation, antigen expression, intracellular signal transduction, inflammatory response, bone destruction, microvascular dysplasia, and other aspects

in the pathogenesis of RA [7–9]. A recent report has shown that exosomes can regulate Thl7/Treg imbalance and inhibit the Th17/IL17 axis [10].

TCM is widely used in China and is effective in treating RA [11]. RA, in light of TCM theory, is considered to be an "impediment disease" (also Bi syndrome), as a consequence of invasion by cold, heat, wind, or dampness pathogens into the meridian channels [12]. Following the principles of TCM theory, dampness and cold elimination and blood circulation promotion contribute to treating severe RA [13]. The current drug administration of RA treatment includes steroidal and non-steroidal anti-inflammatory medication, disease-modifying antirheumatic drugs, and biological preparations in clinical practice [14]. Unfortunately, the previously mentioned medications improve the symptoms slowly and even have certain serious adverse reactions after long-term administration [15]. A meta-analysis has indicated that the treatment protocols that integrated TCM and Western medicines can achieve both effective and satisfactory results in treating RA [16]. The TCM herb *Tripterygium Wilfordii, Caulis Sinomenii*, and *Periploca Forrestii* have been proved effective in alleviating RA progression [17–19]. Triptolide, a component of *Tripterygium Wilfordii* displays an immunosuppressive effect on the RA animal model by downregulating Th17 cells [20]. TCM can realize the overall regulation of body functions through multifaceted and multi-target mechanisms, and it produces a remarkable curative effect on the treatment of RA [11]. However, the underlying mechanism by which TCM helps to alleviate RA remains unknown, thereby hindering its further clinical application.

Our preliminary clinical study confirmed that WTG had a good anti-RA effect in external treatment. The results of the network pharmacological approach indicated that WTG might be of great importance in the Th17 cell differentiation pathway. Based on this, we proposed the hypothesis that the WTG could relieve local joint inflammation and bone destruction by regulating Exo to inhibit the Th17/IL-17 signal axis and relieve systemic inflammation by mediating Th17/Treg balance. The present research explored the anti-arthritis effect using a CIA rat model treated with WTG and the possible mechanism of Th17/Treg balance through exosomes, expecting to offer an experimental foundation for RA treatment in clinical application.

2. Material and Method

2.1. Analysis of Molecular Networks and Signaling Pathways. Based on the principle of network pharmacology, the main components and action targets of compound WTG were predicted to offer a research basis for further study of its mechanism of action. The effective active components and related targets of Da-Xue-Teng (*Sargentodoxae Caulis*), Ji-Xue-Teng (*Spatholobus Suberectus*), Qing-Feng-Teng (*Sinomenium Acutum*), Lei-Gong-Teng (*Tripterygium Wilfordii*), and Hei-Gu-Teng (*Periploca Forrestii* Schltr.) were retrieved via the TCMSP platform (http://lsp.nwu.edu.cn/tcmsp.php), and the genes related to RA were selected from the disease database GeneCard (https://www.genecards.org). Subsequently, the diagram of protein protein interaction (PPI) was constructed using the String website (https://string-db.org/). Analysis of GO and KEGG pathway enrichment of key targets was performed, and the top 30 terms with the lowest P values were selected for visualization analysis.

2.2. Rat CIA Modeling. Animal experiments were approved and performed in accordance with the guidelines of Committee on the Ethics of Animal Experiments of The Second Affiliated Hospital of Guizhou University of Traditional Chinese Medicine, China (No. KYW2019001). A total of 70 SPF grade rats aged 6–8 weeks, weighing approximately 150–180 g were provided by Chongqing Ensiweier Biotechnology Co. Ltd. All animals were given adaptive feeding for one week and marked with numbers. The animal house was provided with an alternative of 12 h–12 h day and night. Water and diets were given at will. The temperature was maintained at 23–25°C.

The laboratory rats were randomly classified into 7 groups: a blank group, a model group, an IL-17 blocking group, a diclofenac diethylamine emulgel (DDE) control group, a high-dose Wu-Teng-Gao group, a medium-dose Wu-Teng-Gao group, and a low-dose Wu-Teng-Gao group, with 10 rats in each group. In the treatment group, high (0.45 g/paw), medium (0.3 g/paw), and low dose (0.15 g/paw) of Wu-Teng-Gao were externally applied on metapedes of the tested rats, respectively. The blank group and model group were fed normally and given an equal dosage of Vaseline for external application. The positive control group was given diclofenac diethylamine emulsion (20 g/tube, produced by Beijing Novartis Pharmaceutical Co., Ltd.), 70 μL/100 g.

The CIA rat model of arthritis is characterized by similar clinical, histopathological, and immunological changes to the human, and it is the animal model of bone destruction commonly used internationally [21, 22]. Collagen II (SolarBio, China) was dissolved by supplementing 0.1 mol/L acetic acids to prepare a 2 mg/mL solution, stirred to be dissolved, and placed in a refrigerator at 4°C overnight. Freund's incomplete adjuvant at the same volume was supplemented, mixed, and emulsified into type II collagen emulsion [23]. The rat model was subsequently injected with a 0.1 mL emulsifier into the tail root intradermally to induce inflammation. The stable CIA model was reproduced, and corresponding drug intervention was initiated to confirm successful modeling. The model assessment followed the below-described criteria: 0 point represented no erythema or swelling; 1 point represented slight erythema or swelling of one toe; 2 points represented erythema or swelling of more than one toes; 3 points represented erythema and swelling of the ankle or wrist; and 4 points represented all erythema and swelling of the toes and ankles or fingers and wrists [24] and failure to bend the ankles or wrists.

2.3. Drug Intervention. Miao medicine Wu-Teng-Gao consists of Hei-Gu-Teng, Ji-Xue-Teng, Qing-Feng-Teng, Da-Xue-Teng, and Lei-Gong-Teng. The preparation was

provided by the Pharmacy Department of The Second Affiliated Hospital of Guizhou University of Traditional Chinese Medicine. Doses of the high, medium, and low treatment groups were calculated by crude drug dose. The medium dose was the same as the crude drug used in clinical patients (the drug volume was about 30 g/paw), according to the conversion coefficient table of drug dose for adults and animals [25]. Drug administration was initiated on day 7 of the modeling. All groups were fixed with nonwoven fabric (patch backing layer), once per day. The course lasted 4 weeks. The IL-17 blocking group was injected with an IL-17 neutralizing antibody, 50 μg/time/rat, once every 3 d. The weight of the rats was measured once a week. On day 28 after administration, the rats were put to death by intraperitoneally injecting 100 mg/kg pentobarbital sodium. Blood samples were obtained from the abdominal aorta and serum samples were collected by centrifugation [26]. The synovial tissues and joint tissues were obtained by removal of the skin on the knee joint and ankle joint of both hind limbs, part of which was fixed with 4% paraformaldehyde, and the remaining were cryopreserved in a refrigerator at −80°C for subsequent detection of various indicators in further experiments.

2.4. HE Staining. The tissues were immersed in a fixation solution containing 4% paraformaldehyde 24 h and prepared into sections at 5 μm thickness. Paraffin sections were baked in an oven set at 60°C for 1 h, dewaxed with xylene, and followed by gradient alcohol hydration. Then they were rinsed with double distilled water for 3 times, 5 min each time. After staining with hematoxylin solution for 5 min, differentiation was performed using hydrochloric acid and alcohol for 2–3 s, saturated lithium carbonate solution turned blue for 1–2 min. After washing with running water for 10 min, drop staining was performed using eosin solution for 1–3 min and washed with running water for 10 min. Conventional gradient alcohol was employed for dehydration and transparency and slice sealing.

2.5. Primary Isolation and Culture of Splenic Lymphocytes. The spleens of the previously described rats were taken after treatment according to the experiment grouping. After surface disinfection, the spleens were dissected, cut into pieces with surgical shears, homogenized manually in an ice bath, and passed through a stainless 200 mesh sieve [27]. The single-cell suspension in the Petri dishes was collected. The operation procedures were conducted following the instructions of the rat spleen lymphocyte separation medium kit (Solarbio, China). An addition of 3 mL separation solution was supplemented to a 15 mL centrifuge tube, and an equal volume of single-cell suspension was added. Centrifugation was performed at room temperature with a horizontal rotor at 500–1000g for 30 min. After centrifugation, a distinct stratification was visualized: the superficial layer was the diluent layer, followed by a layer of lymphocytes presenting a ring of milky white. The third layer was a transparent separation liquid layer. And the fourth was the red blood cell layer. The white layer cells were carefully aspirated into a clean 15 mL centrifuge tube, washed with 10 mL PBS, and centrifugated at 250g for 10 min. The supernatant was removed, and the cells were resuspended with 5 mL PBS or cell cleaning solution, centrifuged at 250g for 10 min, and resuspended for later use.

2.6. Flow Cytometry Detection. Splenic single-cell suspension 300 μL was taken from each sample of each group, and PMA (final concentration 50 μg/L), 1 μL ionomycin (final concentration 1 mg/L), and 1 μL monenomycin (final concentration 1 mg/L) were added and mixed well. The cells were incubated at 37°C in a 5% CO_2 incubator for 6 h, and the cell suspension was resuspended by oscillation once during the process. After incubation, the cell suspension was taken and washed with precooled PBS to remove residual irritants. FITC-labeled anti-rat CD4 antibody 1 μL was added. After incubation at 4°C for 60 min in the dark 900 μL RBC lysate was added, then incubated at room temperature for 7 min avoiding light, and washed with PBS twice. Following centrifugation at 3000 r/min using a high-speed micro-centrifuge for 3 min, the solution was washed with PBS once and the supernatant was discarded. The cells were resuspended in the residual fluid. Samples of each group were added with 1 mL of pre-diluted Foxp3 detection drilling/fixation concentrate three times in advance, rotated, mixed well, and followed by incubation at 4°C for 60 min in darkness. Following a cycle of washing with 2 mL diluted 1× permeation working solution, the cells were centrifuged at 3000 r/min for 3 min, the supernatant was discarded, and washing was repeated once. The supernatant was discarded and the cells were resuspended in the residual fluid. Antibodies anti-rat Foxp3 0.5 μL and anti-rat IL-17A 1 μL were added to each sample, and 1 μL of IgG2a Isotype Control (2A3) was set up and incubated at 4°C for 60 min in the dark. After that, 2 mL of permeation working solution was added to wash the cells twice, and the supernatant was discarded. 500 μL cold PBS was added to resuspend cells. Cells were detected by flow cytometry immediately.

2.7. Real-Time Fluorescence Quantitative PCR (qRT-PCR). RNA was extracted from rat joint tissues and spleen tissues using RNAiso Plus (Takara, Japan). Goldenstar™ RT6 cDNA Synthesis Kit (Beijing, Qingke) was employed to synthesize cDNA. The real-time fluorescence quantitative processes and procedures were followed by the instructions of the 2 × T5 Fast qPCR Mix (SYBR Green I) (Tsingke Biological Technology, Beijing). qPCR amplification procedures were designed as following: 95°C for 30 s with 40 cycles at 95°C for 5 s, 55°C for 30 s, and 72°C for 30 s. Gene expression was relative to GAPDH. Primer sequences were listed (Table 1).

2.8. Western Blot. Joint tissues and spleen tissues of each group were added with lysate containing PMSF and protease inhibitor Cocktail RIPA (Beyotime, China) to obtain total protein [28]. Total proteins 500 μg were extracted from each sample and 5 × SDS loading buffer (China, Jalase) were

Table 1: The primers used for qRT-PCR.

Primers	Sequences
RANKL-F	TACGGCAAGTACCTGCGCG
RANKL-R	CCAGGAGCGCCAGGAACATGA
RORγt-F	GCAAGTCCTACCGAGAGACGT
RORγt-R	CCTCTGGTAGCTGGTCACCT
Foxp3-F	TCCCACAAGCCAGGCTGATC
Foxp3-R	GCAGTGTGTCCGGCTGTACT
GAPDH-F	GGTTACCAGGGCTGCCTT
GAPDH-R	GAGTCATACTGGAACATGT

mixed at the ratio of 4 : 1 to set the proteins at a concentration of about 3.3 μg/μL, and followed by denaturation using a metal bath heated at 100°C for 6 min. The denatured total proteins of 60 g were selected for sample loading. The protein was transferred to a PVDF (Amersham, Germany) membrane. The membrane was removed, washed in TBST for 1 min, and then sealed with 5% skimmed milk blocking buffer at room temperature for 1 h. After sealing, it was washed 3 times using TBST, 5 min each time. The primary antibody was diluted with A primary antibody diluent at 1 : 1000 and incubated overnight at 4°C, followed by three cycles of washing with TBST, 10 min each time. Secondary antibody was diluted at 1 : 2000 concentration with the blocking buffer, incubated for 1 h, then rinsed with TBST for 3 times, 10 min each time. The ECL exposure solution (Thermo, USA) was evenly mixed with liquid A and B at a 1 : 1 rate and evenly spread on the full film surface. After reaction for 1 min, it was loaded in the exposure instrument for detection.

Procedures were performed following the instructions of reagent kits for IL-1, IL-10, IL-17, IL-6, TNF-α, and TGF-β ELISA (Ruixin Biology). Briefly, the reagent kits were balanced at room temperature, and standard wells and sample wells were set. The addition of 50 μL standard solution of different concentrations was supplied to each standard well, and a 10 μL sample was initially supplied to the sample wells and subsequently 40 μL sample dilution for testing. Detection antibody labeled by horseradish catalase 100 μL was supplemented to each standard solution well and sample well, respectively. Following the blocking of well plate with a sealing membrane, incubation was performed at 37°C for 60 min. After incubation, the liquid in wells was discarded and a washing solution was added, standby for 1 min, and discarded with 5 repeats. Following the addition of substrate A and B 50 μL to each well, incubation was performed at 37°C for 15 min in the dark. Termination solution at a quantity of 50 μL was added to each well after incubation. OD values were measured at 450 nm wavelength within 15 min.

2.9. Statistical Analysis. Data analysis was performed using the SPSS 23.0 software. GraphPad Prism 8.0 was employed for plotting. Mean comparison of multiple groups was subjected to one-way ANOVA. The Tukey method was employed for pairwise comparison. The results obtained from all experiments were expressed as the mean ± SD. The value of $P < 0.05$ was regarded as statistically significant.

3. Results

3.1. Results of Network Pharmacological Analysis. A total of 402 targets of WTG were collected from the TCMSP database and 1165 genes related to RA were retrieved from the Gene database (Figure 1(a)). RA and WTG had 85 overlapped targets and the PPI network showed a correlation between them (Figure 1(b)). The top 30 signaling pathways of GO analysis were focused on Th17 cell differentiation, IL-17 signaling pathways, cellular immune response, inflammatory response, and cytokine signaling (Figure 1(c)). Further KEGG analysis showed that the Th17 cell differentiation signaling pathway was identified as the top one common signaling pathway (Figure 1(d)).

3.2. Histopathological Changes in CIA Rats Treated by WTG. Throughout the experiment, body weight of the normal group was heavier than that of the model group and drug treatment group (Figure 2(a)). To evaluate the impact of WTG on CIA-induced joint pathological injury and inflammation, HE staining was performed using knee joint tissues. In the normal group, the surface of articular cartilage was smooth and integrated, and there was neither articular cartilage destruction nor bone destruction. Infiltration of synovial inflammatory cells, proliferation and disorder of synovial cells, and proliferation of capillaries were observed in the model group. Superficial cartilage appeared uneven, defective, and exfoliated. Furthermore, severe damages in both articular cartilage and bone were visualized. The number of inflammatory cells decreased in the IL-17 blocking group and DDE group. Meanwhile, the surface articular cartilage was relatively smooth, and cartilage and bone destruction were greatly alleviated. In the low-dose WTG group, the cartilage surface remained uneven, and the bone was destroyed seriously with disarranged synovial cells. The number of inflammatory cells was declined in the medium and high doses WTG groups. The surface of articular cartilage was slightly rough presenting an integrated structure, and no evident destruction of cartilage or bone tissues was visualized (Figure 2(b)).

3.3. Effect of WTG on the Bone Destruction. Further, the expression of RANKL in joint tissues was subjected to qRT-PCR and Western blot assays, and the influence of WTG on bone destruction was explored in CIA rats. In comparison to the blank group, RANKL mRNA and protein levels were markedly increased, whereas RANKL levels were markedly lower in WTG-treated, IL-17 blocker, and DDE groups. Although WTG could decrease RANKL levels, it remained higher than the blank group (Figures 2(c) and 2(d)). Compared with the model group, TRAP levels in peripheral blood of CIA rats were increased significantly in the WTG group (Figure 2(e)). The data indicated that WTG could suppress the expression of RANKL and inhibit osteoclast differentiation, affecting osteoclast function, and thereby reducing bone destruction.

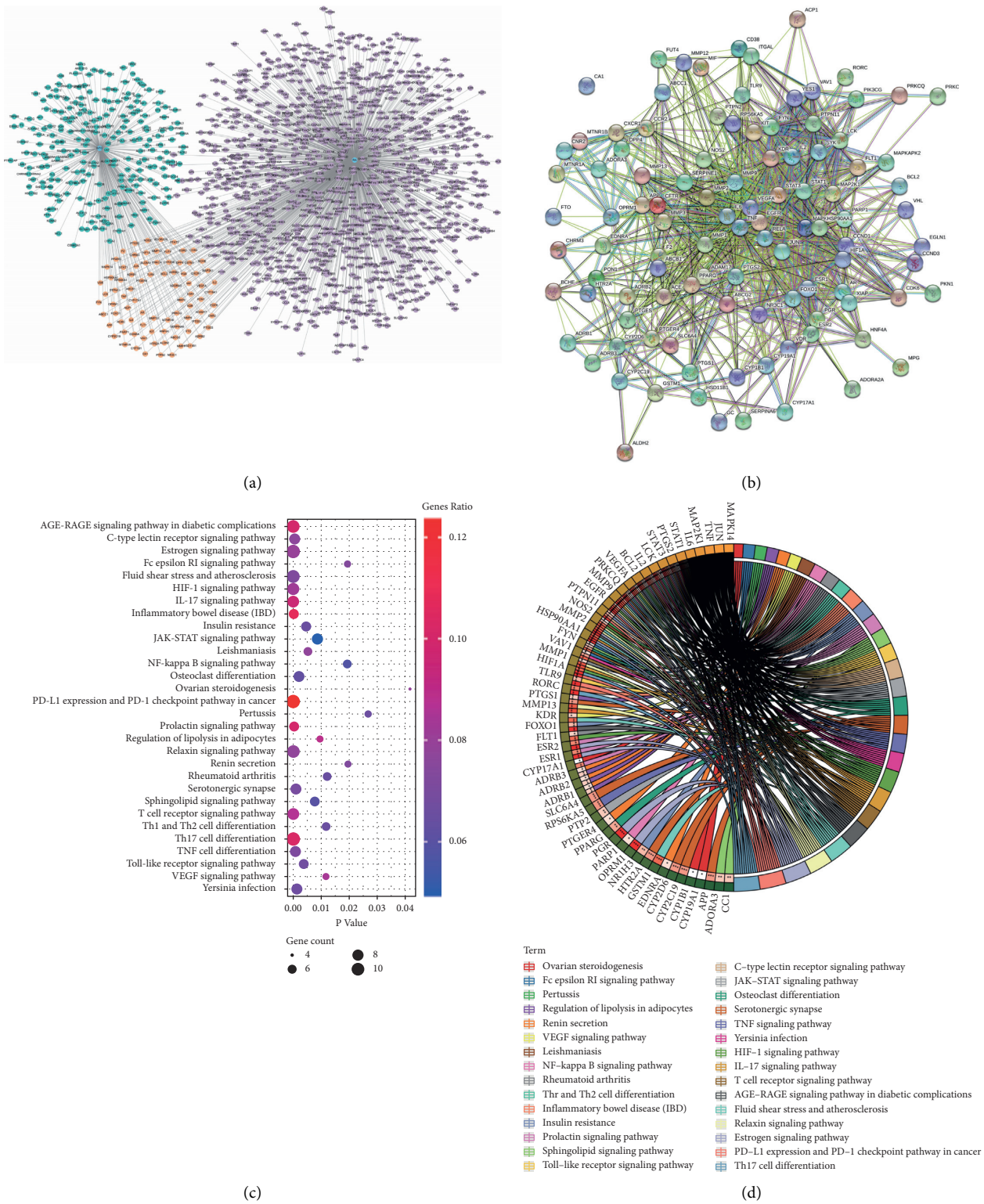

Figure 1: Network pharmacological analysis of Wu-Teng-Gao (WTG) on rheumatoid arthritis (RA). (a) Network of WTG-related targets and RA-related targets. Green represents the WTG-related targets, purple represents the RA-related targets, and yellow represents the common targets between them. (b) Protein protein interaction (PPI) network diagram of overlapped targets. (c) The top 30 GO terms of common targets. The *Y* axis represents GO terms on the left, and the *X* axis represents *P* values. (d) The top 30 KEGG pathway of the overlapped targets. The name of the signaling pathways are presented on the right, and the targets are on the left. The darker the left inner circle, the greater the *P* values of the corresponding gene pathways.

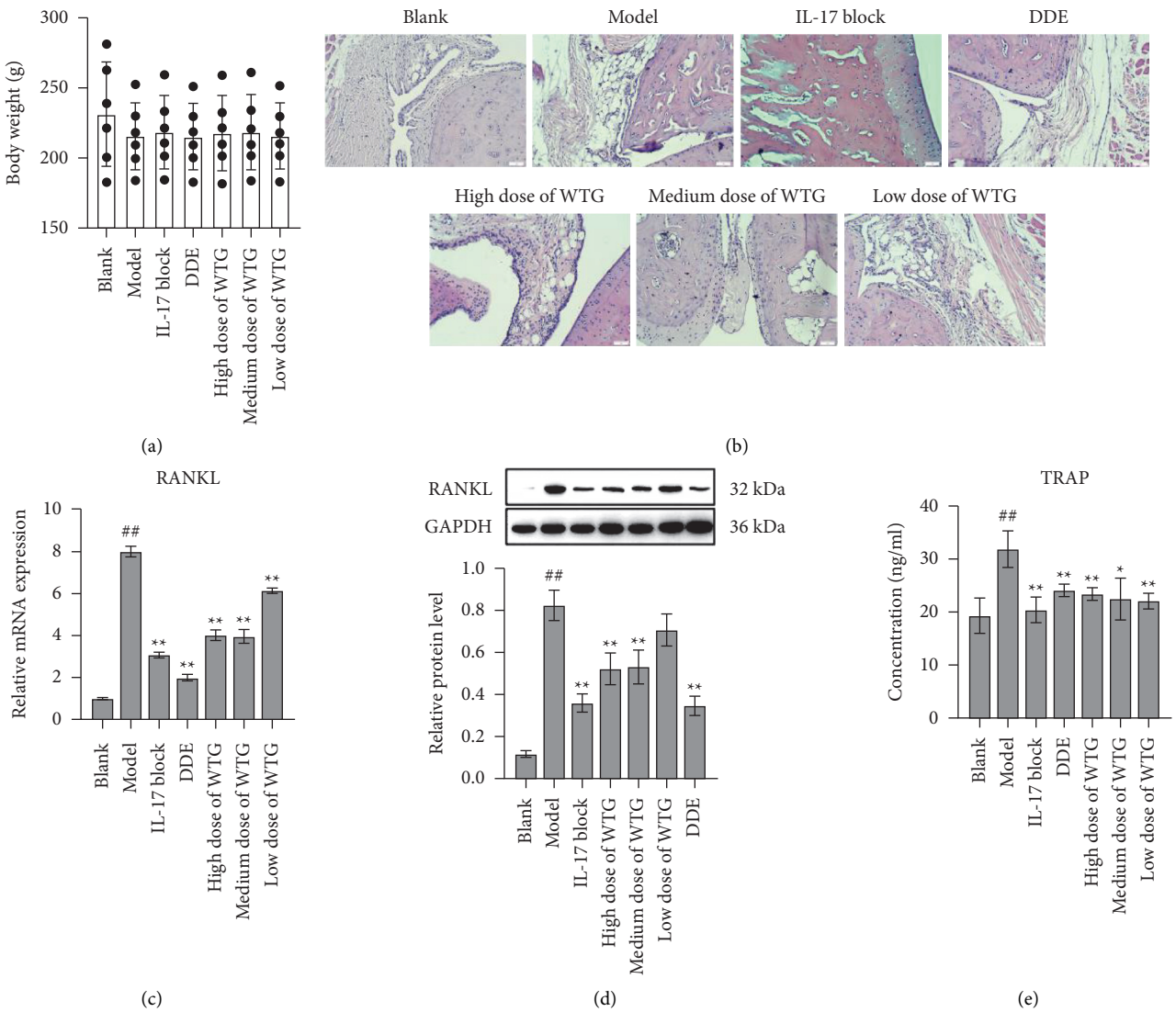

Figure 2: WTG improved bone destruction in CIA rats. (a) Changes in rat body weight after treatment with high (0.45 g/paw), medium (0.3 g/paw), and low doses (0.15 g/paw) of WTG in CIA rats. The body weight was measured before modeling. Drug administration was initiated on day 7 of the CIA modeling, and body weight was measured once a week for 4 consecutive weeks. (b) Histopathological changes in joint tissues after 4 weeks of drug administration. Scale bar = 50 μm. (c) RANKL mRNA levels in joint tissues. (d) RANKL protein levels in joint tissues were tested by Western blot. (e) TRAP levels in serum by ELISA kit. Protein quantification was determined by Image J Mean comparison of multiple groups was subjected to one-way ANOVA with Turkey test. $n = 10$, $^{\#\#}P < 0.01$, compared to Blank; $^{**}P < 0.01$, compared to Model. DDE, diclofenac diethylamine emulsion agent.

3.4. Effect of WTG on Th17/Treg Cells. Expressions of Th17 and Treg cells in splenic lymphocytes were determined using flow cytometry. Compared with the blank group, Th17 cells in the model group increased significantly. The proportion of Th17 cells in the model group declined as the doses increased in the WTG and the IL-17 blocker groups, and the diclofenac diethylamine emulsion (DDE) control group were also markedly reduced (Figure 3(a)). Compared with the blank group, Treg cells were markedly elevated in the model group, whereas those in the WTG, IL-17 blocker, and DDE groups were increased markedly compared with the model group (Figure 3(b)). The ratio of Th17/Treg cells in the model group was significantly increased compared with the blank group. Treatment with different doses of WTG significantly decreased the ratio of Th17/Treg cells, while efficacy in the low-dose group was the least satisfactory (Figure 3(c)). Results of qRT-PCR and Western blot showed that treatment with different doses of WTG significantly decreased RORγt levels while markedly increased Foxp3 levels in the spleen tissue (Figures 3(d) and 3(e)). The results indicated that WTG could improve the balance of Th17/Treg cells in CIA rats. WTG produced similar effects on both IL-17 blockers and DDE.

3.5. Effect of WTG on Inflammatory Response. Expressions of TNF-α, IL-1, and IL-6 in joint tissues and those of IL-17, TNF-α, IL-1, IL-6, IL-10, and TGF-β in peripheral blood were determined by ELISA assay. The results revealed that levels of TNF-α, IL-1, and IL-6 in joint

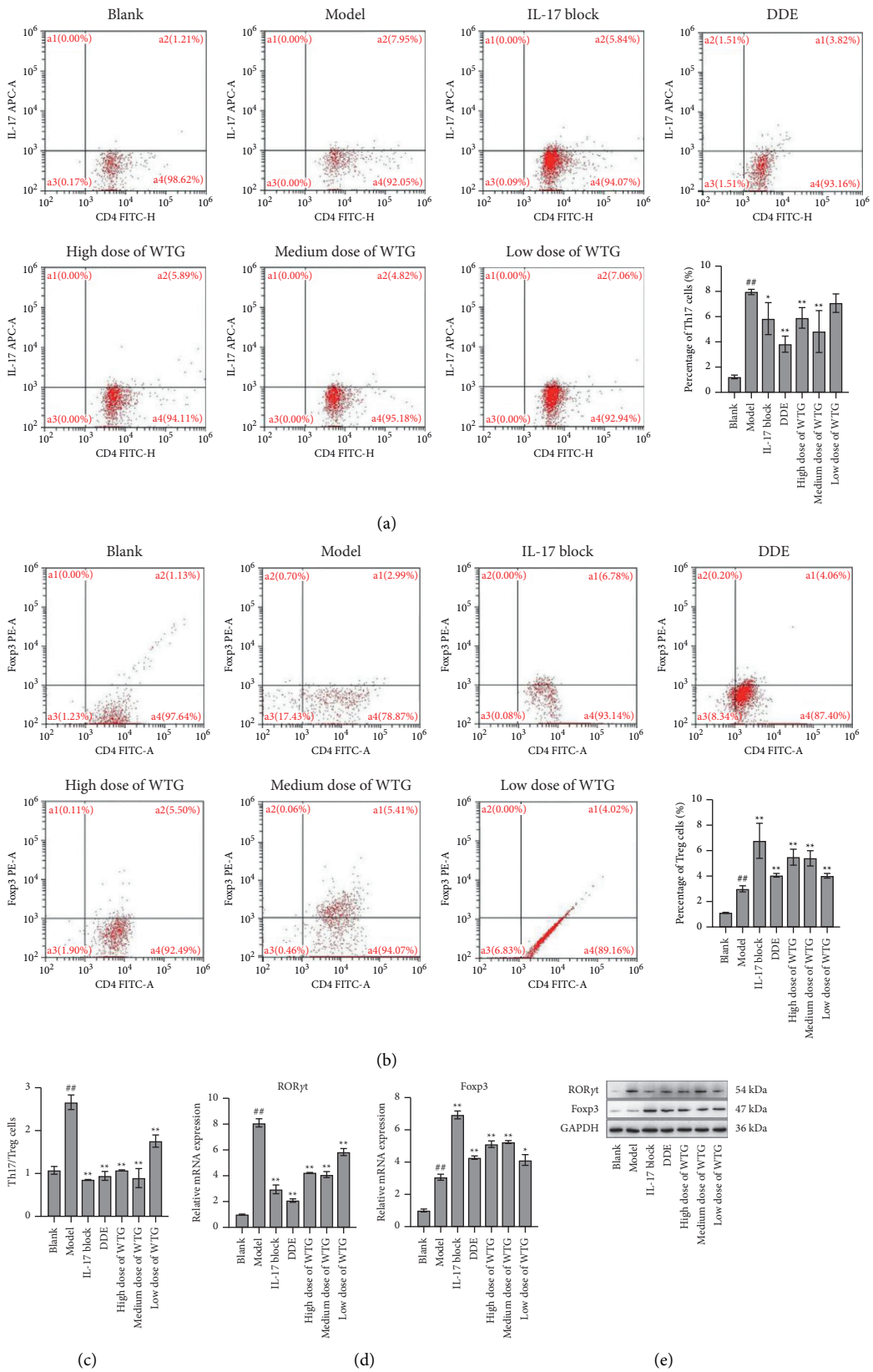

Figure 3: WTG decreased the ratio of Th17/Treg cells in CIA rats. Th17 cell ratio (a) and Treg cell ratio (b) in CD4+ cells after treatment with high (0.45 g/paw), medium (0.3 g/paw), and low doses (0.15 g/paw) of WTG. (c) Ratios of Th17/Treg cells. (d) RORγt and Foxp3 mRNA levels in the spleen tissue. (e) RORγt and Foxp3 protein levels in the spleen tissue. Mean comparison of multiple groups was subjected to one-way ANOVA with Tukey test. $n = 10$, $^{\#\#}P < 0.01$, compared to Blank; $^{*}P < 0.05$, $^{**}P < 0.01$, compared to Model. DDE, diclofenac diethylamine emulsion agent.

tissues were increased substantially in the model group when compared to the blank group, whereas those were obviously reduced following WTG administration (Figure 4(a)). In serum, the levels of anti-inflammatory cytokines IL-10 and TGF-β in WTG groups were higher than in the model group. The levels of pro-inflammatory factors IL-1, IL-17, TNF-α, and IL-6 in WTG groups were lower than in the model group. Moreover, WTG efficacy on these factors was improved with the increase of doses (Figure 4(b)).

4. Discussion

RA represents a frequently encountered chronic autoimmune disorder [29]. In TCM, it has been classified into "Bi syndrome" as a result of evil factor invasion, including wind, cold, dampness, and heat, obstructing joints, and causing pains [11]. This disease presently cannot be eradicated clinically but alleviated through some medication treatment and external application therapy to minimize joint pain and maintain the functions [30]. Numerous clinical trials have testified that TCM contributes to RA treatment with definite efficacy, safety, and less toxic side effects [31–33]. WTG is characterized by dispelling wind, dredging meridians, tonifying qi, and activating blood circulation, thereby benefiting tendon relaxation, collateral activation, blood stasis elimination, and pain relief. As a characteristic external therapy, the external application of TCM can effectively regulate the body balance by local drug penetration to dispel nearby evil and treat internal disorder via an external application [34]. Previous studies have reported that multiple Chinese herbal medicines and extracts in WTG formula produce vital effects on pain improvement in RA patients. For example, Qing-Feng-Teng (*Sinomenium Acutum*), Lei-Gong-Teng (*Tripterygium Wilfordii*), and Hei-Gu-Teng (*Periploca Forrestii Schltr.*) are effective in anti-inflammation and RA treatment [18, 35, 36]. Despite several clinical studies that have been conducted, the molecular mechanism by which WTG alleviates RA progression remains poorly understood. The advances of network pharmacology is new technique for TCM research, and the systematic and integrated research concept is in agreement with characteristics of TCM compounds including multi-components, multi-efficacy, and synergistic actions [37]. Currently, network pharmacology has achieved satisfactory results in the pharmacological mechanism of TCM [38]. The network pharmacological analysis results of WTG indicated that RA treatment might mainly act on biological processes of Th17 cell differentiation, IL-17 signaling pathway response, immune response, and inflammatory response. The present study proposed that external application of WTG might alleviate local joint inflammation and bone destruction in CIA rats by inhibiting the Th17/IL-17 signaling axis, thereby mediating Th17/Treg balance to relieve systemic inflammation through network pharmacological analysis.

Treg and Th17 participate in the occurrence and development of autoimmune diseases, tumors, and infections [39]. Treg is of great significance in autoimmune disorders, and it suppresses the secretion of antibodies produced by inflammatory cytokines and maintains the internal immune environment balance of the body [39]. In contrast to Treg, Th17 can promote the development of autoimmune diseases and mediates pro-inflammatory responses [39]. Additional research has implicated that Th17/Treg balance is the key factor to maintain the presence of RA immune homeostasis [40]. The ratio of Th17/Treg cells presenting in the peripheral blood of RA patients is markedly increased and correlated with disease activity [41]. The controlled Th17/Treg ratio assists in alleviating RA and alleviates disease symptoms, and it also plays a key role in treating autoimmune diseases namely RA [42]. The present study detected spleen lymphocytes in CIA rats by flow cytometry assays and the findings indicated that both medium and low doses of WTG therapy could reduce the Th17/Treg ratio and restore to a certain level, whereas the effect of low-dose group was less effective. Transcription factors are well recognized to be pivotal in cell differentiation and development. RORγt acts as an essential transcription factor in Th17 cells, and its deletion leads to a reduced Th17 cell population and a decreased incidence of autoimmune diseases. Foxp3 is currently recognized as the most sensitive marker and a specific transcription factor of Treg cells. Foxp3 depletion inhibits the differentiation of Treg cells [43]. Foxp3 and RORγt antagonize each other, and their balance can determine the direction of initial $CD4^+$ T cell differentiation to Th17 or Treg cells after antigen stimulation, which affects RA occurrence and development [44]. Our results showed that WTG treatment elevated the expression level of Foxp3 and decreased that of RORγt in the spleen tissues of CIA rats. The results further confirmed that WTG could mediate the expressions of Foxp3 and RORγt, thereby regulating the differentiation of Th17/Treg cells and restoring their ratios to a certain extent.

Th17 mostly secretes the inflammatory mediator IL-17, representing an important pro- and pre-inflammatory cytokine and a fine-tuning factor of the inflammatory response [45]. It also participates in the inflammatory response and progressive damage of RA in multiple ways [46]. IL-17 can induce synovial fibroblasts, osteoclasts, and macrophages to secrete pro-inflammatory cytokines TNF-α, IL-1, and IL-6, which aggravates joint inflammation and causes the occurrence and development of RA [46]. Conversely, Treg cells can secrete anti-inflammatory cytokines IL-10 and TGF-β, inhibit T cells and antigen presentation cells, and exert an immunosuppressive effect by reducing the proinflammatory cytokines secretion [47]. TGF-β influences the differentiation of Th17 cells and participates in regulating Treg functions, especially to maintain the balance of Th17/Treg [48]. The expression levels of TNF-α, IL-1, and IL-6 in the joint tissues of the CIA model group in the current study were markedly higher than those of the blank group. Following external application using WTG, the expressions of TNF-α, IL-1 and IL-6 were largely downregulated compared with the model group. Serum detection results were similar, and external application of WTG to CIA rats reduced the expressions of TNF-α, IL-1, IL-6, and IL-17 in a dose-dependent manner. Furthermore, WTG treatment elevated the expression levels of IL-10 and TGF-β in the serum of CIA rats. The

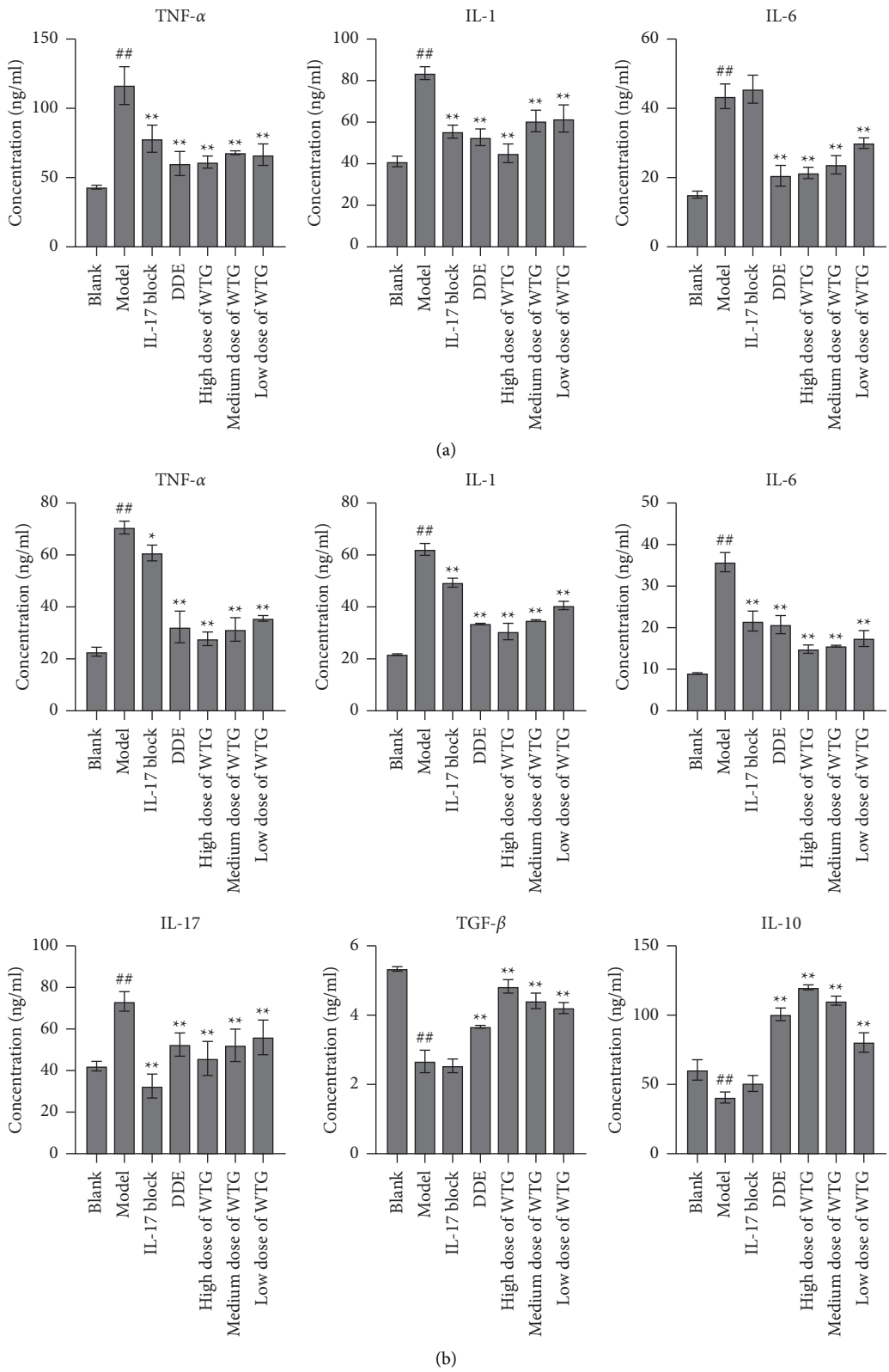

Figure 4: WTG inhibited pro-inflammatory cytokines in CIA rats. (a) Levels of TNF-α, IL-1, and IL-6 in the joint tissues were measured by ELISA assay. (b) Levels of TNF-α, TGF-β, IL-1, IL-6, IL-10, and IL-17 in the serum were measured by ELISA assay. Mean comparison of multiple groups was subjected to one-way ANOVA with the Tukey test. $n = 10$, $^{\#\#}P < 0.01$, compared to Blank; $^{*}P < 0.05$, $^{**}P < 0.01$, compared to Model. DDE, diclofenac diethylamine emulsion agent.

previously described results indicated that WTG treatment in CIA rats could effectively reduce the proinflammatory cytokines IL-17 secreted by Th17 cells and TNF-α, IL-1, and IL-6 induced by Th17 cells, thereby affecting the differentiation of Th17 and Treg and alleviating inflammatory responses of CIA rats.

The principal clinical manifestations of RA are multiple joint erosive synovitis, and the major pathological changes include synovial tissue hyperplasia and the progressive destruction of articular cartilage and bones [6]. The results of HE staining of joint tissues demonstrated that inflammatory cells were reduced in the medium and high dose WTG groups, and the surface of articular cartilage was slightly rough with complete structure in the absence of evident damage of cartilage and bone tissue, suggesting that WTG greatly improved local joint inflammation and bone damage in CIA rats. Previous studies have confirmed that RANKL is highly expressed in RA patients and promotes synovitis and bone destruction in RA [49]. IL-17 can upregulate the expression of RANK, the precursor of osteoclasts, enhance the RANKL signaling pathway and facilitate the differentiation of osteoclasts by inducing RANKL expression [50]. Okamoto and Takayanagi have shown that Treg cells can reduce osteoclast formation by inhibiting the RANKL pathway [51]. Furthermore, IL-10 and TGF-β secreted by Treg can downregulate the expression of RANKL and reduce bone injury [51]. Our results indicated that WTG treatment could substantially reduce the expression of the RANKL gene and protein in the joint tissues of CIA rats, suggesting that WTG might reduce the level of RANKL by inhibiting IL-17 and upregulating IL-10 and TGF-β, thereby improving local joint inflammation and bone destruction.

5. Conclusion

Taken together, this study elucidated that WTG could reduce expressions of pro-inflammatory factors IL-17, TNF-α, IL-1, and IL-6, and increase expressions of anti-inflammatory factors IL-10 and TGF-β. These results indicated that WTG might improve the Th17/Treg imbalance of immune cells in CIA arthritis rats, thereby contributing to alleviating joint inflammation and bone destruction. In future research, we will further explore the molecular mechanism of key monomers in WTG, and use technologies such as molecular docking and microscale thermophoresis to further clarify the direct regulation of WTG.

Data Availability

The data used to support the findings of this study are included within the article.

Additional Points

Highlights. (1) WTG ameliorated the articular inflammation, effectively inhibited the destruction of articular cartilage, and decreased the ratios of Th17 and Treg cells. (2) WTG effectively inhibited the levels of inflammatory cytokines and RNAKL and increased the levels of anti-inflammatory cytokines. (3) WTG might improve the imbalance of Th17/Treg cells in CIA rats by regulating the differentiation of Th17 and Treg cells.

Disclosure

Xueming Yao and Qiuyi Wang are co-first authors.

Conflicts of Interest

The authors declare that there are no conflicts of interest.

Acknowledgments

This work was supported by the National Natural Science Foundation of China (81804127 and 81760884), Guizhou Province Science and Technology Plan Project (Qian Ke He Platform Talents (2016) 5650 and (2020) 2202, Qian Ke He Support (2021) general 006; Qian Ke He Basis (2020]) 1Y361), and National Key Research and Development Program: Research on Modernization of Traditional Chinese Medicine (2017YFC1703904).

References

[1] H. Wang, D. Yang, L. Li, S. Yang, G. Du, and Y. Lu, "Anti-inflammatory effects and mechanisms of rhein, an anthraquinone compound, and its applications in treating arthritis: a review," *Natural Products and Bioprospecting*, vol. 10, no. 6, pp. 445–452, 2020.

[2] M. Zamanpoor, "The genetic pathogenesis, diagnosis and therapeutic insight of rheumatoid arthritis," *Clinical Genetics*, vol. 95, no. 5, pp. 547–557, 2019.

[3] M. Noack and P. Miossec, "Th17 and regulatory T cell balance in autoimmune and inflammatory diseases," *Autoimmunity Reviews*, vol. 13, no. 6, pp. 668–677, 2014.

[4] W. Wang, S. Shao, Z. Jiao, M. Guo, H. Xu, and S. Wang, "The Th17/Treg imbalance and cytokine environment in peripheral blood of patients with rheumatoid arthritis," *Rheumatology International*, vol. 32, no. 4, pp. 887–893, 2012.

[5] A. A. ElAtta, Y. Ali, I. Bassyouni, and R. Talaat, "Correlation of myomir-206 and proinflammatory cytokines (IL-16 and IL-17) in patients with rheumatoid arthritis," *Reumatologia/Rheumatology*, vol. 57, no. 2, pp. 72–77, 2019.

[6] N. Komatsu and H. Takayanagi, "Inflammation and bone destruction in arthritis: synergistic activity of immune and mesenchymal cells in joints," *Frontiers in Immunology*, vol. 3, p. 77, 2012.

[7] A. Anel, A. Gallego-Lleyda, D. de Miguel, J. Naval, and L. Martínez-Lostao, "Role of exosomes in the regulation of T-cell mediated immune responses and in autoimmune disease," *Cells*, vol. 8, no. 2, p. 154, 2019.

[8] F. Tavasolian, A. Z. Hosseini, S. Soudi, and M. Naderi, "miRNA-146a improves immunomodulatory effects of MSC-derived exosomes in rheumatoid arthritis," *Current Gene Therapy*, vol. 20, no. 4, pp. 297–312, 2020.

[9] F. Tavasolian, A. S. Moghaddam, F. Rohani et al., "Exosomes: effectual players in rheumatoid arthritis," *Autoimmunity Reviews*, vol. 19, no. 6, Article ID 102511, 2020.

[10] Y. Ding, L. Wang, H. Wu, Q. Zhao, and S. Wu, "Exosomes derived from synovial fibroblasts under hypoxia aggravate rheumatoid arthritis by regulating Treg/Th17 balance,"

Experimental Biology and Medicine, vol. 245, no. 14, pp. 1177–1186, 2020.

[11] L. Zhang, Z. Cao, Y. Yang, X. Tan, J. Mao, and L. Su, "Traditional Chinese medicine on treating active rheumatoid arthritis: a protocol for systematic review and meta-analysis," *Medicine (Baltimore)*, vol. 99, no. 24, Article ID e20642, 2020.

[12] S. Li, "Advances in TCM symptomatology of rheumatoid arthritis," *Journal of Traditional Chinese Medicine*, vol. 22, pp. 137–142, 2002.

[13] W. Wang, X. Wang, X. Tang, Q. Jiang, and Y. Fan, "Classifying rheumatoid arthritis by traditional Chinese medicine Zheng: a multi-center cross-sectional study," *Journal of Traditional Chinese Medicine*, vol. 39, pp. 425–432, 2019.

[14] M. Abbasi, M. J. Mousavi, S. Jamalzehi et al., "Strategies toward rheumatoid arthritis therapy; the old and the new," *Journal of Cellular Physiology*, vol. 234, no. 7, pp. 10018–10031, 2019.

[15] S. N. Ma, H. Zaman Huri, and F. Yahya, "Drug-related problems in patients with rheumatoid arthritis," *Therapeutics and Clinical Risk Management*, vol. 15, pp. 505–524, 2019.

[16] Q. Xing, L. Fu, Z. Yu, and X. Zhou, "Efficacy and safety of integrated traditional Chinese medicine and western medicine on the treatment of rheumatoid arthritis: a meta-analysis," *Evidence-Based Complementary and Alternative Medicine*, vol. 2020, Article ID 4348709, 15 pages, 2020.

[17] Y. F. Wong, H. Zhou, J. R. Wang, Y. Xie, H. X. Xu, and L. Liu, "Anti-inflammatory and analgesic effects and molecular mechanisms of JCICM-6, a purified extract derived from an anti-arthritic Chinese herbal formula," *Phytomedicine*, vol. 15, no. 6-7, pp. 416–426, 2008.

[18] K. Zheng, Z. Chen, W. Sun et al., "Hei-Gu-Teng Zhuifenghuoluo granule modulates IL-12 signal pathway to inhibit the inflammatory response in rheumatoid arthritis," *Journal of Immunology Research*, vol. 2018, Article ID 8474867, 10 pages, 2018.

[19] W. Zhang, F. Li, and W. Gao, "Tripterygium wilfordii inhibiting angiogenesis for rheumatoid arthritis treatment," *Journal of the National Medical Association*, vol. 109, no. 2, pp. 142–148, 2017.

[20] Y. Wang, L. Jia, and C.-y. Wu, "Triptolide inhibits the differentiation of Th17 cells and suppresses collagen-induced arthritis," *Scandinavian Journal of Immunology*, vol. 68, no. 4, pp. 383–390, 2008.

[21] J.-H. Nho, H.-J. Lee, H.-K. Jung et al., "Effect of Saururus chinensis leaves extract on type II collagen-induced arthritis mouse model," *BMC Complementary and Alternative Medicine*, vol. 19, no. 1, p. 2, 2019.

[22] P. Larsson, S. Kleinau, R. Holmdahl, and L. Klareskog, "Homologous type II collagen-induced arthritis in rats," *Arthritis & Rheumatism*, vol. 33, no. 5, pp. 693–701, 1990.

[23] J. Zhang, X. Hu, X. Dong et al., "Regulation of T Cell activities in rheumatoid arthritis by the novel fusion protein IgD-Fc-Ig," *Frontiers in Immunology*, vol. 11, p. 755, 2020.

[24] S. R. Jitta, P. Daram, K. Gourishetti et al., "Terminalia tomentosa bark ameliorates inflammation and arthritis in carrageenan induced inflammatory model and Freund's adjuvant-induced arthritis model in rats," *Journal of Toxicology*, vol. 2019, Article ID 7898914, 11 pages, 2019.

[25] Z. Wang, W. Yang, P. Yang, B. Gao, and L. Luo, "Effect of radix stemonae concentrated decoction on the lung tissue pathology and inflammatory mediators in COPD rats," *BMC Complementary and Alternative Medicine*, vol. 16, no. 1, p. 457, 2016.

[26] Z. Du, Z. Shu, W. Lei et al., "Integration of metabonomics and transcriptomics reveals the therapeutic effects and mechanisms of Baoyuan decoction for myocardial ischemia," *Frontiers in Pharmacology*, vol. 9, p. 514, 2018.

[27] J. Liu, X. Hong, D. Lin, X. Luo, M. Zhu, and H. Mo, "Artesunate influences Th17/Treg lymphocyte balance by modulating Treg apoptosis and Th17 proliferation in a murine model of rheumatoid arthritis," *Experimental and Therapeutic Medicine*, vol. 13, no. 5, pp. 2267–2273, 2017.

[28] L. Liu, D. Tian, C. Liu, K. Yu, and J. Bai, "Metformin enhances functional recovery of peripheral nerve in rats with sciatic nerve crush injury," *Medical Science Monitor*, vol. 25, pp. 10067–10076, 2019.

[29] M. DiBaise and S. Kohn, "Diagnosing and managing patients with rheumatoid arthritis," *Journal of the American Academy of Physician Assistants*, vol. 34, no. 5, pp. 27–34, 2021.

[30] L. Terslev, C. H. Brahe, M. Østergaard et al., "Using a DAS28-CRP-steered treat-to-target strategy does not eliminate subclinical inflammation as assessed by ultrasonography in rheumatoid arthritis patients in longstanding clinical remission," *Arthritis Research and Therapy*, vol. 23, no. 1, p. 48, 2021.

[31] J.-Y. Wang, X.-J. Chen, L. Zhang et al., "Comparative studies of different extracts from Eucommia ulmoides oliv. against rheumatoid arthritis in CIA rats," *Evidence-Based Complementary and Alternative Medicine*, vol. 2018, Article ID 7379893, 11 pages, 2018.

[32] Z. Wang, J. Wu, D. Li et al., "Traditional Chinese medicine Biqi capsule compared with leflunomide in combination with methotrexate in patients with rheumatoid arthritis: a randomized controlled trial," *Chinese Medicine*, vol. 15, no. 1, p. 36, 2020.

[33] Y.-t. He, A.-h. Ou, X.-b. Yang et al., "Traditional Chinese medicine versus western medicine as used in China in the management of rheumatoid arthritis: a randomized, single-blind, 24-week study," *Rheumatology International*, vol. 34, no. 12, pp. 1647–1655, 2014.

[34] S. Zhang, P. Wang, X. Shi, and H. Tan, "Inhibitory properties of Chinese herbal formula SanHuang decoction on biofilm formation by antibiotic-resistant Staphylococcal strains," *Scientific Reports*, vol. 11, no. 1, p. 7134, 2021.

[35] Z. Shu, Y. Cao, Y. Tao et al., "Polyvinylpyrrolidone microneedles for localized delivery of sinomenine hydrochloride: preparation, release behavior of in vitro & in vivo, and penetration mechanism," *Drug Delivery*, vol. 27, no. 1, pp. 642–651, 2020.

[36] J. Y. Lee, B. H. Lee, N. D. Kim, and J. Y. Lee, "Celastrol blocks binding of lipopolysaccharides to a toll-like receptor4/myeloid differentiation factor2 complex in a thiol-dependent manner," *Journal of Ethnopharmacology*, vol. 172, pp. 254–260, 2015.

[37] S. Li and B. Zhang, "Traditional Chinese medicine network pharmacology: theory, methodology and application," *Chinese Journal of Natural Medicines*, vol. 11, no. 2, pp. 110–120, 2013.

[38] R. Zhang, X. Zhu, H. Bai, and K. Ning, "Network pharmacology databases for traditional Chinese medicine: review and assessment," *Frontiers in Pharmacology*, vol. 10, p. 123, 2019.

[39] I. Mohammad, K. Nousiainen, S. D. Bhosale et al., "Quantitative proteomic characterization and comparison of T helper 17 and induced regulatory T cells," *PLoS Biology*, vol. 16, no. 5, Article ID e2004194, 2018.

[40] A. Paradowska-Gorycka, A. Wajda, K. Romanowska-Próchnicka et al., "Th17/Treg-related transcriptional factor expression and cytokine profile in patients with rheumatoid arthritis," *Frontiers in Immunology*, vol. 11, Article ID 572858, 2020.

[41] D. S. Kim, H.-K. Min, E. K. Kim et al., "Suberoylanilide hydroxamic acid attenuates autoimmune arthritis by suppressing Th17 cells through NR1D1 inhibition," *Mediators of Inflammation*, vol. 2019, Article ID 5648987, 11 pages, 2019.

[42] Y. Takeuchi, K. Hirota, and S. Sakaguchi, "Synovial tissue inflammation mediated by autoimmune T cells," *Frontiers in Immunology*, vol. 10, no. 1989, 2019.

[43] T.-Y. Shao, L.-H. Hsu, C.-H. Chien, and B.-L. Chiang, "Novel Foxp3-IL-10-regulatory T-cells induced by B-cells alleviate intestinal inflammation in vivo," *Scientific Reports*, vol. 6, no. 1, Article ID 32415, 2016.

[44] Y. K. Lee and S. K. Mazmanian, "Has the microbiota played a critical role in the evolution of the adaptive immune system?" *Science*, vol. 330, no. 6012, pp. 1768–1773, 2010.

[45] N. C. Brembilla, L. Senra, and W.-H. Boehncke, "The IL-17 family of cytokines in psoriasis: IL-17A and beyond," *Frontiers in Immunology*, vol. 9, p. 1682, 2018.

[46] L. S. Taams, "Interleukin-17 in rheumatoid arthritis: trials and tribulations," *Journal of Experimental Medicine*, vol. 217, no. 3, 2020.

[47] Q. Dai, J. Li, Y. Yun, and J. Wang, "Toll-Like receptor 4-myeloid differentiation primary response gene 88 pathway is involved in the shikonin treatment of CIA by regulating Treg/Th17 expression," *Evidence-Based Complementary and Alternative Medicine*, vol. 2018, Article ID 2428546, 9 pages, 2018.

[48] L. Zhu, F. Hua, W. Ding, K. Ding, Y. Zhang, and C. Xu, "The correlation between the Th17/Treg cell balance and bone health," *Immunity & Ageing*, vol. 17, no. 1, p. 30, 2020.

[49] M. Papadaki, V. Rinotas, F. Violitzi et al., "New insights for RANKL as a proinflammatory modulator in modeled inflammatory arthritis," *Frontiers in Immunology*, vol. 10, p. 97, 2019.

[50] L. Abusleme and N. Moutsopoulos, "IL-17: overview and role in oral immunity and microbiome," *Oral Diseases*, vol. 23, no. 7, pp. 854–865, 2017.

[51] K. Okamoto and H. Takayanagi, "Regulation of bone by the adaptive immune system in arthritis," *Arthritis Research and Therapy*, vol. 13, no. 3, p. 219, 2011.

Hindawi
Evidence-Based Complementary and Alternative Medicine
Volume 2022, Article ID 6821388, 9 pages
https://doi.org/10.1155/2022/6821388

Research Article

Jin-Wu-Jian-Gu Formulation Attenuates Rheumatoid Arthritis by Inhibiting the IL33-ST2 Signaling Pathway

Daomin Lu,[1] Ying Huang,[1,2] Wukai Ma,[1] Changming Chen,[1] and Lei Hou[1]

[1]*Department of Rheumatology and Immunology, The Second Affiliated Hospital of Guizhou University of Traditional Chinese Medicine, Fei Shan Street, Guiyang 550001, China*
[2]*Guizhou Medical University, Beijing Road, Guiyang, Guizhou Province 550004, China*

Correspondence should be addressed to Wukai Ma; fsmymwk@163.com

Received 28 October 2021; Accepted 29 November 2021; Published 20 January 2022

Academic Editor: Atul Kabra

The present research attempted to investigate the molecular mechanism of Jin-Wu-Jian-Gu Formulation (JWJGF) in inhibiting rheumatoid arthritis (RA) in a pharmacological approach for analysis and experimental validation. First, the potential targets and pathways of JWJGF for RA were predicted by network pharmacology. Second, the effect of JWJGF on RA was observed by hematoxylin-eosin (HE) staining and enzyme-linked immunosorbent assay (ELISA). Further, we observed the effects of JWJGF on the IL33-ST2 signaling pathway by Western blot and quantitative real-time PCR (qPCR) experiments, and finally, we studied the effects of Liquiritigenin on rheumatoid arthritis synovial fibroblast (RASF) cells and the IL33-ST2 signaling pathway. Network pharmacology results showed that the key component of JWJGF was Liquiritigenin and the core target of JWJGF was IL-33. The results of HE and ELISA showed that JWJGF could alleviate RA. Western blot and qPCR findings indicated that JWJGF could inhibit the IL33-ST2 signaling pathway. Furthermore, JWJGF could inhibit the proliferation of RASF cells and the IL33-ST2 signaling pathway. In conclusion, this study revealed that JWJGF attenuated RA by inhibiting the IL33-ST2 signaling pathway.

1. Introduction

RA represents a frequently encountered chronic systemic disorder in the immune system. It is characterized by infiltration of a large number of inflammatory cells, proliferation of synovial tissue, increase of inflammatory factors, and serious damage of articular cartilage and bone tissue. Abnormal proliferation and inhibition of apoptosis of RASF develop in RA patients, which promotes the development of RA [1–4].

Interleukin- (IL-) 33 is a cytokine of the IL-1 family originating from epithelial cells. The receptor for IL-33, growth stimulation expressed gene 2 (ST2), is expressed in a wide range of cells including immunocytes. ST2 has two main forms: soluble growth stimulation expressed gene 2 (sST2) and transmembrane (ST2). A study has reported that the organism can release intracellular IL-33 under stress and infection, which plays an important role in an allergic reaction, inflammation, autoimmune disease, and host defense [5–7].

JWJGF is a long-term clinical study of the vaccine prescription of this research group. It produces a satisfactory curative effect on RA. JWJGF is composed of *Herba Cibotium barometz* (JM), *Herba homalomena* (QN), *Herba Periploca forrestii Schltr* (HG), *Herba Zaocys dhumnades* (WS), *Herba Sabia parviflora Wall* (XH), and *Herba pseudoginseng* (SQ). Liquiritigenin (LQ) is a common component of SQ and QN. As a dihydroflavonoid compound, LQ exerts certain effects on the cardiovascular system and nervous system. In addition, it functions in antivirus, antioxidant, antitumor, and other pharmacological effects [8–11].

Initially, the possible targets and pathways of JWJGF for RA were predicted using network pharmacology and it was found that the key component of the JWJGF was LQ and the core target of the JWJGF was IL-33. Subsequently, the effect of JWJGF on RA was verified by constructing an RA model. Further, the role and molecular mechanism of JWJGF were investigated through Western blot and qPCR experiments.

Finally, we examined the effects of LQ on RASF cells and the IL33-ST2 signaling pathway.

2. Methods

2.1. Experimental Herbal Formulation. JWJGF is a long-term clinical study of the vaccine prescription of this research group, which has been proved to exert a satisfactory curative effect on RA. Herbs were immersed in 1 000 mL drinking water for 1 h before decoction for 30 min. All of the medicine was decocted with 500 mL water for 30 min. Both were mixed and concentrated to 1 g/mL of the raw medicine by evaporation.

2.2. Experimental Animals. Male Sprague Dawley (SD) rats weighing approximately 150–180 g were prepared. Animal experiments were approved and performed as per the guidelines of Committee on the Ethics of Animal Experiments of the Second Affiliated Hospital of Guizhou University of Traditional Chinese Medicine, China. The laboratory animal license is SCXK (Xiang) 2019–0004. The laboratory animals were fed under a condition of 12 h light-dark alternatives with food and water available at will.

The rats were randomly classified into 7 groups as follows: control group, RA model group, RA + prednisone group, RA + GTW group, RA + L-JWJGF group, RA + M-JWJGF group, and RA + H-JWJGF group ($n = 15$/group). Complete Freund's adjuvant at 0.1 mL was commenced by intradermal administration into the left posterior metatarsal footpad to induce arthritis. On day 12 following model establishment, the rats in the control group were given intradermal injections while the remaining groups were given 0.5% sodium carboxymethylcellulose intragastrically. The animals were treated with prednisone (50 mg/kg) and glycosides of *Tripterygium wilfordii* (GTW, 100 mg/kg) by gavage. The low-dose JWJGF group was administered at a dose of 5 g/kg, the medium-dose JWJGF group of 10 g/kg, and the high-dose JWJGF group of 20 g/kg, and all were given by gavage. The treatment of the three groups lasted for four weeks.

2.3. Cell Cultures and Experimental Treatments. RASF cells were bought from American Type Culture Collection (ATCC) (Manassas, USA), grown in DMEM by addition of 10% fetal bovine serum and followed by administration of Liquiritigenin (50, 100, and 150 μM), prednisone (200 ng/mL), and glycosides of *Tripterygium wilfordii* (30 μg/mL) for 24 h.

2.4. Network Pharmacology Analysis. Targets of active components contained in JWJGF were retrieved from website (http://www.swisstargetprediction.ch/). The human RA genes were screened out from GeneCards (https://www genecards.org/), a disease database. A PPI network diagram was created and exported from String (https://string-db.org/), and a drug-component-target network was constructed via Cytoscape 3.6.0. The GO analysis and KEGG pathway analysis were performed on target sites using ClueGO, a plugin of the Cytoscape software, and the enrichment analysis results were visualized ultimately.

2.5. Western Blot Analysis. Cells were collected and added to radio-immunoprecipitation assay (RIPA) lysate including PMSF and proteinase inhibitor cocktail. Following treatment at 4°C and 13 000 rpm centrifugation for 20 min, the supernatant was transferred into a precooled 1.5 mL centrifuge tube for concentration determination. Total protein was added at a quantity of 30 μg/well, boiled at 100°C for 10 min, separated by 10% polyacrylamide gel electrophoresis (SPS-PAGE), and followed by transference to a phenylmethanesulfonyl fluoride (PDVF) membrane. Following being sealed with 5% skimmed milk for 1 h at room temperature, the membrane was rinsed 3 times using TBST, 5 min each time. BSA primary antidilution solution at 3% was diluted with 1 : 1 000~2 000, incubated at 4°C overnight, and incubated by supplemented secondary antidilution solution (1 : 1 000) for 1 h on the next day.

2.6. qPCR Assay. Total RNA extraction was subsequently performed using Trizol reagent (Takara, Japan) as per the instructions of use. The reverse transcription of CDNA was conducted using PrimeScript TMR *T* kit (Takara, Japan). The response system and procedures for qRT-PCR were conducted as described in the instructions of TB Green Premix Ex Taq II (Takara, Japan), and a real-time system employed CFX96 (Bio-Rad, USA). Relative expression levels of genes were calculated using the $2^{-\Delta\Delta CT}$ algorithm. Primer sequence of each gene was as follows: sST2-F(GGTGTGACCGACAAGGACT), sST2-R(TTGTGAGAGACACTCCTTAC), ST2L-F(AGTTGTGCATTTACGGGAGAG), ST2L-R(GGATACTGCTTTCCACCACAG), IL-33-F(GTGCAGGAAAGGAAGACTCG), IL-33-R(TGGCCTCACCATAAGAAAGG), GAPDH-F(GCAAGTTCAACGGCACAG), and GAPDH-R(GCCAGTAGACTCCACGACATA).

2.7. EDU Assay. RASF cells were inoculated into a 24-well plate. According to the instructions of the EdU kit, 2 × EdU reaction solution was prepared and added to a 24-well plate. The cells were incubated in the reaction solution for 2 h in the dark, fixed by 4% paraformaldehyde for 20 min at room temperature, and supplemented with 500 μL 0.3% Triton X-100. After reaction for 10 min at room temperature, the cells were rinsed 3 times using PBS. AZIDE 555-Click reaction solution was prepared, and 200 μL was added to each well and incubated in the dark at room temperature for 30 min. Following the removal of the reaction solution and three cycles of washing with PBS, the nucleus was restained by Hoechst, and immunofluorescence was conducted subsequently.

2.8. TUNEL Assay. The slides were fixed with paraformaldehyde at room temperature for 15–30 min and followed by three cycles of washing with PBS. A sealing medium was

subsequently supplied for cell culture at room temperature for 10 min. After rinsing with PBS, the cells were added with a membrane-penetrating solution and incubated at room temperature for 30 min. The TUNEL reaction mixture was prepared and then mixed with 50 μL TdT+450 μL fluorescein-labeled dUTP solution. Reaction time was set as 30 min at room temperature. The cells were added with 50 μL TUNEL reaction mixture, and reacted in a dark wet chamber at 37°C for 60 min. The apoptotic cells were counted under a fluorescence microscope with 1 drop of PBS.

2.9. HE Staining. Freshly prepared paraformaldehyde (4%) was employed to fix the samples and sections were embedded in paraffin as per routine histological procedures. After that, the sections were made into 4.5 μm thickness and ready for hematoxylin and eosin (HE) staining. Following the scanning of the stained slides using Pannoramic Scan 250 Flash, photographs were captured using Pannoramic Viewer.

2.10. ELISA Assay. Quantification of inflammatory cytokines TNF-α, TNF-γ, IL-1, IL-5, IL-6, IL-13 IL-17, and IL-1β in rat serum was detected by ELISA (Kehua Bio-Engineering, Shanghai, China), and all procedures were performed as the description of the manufacturer's instructions.

2.11. Statistical Analysis. SPSS 23.0 was used to analyze the data. The mean of both groups of independent samples was compared using *t*-tests, and the mean value of multiple groups of samples was analyzed by one-way ANOVA, $P < 0.05$. The experimental results were expressed as mean value ± standard deviation and each experiment was repeated three times independently.

3. Results

3.1. Common Targets and Network Visualization of JWJGF and RA. To elucidate the potential action mechanism of JWJGF in RA, we first predicted 592 targets of JWJGF active components in the SwissTargetPrediction database, screened 1374 targets of RA-related genes in the GeneCards database, and obtained 241 overlapped genes as the Venn diagram presented (Figure 1(a)). Finally, Cytoscape 3.6 was used to analyze JWJGF, its components, and targets and a drug-active component-target network diagram was plotted. We found that Liquiritigenin had the most connections, and CYP19A1, ESR2, F2, and IL-33 were the potential target proteins (Figure 1(b)). IL-33 was an epithelial cell-derived cytokine found in recent years which could bind with the ST2 receptor to regulate inflammatory factor secretion. There were two secretions of IL-33: active secretion by immune cells and passive excretion by damaged cells. ST2 was a high-affinity receptor for IL-33, and it presented in many immune cells and nonconstructive blood cells. It was found that IL-33 could be released after stress and infection, which played an important role in an allergic reaction, inflammation, autoimmune disease, and host defense.

3.2. Effect of JWJGF on the Fibroblast-like Synoviocyte Proliferation and Inflammatory Factors of RA Rats. The main pathological changes of RA are synovial tissue hyperplasia and infiltration of inflammatory cells. The joint synovial tissue cells from the control group were arranged regularly in the absence of both synovial cell hyperplasia and inflammatory cell infiltration. Conversely, hyperemia and edema were recorded in the synovial tissues of RA group. Meanwhile, the apparent proliferation of synovial cells, inflammatory infiltration, and chondrocyte injury was revealed. The hyperemia and edema of synovial tissues in the low- and medium-dose groups of JWJGF decreased slightly, and a small number of synovial cells proliferated inflammatory cells infiltrated. In RA + prednisone group and RA + GTW group, slightly hyperemia, edema, synovial cell proliferation, and a few inflammatory cells infiltration were revealed in the synovial tissues. There was no hyperemia, edema, nor synovial cell proliferation but only a little inflammatory cell infiltration was visualized in the synovial tissues of JWJGF group (Figure 2(a)). There are many inflammatory factors that participated in the pathogenesis of RA. TNF-α and IL-1 are recognized as the most important factors, and both of them usually exist at the same time. TNF-α and IL-1 are mainly secreted by monocytes and macrophages. TNF-α is an important physiological inflammatory mediator. TNF-α is secreted at high levels in the active or progressive stage of RA disease, which can cause local joint destruction and corresponding clinical symptoms. At present, it is suggested that the mechanism of TNF-α and IL-1β inducing joint inflammation is to promote the activation and induction of synovial cells and chondrocytes. Meanwhile, the synthesis of a series of inflammatory mediators, IL-8 and IL-6, produces a powerful proinflammatory effect, leading to synovial inflammation, cartilage destruction, and bone erosion, thereby stimulating the proliferation of synovial fibroblasts. The results of ELISA showed that the expressions of TNF-α, TNF-γ, IL-1, IL-5, IL-6, IL-13, IL-17, and IL-1β in the serum of rats were markedly higher in the model group than those of the control group ($P < 0.01$). Conversely, the serum levels of TNF-α, TNF-γ, IL-1, IL-5, IL-6, IL-13, IL-17, and IL-1β in JWJGF, prednisone, and GTW groups were all decreased to a different extent compared with the control group, and the expression level of Jin-Wu-Jian-Gu decoction in high-dose group was substantially lower than RA group ($P < 0.01$). However, no significant difference was revealed between the prednisone and GTW groups ($P > 0.05$) (Figure 2(b)). The results showed that JWJGF could fight against inflammation by downregulating the inflammatory factors (TNF-α, TNF-γ, IL-1, IL-5, IL-6, IL-13, IL-17, and IL-1β), inhibiting the infiltration of inflammatory cells and the proliferation of synovial tissues, and minimizing destruction of cartilage.

3.3. Effect of JWJGF on the IL33-ST2 Signaling Pathway in RA Rats. The IL33-ST2 signaling pathway exerts a pivotal effect in many diseases. The change of ST2 in the course of disease development has become a hot topic in recent years. SST2 may function as a marker of disease activity in the course of chronic kidney diseases (CKD), and its mechanism in the

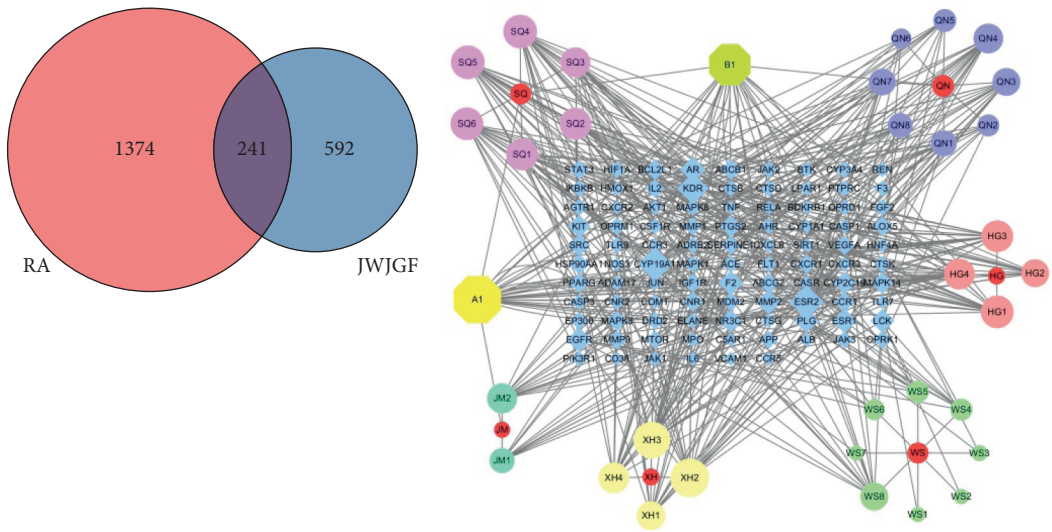

(a) (b)

Figure 1: Analysis of key components and core targets of JWJGF therapy for RA based on network pharmacology. (a) Venn diagram of overlapped gene between JWJGF and RA targets. (b) JWJGF-compound-target-RA network diagram. Blue diamonds represented candidate targets of JWJGF against RA, and circular and hexagon shapes represented active ingredients of JWJGF.

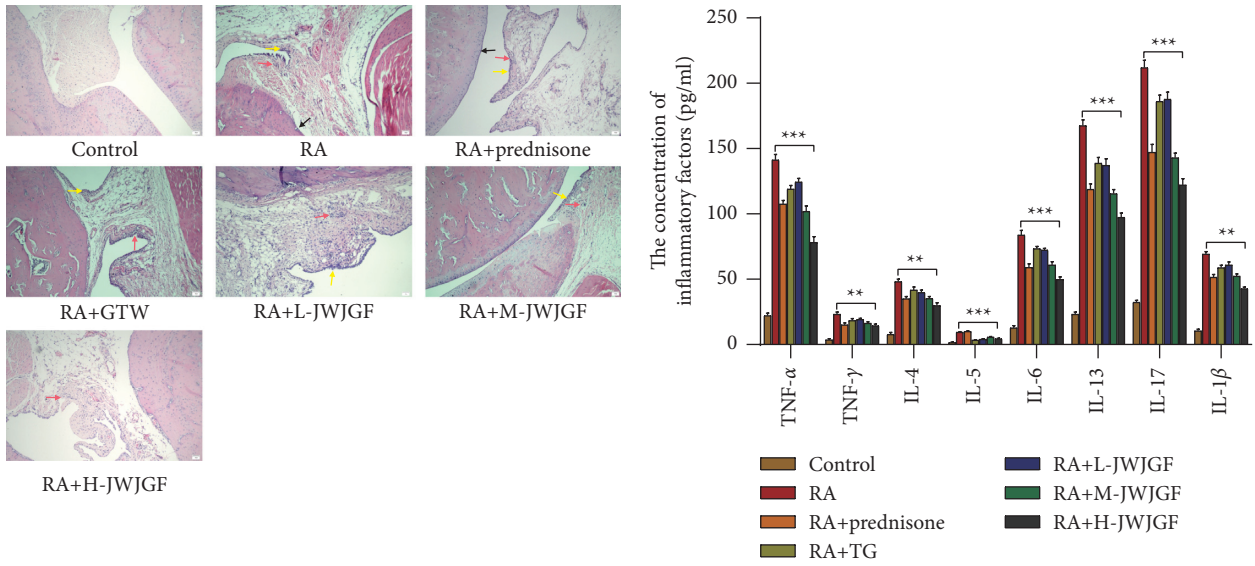

(a) (b)

Figure 2: FLS proliferation and inflammatory factors of the RA rat model were suppressed after JWJGF administration. (a) Histological examinations were performed in the hind paw joints (yellow arrows indicated synovial hyperplasia, black arrows indicated chondrocyte injury, and red arrows represented inflammatory cell infiltration. The scale bar was 50 μm). (b) Comparison of various inflammatory factors (TNF-α, TNF-γ, IL-1, IL-5, IL-6, IL-13, IL-17, and IL-1β) of each group using ELISA. Levels of the previously described inflammatory factors were determined after 4 d treatment. All data obtained from experiments were expressed as mean ± SD ($n > 3$). $^{*}p < 0.05$, $^{**}p < 0.01$, $^{***}p < 0.001$, and $^{***}p < 0.0001$ based on either pairwise comparison using Student's t-tests or one-way ANOVA using Tukey's tests for multiple groups.

development of CKD may be the focus of future research. Through network pharmacology, we found that IL-33 could serve as a potential target of JWJGF. To investigate the effect of JWJGF on the IL33-ST2 signaling pathway, we observed the effect of JWJGF on the IL33-ST2 signaling pathway in RA rats through Western blot and qPCR assays. The findings indicated that the expression levels of IL-33, sST2, and ST2L were markedly higher in RA group than those of control group ($P < 0.01$), whereas the levels were apparently lower in prednisone and GTW groups than model group ($P < 0.01$). In prednisone and GTW groups, protein expression levels of IL-33, sST2, and ST2L declined markedly in comparison to

model group ($P < 0.01$). Furthermore, the protein expression levels of IL-33, sST2, and ST2L decreased greatly in the JWJGF groups administered at three doses compared with model group ($P < 0.01$) (Figure 3(a)). This indicated that JWJGF decreased the protein expression levels of IL-33, sST2, and ST2L in RA rats. Similarly, the same conclusion was obtained by qPCR (Figure 3(b)).

3.4. Effects of Liquiritigenin on RASF Cells. Using the network pharmacological approach, we found that LQ had the largest number of connections among all compounds. It is extracted from the stems of *Glycyrrhiza uralensis Fisch* and known as 7,4-dihydroxy-dihydroflavone with the chemical formula $C_{15}H_{12}O_4$ and molecular weight of 256.25. As a dihydroflavonoid compound, LQ has certain effects on the cardiovascular system and nervous system. In addition, it has various pharmacological effects such as antiviral, antioxidant, antitumor, and estrogen effects. To figure out the effect of LQ on RASF cells, the effect of LQ on RASF cells was verified using EDU and TUNEL experiments. EDU results revealed that the positive EDU cell count was apparently elevated in TNF-α group compared with control group ($P < 0.01$), whereas that was decreased markedly in prednisone and GTW groups compared with TNF-α group ($P < 0.01$). Meanwhile, the positive EDU cell count in high-dose LQ group was substantially decreased compared with TNF-α group, indicating that LQ effectively inhibited the proliferation of RASF cells (Figure 4(a)). Simultaneously, TUNEL assay findings revealed that the positive TUNEL cell count in TNF-α group was markedly declined compared with control ($P < 0.01$), those in prednisone and GTW groups were substantially elevated in TNF-α group ($P < 0.01$), and those in high-dose LQ group were also greatly increased compared with TNF-α group, suggesting that LQ significantly promoted apoptosis of RASF cells. It was confirmed that LQ could inhibit the proliferation of RASF cells by EDU and TUNEL (Figure 4(b)).

3.5. Effect of Liquiritigenin on the IL33-ST2 Signaling Pathway in RASF Cells. To explore the effect of LQ on the IL33-ST2 signaling pathway of RASF cells, we verified its effect using Western blot and qPCR experiments. Western blot assay indicated a marked increase in expression levels of IL-33, sST2, and ST2L in TNF-α group compared with control group ($P < 0.01$), whereas a substantial decrease in expression levels of IL-33, sST2, and ST2L in prednisone group and GTW group was exhibited compared with TNF-α group ($P < 0.01$), and those in high-dose LQ group were also significantly decreased compared with TNF-α group (Figure 5(a)). These findings displayed that LQ effectively inhibited expressions of IL-33, sST2, and ST2L proteins, and the qPCR experiment confirmed the same results (Figure 5(b)).

4. Discussion

The main pathological manifestations of RA are synovial cell proliferation, synovial inflammation, and the formation of vascular opacities, which in turn erode cartilage and bone, ultimately leading to joint deformity and mobility impairment. The pathogenesis of RA is complex, involving genetic, environmental, and immune factors [12–14]. T cell-mediated autoimmunity is also a key factor in RA occurrence and $CD4^+$ T cells have been reported to be associated with the pathogenesis of RA. At present, options for RA treatment have been improved from initial nonsteroidal anti-inflammatory drugs and traditional disease improvement antirheumatic drugs (cDMARDs) to targeted biologics and targeted small molecule drugs. Biological agents targeted for RA are mainly concentrated on various inflammatory factors downstream of pathogenesis including TNF-, IL-6, and IL-17 [15–17].

JWJGF is a long-term clinical study of the vaccine prescription of this research group presenting a satisfactory curative effect on RA treatment. To explore whether JWJGF was effective in RA treatment, we identified the key component (Liquiritigenin) and core target (IL-33) of JWJGF through network pharmacology. LQ is a compound extracted from the stems of *Glycyrrhiza uralensis Fisch*. As a dihydroflavonoid compound, LQ has certain effects on the cardiovascular system and nervous system. Besides, LQ has various pharmacological effects such as antiviral, antioxidant, antitumor, and estrogen effects. LQ indicated a role in inhibiting the proliferation of human cervical cancer HeLa cells and inducing cell apoptosis. LQ reduces vascular growth in transplanted tumors by inhibiting vascular endothelial growth factors and ultimately suppressing tumor progression. Kim had found that LQ can activate p53 and further activate p21, eventually causing the cervical cancer cell cycle to stagnate G1 and G2/M phases [18–21]. IL-33, derived from epithelial cells, is recognized as a cytokine of the IL-1 family. It can be combined with ST2 and regulate the secretion of inflammatory factors. IL-33 mainly originates from epithelial and endothelial cells and fibroblasts. It has dual biological roles like other IL-1 family members. It functions both as a transcription factor when localized in the nucleus and as a cytokine when secreted outside the cell. ST2 is expressed in many immune cells and nonconstructive blood cells as a high-affinity receptor of IL-33. IL-33 can also be released after stress and infection, which plays an important role in an allergic reaction, inflammation, autoimmune disease, and host defense. Lately, increasing studies have reported that IL-33 is closely related to heart-related diseases, diabetes, kidney disease, and autoimmune development. IL-33 binds to ST2 receptors to regulate inflammatory factor secretion [22–24].

To find out the molecular mechanism of JWJGF in RA treatment, we constructed a model of RA rats to verify the effects of JWJGF on synovial tissues, the infiltration of inflammatory cells, and chondrocyte injury. Compared with RA group, neither hyperemia, edema, nor synovial cell proliferation was reported in JWJGF group. Little infiltration of inflammatory cells was found.

Compared with mock group, expression levels of IL-1, IL-5, IL-6, IL-13, IL-17, IL-1β TNF-α, and TNF-γ in the high-dose JWJGF group were greatly declined compared with RA group ($P < 0.01$), indicating JWJGF could inhibit both synovial tissue proliferation and inflammation. To

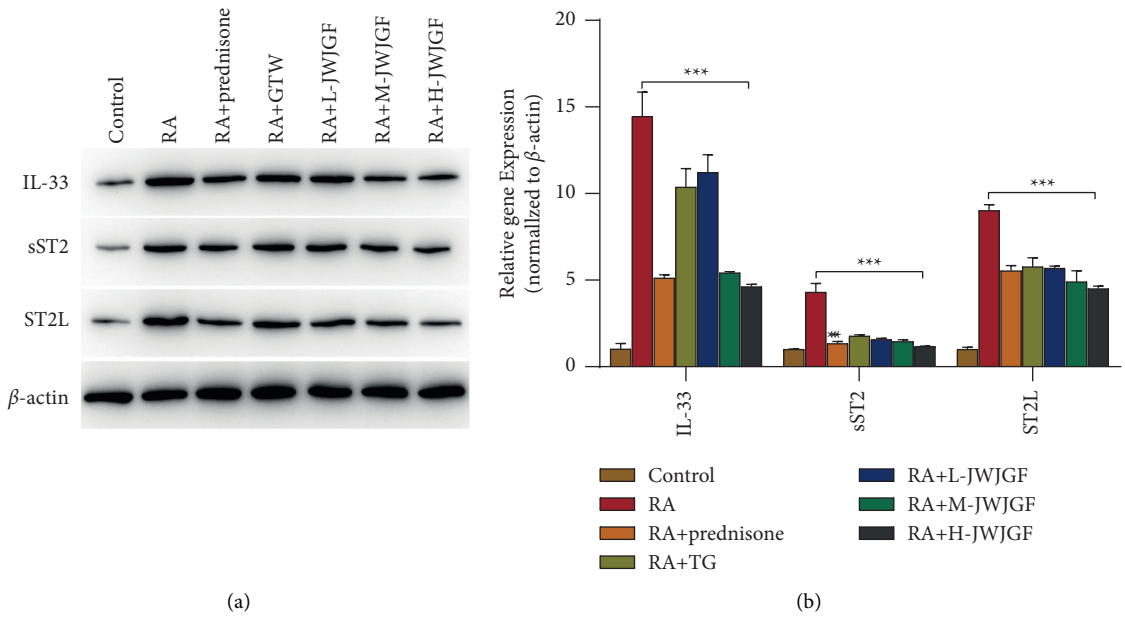

Figure 3: The effects of JWJGF on the IL33-ST2 signaling pathway in RA rats were verified using Western blot and qPCR. (a) Detection of protein expression levels of IL-33, sST2, and ST2L in each group using Western blot. (b) qPCR detection of the relative gene expressions of IL-33, sST2, and ST2L in each group. The data obtained were expressed as mean ± SD ($n \geq 3$). $^{*}p < 0.05$, $^{**}p < 0.01$, $^{***}p < 0.001$ and $^{****}p < 0.001$ based on either Student's t-tests for pairwise comparison or one-way ANOVA using Tukey's tests for multiple group comparison.

further explore the mechanism of JWJGF in the treatment of RA, we observed the effect of JWJGF on the IL33-ST2 signaling pathway in RA rats by Western blot and qPCR assays. The results presented a great decrease in protein expression levels of IL-33, sST2, and ST2L in JWJGF group ($P < 0.01$). This suggested that JWJGF might inhibit inflammation by inhibiting the IL33-ST2 signaling pathway.

Through network pharmacology, LQ was mostly connected with edges. To explore whether LQ acted on RASF cells, we observed the effect of LQ on RASF cells by EDU and TUNEL experiments. Findings of EDU assays indicated a sharp decrease in the number of positive EDU cells in the high-dose LQ group compared with TNF-α group. The results indicated that LQ significantly inhibited RASF cell proliferation. TUNEL assay findings indicated an apparent elevation in the number of positive TUNEL cells in the high-dose LQ group compared with TNF-α group. The results suggested that LQ significantly promoted RASF cell apoptosis. To further investigate LQ action on the IL33-ST2 signaling pathway in RASF cells, we compared effects of Liquiritigenin on the IL33-ST2 signaling pathway between high-dose LQ group and TNF-α group by Western blot and qPCR assays. The protein expression levels of sST2 and ST2L decreased substantially ($P < 0.01$). The results exhibited that LQ significantly inhibited the expressions of IL-33, sST2, and ST2L proteins, and the qPCR experiment confirmed the same findings. This suggested that Liquiritigenin might mediate the proliferation of RASF cells by inhibiting the IL33- ST2 signaling pathway.

JWJGF produces little toxicity, and it is safe to be applied clinically as per the prescribed dose and course of treatment. In the preliminary research of this research team, the toxicity of JWJGF was detected by performing acute and chronic toxicity tests. The acute toxicity test was designed as follows: 40 Kunming mice were randomly divided into a blank group and a JWJGF group, 20 in each group. The JWJGF group was administered at the maximum dose of 24.3 g/kg once, and the blank group was given an equal volume of distilled water. After 14 days, the mice were sacrificed and the main organs were harvested for pathological section comparison. The chronic toxicity test was designed as follows: a total of 80 rats were randomly divided into 4 groups, 20 in each group. A control group, JWJGF high-, medium-, and low-doses groups were prepared. The animals were given different concentrations of drugs by gavage for 6 d a week for 3 consecutive months. The control group was given an equal quantity of distilled water. The general manifestations of rats, poisoning reactions, and death before and after gavage were observed, and hemocytology and blood biochemical indexes, organ coefficients, and pathological examinations of main organs were recorded. The results in the acute toxicity experiment indicated that both groups of mice were generally stable following 2 to 14 d administration, with normal diets. No toxicity or death cases were reported. After anatomy, there were no abnormal changes in the organs. Pathological examinations revealed chronic inflammation in the partial trachea, and no obvious lesions were visualized in other organs. The chronic toxicity test revealed that the rats were administered with JWJGF at 10, 25, and 50 times of the recommended daily dose of adults in clinical practice by continuous intragastric administration for 3 months, and no death was reported. There were no obvious changes in general condition, weight, main organs, and hematological indexes of each drug group [25]. It is therefore obtained that

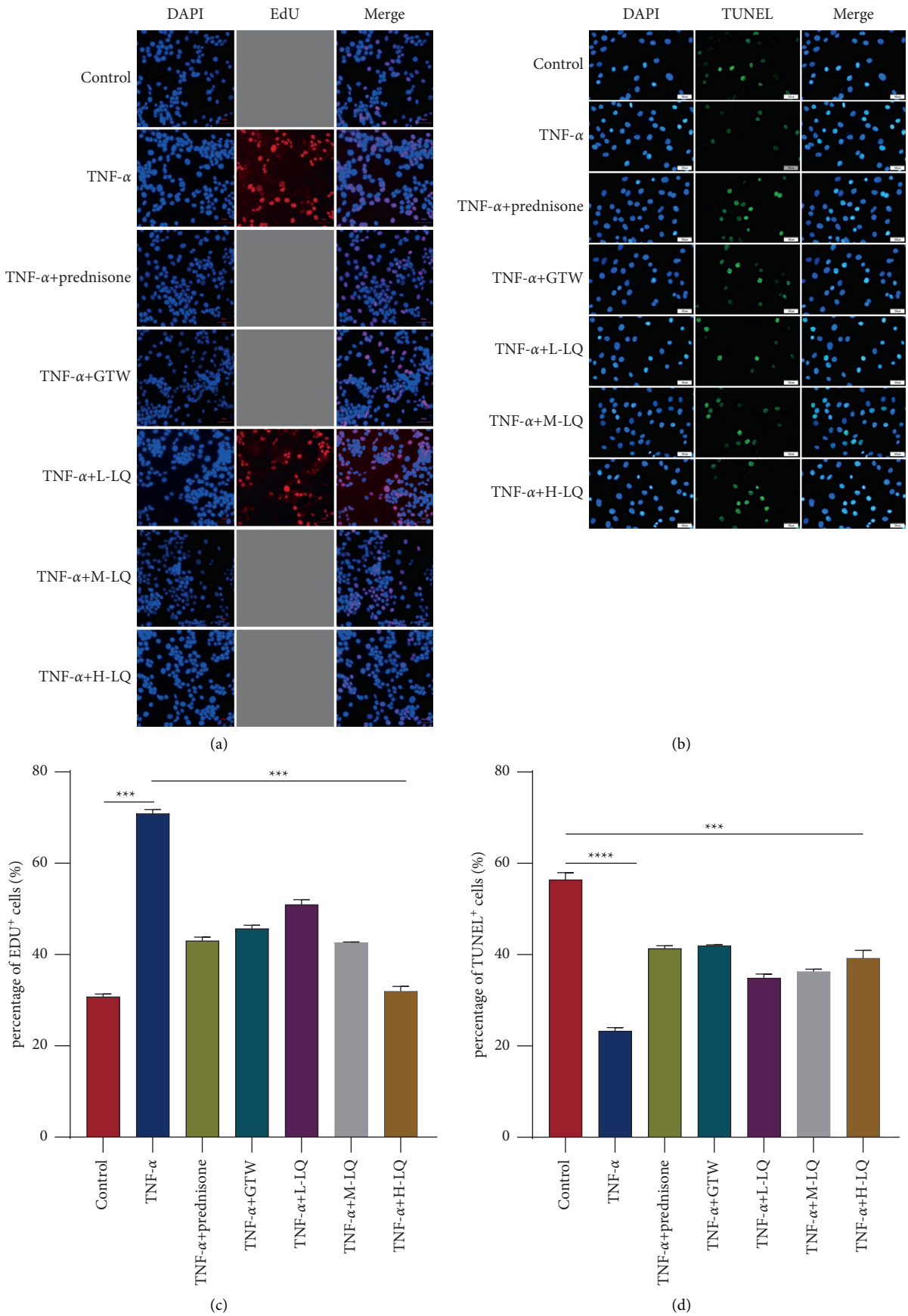

Figure 4: LQ action on RASF cell proliferation was detected using EDU assay and TUNEL assay. (a, b) Representative images and quantification. (c) Results of EdU assays. (d) Results of TUNEL assays. RASF cells were treated with TNF-α (10 ng/mL), LQ (50 μM, 100 μM, and 150 μM), prednisone (200 ng/mL), and GTW (30 μg/mL) for 24. (h) Data of the assays were expressed as mean ± SD ($n \geq 3$). $^{*}p < 0.05$, $^{**}p < 0.01$, $^{***}p < 0.001$, and $^{****}p < 0.001$ based on either Student's t-tests for pairwise comparison or one-way ANOVA using Tukey's tests for multiple group comparison.

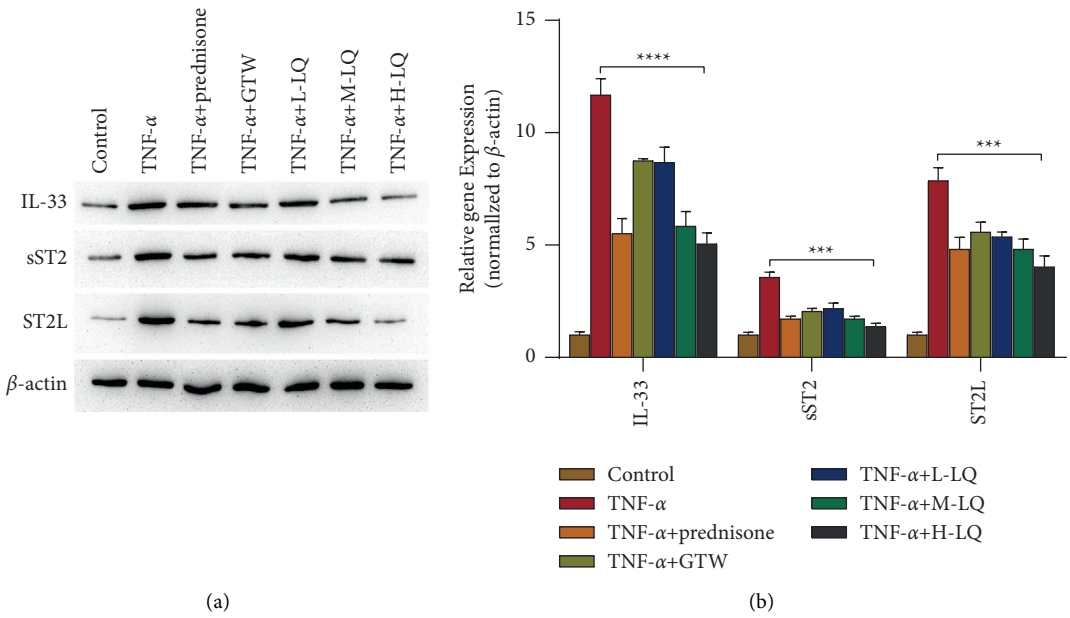

Figure 5: Detection of the effect of LQ on IL33-ST2 signaling pathway in RASF cells by Western blot and qPCR. (a) The relative protein expression levels of IL-33, sST2, and ST2L in all groups were subjected to Western blot. (b) The relative gene expressions of IL-33, sST2, and ST2L of each group were detected by qPCR. All data were presented as mean ± SD ($n > 3$ experiments). $^{*}p < 0.05$, $^{**}p < 0.01$, $^{***}p < 0.001$, and $^{****}p < 0.0001$ based on using Student's t-tests for pairwise comparison or one-way ANOVA using Tukey's tests for multiple groups.

the drug concentration selected in the present study on the basis of previous research is appropriate.

5. Conclusion

We firstly predicted possible targets and pathways of JWJGF for RA in a network pharmacology approach. The key component (LQ) and the core target (IL-33) of JWJGF were identified. Further, we found that JWJGF could inhibit the IL33-ST2 signaling pathway using Western blot and qPCR assays. Finally, JWJGF was verified as being responsible for inhibiting proliferation of RASF cells and the IL33- ST2 signaling pathway.

Data Availability

The data used to support the findings of this study are included within the article.

Disclosure

Daomin Lu and Ying Huang are the co-first authors.

Conflicts of Interest

The authors declare that they have no conflicts of interest.

Acknowledgments

This work was supported by the National Natural Science Foundation of China (nos. 81760829 and 82060909) and Growth Project of Young Scientific and Technological Talents of Guizhou Provincial Department of Education (Qian Jiao He KY Zi no. [2018] 218).

References

[1] J. A. Sparks, "Rheumatoid arthritis," *Annals of Internal Medicine*, vol. 170, 2019 Itc1-itc16.

[2] N. Choudhary, L. K. Bhatt, and K. S. Prabhavalkar, "Experimental animal models for rheumatoid arthritis," *Immunopharmacology and Immunotoxicology*, vol. 40, pp. 193–200, 2018.

[3] D. Aletaha and J. S. Smolen, "Diagnosis and management of rheumatoid arthritis: a review," *The Journal of the American Medical Association*, vol. 320, pp. 1360–1372, 2018.

[4] D. Giannini, M. Antonucci, F. Petrelli, S. Bilia, A. Alunno, and I. Puxeddu, "One year in review 2020: pathogenesis of rheumatoid arthritis," *Clinical & Experimental Rheumatology*, vol. 38, pp. 387–397, 2020.

[5] I. Pusceddu, B. Dieplinger, and T. Mueller, "ST2 and the ST2/IL-33 signalling pathway-biochemistry and pathophysiology in animal models and humans," *Clinica Chimica Acta*, vol. 495, pp. 493–500, 2019.

[6] W. Y. Chen, T. H. Tsai, J. L. Yang, and L. C. Li, "Therapeutic strategies for targeting IL-33/ST2 signalling for the treatment of inflammatory diseases," *Cellular Physiology and Biochemistry*, vol. 49, pp. 349–358, 2018.

[7] G. Liu and F. Liu, "[Advances of IL-33/ST2 signaling pathway in allergic rhinitis]," *Lin Chung Er Bi Yan Hou Tou Jing Wai Ke Za Zhi*, vol. 34, pp. 565–568, 2020.

[8] M. Ramalingam, H. Kim, Y. Lee, and Y. I. Lee, "Phytochemical and pharmacological role of Liquiritigenin and isoliquiritigenin from radix glycyrrhizae in human health and disease models," *Frontiers in Aging Neuroscience*, vol. 10, p. 348, 2018.

[9] F. Liang, H. Zhang, H. Gao et al., "Liquiritigenin decreases tumorigenesis by inhibiting DNMT activity and increasing BRCA1 transcriptional activity in triple-negative breast cancer," *Experimental Biology and Medicine*, vol. 246, pp. 459–466, 2021.

[10] F. C. Meng and J. K. Lin, "Liquiritigenin inhibits colorectal cancer proliferation, invasion, and epithelial-to-mesenchymal transition by decreasing expression of runt-related transcription factor 2," *Oncology Research Featuring Preclinical and Clinical Cancer Therapeutics*, vol. 27, pp. 139–146, 2019.

[11] C. Shi, H. Wu, K. Xu et al., "Liquiritigenin-loaded submicron emulsion protects against doxorubicin-induced cardiotoxicity via antioxidant, anti-inflammatory, and anti-apoptotic activity," *International Journal of Nanomedicine*, vol. 15, pp. 1101–1115, 2020.

[12] G. R. Burmester and J. E. Pope, "Novel treatment strategies in rheumatoid arthritis," *Lancet*, vol. 389, pp. 2338–2348, 2017.

[13] F. Tang, X. M. Yao, and W. K. Ma, "Rheumatoid arthritis," *Nature Reviews Disease Primers*, vol. 4, Article ID 18002, 2018.

[14] J. S. Smolen, D. Aletaha, and I. B. McInnes, "Rheumatoid arthritis," *Lancet*, vol. 388, pp. 2023–2038, 2016.

[15] E. A. Littlejohn and S. U. Monrad, "Early diagnosis and treatment of rheumatoid arthritis," *Prim Care*, vol. 45, pp. 237–255, 2018.

[16] F. Ferro, E. Elefante, N. Luciano, R. Talarico, and M. Todoerti, "One year in review 2017: novelties in the treatment of rheumatoid arthritis," *Clinical & Experimental Rheumatology*, vol. 35, pp. 721–734, 2017.

[17] J. Narváez, "[Treatment of rheumatoid arthritis]," *Medical Clinics of North America*, vol. 147, pp. 176–180, 2016.

[18] Y. Liu, S. Xie, Y. Wang, K. Luo, Y. Wang, and Y. Cai, "Liquiritigenin inhibits tumor growth and vascularization in a mouse model of HeLa cells," *Molecules*, vol. 17, pp. 7206–7216, 2012.

[19] X. Yuan, B. Zhang, N. Chen et al., "Isoliquiritigenin treatment induces apoptosis by increasing intracellular ROS levels in HeLa cells," *Journal of Asian Natural Products Research*, vol. 14, pp. 789–798, 2012.

[20] X. Yuan, B. Zhang, L. Gan et al., "Involvement of the mitochondrion-dependent and the endoplasmic reticulum stress-signaling pathways in isoliquiritigenin-induced apoptosis of HeLa cell," *Biomedical and Environmental Sciences*, vol. 26, pp. 268–276, 2013.

[21] I. Park, K. K. Park, J. H. Park, and W. Y. Chung, "Isoliquiritigenin induces G2 and M phase arrest by inducing DNA damage and by inhibiting the metaphase/anaphase transition," *Cancer Letters*, vol. 277, pp. 174–181, 2009.

[22] C. Cayrol and J. P. Girard, "Interleukin-33 (IL-33): a nuclear cytokine from the IL-1 family," *Immunological Reviews*, vol. 281, pp. 154–168, 2018.

[23] B. Griesenauer and S. Paczesny, "The ST2/IL-33 Axis in immune cells during inflammatory diseases," *Frontiers in Immunology*, vol. 8, p. 475, 2017.

[24] E. Vianello, E. Dozio, L. Tacchini, L. Frati, and M. M. Corsi Romanelli, "ST2/IL-33 signaling in cardiac fibrosis," *The International Journal of Biochemistry & Cell Biology*, vol. 116, Article ID 105619, 2019.

[25] H. Xu, Y. Huang, Y. Wang, F. Tang, X. M. Yao, and W. K. Ma, "Experimental study on toxicology of miao medicine Jinwujiangu capsule," *Journal Of Guizhou University Of Traditional Chinese Medicine*, vol. 42, pp. 18–22, 2020.